SOME MINERALOGICAL, PHYSICAL AND CHEMICAL PROPERTIES OF VOLCANICALLY AFFECTED SOILS UNDER IRRIGATED SUGARCANE IN TANZANIA

Terri Storm Taylor

BSc Hons; MSc

Submitted in fulfilment of the academic requirements for the degree of

Doctor of Philosophy

Discipline of Soil Science

School of Agricultural, Earth and Environmental Sciences

College of Agriculture, Engineering and Science

University of KwaZulu-Natal

Pietermaritzburg

2013

COLLEGE OF AGRICULTURE, ENGINEERING AND SCIENCE

DECLARATION 1 - PLAGIARISM

I, Terri Storm Taylor, declare that

1. The research reported in this thesis, except where otherwise indicated, is my original research.

2. This thesis has not been submitted for any degree or examination at any other university.

3. This thesis does not contain other persons' data, pictures, graphs or other information, unless specifically acknowledged as being sourced from other persons.

4. This thesis does not contain other persons' writing, unless specifically acknowledged as being sourced from other researchers. Where other written sources have been quoted, then:
   a. Their words have been re-written but the general information attributed to them has been referenced.
   b. Where their exact words have been used, then their writing has been placed in italics and inside quotation marks, and referenced.

5. This thesis does not contain text, graphics or tables copied and pasted from the Internet, unless specifically acknowledged, and the source being detailed in the thesis and in the References.

Signed: ……. Name: T.S Taylor Date:

As the candidate's supervisor I have/have not approved this dissertation for submission

Signed: ……. Name: Prof. J.C. Hughes Date:

As the candidate's co-supervisor I have/have not approved this dissertation for submission

Signed: ……. Name: Dr. L.W. Titshall Date:

ACKNOWLEDGEMENTS

Mr. Jan Meyer for getting the project started and giving valuable information and advice throughout the project.

TPC Ltd. for funding the project and providing a postgraduate student bursary.

Mr. Pierre Noel for his time in organising the various aspects of the field work and his input and interest throughout the duration of the project.

Mr. Jean Robert Lincoln for his enthusiasm and interest in the project, as well as sharing valuable information.

The TPC Agronomy Department, especially Ramadhani Hasani and Jacob Jeremia Mmary who helped with all the field work and soil preparation with never-ending enthusiasm.

TanzaniteOne Ltd. who allowed a better understanding of the area's geology by providing their time and a tour of the tanzanite mining area.

To those in the soil science department at UKZN, both past and present, who made working on this project that much more enjoyable. A special thanks to Tezi Nala, Jothan Buthelezi, Tad Dorasamy and Irene Bame.

To Shirley Mackellar who helped with the TEM work, Bheki Dlamini for assistance with the ICP and Hanlie Botha who provided the SSA data.

Prof. Jeffrey Hughes for his time and guidance through many years, both in and out of academia. Your support and help throughout my university career is hugely appreciated.

Dr. Louis Titshall for his effort, time and remarkable ability of making the complicated seem simpler. Thank you for many years of thought-provoking conversations and your support.

My parents, Lindsay and Jennifer Bassett. Thank you for everything you have done that has given me this incredibly blessed life to live.

To my husband, Guy Taylor, for making this life the most exciting adventure ever. Your support and love mean the world to me… two is better than one.

ABSTRACT

TPC is a 16 000 hectare estate located in Moshi, Tanzania and is currently planted under 8 800 hectares of sugarcane and produces over 60 000 tons of sugar per annum. The influence of volcanic parent material and volcanic ash over TPC, together with the alluvial nature of many of the soils, has imparted a unique combination of soil mineralogical, physical and chemical properties. Furthermore, irrigation with poor quality water has led to sodicity problems on the estate. Understanding the mineralogy and sodicity effects on soil hydraulic properties across the estate can lead to better irrigation management where it is important to prevent the build-up of salts due to over-irrigation.

In response to this need, a study was carried out with the aim of characterising the mineralogical, physical and chemical properties in the five management areas of the estate (North, East, West, South and Kahe), in order to determine the relationships between various measured parameters.

A total of 70 fields across TPC, as well as four sites outside the estate and two ash layers, were chosen for sampling. Undisturbed soil cores and bulk samples were collected from the A and B horizons from 45 of these fields and the four sites outside. Selected fields were sampled at more than one site to assess field variability, and where cane growth was patchy selected fields were sampled in a patch of poorly growing cane and an adjacent patch of better cane growth. Bulk soil samples were collected from the remaining fields and the two ash layers.

Double ring infiltration measurements were carried out on 25 of the selected fields. X-ray diffraction, transmission electron microscopy and aluminium, iron and silica extractions were carried out to determine the mineralogy. Physical and chemical measurements included water retentivity, saturated hydraulic conductivity, bulk density, particle size distribution, organic carbon, pH (H_2O), electrical conductivity, water soluble and exchangeable cations (Ca, Mg, K and Na), cation exchange capacity and clay specific surface area.

The particle size distribution showed that the soils were mainly loams and sandy loams. Organic carbon values were generally greater in the A horizon compared to the B horizon and varied

between 0.4 and 2.5 % in the topsoil and 0.3 and 2.1 % (with the exception of field 11 which had an organic carbon of 4.0 %) in the subsoil. X-ray diffraction patterns of sand and silt fractions were dominated by sanidine while clay patterns were weak and had high backgrounds and very broad peaks, suggesting the presence of poorly ordered material in the clay fraction. The Al and Fe extraction methods and electron micrographs indicated that this poorly ordered material was allophane. However, the dominant clay mineral across the estate was halloysite, in both tubular and spheroidal form, as well as very small (<< 0.5 µm) kaolinite particles. There was also gibbsite in some of the samples analysed. The combination of allophane, halloysite, kaolinite and gibbsite indicated that the primary volcanic minerals have weathered to various degrees across the estate. This is reflected in the alluvial nature of the soils where less weathered material has been periodically deposited onto older, more weathered material over some parts of the estate. The south and west areas had a slightly higher Al_o + ½ Fe_o ratio than the other areas in both the topsoil (1.07 and 0.95, respectively) and the subsoil (1.16 and 1.06, respectively), a possible consequence of less weathered alluvial material that was deposited in these areas. Although the concentration of allophane was low (< 5 %), even in the south and west areas, its presence greatly increased the clay specific surface area (up to 145.94 m^2 g^{-1}) and consequently had a significant influence on the soil physical and chemical properties.

Water retention across TPC was high, particularly at the lower matric potentials (between 0.13 and 0.45, and 0.09 and 0.24 m^3 m^{-3} at -33 kPa and -1500 kPa, respectively). The high water retention is a result of allophane which gives the soils a high adsorption capacity and a porosity that is dominated by micro-pores. Generally, the south area had the highest water retention at the various measured matric potentials which corresponds to the higher allophane content. Variability in water retentivity across areas and within fields limited further interpretation and correlation with the mineralogical results.

Infiltration rate was lowest in the south (60.85 mm hr^{-1}) and highest in the Kahe area (171.20 mm hr^{-1}). The main factor influencing the final infiltration rate was the concentration of sodium in the soil, with higher concentrations causing soil dispersion and blockage of soil pores. Clay dispersion has led to the development of calcareous surface crusts and reduced porosity, thus reducing the infiltration rate.

Sodium concentration in the soil is likely to have had a dominating effect over the mineralogical composition of the soil. Poor cane growth in the south and west areas corresponded to higher pH (up to 10.32), electrical conductivity (up to 614 mS m^{-1}), sodium absorption ratio (up to 20.63) and water soluble and exchangeable sodium (up to 53.20 $mmol_c$ l^{-1} and 14.87 $cmol_c$ kg^{-1} soil, respectively) in these areas. The soils are thus more dispersive and the combination of sodicity and allophane has resulted in "fluffy" soils with small particles clogging soil pores and thus surface crusts have formed easily.

The combined effect of mineralogy and sodicity in the south is further complicated by the presence of perched water tables. High adsorption capacities and the dominance of micro-pores allow the occurrence of significant capillary rise which brings salts to the soil surface, further exacerbating the sodicity problem. Therefore, over-irrigation should be avoided where soils are prone to sodicity from a combination of irrigation with poor quality water, perched water tables and strong capillary rise action. Fields which are currently experiencing the negative effects of high sodicity, require irrigation with good quality water and adequate sub-surface drainage to ensure the leaching of salts.

Further studies with specific focus on the south and west areas would be beneficial in accounting for the variability and in drawing correlations between the mineralogy and sodium content of the soils with the other measured properties. Fields which are prone to increased sodicity through over-irrigation with poor quality water, have strong capillary rise from perched water tables and which require remediation through sub-surface drains can thus be distinguished and the factors influencing sugarcane growth can be more clearly understood. Growth depends on the combination of these soil's unique mineralogy and sodium content and the influence they have on the infiltration rate, adsorption capacity, micro-porosity and capillary rise from the water table. For future work, water movement modelling to predict saturated and unsaturated flow, as well as *in situ* measures of unsaturated flow, will lead to further understanding of the soil hydraulic properties and aid in improved irrigation management.

TABLE OF CONTENTS

Page

DECLARATION……... ii

ACKNOWLEDGEMENTS…….. iii

ABSTRACT……... iv

TABLE OF CONTENTS…….. vii

LIST OF FIGURES…….. x

LIST OF TABLES…… xiv

LIST OF PLATES…… xvi

LIST OF APPENDICES…….. xvii

ABBREVIATIONS AND SYMBOLS……. xx

CHAPTER 1: INTRODUCTION……..... 1

CHAPTER 2: BACKGROUND…….. 4

2.1 Site description…….. 4

2.2 Historical research……..... 5

CHAPTER 3: THE INFLUENCE OF MINERALOGY ON THE PHYSICAL AND CHEMICAL PROPERTIES OF ANDISOLS AND SOILS WITH ANDIC PROPERTIES…… 10

3.1 Introduction…….. 10

3.2 Volcanic ash soils…….. 11

3.2.1 Mineralogy of volcanic ash soils……... 12

3.2.2 Physical properties of volcanic ash soils……... 17

3.2.2.1 Structure and water retention……... 17

3.2.2.2 Infiltration rate and hydraulic conductivity…….. 19

3.2.3 Chemical properties of volcanic ash soils…… 21

3.2.3.1 Cation exchange capacity, anion exchange capacity and specific surface area……... 21

3.3 Conclusions……... 24

CHAPTER 4: MATERIALS AND METHODS…… 26
4.1 Field sampling…… 26
4.1.1 Field sampling protocol…….. 26
4.1.2 Bulk soil samples……..... 26
4.1.3 Soil cores……. 27
4.1.4 Infiltration measurements……... 27
4.2 Laboratory analysis……... 27
4.2.1 Mineralogical properties……. 27
4.2.1.1 X-ray diffraction…….. 27
4.2.1.2 Transmission electron microscopy……. 28
4.2.2 Physical properties…….. 28
4.2.2.1 Water retention characteristics, saturated hydraulic conductivity and bulk density……... 28
4.2.2.2 Determination of field capacity: Free drainage method……. 30
4.2.2.3 Particle size distribution…….. 30
4.2.2.4 Specific surface area…… 30
4.2.3 Chemical properties…… 31
4.2.3.1 Organic carbon……. 31
4.2.3.2 Electrical conductivity and pH……. 31
4.2.3.3 Extractable silica, aluminium and iron……. 31
4.2.3.4 Water soluble cations, exchangeable cations and cation exchange capacity…….. 31
4.3 Statistical analysis…….. 32

CHAPTER 5: RESULTS AND DISCUSSION…….. 34
5.1 Introduction……..... 34
5.2 Mineralogical analysis……... 34
5.2.1 X-ray diffraction of oriented clay samples……. 34
5.2.2 X-ray diffraction of random powder sand and silt samples…….. 39
5.2.3 Transmission electron microscopy…….. 42
5.2.4 Extractable silica, aluminium and iron……... 45

5.3 Physical analysis…… 50
5.3.1 Final infiltration rate…….. 50
5.3.2 Water retention……..... 53
5.3.2.1 Good and bad patches of cane growth……..... 53
5.3.2.2 Variability within fields……... 59
5.3.2.3 Water retention across TPC estate……. 62
5.3.3 Hydraulic conductivity……..... 66
5.3.4 Bulk density……..... 67
5.3.5 Particle size distribution…….. 69
5.3.6 Specific surface area……... 70
5.4 Chemical analysis……... 73
5.4.1 Organic carbon…… 73
5.4.2 pH (H_2O)…… 74
5.4.3 Electrical conductivity…… 76
5.4.4 Water soluble cations of a saturated paste…….. 78
5.4.5 Water soluble cations of the soil……. 81
5.4.6 Exchangeable cations…….. 82
5.4.7 Cation exchange capacity…… 83

CHAPTER 6: GENERAL DISCUSSION, CONCLUSION AND RECOMMENDATIONS…… 85
6.1 Recommendations and possible future work……... 88
REFERENCES……. 90
APPENDICES…….. 100

LIST OF FIGURES

Page

Figure 2.1: Location of Tanzania within Africa (http://www.worldatlas.com/webimage/countrys/africa/tz.htm) and the approximate location of TPC sugar estate within Tanzania (modified from http://www.infoplease.com/atlas/country/tanzania.html)……. 4

Figure 3.1: X-ray diffraction patterns of naturally occurring imogolite and allophane (Wilson, 1987; cited by Harsh *et al*., 2002)…….. 13

Figure 3.2: Gravimetric water content at -1, -10, -33, -100 and -1500 kPa matric potential for an Andisol (numbered 0) and cultivated volcanic soils (numbered 1 to 5 according to their decreasing andic character: 0>1>2≈3≈4>5) (modified from Armas-Espinel *et al*., 2003)……..... 18

Figure 3.3: Cation exchange capacity and clay contents in soils dominated by illitic and amorphous clay minerals (1V indicates the soil of site 1 under virgin conditions, 5A indicates the soil of site 5 under agricultural conditions) (Hepper *et al*., 2006)……... 23

Figure 5.1: X-ray diffraction patterns with labelled peaks (Å) of oriented clay samples treated with magnesium (Mg) and potassium (K) and analysed as air-dry samples (AD), heated at 550 ^{o}C (Htd) and analysed after treatment with ethylene glycol (EG) and glycerol (Gly) for the a) A horizon and b) B horizon in field 5[1]……... 36

Figure 5.2: X-ray diffraction patterns with labelled peaks (Å) of random powder samples of the sand fraction for specimens N91 A horizon, L1S B horizon, E6 A horizon and R8 ash layer. All labelled peaks are K-feldspar peaks with the exception of the peaks at 3.03/ 3.01Å, 2.28Å and 2.09Å which represent calcite and the 7.29Å and 4.47Å peaks of kaolin…… 40

Figure 5.3: X-ray diffraction patterns with labelled peaks (Å) of random powder samples of the silt fraction for specimens N91 A horizon, L1S A horizon, N34N A horizon and E6 B horizon. All labelled peaks are K-feldspar peaks with the exception of the peaks at 7.22/ 7.30/ 4.44Å which represent kaolin, the 10.11Å peak which represents illite and the 8.38Å peak of amphibole.……... 41

Figure 5.4: Transmission electron microscope images of the R8 ash layer, borehole ash, N65 A and B horizons, E6 A and B horizons, 10K A and B horizons (Good), KH29 A and B horizons, 1 A and B horizons (Good). Scales are indicated on each photomicrograph……. 44

Figure 5.5: Iron extracted by acid oxalate (Fe_o) and citrate-bicarbonate-dithionite (Fe_d) in the a) A horizon and b) B horizon and iron extracted by sodium pyrophosphate (Fe_p) in the c) A horizon and d) B horizon for the north, west, east, south and Kahe areas, and the ash layers (R8 ash and borehole ash (BH Ash)) of TPC sugar estate…….. 46

Figure 5.6: Allophane content for the various areas and ash layers of TPC sugar estate for the A and B horizons……..... 48

Figure 5.7: Water retentivity curves of a selection of fields with good and bad patches of cane growth…… 55

Figure 5.8: The pore size distribution of the good and bad patches of cane growth in the a) A horizon and b) B horizon…… 57

Figure 5.9: Pore size distribution of the A and B horizons for the different areas of TPC sugar estate……... 60

Figure 5.10: Principal component analysis (PCA) of water retention characteristics for the A horizon. Open circles represent each sample point, inverted solid triangles represent the average value for samples collected from the five regions and the vectors represent the magnitude and direction of change for the volumetric water content at various matric potentials (-kPa). Sample point P4N was excluded as an outlier, while some of the measured WRC values are not shown for sake of clarity (-1 and -8 kPa). PCA axis 1 accounted for 68.4 % and PCA axis 2 accounted for 11.8 % of the variation in the data (86.4 % combined)……. 62

Figure 5.11: Principal component analysis (PCA) of water retention characteristics for the B horizon. Open circles represent each sample point, inverted solid triangles represent the average value for samples collected from the five regions and the vectors represent the magnitude and direction of change for the volumetric water content at various matric potentials (-kPa). Sample point P4N was excluded as an outlier, while some of the measured WRC values are not shown for sake of clarity (-1 and -8 kPa). PCA axis 1 accounted for 72.8 % and PCA axis 2 accounted for 15.9 % of the variation in the data (88.7 % combined)……. 63

Figure 5.12: Bulk density of the A and B horizons of the various areas within TPC sugar estate…….. 67

Figure 5.13: The percentage of a) sand, b) silt, and c) clay of the various areas of TPC sugar estate for the A and B horizons……..... 69

Figure 5.14: pH (H_2O) for the different areas of TPC sugar estate for the A and B horizons….. 74

Figure 5.15: Electrical conductivity (EC_e) of a saturated paste sample for the various areas of TPC sugar estate in the A and B horizons…….. 77

Figure 5.16: Calcium (Ca), magnesium (Mg), sodium (Na), potassium (K) and sodium adsorption ratio (SAR) for the different areas of TPC sugar estate in the a) A horizon and b) B horizon…… 79

Figure 5.17: Water soluble calcium (Ca), magnesium (Mg), sodium (Na) and potassium (K) and the sodium adsorption ratio (SAR) for the different areas of TPC sugar estate in the a) A horizon and b) B horizon…… 81

Figure 5.18: Exchangeable calcium (Ca), magnesium (Mg), sodium (Na), potassium (K) and the sum of exchangeable bases (Ex. bases) in the different areas of TPC sugar estate in the a) A horizon and b) B horizon…… 82

Figure 5.19: Cation exchange capacity in the different areas of TPC sugar estate in the A and B horizons……..... 83

LIST OF TABLES

Page

Table 2.1: Water quality of irrigation water in rivers and TPC management areas averaged from January to June 2013 (data supplied by TPC management) 9

Table 3.1: Bulk density (ρb), Al_o + ½ Fe_o percentage and phosphorus (P) retention for five soils from Tenerife with decreasing andic characteristics. Soils (0 = reference Andisol, 1 to 5 = cultivated volcanic soils) numbered according to their decreasing andic character: 0>1>2≈3≈4>5 (modified from Armas-Espinel *et al*., 2003)…….. 12

Table 3.2: Frequency of hydraulic conductivity classes for the studied soils (0 = reference Andisol, 1 – 5 = cultivated volcanic soils, numbered according to decreasing andic character 0>1>2≈3≈4>5). n = number of samples (modified from Armas-Espinel *et al*., 2003)…….. 20

Table 3.3: Cation exchange capacity (CEC) and surface area of common soil minerals (adapted from Brady and Weil, 2002)……. 22

Table 5.1: The range and average (n = 32) of Fe, Al and Si extracted by the acid oxalate, citrate-bicarbonate-dithionite and pyrophosphate methods for the A and B horizons of the sampled soils of TPC sugar estate…….. 45

Table 5.2: Final infiltration rates for each area of the TPC estate……. 50

Table 5.3: Probability (P = 0.05) from paired t-tests used to compare the water retentivity at various tensions, the readily available water (RAW) and the plant available water (PAW) between the good and bad patches of cane growth from both the A and B horizons……..….. 56

Table 5.4: Volumetric water content (m^3 m^{-3}) at various matric potentials (kPa) for the fields where sampling was done at more than one site…… 61

Table 5.5: Plant available water (PAW), readily available water (RAW) and volumetric water content (m^3 m^{-3}) at -10, -33 and -1500 kPa for red, black and grey soils typically found in the South African sugarcane industry (modified from Johnston, 1973)…….... 64

Table 5.6: Readily available water (RAW) and plant available water (PAW) in the A and B horizons for the five areas of TPC sugar estate…… 66

Table 5.7: Percentage of samples within each area of TPC sugar estate with a bulk density of below 1.1g cm^{-3} for the A and B horizon……... 68

Table 5.8: Specific surface area of selected PSU clay (< 2 µm) samples from TPC sugar estate……... 71

Table 5.9: Hypothetical calculation for clay BET specific surface area at TPC……. 72

Table 5.10: Average soil organic carbon (%) for each area of the TPC estate…… 73

Table 5.11: Average soil organic carbon (%) for the good and bad patches in the A and B horizons……... 74

Table 5.12: pH (H_2O) of the fields measured in a patch of poorly growing cane (Bad) and better growing cane (Good) for the A and B horizons……... 76

Table 5.13: The sodium adsorption ratio (SAR) of the A and B horizons in good and bad patches of cane growth……... 80

LIST OF PLATES

Page

Plate 5.1: Calcrete exposed in a drain in Field D28 (East area). Hammer on the left is 30 cm long.……...…….. 39

Plate 5.2: Surface crust in field R8N (South area)……. 50

Plate 5.3: Precipitated salts on the soil surface in the south area…….. 51

Plate 5.4: Saturated soil in field D19 (East area)……... 52

LIST OF APPENDICES

Page

Appendix 4.1: Sample collection summary from a) PSU sites (Undisturbed soil cores and bulk sample from A and B horizons collected), b) non-PSU sites (Undisturbed soil cores and bulk sample from A and B horizons collected), c) bulk sites (Bulk sample collected from A and B horizon, no undisturbed soil cores collected) and d) the two ash layers from the borehole (BH Ash) and field R8 (R8 Ash)……. 101

Appendix 4.2: Map of sample points taken over TPC estate…….. 106

Appendix 5.1: X-ray diffraction patterns with labelled peaks (Å) of oriented clay samples treated with magnesium (Mg) and potassium (K) and analysed as air-dry samples (AD), heated at 550^{o}C (Htd) and analysed after treatment with ethylene glycol (EG) and glycerol (Gly) for the A and B horizons of selected fields from the a) north, b) west, c) east, d) south, e) Kahe areas and f) the ash layers of TPC sugar estate…….. 107

Appendix 5.2: X-ray diffraction patterns of random powder samples of the sand fraction from the A and B horizon for specimens N91, N65 and N34N (North), L1S (West), E6 (East), 17B and G2 (South), KH4 and KH29 (Kahe), and R8 Ash and BH Ash (Ash layers)…….. 162

Appendix 5.3: X-ray diffraction patterns of random powder samples of the silt fraction from the A and B horizon for specimens N91, N65 and N34N (North), L1S (West), E6 (East), G2 (South), KH4 and KH29 (Kahe), and R8 Ash and BH Ash (Ash layers)……... 169

Appendix 5.4: Acid oxalate extractable Fe, Al and Si (Fe_o, Al_o, Si_o), citrate-bicarbonate-dithionite extractable Fe and Al (Fe_d, Al_d) and sodium pyrophosphate extractable Fe and Al (Fe_p, Al_p) for TPC soil samples in the A horizon (A) and B horizon (B)..…….. 175

Appendix 5.5: Amount of ferrihydrite, allophane and Al_o + ½ Fe_o in soils from TPC sugar estate from the A horizon (A) and B horizon (B)…… 177

Appendix 5.6: Final infiltration rate (mm hr^{-1}) of measured fields across TPC sugar estate…….. 179

Appendix 5.7: The volumetric water content (m^3 m^{-3}) for the A horizon (A) and B horizon (B) at each measured matric potential (kPa) at each sampled site across TPC sugar estate…… 181

Appendix 5.8: Trends in water retention characteristics for each sampled site…….. 188

Appendix 5.9: Saturated hydraulic conductivity (K_s) of undisturbed soil cores from the A and B horizons for TPC sugar estate……..... 196

Appendix 5.10: Bulk density of soil samples from TPC sugar estate for the A and B horizon…….. 201

Appendix 5.11: Particle size distribution of sampled fields across TPC sugar estate……. 203

Appendix 5.12: Soil organic carbon (%) from the A and B horizons of fields sampled at TPC sugar estate……... 209

Appendix 5.13: pH (H_2O) in the A and B horizons of the sampled fields across TPC sugar estate... 212

Appendix 5.14: Electrical conductivity of a saturated paste sample for TPC sugar estate fields in the A and B horizons……. 215

Appendix 5.15: Water soluble cations and the sodium adsorption ratio (SAR) of a saturated paste for the A horizon (A) and B horizon (B) of sampled fields across TPC sugar estate…… 218

Appendix 5.16: Water soluble cations (Ca, Mg, Na and K) and the sodium adsorption ratio (SAR) of the A horizon (A) and B horizon (B) of sampled fields across TPC sugar estate……. 221

Appendix 5.17: Exchangeable Ca, Mg, Na, K and the sum of exchangeable bases (Ex. bases) in the A horizon (A) and B horizon B of sampled fields across TPC sugar estate…….. 222

Appendix 5.18: Cation exchange capacity (CEC) of the A horizon (A) and B horizon (B) of measured fields across TPC sugar estate……... 224

Appendix 5.19: Correlations (r value) between amorphous mineral content of the soils from TPC sugar estate and other measured soil properties in the a.) A horizon and b.) B horizon…… 225

Appendix 5.20: Correlations (r value) between water retention characteristics and other measured soil properties in the a.) A horizon and b.) B horizon…… 227

Appendix 5.21: Correlations (r value) between pH and electrical conductivity (EC) of the soils from TPC sugar estate with exchangeable cations in the a.) A horizon and b.) B horizon (n = 7)….. 231

ABBREVIATIONS AND SYMBOLS

AAS	Atomic absorption spectrophotometry
AEC	Anion exchange capacity
Al_d	Citrate-bicarbonate-dithionite extractable Al
Al_o	Acid ammonium oxalate extractable Al
Al_p	Sodium pyrophosphate extractable Al
AWC	Available water capacity
BET	Brunauer, Emmett, and Teller Equation
CBD	Citrate-bicarbonate-dithionite
CEC	Cation exchange capacity
EC_e	Electrical conductivity of a saturated paste
EGME	Ethylene glycol monoethyl ether
ERD	Effective rooting depth
ESP	Exchangeable sodium percentage
Fe_d	Citrate-bicarbonate-dithionite extractable Fe
Fe_o	Acid ammonium oxalate extractable Fe
Fe_p	Sodium pyrophosphate extractable Fe
FIR	Final infiltration rate
HIV	Hydroxyl interlayed vermiculite
ICP-ES	Inductively coupled plasma emission spectrometry
K_s	Saturated hydraulic conductivity
OC	Organic carbon
OM	Organic matter
PAW	Plant available water
PSU	Permanent sampling unit
RAW	Readily available water
SAR	Sodium absorption ratio
SASRI	South African Sugar Research Institute
SEM	Scanning electron microscope

Si_o	Acid ammonium oxalate extractable Si
SRO	Short-range order
SSA	Specific surface area
TAM	Total available moisture
TEM	Transmission electron microscopy
UKZN	University of KwaZulu-Natal
VAS	Volcanic ash soils
WHC	Water holding capacity
WRB	World Reference Base soil classification
XRD	X-ray diffraction
ρb	Bulk density

CHAPTER 1
INTRODUCTION

Soils found in volcanic regions around the world often have a unique assembly of clay minerals comprising both non-crystalline and layered silicate minerals (Armas-Espinel *et al*., 2003). The presence of non-crystalline minerals, even in small quantities, has a strong influence on the soil chemical and physical properties due to their large reactive surface area (Gama-Castro *et al*., 2000) and their strong aggregating effect (Armas-Espinel *et al*., 2003). Soil properties, such as water retention and cation exchange capacity, have been found to greatly increase with the amount of non-crystalline volcanic minerals (Nanzyo *et al*., 1993; Gama-Castro *et al*., 2000; Armas-Espinel *et al*., 2003; Fontes *et al*., 2004; Hepper *et al*., 2006).

The highland regions of Tanzania, on which the TPC sugar estate is situated, form part of the East African rift system which developed due to crustal tension, rift faulting and volcanic activity. The geology of the rift zone is mainly comprised of basaltic intrusive and volcanic rocks, with some rare alkaline rocks and igneous carbonates. This geology greatly influences the groundwater quality in the rift zone which is mostly alkaline, with low calcium and magnesium contents, and high pH and sodium concentrations (British Geological Survey, 2000). Despite the intensive commercial agriculture in the rift zone, studies on the properties of these soils due to the combined effect of their volcanic origin and irrigation with poor quality water are scarce.

The soils of the TPC sugar estate have been strongly influenced by the volcanic history of Mt. Kilimanjaro and Mt. Meru, situated about 50 km to the north. The alluvial deposition of volcanic materials over many parts of the estate, as well as irrigation with poor quality water, provided an opportunity to assess the influence on soil physical and chemical properties due to a combined effect of minerals of a volcanic origin and soil salinity and sodicity.

According to Meyer *et al*. (2009), one of the greatest challenges for the TPC sugar estate is “How to improve water-use efficiency and the quality of the irrigation water in the south, and how to reduce deep percolation water losses from irrigation areas which is exacerbating the build-up of groundwater tables in the south and east”. One of the suggestions made to address

this is to base irrigation scheduling on total available moisture (TAM). Leroy (2004) suggests that regular measuring of electrical conductivity and determination of the water use by measuring volumetric water content can help in timing irrigation and leaching events to meet the water need and prevent over-irrigation and the build-up of salts. Although Meyer *et al*. (2009) calculated TAM by multiplying an estimated value of available water capacity (AWC) by effective rooting depth, it is likely that the AWC estimation based on clay percentage results in an under-estimation of TAM due to the presence of non-crystalline clay minerals.

In response to this need, this study aimed at relating the mineralogy (and other selected soil physical and chemical attributes) to water retention and transmission properties at TPC with the purpose of guiding improved irrigation management. It is suggested that an increase in amorphous minerals, predominately allophane, results in a greater amount of water being retained in the soil by increasing the soil's specific surface area and adsorption properties. Consequently, greater quantities of allophane are likely to drive increased capillary rise bringing salts from the groundwater table to the soil surface. It is hypothesised that where the soils are sodic, the aggregating effect of allophane will be unable to offset the dispersion of clay particles and consequently infiltration rates and hydraulic conductivity will be low due to the development of surface crusts and blockage of soil pores by dispersed clay particles.

The overall objectives of the study were to:

- determine the mineralogical composition of these samples;
- determine water retention and water movement characteristics, along with other selected physical parameters, at the sampled sites;
- chemically characterise soils from "benchmark" sites and other selected areas;
- investigate the relationship between physical, mineralogical and chemical parameters; and
- suggest possible action and further research for improved water and salt management at the TPC sugar estate.

The thesis is structured as follows:

- Chapter 2 gives the background for the initiation of this study and a site description.
- Chapter 3 presents a review of the current literature on the influence of mineralogy on the physical and chemical properties of soils, with an emphasis on Andisols and soils with andic properties.

- Chapter 4 gives a description of the materials and methods used in this study.
- Chapter 5 reports and discusses the mineralogical, physical and chemical properties, as well as the relationships between these properties, of the soils analysed from the TPC sugar estate.
- Chapter 6 presents a general discussion, draws overall conclusions and provides recommendations and suggestions for future work for improved irrigation and salt management at the TPC sugar estate.

CHAPTER 2
BACKGROUND

2.1 Site description

TPC is located in Moshi, Tanzania (Figure 2.1) and is a 16 000 hectare estate planted under 8 800 hectares of sugarcane that currently produces over 60 000 tons of sugar per annum.

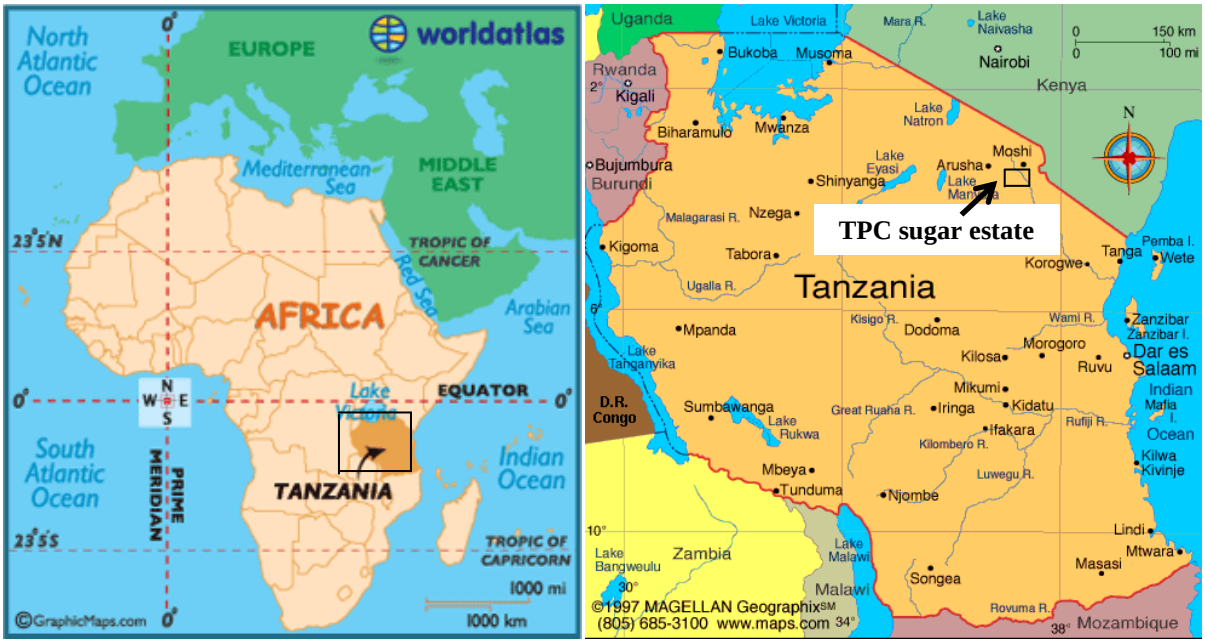

Figure 2.1: Location of Tanzania within Africa (http://www.worldatlas.com/webimage/countrys/africa/tz.htm) and the approximate location of TPC sugar estate within Tanzania (modified from http://www.infoplease.com/atlas/country/tanzania.html).

The area forms part of the East African Rift Valley system and has a semi-arid climate with an average annual rainfall ranging between 500 mm in the south of the estate to 700 mm in the north (Meyer *et al*., 2009), and a maximum temperature which ranges between 17 and 30 ^{o}C (Brogna, 2004). The potential evaporation A pan reading averages 2313.5 mm per annum. The topography is gently undulating with a slight decline in altitude from north to south (Meyer *et al*., 2009).

2.2 Historical research

During the period between September 2007 and September 2008, Messrs. Jan Meyer and Warren Heathman were appointed by MWH, a European based consulting consortium, to complete a detailed soil survey of the TPC sugar estate. This survey was completed in response to one of the key recommendations made as part of the 'Irrigation and Drainage Master Plan for TPC' (Hardy, 2007), with the intention of improving field management practices (i.e. irrigation, drainage and nitrogen application). The soil survey, therefore, aimed at gaining an understanding of the occurrence and distribution of the various soil types on the estate, as well as the physical and chemical properties of these soils (Meyer *et al*., 2009).

For the soil survey, 865 pits (2 x 2 x 2 m) were sampled with bulk soil samples taken from depths of 0 to 30, 30 to 60 and 60 to 90 cm. The bulk soil samples were analysed for pH, exchangeable cations (Ca, Mg, K and Na), exchangeable sodium percentage (ESP), cation exchange capacity (CEC), water soluble cations in a saturated paste, electrical conductivity of a saturated paste (EC_e), sodium absorption ratio (SAR), moisture saturation and particle size distribution. The topsoil horizon from each pit was further analysed for sample density, organic carbon (OC), nitrogen mineralisation potential and N fertiliser volatilization potential.

The results of the soil survey indicate that 82 % of the parent material on the estate is alluvium, 7 % is volcanic igneous rock and 11 % is a colluvial mixture of alluvium and volcanic rock parent material. The geology in the north of the estate consists of young, acid, volcanic rock (part of the Kilimanjaro lava flow) which is intruded into undifferentiated granites in the south. This geology is overlain by alluvial deposits (gravel, boulders, sand, silt and clay) ranging in depth from 3 m in the south eastern area to greater than 80 m in the west and northwest areas. In the south and in the Kahe section of the estate (situated to the east) there are deposits of silcrete and murrum (the name given to the clayey material containing rounded pebbles used as road building quarry), believed to be contributing to the perched water table in these areas due to their impermeable nature.

Meyer *et al*. (2009) recognised four main soil groups, namely: 1) volcanically derived medium to heavy clay soils; 2) medium clay, structured soils which are wet and non-wet; 3)

young sandy and silty, non-wet soils; and 4) sandy and silty, alluvial, wet soils. The majority of these soils also consist of colluvial and alluvial deposition of volcanic ash and there is evidence to suggest that there are significant amounts of allophane and sanidine in the mineralogical make-up of the soil (Meyer *et al*., 2009).

The dominant soil type (Soil Classification Working Group, 1991) over the estate is Oakleaf, followed by the Tukulu soil form which dominates in the south. The Tukulu soil form is mostly found in the low-lying areas that consist of sandy and silty alluvial soils which effervesce strongly with 1M HCl due to sodium bicarbonate transferred by capillary action where groundwater is of poor quality. The volcanically derived medium to heavy clay soils in the north and west are mostly Shortlands and Swartland soil forms that generally have a well-developed structure with good TAM (120 – 150 mm) and aeration. The alluvially derived medium clay soils are mostly found in the central and eastern parts of the estate and are dominated by the Valsrivier and Sepane soil forms. Due to the Sepane form being waterlogged at depth, this soil type is prone to sodicity problems. The sandy and silty loam soils consist of Oakleaf, Clovelly and Hutton soil forms, while the loamy sands are mostly Dundee and Fernwood soil forms. These soils are found mostly in the central and western part of the estate (Meyer *et al*., 2009).

The most widespread World Reference Base (IUSS Working Group WRB, 2006) soil units on the estate are Cambisols (young soils, weak B horizon development, no appreciable quantities of alluvial clay, organic matter (OM) or Fe and Al oxides. Good structural stability, high porosity, good water holding capacity (WHC), and good drainage), which account for 66 % of the soils, followed by 17.2 % Luvisols and 6.7 % Plinthosols (Meyer *et al*., 2009).

The organic matter content is low (≤ 1.5 %) in 60 % of the soils, with the lowest levels of OM occurring in the north and central east areas. Only 9 % of the soils across the estate have a moderate to high OM level (> 2.5 %), mostly occurring in the west and south areas. The majority of the soils are alkaline with 43 % having a pH (H_2O) between 8 and 9. Alkalinity increases north to south and east to west. The soils in the north of the estate have a lower CEC than elsewhere. The effective rooting depth (ERD) is greater than 110 cm in 61 % of the soils, mostly occurring in the west of the estate. The south and east areas have the lowest ERD. Particle size analysis shows that < 1 % of the soils are heavy clays, 40 % are sandy clay loams, 58 % sandy loams to loamy sands, and < 3 % are sandy soils (Meyer *et al*.,

2009). TPC soils are rich in potassium (can be over 2000 ppm) and phosphorus (Brogna, 2004; Meyer *et al*., 2009).

The results of the soil survey suggest that alluvial volcanic ash, tuff and pumice that originated from the north of the estate are weathering and contributing to significant amounts of amorphous materials in the mineral make-up of the soil, especially in the southern areas of TPC. The last major eruption from Kilimanjaro dates back to between 150 000 and 200 000 years ago (Nonnotte *et al*., 2008) and volcanic ash has likely being deposited over TPC estate by both aeolian and alluvial deposition. Evidence supporting the presence of amorphous materials includes many of the soils having a very large CEC equivalent of between 120 and 160 $cmol_c$ kg^{-1} clay and some soils which hold up to 120 % moisture at saturation. Furthermore, the sample density of disturbed soil with a clay content between 15 and 25 % ranges between 0.8 and 1.2 g ml^{-1}, whereas the sample density for a 'normal' alluvial soil with a similar clay content should be between 1.2 and 1.6 g ml^{-1} (Meyer *et al*., 2009). The powdery nature of the topsoil upon drying and the large macro-porosity leads to strong capillary rise and also points towards the presence of allophane. Previous studies carried out at TPC also allude to the presence of allophane and other associated minerals such as zeolites and halloysite (Moberg, 1981 and Sloot, 1987; cited by Meyer *et al*., 2009). As a consequence of the assumed presence of these minerals, it is suspected that the moisture retention at field capacity and wilting point is high and Meyer *et al*. (2009) suggested in their report that undisturbed soil cores be collected from areas where capillary rise is marked and the available moisture content determined between field capacity (-10 kPa) and wilting point (-1500 kPa).

The refinement of soil management at TPC is particularly necessary given that 26 % of the soils between 0 and 60 cm deep are prone to sodification, which is based on an SAR value ≥ 8 and an ESP value ≥15. An SAR value of 8 was used by Meyer *et al*. (2009) as it represents the average of the values recommended by the South African Sugar Research Institute (SASRI) for duplex soils (SAR 6) and non-duplex soils (SAR 10). Only 7.5 % of the soils have an ECe value in excess of 200 mS m^{-1}, and generally also have an ESP above 15, making these soils saline-sodic. These results indicate that sodicity is a bigger problem than salinity. Leroy (2004) recorded that approximately 40 % of the fields in the south are affected by saline/saline-sodic conditions, while another 30 % are affected by saline/saline-sodic conditions elsewhere on the estate. Thouvenot (2002) and Meyer *et al*. (2009) found that soils

in the south of the estate have the highest average EC_e, ESP and SAR indicating greater saline/sodic conditions than in other parts of the estate. On average, ESP values are higher than the SAR, except in the south where the SAR is double the ESP (Meyer *et al*., 2009).

Brogna (2004) used remote sensing techniques to map the patchy cane growth resulting from one or more of salinity, sodicity and white grub infestation. Brogna (2004) concluded that the south and east are more affected by patchy cane growth due to salinity/sodicity than the north and west, and that patchy cane growth occurs over 10 % of the estate, which is equivalent to a loss of 150 000 tons of sugar per annum (*pers. comm*., Lincoln[1], 2010).

Factors contributing to the sodicity and salinity problems are the poor quality irrigation water used in the southern and eastern parts of the estate and a shallow, saline groundwater table (particularly in the south and east) which can lead to capillary rise bringing salts to the soil surface, especially when there is over-irrigation and/or poor drainage (Thouvount, 2002; Leroy, 2004; Meyer *et al*., 2009). The sodicity and salinity problems in the west, where the water table is relatively low, are probably due to under-irrigation with poor quality irrigation water which does not allow the build-up of salts around the root zone to be leached away (Thouvenot, 2002).

The Karanga River runs from the northern point of TPC along the western boundary and is joined by the Weru Weru River at field N70. These two rivers serve to irrigate the north and west by overhead irrigation. The Kikafu River water then joins at field N33, followed by the Kikuletwa River, which joins in at field H3. The Kikuletwa River then serves to irrigate the south and east mostly by furrow irrigation via canals (Leroy, 2004; Meyer *et al*., 2009). The estate also has high quality natural seepage water, Miweleni Springs, which serves to irrigate the Kahe section by furrow irrigation (Meyer *et al*., 2009). The Kikuletwa River water is saline with high sodium bicarbonate levels (Meyer *et al*., 2009) and according to the SASRI classification is classified as class D, which is unsuitable for irrigation of sugarcane under normal irrigation practices. Consequently, this water is only used for irrigation in the driest months of the year (Thouvenot, 2002). The Weru Weru River water is classified as class A (suitable irrigation water on all soil types) (Thouvenot, 2002). However, irrigation water from the Weru Weru River may cause a reduction in the infiltration rate even if Na is low due to

[1] Lincoln J.R. Group Agricultural Development Manager, Ciel agro-industry

low levels of Ca and Mg (Thouvenot, 2002; Leroy, 2004). Table 2.1 provides a summary of water quality measured by TPC in the first half of 2013, for two of the major rivers used for irrigation and for each area, taken from piezometers and boreholes in various field. The water quality is relatively consistent throughout the year from each measured point.

Table 2.1: Water quality of irrigation water in rivers and TPC management areas averaged from January to June 2013 (data supplied by TPC management)

		EC	Ca_2^+	Mg_2^+	Na^+	K^+	HCO_3^-	SAR
		mS/m	……mmol$_c$/L……					
North		49.8 ± 2.42	1.05 ± 0.12	0.78 ± 0.09	2.56 ± 0.30	0.38 ± 0.04	5.71 ± 0.36	2.56 ± 0.23
	n	36	37	37	50	50	41	28
West		74.4 ± 7.75	1.70 ± 0.38	1.76 ± 0.09	3.50 ± 0.26	0.36 ± 0.05	9.18 ± 0.97	2.51 ± 0.37
	n	14	18	18	21	21	14	11
Kikuletwa		130 ± 22.6	1.68 ± 0.28	3.60 ± 0.72	7.03 ± 0.75	0.65 ± 0.17	16.0 ± 2.08	4.21± 0.24
	n	7	7	7	9	9	7	5
East		75.0 ± 4.58	2.02 ± 0.37	1.96 ± 0.20	2.87 ± 0.32	0.45 ± 0.06	9.67 ± 0.78	2.11± 0.64
	n	7	10	10	11	11	7	6
South		127 ± 2.59	1.00 ± 0.17	1.75 ± 0.11	8.98 ± 1.51	0.58 ± 0.09	16.4 ± 1.06	7.62 ±1.51
	n	10	10	10	10	13	10	7
Miwaleni		33.4 ± 9.64	1.18 ± 0.37	1.36 ± 0.46	0.73 ±0.12	0.13 ± 0.05	4.21 ± 1.03	0.64 ± 0.03
	n	7	7	7	9	9	7	5
Kahe		145 ± 13.9	0.49 ± 0.14	0.34 ± 0.09	11.5 ± 0.80	0.48 ± 0.07	18.6 ± 1.75	25.4 ± 3.44
	n	21	21	21	27	27	21	15

To manage the water and salt balance, the estate is currently using drains in some areas and there are a number of piezometers spread throughout the estate to record water table height. Monitoring the water table height and the quality of the soil water is important so that salinity caused by capillary rise can be assessed (Leroy, 2004). A salinity/sodicity reclamation trial under both furrow and overhead irrigation was set-up in 2001 in an affected field (11E) and consists of subsurface drains and the use of ameliorants (Brogna, 2004).

Sugarcane requires between 1 100 and 2 000 mm of water per annum and therefore irrigation at TPC is necessary (Brogna, 2004). Given the long history of sodicity/salinity problems and the economic considerations, it is imperative that optimal irrigation management is achieved by understanding the effect of these soils' unique properties on soil hydraulic behaviour.

CHAPTER 3
THE INFLUENCE OF MINERALOGY ON THE PHYSICAL AND CHEMICAL PROPERTIES OF ANDISOLS AND SOILS WITH ANDIC PROPERTIES

3.1 Introduction

The clay sized fraction of soil (< 2 µm) is comprised primarily of phyllosilicates, which largely control the physical and chemical properties of the soil due to their small particle size, high specific surface areas and cation exchange properties (Schulze, 2002). However, clay minerals vary both in their physical and chemical properties due to differences in degree of 'crystallinity' (short range vs. long range order) and chemical composition.

Most minerals have a long-range structure (a regular repeating of structural units that extends from a few hundred nanometres to millimetres) but some minerals have a short-range structure (regular repeating of structural units extends over only a few nanometres). The long-range order minerals have been referred to as crystalline and the short-range order (SRO) minerals as amorphous or poorly crystalline (Amonette, 2002). Usually X-ray diffraction (XRD) provides sufficient information for the general identification of minerals with long-range order but other analytical techniques may be used for confirmation (Amonette, 2002). Also the presence of amorphous substances which cannot be detected by XRD requires the use of other methodologies. Transmission electron microscopy (TEM) is a useful technique for imaging clay sized minerals and obtaining elemental composition and structural information as the wavelength used in TEM is 400 x shorter than that used for XRD (Amonette, 2002).

Many of the basic influences of mineralogy on soil properties are well-known and thus this literature review will focus on the effect of the minerals common in poorly crystalline clays that tend to typify andic soils and soils with some andic characteristics. Identifying mineral types and quantities, and examining the changes in soil properties as influenced by volcanically derived clay minerals, can greatly aid in the classification and agronomic

management of soils in volcanic regions (Whittig and Allardice, 1986; Amonette, 2002; Hepper *et al*., 2006).

3.2 Volcanic ash soils

Volcanic ash soils (VAS) are distributed over approximately 0.84 % of the Earth's surface (Shoji *et al*., 1993; Drouza *et al*., 2007) and cover approximately 124 million hectares (Shoji *et al*., 1993; Tsai *et al*., 2010). Volcanic ash soils are commonly, but not always, represented by the term Andisols (Shoji *et al*., 1993). Ndayiragije and Delvaux (2003) described the formation of Andisols as the rapid weathering of porous, permeable, fine-grained parent material, containing glass and microlites, in the presence of organic matter. Consequently, VAS are generally rich in organic matter (15 – 30 % in the A horizon; Velde and Barré, 2010) and contain active (often amorphous or poorly crystalline) forms of Al and Fe (Shoji *et al*., 1993; Fontes *et al*., 2004).

The main contributors to the amorphous materials in soil are allophane, imogolite and ferrihydrite which are measured by extracting Al, Fe and Si from the soil using acid ammonium oxalate (Al_o, Fe_o and Si_o) (Armas-Espinel *et al*., 2003). The allophane content of a soil can be estimated using selective dissolution methods with extracting solutions of sodium pyrophosphate and acid ammonium oxalate. The assumption is that sodium pyrophosphate only removes organically bound Al (Al_p) and the acid oxalate removes the organically bound and the SRO Si and Al (Si_o and Al_o). The Si/Al ratio and Si_o can be used to calculate the percentage of allophane (Si_o/ (-0.067Al/Si + 0.27)), where the Si/Al ratio of allophane and imogolite = Si_o/ ($Al_o - Al_p$) (Harsh *et al*., 2002).

The discovery, characterisation, and significance of non-crystalline colloidal materials and SRO clay minerals, such as imogolite, allophane, laminar opaline silica, ferrihydrite and Al- and Fe-humus complexes, owe their recognition to the intensive studies of VAS and efforts to classify these soils (Shoji *et al*., 1993). Andisols must have a defining bulk density (ρb) that is ≤ 0.9 g cm^{-3} (Armas-Espinel *et al*., 2003) and exhibit andic or vitric soil properties (Andic = $Al_o + {}^1/_2\ Fe_o \geq 2$ % and P retention ≥ 85 %; Vitric = $Al_o + {}^1/_2\ Fe_o \geq 0.4$ % and P retention $\geq$ 25 %) (Drouza *et al*., 2007). Armas-Espinel *et al*. (2003) reported that ρb increased and the percentage of $Al_o + {}^1/_2\ Fe_o$ and P retention decreased with a decrease in andic characteristics.

These authors report that although the soils in their study did not meet the criteria to be classified as Andisols, soils 1 – 4 in Table 3.1, have values which are very near the threshold values.

Table 3.1: Bulk density (ρb), Al_o + ½ Fe_o percentage and phosphorus (P) retention for five soils from Tenerife with decreasing andic characteristics. Soils (0 = reference Andisol, 1 to 5 = cultivated volcanic soils) numbered according to their decreasing andic character: 0>1>2≈3≈4>5 (modified from Armas-Espinel *et al*., 2003).

Soil	ρb (g cm^{-3})	Al_o + ½ Fe_o (%)	P retention (%)
0	0.58 ± 0.07	8.6 ± 0.2	96.4 ± 0.2
1	0.82 ± 0.02	4.1 ± 0.3	80.9 ± 2.4
2	0.96 ± 0.02	2.1 ± 0.1	74.2 ± 1.0
3	0.99 ± 0.03	2.4 ± 0.2	62.5 ± 1.2
4	1.07 ± 0.04	2.2 ± 0.2	68.9 ± 5.4
5	1.11 ± 0.03	0.8 ± 0.04	20.0 ± 2.0

Soils influenced by volcanic ash, even if they do not meet all the criteria to be classified as Andisols, often have unique morphological, physical and chemical properties due to the formation of poorly crystalline and non-crystalline minerals that are commonly products of volcanic ash weathering (Shoji *et al*., 1993; Tsai *et al*., 2010). Understanding the unique properties of soils influenced by volcanic ash allows improved management of these soils which aids in maximising soil productivity while minimising degradation (Shoji *et al*., 1993).

3.2.1 Mineralogy of volcanic ash soils

Volcanic ash is dominated by volcanic glass which is amorphous in nature and weathers rapidly. This rapid weathering releases elements faster than crystalline minerals can form and therefore the soil solution is often over-saturated with Al and Si. These precipitate as poorly ordered solid phase minerals (Shoji *et al*., 1993; Harsh *et al*., 2002), resulting in VAS having a unique assembly of clay size minerals (commonly, allophane and imogolite) (Shoji *et al*., 1993; Harsh *et al*., 2002; Drouza *et al*., 2007). Hepper *et al*. (2006) studied the loess soils of the semi-arid Argentinean Pampas, which contain variable amounts of volcanic ash, and found that the clay fraction is dominated by illite in ash-free soils, whereas ash-enriched soils

are dominated by amorphous minerals and poorly crystalline montmorillonite. Similarly, the fine clay fraction was found to be dominated by illite and illite-smectite intergrades in the ash-free soils, while ash-enriched soils were dominated by amorphous minerals.

Under high rainfall and well-drained conditions, Si is quickly leached resulting in low soluble Si concentrations and the formation of allophane (Broquen *et al*., 2005). When present, imogolite is often found with allophane, but in smaller amounts (Harsh *et al*., 2002). Allophane and imogolite are poorly crystalline hydrous aluminosilicates (Harsh *et al*., 2002; Fontes *et al*., 2004) and are characterised by their small particle size, high specific surface area (SSA) and their permanent and/or variable charge (Harsh *et al*., 2002). Allophane consists of hollow, irregularly-shaped particles with outside diameters of 3.5 to 5 nm and a wall thickness of 0.7 to 1 nm (Shoji *et al*., 1993). Allophane has broad XRD peaks at 0.33 and 0.25 nm (Figure 3.1) due to poor crystallinity and variations in shape and size of particles (Harsh *et al*., 2002).

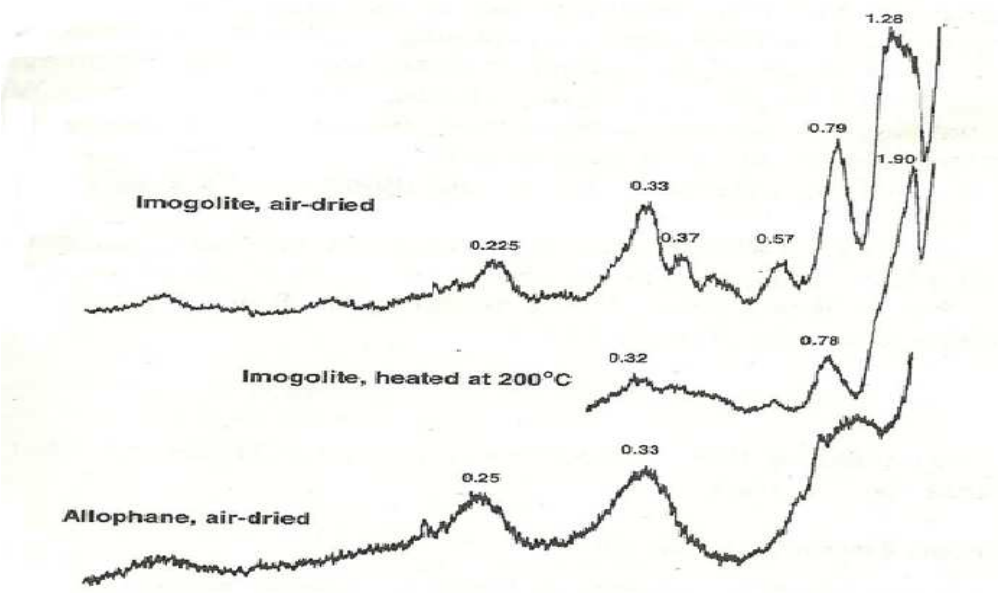

Figure 3.1: X-ray diffraction patterns of naturally occurring imogolite and allophane (Wilson, 1987; cited by Harsh *et al*., 2002).

Imogolite can have medium and long-range structure, as well as short-range structure. Imogolite consists of closely packed bundles of hollow fibres, usually several micrometres in length and approximately 2 nanometres in diameter (Shoji *et al*., 1993; Harsh *et al*., 2002). The large SSA of allophane and imogolite mean that these minerals dominate the soil

properties even if only small amounts are present (Kaufhold *et al*., 2010). The typical SSA measured by ethylene glycol monoethyl ether adsorption for allophane, ranges between 400 and 600 m^2 g^{-1} and between 70 and 170 m^2 g^{-1} for nitrogen adsorption using the Brunauer, Emmett, and Teller Equation (BET) (Paterson, 1977).

Soil pH is a critical factor in the formation of allophane (Drouza *et al.*, 2007). Between pH values of 5 and 7, the formation of allophane increases with increasing pH and free Al and Fe form allophane, imogolite and crystalline phyllosilicate minerals (Drouza *et al.*, 2007). However, in soils with high organic matter content and a pH (H_2O) < 5, Al- and Fe-humus complexes form, lowering the Al activity and inhibiting the formation of allophane and imogolite. This is known as the "anti-allophanic effect" (Shoji *et al*., 1993; Broquen *et al*., 2005; Drouza *et al.*, 2007). The excess Si precipitates as opaline silica (Shoji *et al*., 1993). As a consequence of metal-humus formation the A horizons of VAS are often characterised by accumulation of organic matter, organic matter stabilisation of active Al and Fe, carbonic acid weathering and formation of laminar opaline silica rather than allophane (Shoji *et al*., 1993; Harsh *et al*., 2002). However, the surface soil properties often represent those of allophanic soils, such as low ρb, high extractable Al, low pH and high WHC (Harsh *et al*., 2002). Ndayiragije and Delvaux (2003), estimated the allophane content at 3 % in the A horizon and 26 % in the B horizon of an Andisol from the island of Barra-Terre, which suggests Al is incorporated in Al-humus complexes in the A horizon (anti-allophanic effect). In contrast, a study carried out on the VAS of the Andinopatogonian region, in the province of Neuquén, Argentine, showed that the content of allophane was highest where the level of OC was highest, indicating that Al-humate formation had not prevented allophane formation (Broquen *et al*., 2005).

Under conditions where weathering is slow, the amount of Si and Al in the soil solution is usually insufficient to form allophane. A study in the dry Mediterranean Nisyros region of Greece by Drouza *et al*. (2007) found no allophane or ferrihydrite formation, low P-retention and no active forms of Al and Fe in a volcanic soil. This was attributed to slow weathering rates and low OM content resulting from the low precipitation and a long dry season. Similarly, Hepper *et al*. (2006) suggest the slow weathering rate of a recently deposited volcanic ash in the semi-arid Argentinean Pampas as the cause for the majority of the amorphous materials consisting of Al and Fe oxides and the absence of allophane.

In some soils under a drier climate, and where there is high soluble Si, halloysite forms preferentially in place of allophane and imogolite (Shoji *et al*., 1993; Harsh *et al*., 2002; Ndayiragije and Delvaux, 2003). Soil solution Si concentrations of less than $10^{-3.45}$ M favours Al-rich allophane, whereas a greater soil solution Si concentration favours halloysite formation. In soils from the volcanic region of Tenerife, Canary Islands, with characteristics that are near those needed to be classified as Andisols, the dominant phyllosilicate is halloysite (Armas-Espinel *et al*., 2003). In xeric environments with seasonal rainfall, the wet/dry fluctuations can allow halloysite to co-exist with allophane and imogolite as there are periods where there is more and periods where there is less silica (Harsh *et al*., 2002). The shape of halloysite is related to its genesis. Spheroidal halloysite tends to form from volcanic glass, while tubular halloysite tends to form from more crystalline minerals such as mica and feldspars (Adamo *et al*., 2001; Singer *et al*., 2004). There is speculation as to whether the SiO_2/Al_2O_3 ratio affects halloysite shape; however, the different results reported in the literature are insufficient to warrant structural interpretations (Singer *et al*., 2004).

As weathering proceeds, the silica content diminishes as the quantity of glass is depleted. This results in the formation of more stable, crystalline aluminosilicates and Al- or Fe-oxide minerals (Shoji *et al*., 1993; Harsh *et al*., 2002). In young volcanic ash soils, the soil is dominated by allophane and imogolite, with an Al:Si ratio of about 2. As weathering proceeds, the minerals which dominate in the initial weathering phase (i.e. allophane, imogolite, opaline silica and ferrihydrite) are transformed to halloysite or are the end-product if they are preserved as buried deposits. In older volcanic soils, gibbsite and goethite tend to accumulate (Nieuwenhuyse *et al*., 2000). Gibbsite often forms under conditions where there is strong leaching (Harsh *et al*., 2002; Watanabe *et al*., 2006) and desilication of kaolin (kaolinite and halloysite) or non-crystalline intermediates (Nieuwenhuyse *et al*., 2000; Ndayiragije and Delvaux, 2003). Gibbsite may also form directly from volcanic minerals, especially in permeable parent materials under high rainfall as formation of Al-silicates is prevented due to low silica concentrations. With soil age, iron compounds accumulate and poorly crystalline forms (i.e. ferrihydrite) transform into more stable minerals (Nieuwenhuyse *et al*., 2000). Egli *et al*. (2008) studied soils around the Mt. Etna volcano in southern Italy and found that the main mineral transformation was from volcanic glass to imogolite-like allophanes, then halloysite, followed by kaolinite.

The nature of the parent material (i.e. rock type and particle size) significantly determines the rate of weathering, the pH and the type of minerals which form (Shoji *et al*., 1993). Silica content increases in the order: basalt < andesite < dacite < rhyolite. Soils derived from low Si parent material tend to have lower Si in the soil solution. Allophane can form from biotite and feldspar but feldspar only weathers rapidly enough to form SRO clays at a pH below 5. However, allophane does not form easily below a pH of 4.8, thus the band for allophane formation is narrow where feldspar is dominant (Harsh *et al*., 2002). X-ray diffractograms of the silt fraction of soils from humid regions of Asia indicate that mica is absent when the parent material is andesitic or mafic, but is present when the parent material is sedimentary or felsic igneous rock (granite or rhyolite). When mica is present in the silt fraction then it is also present in the clay fraction together with vermiculite and hydroxyl interlayered vermiculite (HIV) (Watanabe *et al*., 2006). Volcanic ash parent material usually contains a few minerals (i.e. chlorite and mica) that can weather directly to 2:1 and 1:1 phyllosilicates. Volcanic ash may also contain accessory minerals formed by weathering and/or hydrothermal alteration of materials comprising the cone of the volcano (i.e. opal, cristobalite, kaolinite, allophane, halloysite, smectite and interstratified layer silicates) (Shoji *et al*., 1993).

The presence of 2:1 and hydroxyl-Al-interlayered 2:1 silicate minerals in volcanic soils may be from a) inheritance from the primary minerals in the parent material through hydrothermal processes (Nieuwenhuyse *et al*., 2000; Ndayiragije and Delvaux, 2003; Egli *et al*., 2008); b) an aeolian deposit or weathered products of an aeolian deposit (Ndayiragije and Delvaux, 2003; Egli *et al*., 2008); c) incorporation of lithic fragments into tephra during eruption; and d) neoformation in specific micro-environments (Ndayiragije and Delvaux, 2003). Watanabe *et al*. (2006) attributed the dominance of smectite in the silt fraction to inheritance from parent rocks. In “gibbsitic” Andisols, there are often hydroxyl-Al-interlayered 2:1 clay minerals due to incorporation into tephra during eruption or as a result of pedogenic Al interlayering of inherited 2:1 clay minerals (Ndayiragije and Delvaux, 2003). In a study of the mineralogical evolution of a dated chronosequence of three soils on an andesitic lava in perudic tropical Costa Rica, the soil on the youngest lava (2 000 years old) was dominated by non-crystalline material throughout the profile. This soil has a low ρb, Al_o, Fe_o, Si_o, Al_p, Fe_p, and high P-retention and pH-NaF values, an Al:Si ratio > 2 and Al- and Fe-humus complexes dominating the secondary minerals. A greater percentage of allophane in the B horizon

compared to the A horizon indicates that much of the Si was released from the primary minerals. The soil developed on the second oldest lava (18 190 years old) consists of mainly non-crystalline material, and allophane and imogolite are present. There is also some gibbsite due to desilication of allophane and imogolite with weathering. This soil has a high P-retention, pH-NaF, and Al_o, Fe_o, Si_o content in A and B horizons, and high Al_p and Fe_p in the A horizon (indicating dominance of non-crystalline material). Low allophane content in the A horizon of soils developed on the two youngest lava flows may be due to the anti-allophanic effect. Micromorphological data and low Al_o, Fe_o, Si_o values in the oldest lava indicate absence of non-crystalline material and Al- and Fe-humus complexes.

3.2.2 Physical properties of volcanic ash soils

3.2.2.1 Structure and water retention

Porosity and pore size distribution (which determine the soil physical properties) are dependent on the development of soil structure (Nanzyo *et al*., 1993). Ideally, soil aggregates should possess pores that are larger than 75 µm and pores which are between 30 and 0.2 µm, to hold capillary water (Velde and Barré, 2010). Large pores between the soil aggregates allow rapid infiltration of water as well as free drainage so that the soil remains aerobic (Velde and Barré, 2010). Allophanes, Fe- and Al-oxyhydroxides (e.g. ferrihydrite) and high OM, which are commonly present in soils from volcanic regions, induce strong aggregation (Nanzyo *et al*., 1993; Armas-Espinel *et al*., 2003; Velde and Barré, 2010). Consequently, Andisols tend to have a well-developed structure and contain an abundance of inter- and intra-particle pores which allows for high porosity and large amounts of water to be retained at various matric potentials (Nanzyo *et al*., 1993; Armas-Espinel *et al*., 2003; Fontes *et al*., 2004). Furthermore, the presence of allophane contributes to high water retention due to its small particle size and hollow spheroidal structure (Gama-Castro *et al*., 2000; Tsai *et al*., 2010). Armas-Espinel *et al*. (2003) found that the gravimetric water content at various matric potentials decreased as the soil andic character decreased (Figure 3.2).

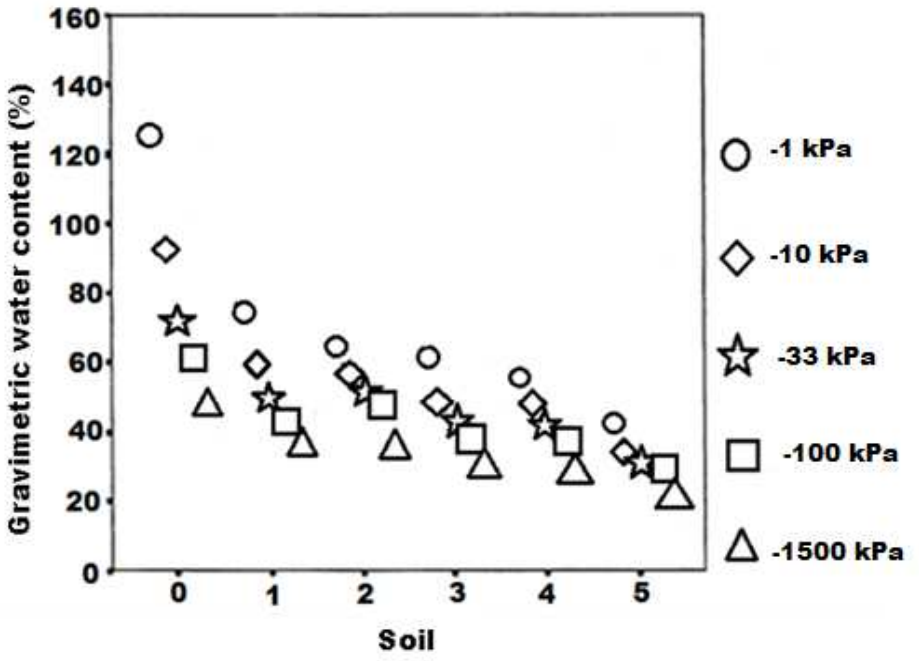

Figure 3.2: Gravimetric water content at -1, -10, -33, -100 and -1500 kPa matric potential for an Andisol (numbered 0) and cultivated volcanic soils (numbered 1 to 5 according to their decreasing andic character: 0>1>2≈3≈4>5) (modified from Armas-Espinel *et al*., 2003).

Similarly, Tsai *et al*. (2010) found that as the andic properties of soils from the Tatun Volcanic Group in Taiwan increased, the water retention at -33 kPa and -1500 kPa increased. A positive correlation between allophane and water retention at -1500 kPa was found ($r = 0.27$, $p < 0.05$) (Tsai *et al*., 2010). Studies from the eastern Hokkaido region on allophanic Andisols (Ito *et al*., 1991) obtained a relationship between water retention at -1500 kPa and the concentration of non-crystalline materials and organic matter as follows:

-1500 kPa water retention of undried samples (%)

$$= 1.93\,(1.7 \times \text{organic carbon (\%)}) + 1.47\,(8 \times Si_o\ (\%)) + (2 \times Fe_o\ (\%)) - 0.92.$$

The strong correlation ($r = 0.944$, $n = 37$) indicates that both allophanic clays and humus contribute to the water retention at -1500 kPa (Shoji *et al*., 1993). Armas-Espinel *et al*. (2003) found that the water retention at -1500 kPa to clay ratio to be higher as soils increased in andic character, indicating that the SRO minerals are contributing more to water retention at -1500 kPa than the amount of clay.

Andisols can hold more than 30 % plant available water (PAW) by volume. Plant available water is held primarily by the meso-pores and is defined as the water content between field capacity and wilting point (Nanzyo *et al*., 1993).

Armas-Espinel *et al*. (2003) reported a significant and linear relationship between gravimetric water content and Al_o at low to intermediate matric potentials. The lack of the same trend between Al_o and the higher gravimetric water contents was reported by Dorel *et al*. (2000) to be a consequence of OM contributing to the macro-porosity. However, the volcanic soils studied by Armas-Espinel *et al*. (2003) had low contents of OM and this was suggested by the authors as an unlikely source of increased macro-porosity.

Water retention in VAS shows strong hysteresis with drying due to allophanic clays (Nanzyo *et al*., 1993). In the study by Armas-Espinel *et al*. (2003) the gravimetric water content at all matric potentials was lower than that predicted by the Al_o values and was thought to be a consequence of the soil drying out during transport and/or land preparation which caused an irreversible loss of water retention capacity. It is postulated that much of this water is contained within the micro-spheres of allophane and once dry these spheres collapse and they are unable to be re-hydrated to their original size (Neall, 2009).

3.2.2.2 Infiltration rate and hydraulic conductivity

Infiltration rate and hydraulic conductivity are dependent on the number, size distribution and continuity of pores, which are a function of texture and structure, as well as initial soil water content, vegetation cover and topography (Levy, 1988; Bamutaze *et al*., 2010).

The infiltration and saturated and unsaturated hydraulic conductivity (K_s) of Andisols is generally high due to the low ρb and highly stable aggregates which form a granular structure (Harsh *et al*., 2002; Jordán, *et al*., 2009). Armas-Espinel *et al*. (2003) found that the K_s was higher in allophanic soils than crystalline clay soils (Table 3.2).

Table 3.2: Frequency of hydraulic conductivity classes for the studied soils (0 = reference Andisol, 1 – 5 = cultivated volcanic soils, numbered according to decreasing andic character 0>1>2≈3≈4>5). n = number of samples (modified from Armas-Espinel *et al*., 2003).

Soil	0	1	2	3	4	5
n	3	19	9	4	6	8
Very low (< 8 mm hr^{-1})	-	5 %	44 %	-	-	-
Low (8 – 20 mm hr^{-1})	-	5 %	-	-	17 %	13 %
Moderate (20 – 60 mm hr^{-1})	-	56 %	22 %	-	-	13 %
Moderately (60 – 80 mm hr^{-1})	-	11 %	11 %	-	-	-
Rapid (80 – 125 mm hr^{-1})	-	11 %	22 %	-	-	13 %
Very rapid (>125 mm hr^{-1})	100%	42 %	-	100 %	83 %	63 %

Another important factor influencing infiltration rate and hydraulic conductivity is soil sodicity. A high ESP leads to aggregate breakdown (slaking) and clay dispersion, which in turn results in the clogging of soil pores and the formation of surface seals and crusts (Levy, 1988; Jalali *et al*., 2008). Results on four South African soils, differing in clay mineralogy, indicate that crusting becomes more pronounced with an increase in ESP (Levy, 1988). An increase in the ESP results in greater swelling, particle dispersion and slaking which tend to reduce the porosity and changes the pore size distribution (Levy, 1988). The results of Elgabaly and Elghamry (1970) and Frenkel *et al*. (1978) show that high levels of exchangeable sodium adversely affect the hydraulic conductivity of kaolinitic soils, where an ESP > 10 significantly reduces the hydraulic conductivity (Levy, 1988). Levy (1988) used scanning electron microscope (SEM) micrographs to view the surface of crusts after final infiltration rate (FIR) was reached on a soil treated with solutions with an ESP value of 1 (low) and an ESP value of 15 (high) and found that at the higher ESP value there were more loose clay particles (i.e. clay dispersion) and a lower FIR than at the lower ESP value. These

results were attributed to the lower aggregate stability of the soil at a higher ESP, which results in the clogging of soil pores by dispersed clay particles. Similar results were found by Gal *et al*. (1984) where SEM micrographs show that at a low ESP the soil crust consists of a thin upper skin, whereas at a higher ESP there is an upper skin as well as a "washed in" layer where dispersed clay particles have clogged conducting soil pores.

The strong cementing action of the Al and Fe in volcanic soils may maintain a relatively high hydraulic conductivity due to the formation of stable aggregates even under conditions of high ESP and low salt concentrations (Levy, 1988). Armas-Espinel *et al*. (2003) report that when Al_o values are lower than 3 %, the hydraulic conductivity is very low due to the aggregating effect of allophane not being able to counterbalance the structural deterioration of clay minerals caused by high sodium content.

The variable charge nature of allophane may result in colloidal dispersion at pH values several units removed from the point of zero charge (Harsh *et al*., 2002). Nakagawa and Ishiguro (1994) found that the K_s of an allophanic Andisol was highest at pH 6 and decreased by 93 and 75 % when the pH was changed to 3 and 11, respectively. The dispersion of positively charged (pH 3) and negatively charged (pH 11) colloids disrupts the soil aggregates and leads to clogging of soil pores.

3.2.3 Chemical properties of volcanic ash soils

3.2.3.1 Cation exchange capacity, anion exchange capacity and specific surface area

The weathering of primary minerals inherited from parent material results in secondary minerals which can either have a high or a low activity. High activity minerals form under less well weathered conditions and are characterised by a high CEC and large surface area (smectites, vermiculite, illite and mica). Low activity minerals form under strongly weathered conditions and have a low CEC and surface area, and may also have an anion exchange capacity (Table 3.3) (Brady and Weil, 2002).

Table 3.3: Cation exchange capacity (CEC) and surface area of common soil minerals (adapted from Brady and Weil, 2002).

Mineral	Type	CEC ($cmol_c\ kg^{-1}$)*	Surface area ($m^2\ g^{-1}$)
Smectite	High activity clay	-80 to -150	80 to 150
Vermiculite	High activity clay	-100 to -200	70 to 120
Fine mica	High activity clay	-10 to -40	70 to 175
Chlorite	High activity clay	-10 to -40	70 to 100
Kaolinite	Low activity clay	-1 to - 15	5 to 30
Gibbsite	Al-oxide	+10 to -5	80 to 200
Goethite	Fe-oxide	+20 to -5	100 to 300
Allophane	Amorphous	+10 to -150	100 to 1000
Humus	Organic	-100 to -500	Variable

**Negative signs indicate cation exchange capacity, while positive sign indicates that the minerals no longer exhibit a cation exchange capacity, but rather an anion exchange capacity.*

Cation exchange capacity is the soil's ability to attract, retain and supply nutrients (positively charged cations) and generally increases with increasing content of fine particles, amount of 2:1 clay minerals and content of soil organic matter (Hepper *et al*., 2006). Curtin and Smillie (1976) found that the CEC in Irish soils, developed on a wide range of parent materials, is significantly correlated to the OM and fine clay content. In the semi-arid Argentinean Pampas the CEC is highly influenced by the silt fraction as it contains high amounts of 2:1 minerals, mainly illites (Hepper *et al*., 2006). Cation exchange capacity is also influenced by amorphous minerals in the soil. Hepper *et al*. (2006) found that illitic soil with a low OM content had the lowest CEC while the highest CEC corresponded to ash-enriched soil with a high silt and clay content and high SSA. The mean CEC of ash-enriched soils was significantly ($p < 0.05$) higher than the mean CEC of illitic soils at any given clay content (Figure 3.3), suggesting amorphous minerals contribute more to CEC than illites.

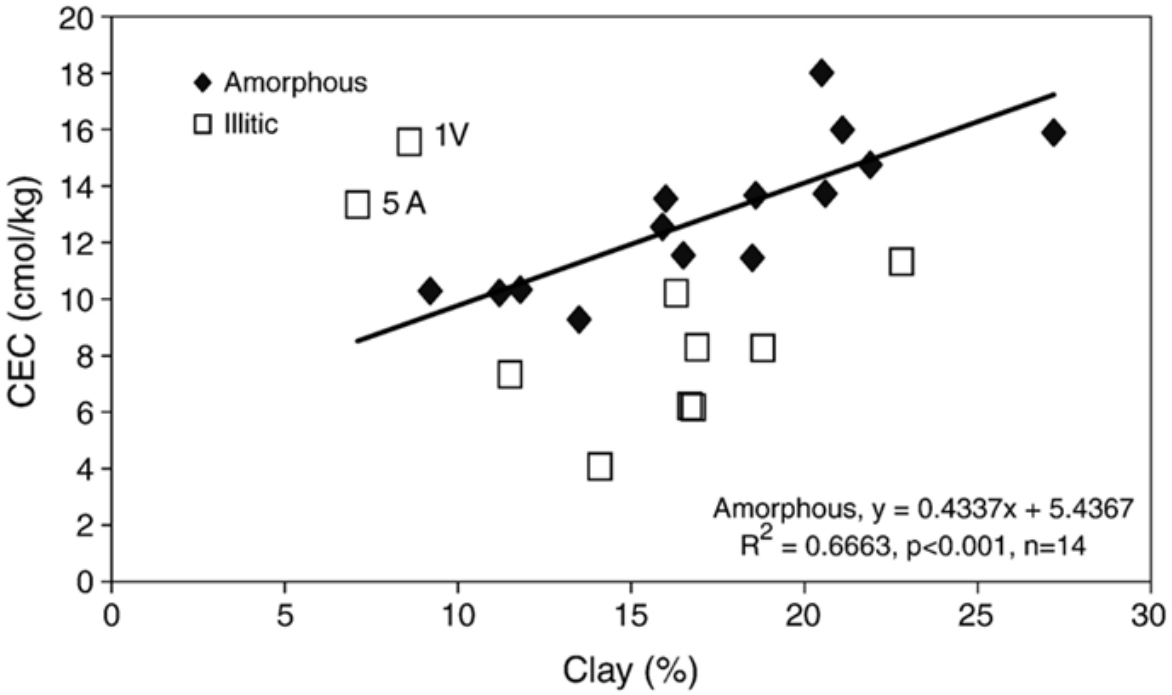

Figure 3.3: Cation exchange capacity and clay contents in soils dominated by illitic and amorphous clay minerals (1V indicates the soil of site 1 under virgin conditions, 5A indicates the soil of site 5 under agricultural conditions) (Hepper *et al*., 2006).

In the study by Hepper *et al*. (2006), sites 1V and 5A were the only soils found where the CEC was higher than that expected for the measured clay content (Figure 3.3) and is expected to be a consequence of Site 1V having the highest OM content and site 5A having an extremely high montmorillonite content (70 %). Therefore, in soils dominated by amorphous materials the CEC depends more on inorganic colloids, whereas in illitic soils the CEC depends on OM content (Hepper *et al*., 2006). Gama-Castro *et al*. (2000) found that the CEC of alluvial pumiceous soils from the Nayarit region of Mexico increases with the amount of weathered pumice and that CEC is largely controlled by the amount of amorphous material in these soils. Similarly, the CEC of Andisols and related soils from the Azores, Portugal, correlates with the Al_o percentage and OC (Madeira *et al*., 2003), indicating that both organic and amorphous constituents influence CEC. In soils forming on volcanic parent material in the Nisyros region of Greece the CEC range was found to be low (5.5 – 8.1 $cmol_c\ kg^{-1}$) and is attributed to the low OM content and slow weathering rates which prevent the formation of non-crystalline minerals (Drouza *et al*., 2007).

3.3 Conclusions

Minerals common in volcanic ash primarily have a short-range structure and include allophane, imogolite, laminar opaline silica, ferrihydrite and Al- and Fe-humus complexes (Shoji *et al*., 2003). These volcanically derived minerals have a substantial influence on the morphological, physical and chemical properties of soils (Shoji *et al*., 2003; Tsai *et al*., 2010). An increase in andic character is associated with a decrease in ρb and an increase in the percentage of Al_o + ½ Fe_o and P retention (Armas-Espinel *et al*., 2003). The rapid weathering of volcanic glass in volcanic ash results in an over-saturation of Al and Si which precipitate as poorly ordered minerals, such as allophane and imogolite (Harsh *et al*., 2002). The small particle size and hollow structure of allophane, results in soils having a very large CEC and SSA (Harsh *et al*., 2002).

The specific mineralogy resulting from the weathering of volcanic ash is dependent on a number of variables such as pH, organic matter content, rate and extent of weathering and parent material. A high OM content in low pH soils (< 5) can result in the "anti-allophanic effect" which prevents the formation of allophane and imogolite and results in the dominance of opaline silica and Fe- and Al-humus complexes (Harsh *et al*., 2002; Shoji *et al*., 2003). In environments with annual precipitation of less than 1 700 mm (Prado *et al*., 2007) halloysite generally forms preferentially to allophane and imogolite (Harsh *et al*., 2002; Shoji *et al*., 2003; Ndayiragije and Delvaux, 2003). As weathering proceeds more stable, crystalline minerals and Al- and Fe-oxide minerals form (Harsh *et al*., 2002; Shoji *et al*., 2003), and the general weathering sequence is from volcanic glass to allophane and imogolite, then halloysite, followed by kaolinite (Egli *et al*., 2008). The parent material also affects mineralogy as determined by the silica content and inherited minerals which weather directly to 2:1 and 1:1 layer silicates (i.e. chlorite and mica) (Shoji *et al*., 2003).

Volcanic ash soils generally have good structural properties due to the aggregating effect of allophanes and Fe- and Al-oxides (Nanzyo *et al*., 1993, Armas-Espinel *et al*., 2003; Velde and Barré, 2010). This, together with high surface area induced by the small particle size and hollow structure of allophane, allows VAS to retain a high quantity of water at the various matric potentials (Gama-Castro *et al*., 2000; Tsai *et al*., 2010). Furthermore, the low ρb and

structural stability commonly found in VAS result in high infiltration rates and hydraulic conductivity (Harsh *et al*., 2002; Jordán, *et al*., 2009), although if soils have a high ESP the infiltration rate and hydraulic conductivity can be severely reduced due to soil dispersion and clogging of soil pores (Levy, 1988; Armas-Espinel *et al*., 2003).

CHAPTER 4
MATERIALS AND METHODS

4.1 Field sampling

4.1.1 Field sampling protocol

The TPC sugar estate has been divided into five management areas, namely the north, east, south, west and Kahe. Within these broad areas TPC management selected 21 fields as permanent sampling units (PSUs). A PSU is considered representative of the local area in terms of soil, yield, water source, and other similar attributes. In addition to the 21 PSUs, 49 other fields, four sites outside of the TPC estate and two ash layers were selected for sampling (Appendix 4.1). Bulk soil samples and undisturbed soil cores were collected from the 21 PSUs, 24 additional fields, as well as from the four sites outside the TPC estate. Only bulk soil samples were collected from the remaining 25 additional fields and from the two ash layers found in field R8 (R8 Ash) and in a borehole in the north (BH Ash). Of the 45 fields sampled for both bulk samples and undisturbed soil cores, nine fields were sampled from more than one site indicated by e.g. 'R3S (2.1 etc.)' and seven fields which experience patchy cane growth were chosen to be sampled in a patch of poor growing cane (Bad) and in an adjacent patch of better growing cane (Good). Field infiltration rate was measured in 25 selected fields from where bulk samples and undisturbed soil cores were also collected. The majority of the samples were collected from the inter-rows. Sampling was only done within cane rows either where there was young cane under furrow irrigation where the irrigation furrows are initially made in the same row as the cane or where a field had been recently harvested and thus rows and inter-rows could not be clearly distinguished. The sample points are shown in Appendix 4.2. Samples were collected during two visits to TPC, the first of which was in July 2010 and the second in September 2011 (Appendix 4.1).

4.1.2 Bulk soil samples

Bulk soil samples were collected from the A and B horizons using a spade and hand trowel, air-dried, gently milled by mortar and pestle to pass a 2 mm sieve and stored for further analysis.

4.1.3 Soil cores

Undisturbed soil cores were taken by inserting a labelled stainless steel core ring (50 mm in height and 75 mm in diameter) into the soil using the core sleeve guide. A hammer was used to insert the core to the correct depth. Three undisturbed soil cores were collected from each of the A and B horizons in each field at a single location. The A horizon cores were collected after removing loose material from the soil surface, while a pit was excavated to create a terrace in the B horizon for core sampling. The excess material protruding at the ends of each core after extraction from the soil was removed in-field to permit better packaging. A lid was placed on each end of the soil core that was then wrapped with masking tape. The wrapped soil core was then placed in a plastic bag and wrapped with packaging tape to minimise damage and water loss during transport from TPC to South Africa.

4.1.4 Infiltration measurements

Steady state infiltration measurements were taken at the same locations used for the collection of the soil cores, using the double ring infiltrometer method (Bouwer, 1986). The outer ring was 150 mm in height by 400 mm in diameter and the inner ring was 150 mm in height by 200 mm in diameter.

4.2 Laboratory analysis

4.2.1 Mineralogical properties

4.2.1.1 X-ray diffraction

The mineralogical composition of soils from the PSU's for the clay fraction was characterised using X-ray diffraction (XRD) on oriented specimens. The clay fraction (< 2 μm) was obtained from the soil by using sedimentation flasks and applying Stokes' Law. Prior to preparation of the oriented specimens on glass slides, one third of the separated clay fraction was saturated with Mg^{2+} and one third was saturated with K^{+}. The remaining one third of the separated clay was stored for surface area determination. Three oriented specimen glass slides were then prepared with the Mg-saturated clay and two oriented specimen glass

slides with the K-saturated clay. The three Mg-saturated specimens were air-dried, treated with ethylene glycol at 60 ^{o}C overnight and treated with glycerol at 85 ^{o}C overnight, respectively, and the two K-saturated specimens were air-dried and heated at 550 ^{o}C for four hours, respectively (Bühmann *et al.*, 1985). After the clay was separated by means of the settling flask the remaining fraction (mostly silt and sand) was wet sieved to pass through a 500 µm sieve and the separated sand and silt fractions were collected and dried in an oven for 24 hours before each was analysed as random powder specimens by means of XRD for mineralogical composition. X-ray diffraction analysis was carried out using a Philips X-ray diffractometer with a graphite monochromator at 40 kV and 40 mA. Oriented and random powder specimens were scanned at 1^{o}/min with a step-scan of 0.02^{o} over the 3 to 40^{o} range and 3 to 75^{o} range, respectively.

4.2.1.2 Transmission electron microscopy

After XRD analysis was carried out on the clay fraction, 31 of these clay fraction samples from 12 fields (representing the 5 areas across the estate) and the two ash layers were selected for transmission electron microscopy (TEM) (JEOL 1400) viewing in order to further investigate clay type, size and shape.

4.2.2 Physical properties

4.2.2.1 Water retention characteristics, saturated hydraulic conductivity and bulk density

The undisturbed soil cores were prepared and analysed for water retentivity characteristics, saturated hydraulic conductivity (K_s) and bulk density (ρb) on the same sample core using the method of Moodley *et al*. (2004). In brief, the method involves placing a pre-weighed piece of nylon cloth and elastic band onto the lower end of a soil core that has been trimmed level with the upper and lower surface of the ring. The core was then slowly saturated by capillary water movement to saturate the micro-pores and then by flooding to saturate the larger pores. Immediately after complete saturation the cores were weighed to obtain saturated water content. The cores were then placed on a tension table (sand bath construction; Avery and Bascomb, 1974) using a continuous hanging water column to achieve a matric potential of -1 kPa. The cores were allowed to equilibrate to constant mass before being re-weighed and returned to the tension table. The hanging water column was then lowered to achieve a matric

potential of -2 kPa. This process was repeated for matric potentials of -4, -6, -8 and -10 kPa. The cores were then transferred to ceramic pressure plates in a pressure chamber apparatus. The cores were equilibrated at matric pressures equivalent to -33 and -100 kPa and weighed at each respective pressure once constant mass was reached. The cores were then oven-dried at 105 ^{o}C for 48 hours to determine ρb and mass moisture content of the soil for each respective matric potential. The mass moisture content was converted to volumetric water content as follows:

$$\frac{\text{Gravimetric water content x Bulk density}}{\text{Water density}} \quad (m^3\ m^{-3}) \qquad \text{(Equation 4.1)}$$

where the density of water is taken as 998 kg m^{-3}.

Wilting point moisture content was determined at -1500 kPa in a high pressure chamber apparatus using re-packed samples. Rings (10 mm height x 50 mm diameter) were filled with loosely packed soil (< 2 mm) and saturated by capillary wetting overnight. The rings were then placed in the pressure chamber and allowed to equilibrate for approximately 2 weeks until constant mass was reached. After removal from the pressure chamber the mass moisture content of the soil was determined by oven drying at 105 ^{o}C for 24 hours. The mass moisture content of the soil was converted to volumetric water content using Equation 4.1, where the bulk density used was calculated from the repacked rings.

Prior to oven-drying the soil cores (and directly after the soil retentivity measurements), the K_s was determined using the method of Moodley *et al*. (2004). This required taping a second empty core ring to the top of the soil core to increase the length and re-saturating the core. The core was then placed on a steel mesh held inside a funnel and K_s measured by the constant head method (Klute and Dirksen, 1986). The K_s was calculated using Darcy's equation for saturated flow under constant head conditions as follows:

$$K_s = ((V / (A \times t)) \times (L / \Delta H)) \times 10 \ (\text{mm hr}^{-1}) \qquad \text{(Equation 4.2)}$$

where

V = Volume of water in cm^3 collected for a time period of t (hours)

A = cross sectional area of the core (cm^2)

L = Length of soil column (cm)

ΔH = total hydraulic head (cm)

4.2.2.2 Determination of field capacity: Free drainage method

To estimate the likely field capacity of the soils under field conditions, 25 randomly selected cores were re-saturated after the measurement of K_s and then allowed to drain until the core no longer dripped water for a period of 1 hour. This point was reached after approximately 20 hours, suggesting that all free water had drained away and thus the core was assumed to be at its field capacity water retention. The tension at which the free-drainage field capacity was reached could therefore be determined by comparing the weight of the soil in the soil core after 20 hours of drainage against the water retention curve for that soil. For most of the randomly selected cores the tension at which field capacity was reached was at approximately -10 kPa and thus the volumetric water content at -10 kPa is used here to represent field capacity.

4.2.2.3 Particle size distribution

Bulk soil samples were analysed for particle size distribution by the pipette method (Gee and Bauder, 1986) after treatment with Calgon to ensure complete particle dispersion. Due to low levels of organic matter in the analysed soils, organic matter combustion was not preformed before analysis.

4.2.2.4 Specific surface area

Samples from the A and B horizons of seven PSUs (one from each of the north, east and west areas, and two from each of the south area and Kahe) were selected for the determination of specific surface area (SSA) using an ASAP 2010 (Accelerated Surface Area and Porosimetry System) from Micromeritics Instrument Corporation. The surface area was determined on a sample that was first freed of moisture and atmospheric vapors by application of heat and evacuation. The temperature of the sample was then reduced to that of liquid nitrogen and the absorbing gas (nitrogen) was admitted in incremental doses. The accumulated gas quantity adsorbed *vs.* gas pressure data at one temperature was then graphed to generate an adsorption

isotherm and the data was treated in accordance with the Brunauer, Emmett, and Teller Equation (BET) gas adsorption theory to determine SSA (Carter *et al*., 1986).

4.2.3 Chemical properties

4.2.3.1 Organic carbon

Bulk soil samples from the PSUs were analysed for soil organic carbon content by acid dichromate oxidation (Walkley, 1947).

4.2.3.2 Electrical conductivity and pH

Bulk soil samples were analysed for pH (NSAWC, 1990) in water using a soil: solution ratio of 1:2.5 and for electrical conductivity on an aliquot from a saturated paste extraction (Richards, 1954).

4.2.3.3 Extractable silica, aluminium and iron

The soil samples from the PSUs were analysed for extractable silica, aluminium and iron using acid ammonium oxalate (McKeague and Day, 1966) for the amorphously bound fraction, and aluminium and iron using citrate-bicarbonate-dithionite (CBD; Mehra and Jackson, 1960) for the crystalline fraction and sodium pyrophosphate (McKeague, 1967) for the organically bound fraction.

4.2.3.4 Water soluble cations, exchangeable cations and cation exchange capacity

Water soluble cations (Ca, Mg, Na and K) from the PSU samples collected during the July 2010 sampling were extracted from 5 g of soil by adding 20 ml of deionized water, shaking for 15 minutes, centrifuging at 3000 rpm for 10 minutes and filtering through Whatman No. 1 filter paper. This extraction procedure was repeated twice. After filtering it was necessary to use a milli-pore (mesh size: 0.22 µm) to remove suspended particles from the extractant. The concentrations of Ca, Mg, Na and K in the extract were then measured using inductively coupled plasma emission spectrometry (ICP-ES) (Varian 720-ES).

Water soluble Ca, Mg, Na and K were also determined on a saturated paste sample in the TPC laboratory using atomic adsorption spectrophotometry (AAS) (Varian 240-FS) (Richards, 1954).

Exchangeable Ca, Mg, Na and K from the PSU samples collected during the July 2010 sampling were measured by modifying the method of Tan (2005). Exchangeable Ca, Mg, Na and K were extracted from 5 g of soil by adding 20 ml of 0.2 M $BaCl_2$ – TEA (buffered at pH 8.2), shaking for 15 minutes, centrifuging at 3000 rpm for 10 minutes and filtering through Whatman No. 1 filter paper. This extraction procedure was repeated twice and the extractions combined. The concentrations of Ca, Mg, Na and K in the extractant were then measured using ICP-ES.

Cation exchange capacity (CEC) was measured on the same soil sample which had undergone exchangeable cation extraction with the 0.2 M $BaCl_2$ – TEA. After washing twice with 50 % ethanol, 25 ml of 0.3 M $CaCl_2$ was added to the soil sample, shaken for 15 minutes and centrifuged at 3000 rpm for 10 minutes to allow the Ca to exchange the Ba on the exchange sites. This procedure was repeated twice followed by the addition of 30 ml of deionized water to the soil sample. After shaking and centrifuging, the supernatant from the two extractions with $CaCl_2$ and the one extraction with deionized water were combined and the concentration of Ba measured by ICP-ES.

4.3 Statistical analysis

Overall differences between the patches of poorly growing cane (Bad) and patches of better growing cane (Good) were assessed using paired t-tests (GENSTAT, 14th edition). Paired t-tests were performed for matric potentials of 0, -10, -33, -100 and -1500, as well as for readily available water (RAW), plant available water (PAW), soil organic carbon and pH. Paired t-test for other measured variables were not possible due to insufficient number of fields sampled in a good and bad patch for these other variables.

Principal component analysis (CANOCO, version 4.56) was used to assess the relationship between the water retention characteristics with location and their interaction with each other.

Correlation matrices were produced (GENSTAT, 14th edition) between the measures of amorphous minerals in the soil (allophane, ferrihydrite and the $Al_o + {}^1/_2\ Fe_o$ ratio), and the water retention variables (0 kPa, -10 kPa, -33 kPa, -100 kPa, -1500 kPa, PAW and RAW), with the other measured soil properties. Individual correlation matrices between the measured soil properties with the amorphous mineral content and water retention variables were created to maximise the number of observation points before individual correlation matrices were merged into a single table.

CHAPTER 5
RESULTS AND DISCUSSION

5.1 Introduction

The five management areas (north, east, south, west and Kahe) are based on location within the estate for ease of management and not necessarily on any similar properties such as yield, soil characteristics, water source, etc. As such, it was expected that the various areas would have considerable variability between fields in terms of measured properties. However, a comparison between areas in the measured properties is useful to indicate general differences and any trends that may be present from north to south or east to west across the estate. A number of measured soil properties showed north-south and east-west trends in Meyer *et al*. (2009) and therefore it was decided for this study to provide averages of measured properties for the respective areas for purposes of an overall comparison. Any values for a particular property which are relatively high or low with regards to that area's average are discussed and all measured soil properties are provided as Appendices with the results from each sampled site in each field.

5.2 Mineralogical analysis

5.2.1 X-ray diffraction of oriented clay samples

The X-ray diffractograms for all clay samples analysed were very similar. All patterns are weak, indicating poorly crystalline material in the sample, probably as allophane. All samples have kaolin, K-feldspar, illite or an Al hydroxyl interlayed vermiculite (HIV) and a small quantity of hematite. The kaolin is probably present as halloysite, rather than kaolinite, as the 002 reflection is much stronger than the 001 reflection which in most samples has a d-spacing >> 7.03Å, which would represent low defect kaolinite. This together with the broadness of the peaks suggests that there is a high level of disorder within the kaolin mineral. These results are similar to those found previously on samples taken from fields 11F and N83 (*pers. comm.*, Maud[1], 2004). The height of the kaolin and illite peaks differ in the XRD patterns

[1] Maud. R., 2004. Drennan, Maud and Partners.

between clay samples, indicating variable quantities between fields. However, there seems to be no trend for specific areas. 1 Bad, 5^1 and 12C Bad samples also have a small amount of gibbsite present. Samples from field 5^1 also have a small amount of talc present. Calcite is present in samples from fields 10K and R3S.

Similar mineralogy was found in a study on volcanic ash in five pedons in the Matese Massif, southern Italy, which revealed the dominant presence of allophane, as well as unweathered volcanic glass, sanidine (direct from parent material), vermiculite, HIV, mica, kaolinite and a mica-kaolinite intergrade. Gibbsite was also found in the deepest horizons of two pedons which were identified as buried horizons that had undergone more weathering than the overlying horizons (Sellitto *et al*., 2010). Furthermore, three pedons derived from volcanic ash from the Roccamonfina volcano in south-central Italy contained allophane, imogolite and some halloysite and HIV (Vacca *et al*., 2003). A study done on the soils in the woodlands of the Serengeti National Park in Tanzania also reveal the influence of volcanic ash on the soil mineralogy where the dominant minerals are amorphous in nature (Jager, 1982). Funakawa *et al*. (2012) studied the determining factors of soil fertility across Tanzania and found that the soil mineralogy around the town of Moshi had a large amount of amorphous material which was attributed to the volcanic parent material.

The A and B horizons from field 5^1 have been chosen as representative examples of the oriented clay XRD patterns found for the soils analysed from TPC (Figure 5.1). X-ray diffraction patterns for all samples analysed are given in Appendix 5.1.

a)

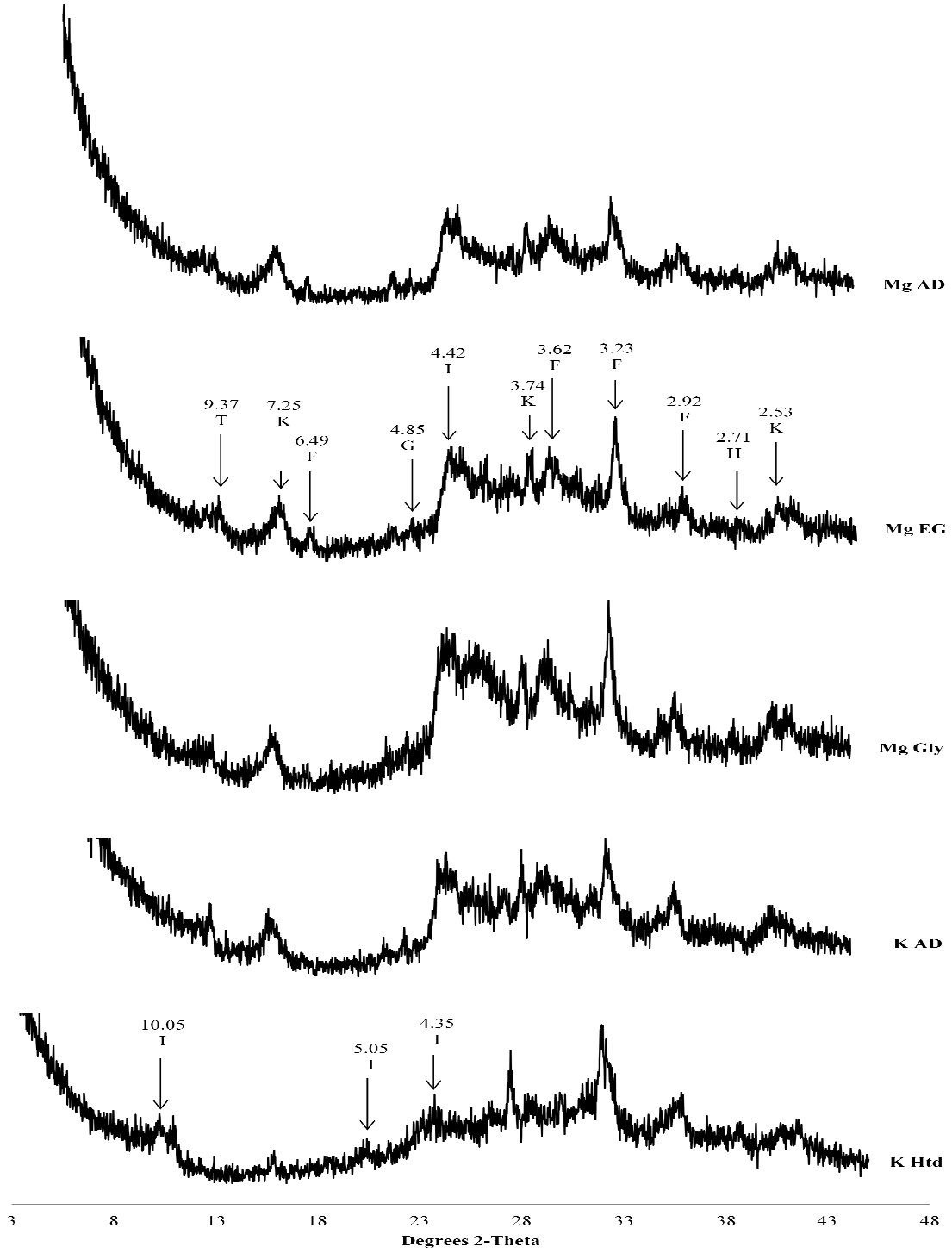

Figure 5.1: X-ray diffraction patterns with labelled peaks (Å) of oriented clay samples treated with magnesium (Mg) and potassium (K) and analysed as air-dry samples (AD), heated at 550^{o}C (Htd) and analysed after treatment with ethylene glycol (EG) and glycerol (Gly) for the (a) A horizon and (b) B horizon from field 5[1]. T - talc, K - kaolin, F - feldspar, G - gibbsite, H - hemitite, I - illite.

b)

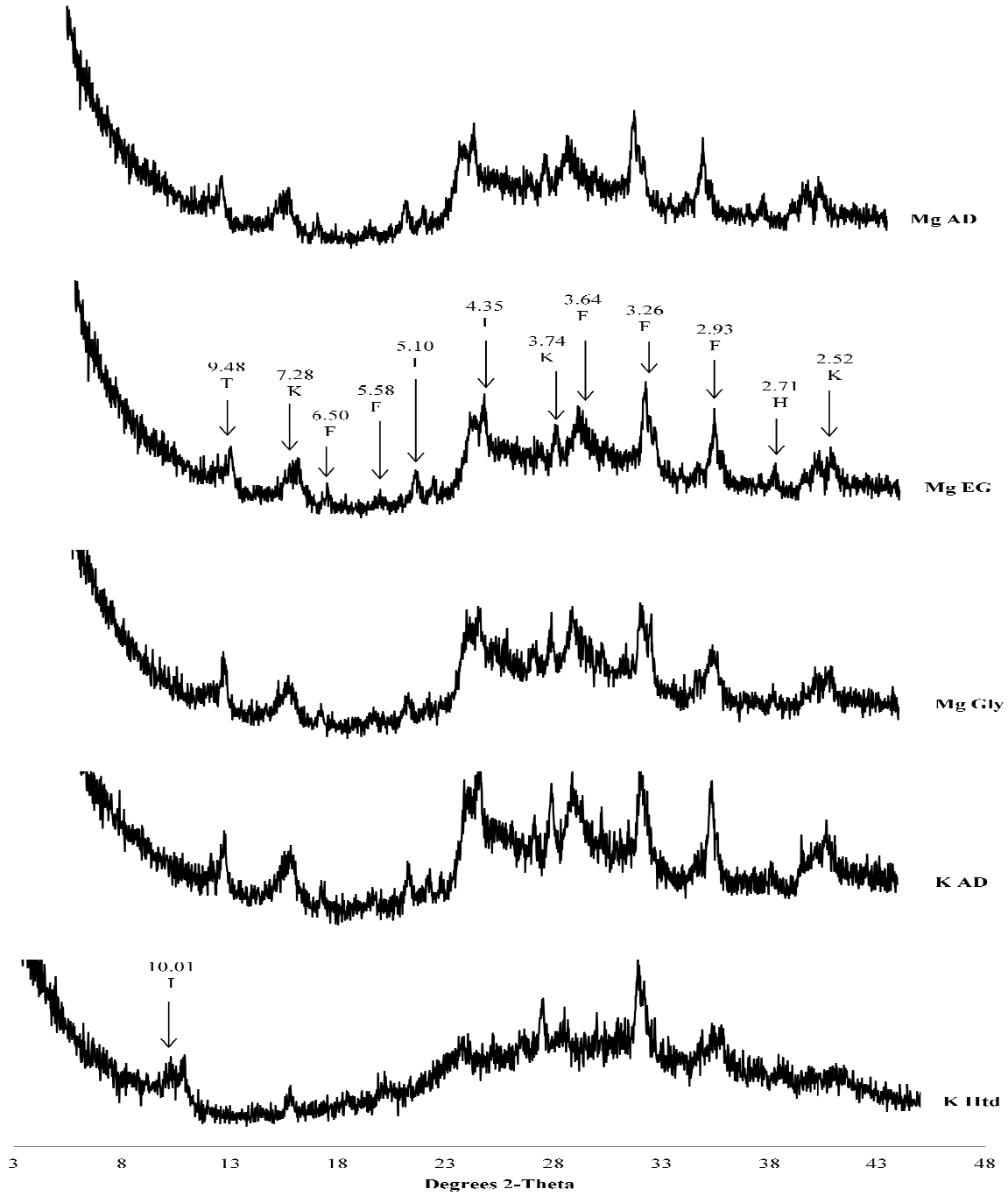

Figure 5.1 continued: X-ray diffraction patterns with labelled peaks (Å) of oriented clay samples treated with magnesium (Mg) and potassium (K) and analysed as air-dry samples (AD), heated at 550^{o}C (Htd) and analysed after treatment with ethylene glycol (EG) and glycerol (Gly) for the (a) A horizon and (b) B horizon from field 5[1]. T - talc, K - kaolin, F - feldspar, H - hemitite, I - illite.

It is well recognised that the mineralogy of volcanic ash-enriched soils usually consists of amorphous and poorly crystalline minerals (Hepper *et al*., 2006) and the dominance of poorly crystalline material in all the samples rather than more crystalline materials indicates the strong influence of volcanic ash in the soils across all of TPC.

The presence of halloysite together with allophane in all samples is likely indicative of the semi-arid climate. Harsh *et al.* (2002) state that halloysite can co-exist with allophane and imogolite in xeric conditions with seasonal rainfall where there are periods of more and less silica in solution. Vacca *et al*. (2003) suggest that allophane formation is favoured in young, porous and permeable ash deposits, while non-allophanic soils consisting of halloysite and HIV develop in older and less porous material, thus allowing the co-existence of allophanic and non-allophanic soils in the same environment. The alluvial nature of the soils at TPC would allow both young and older ash deposits to co-exist and thus allow the presence of both allophane and halloysite. Sellito *et al*. (2010) believe halloysite forms due to the release and leaching of K and Na from sanidine and mica.

Similarly to the study by Sellitto *et al*. (2010), the illite in the clay fraction at TPC is likely to be inherited from the parent material, while the HIV probably results due to weathering of the illite. The presence of a small amount of gibbsite indicates that there has been weathering of some of the halloysite. The combination of allophane and halloysite, together with a small quantity of gibbsite may be a consequence of the alluvial nature of the TPC soils. The deposited material likely consists of material at different stages of weathering. Halloysite is usually the first alteration stage from feldspar weathering, followed by gibbsite with the removal of silica from the halloysite (Bates, 1960). Bates (1960) found large quantities of both halloysite and gibbsite in soils weathered from basalitic rocks in the Hawaiian Islands which is attributed to different local conditions in terms of rainfall, slope and rock texture which affect the degree of weathering. The quantities of both gibbsite and talc in the samples where they were found are very small and unlikely to play a significant role in any management properties.

5.2.2 X-ray diffraction of random powder sand and silt samples

All sand and silt samples have strong K-feldspar peaks which represent sanidine, a mineral commonly found in volcanic rocks (Sellitto *et al.*, 2010). The d-spacings of the peaks indicate that the sanidine is likely to be mixed with other K-feldspars such as microcline and orthoclase. The sand sample from the R8 ash layer also contained calcite.

The X-ray diffraction patterns of four sand specimens (Figure 5.2) and four silt specimens (Figure 5.3) have been chosen as representative examples of the mineralogical composition of the sand and silt fractions, respectively. X-ray diffraction patterns for all sand and silt samples analysed are given in Appendix 5.2 and 5.3, respectively.

The presence of calcite is probably due to high levels of bicarbonate in the irrigation water (*pers. comm.*, Lincoln[2], 2010) which causes the calcium to precipitate in the form of calcium carbonate. Hardpans with precipitated calcium carbonate (calcrete) were observed in some areas of the TPC estate which further verifies that the high levels of bicarbonate in the water is causing the calcium to precipitate (Plate 5.1).

Plate 5.1: Calcrete exposed in a drain in Field D28 (East area). Hammer on the left is 30 cm long.

[2] Lincoln J.R. Group Agricultural Development Manager, Ciel agro-industry

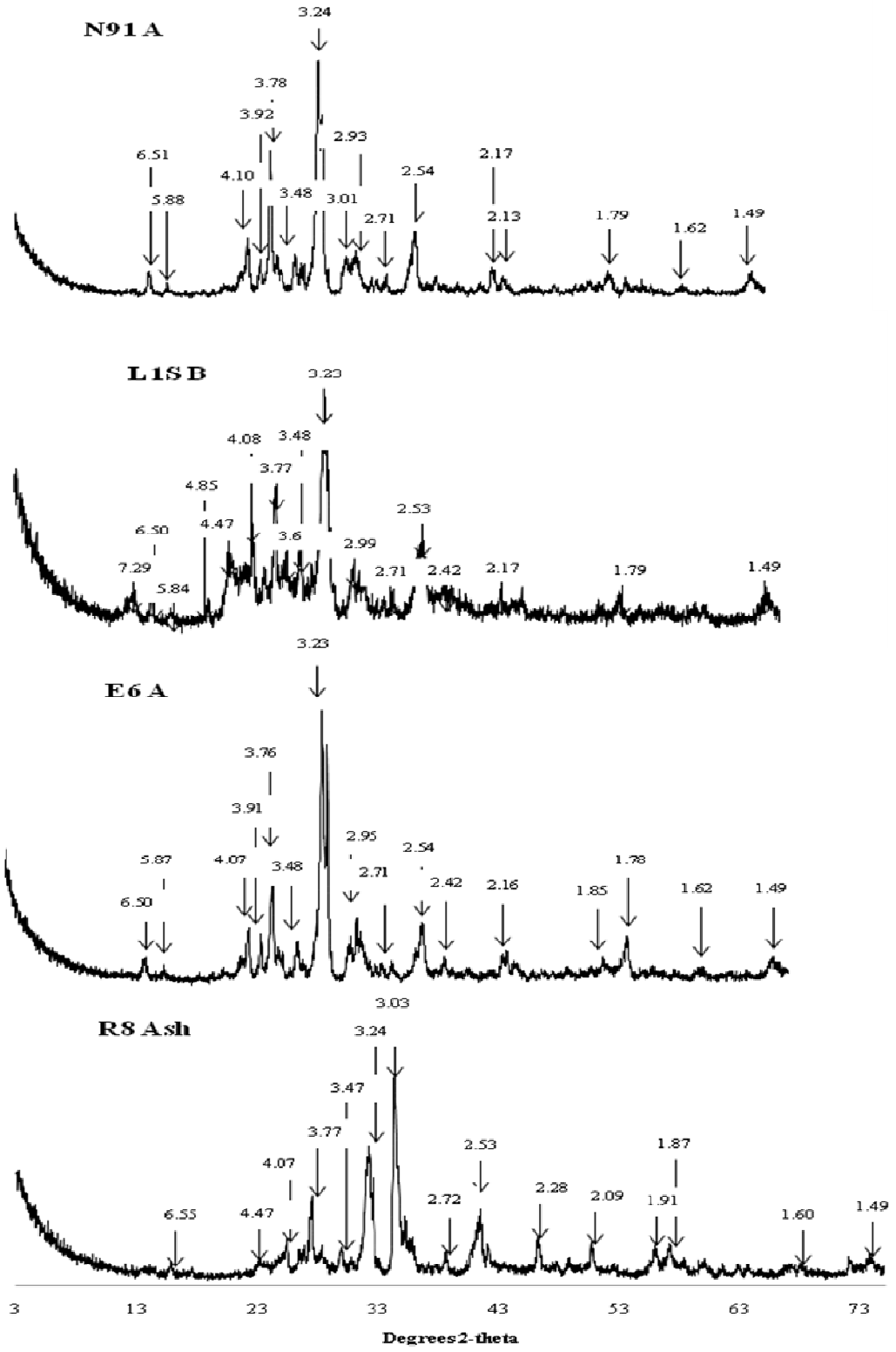

Figure 5.2: X-ray diffraction patterns with labelled peaks (Å) of random powder samples of the sand fraction for specimens N91 A horizon, L1S B horizon, E6 A horizon and R8 ash layer. All labelled peaks are K-feldspar peaks with the exception of the peaks at 3.03/ 3.01Å, 2.28Å and 2.09Å which represent calcite and the 7.29Å and 4.47Å peaks of kaolin.

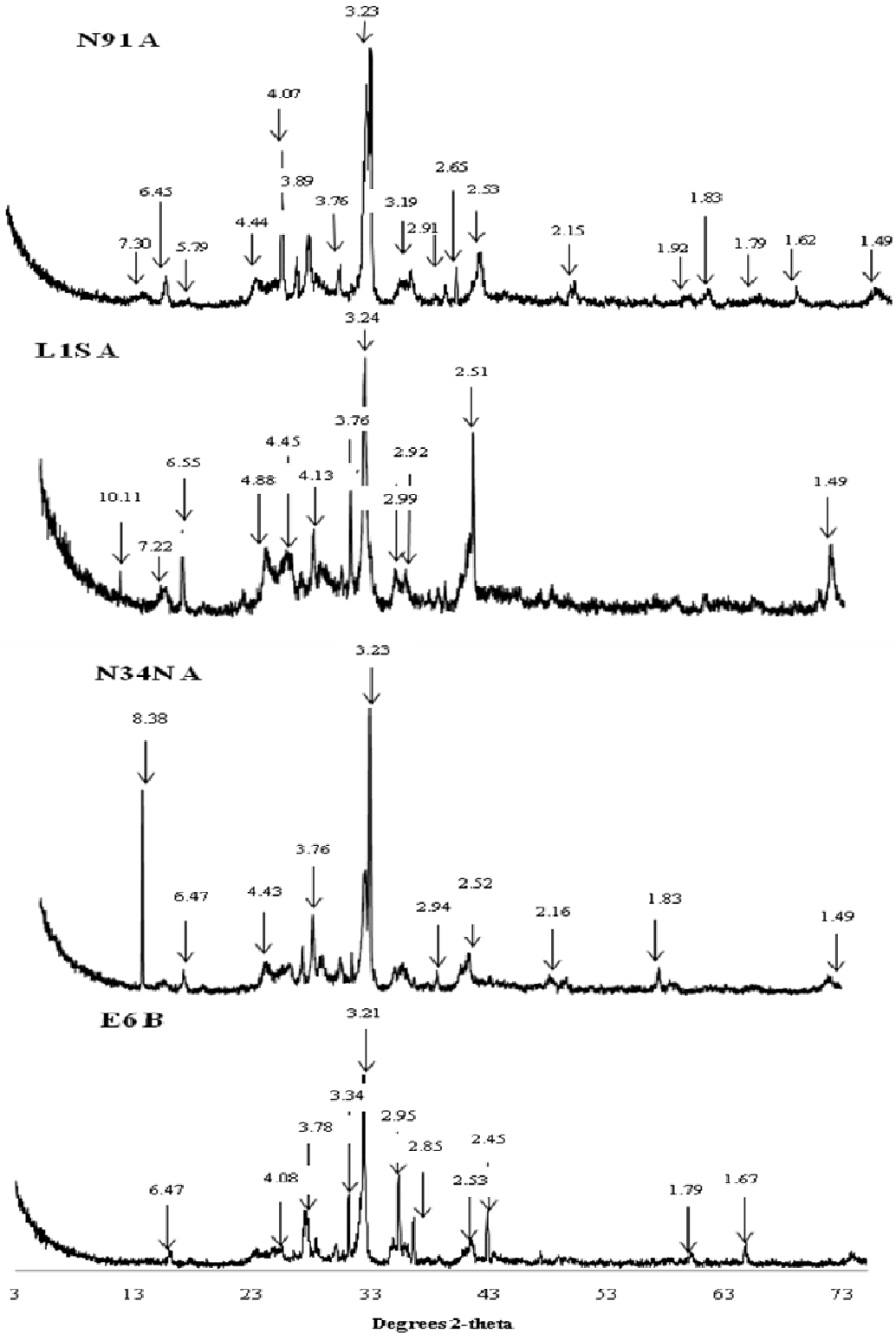

Figure 5.3: X-ray diffraction patterns with labelled peaks (Å) of random powder samples of the silt fraction for specimens N91 A horizon, L1S A horizon, N34N A horizon and E6 B horizon. All labelled peaks are K-feldspar peaks with the exception of the peaks at 7.22/ 7.30/ 4.44Å which represent kaolin, the 10.11Å peak which represents illite and the 8.38Å peak of amphibole.

5.2.3 Transmission electron microscopy

Transmission electron microscope (TEM) analysis was carried out on the clay fractions from the A and B horizons of fields 1, 10K, 12C, 16B, 17B, E6, G2, KH4, KH29, N65, N84, R3S and the ash collected in field R8 and from the borehole in the north. These samples were selected for TEM to ensure a sample from each area of the estate was represented, with the majority of the samples selected coming from the south as this area was suspected to have the most amorphous material present. Images from five of the selected fields have been shown to indicate the minerals present, as well as the variation between the areas of TPC estate (Figure 5.4).

R8 Ash Layer

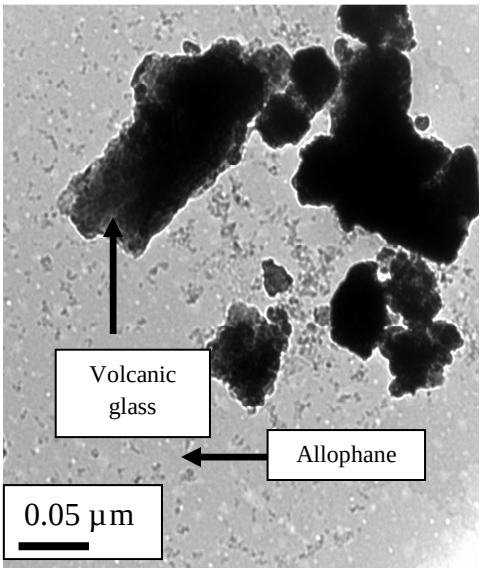

Borehole Ash

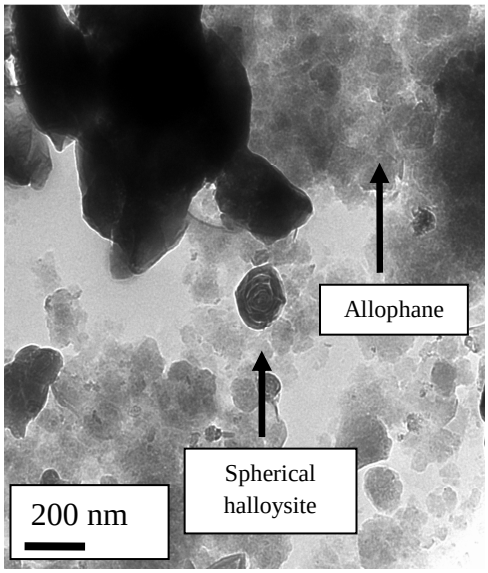

N65 A

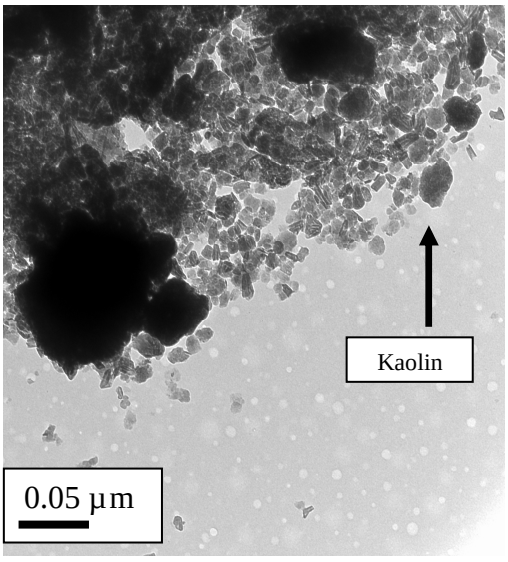

N65 B

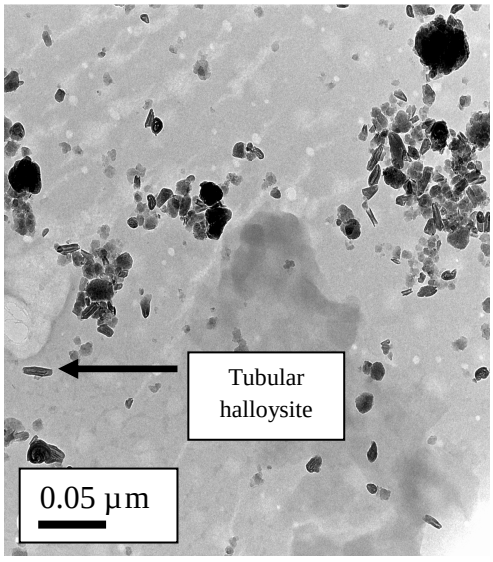

E6 A

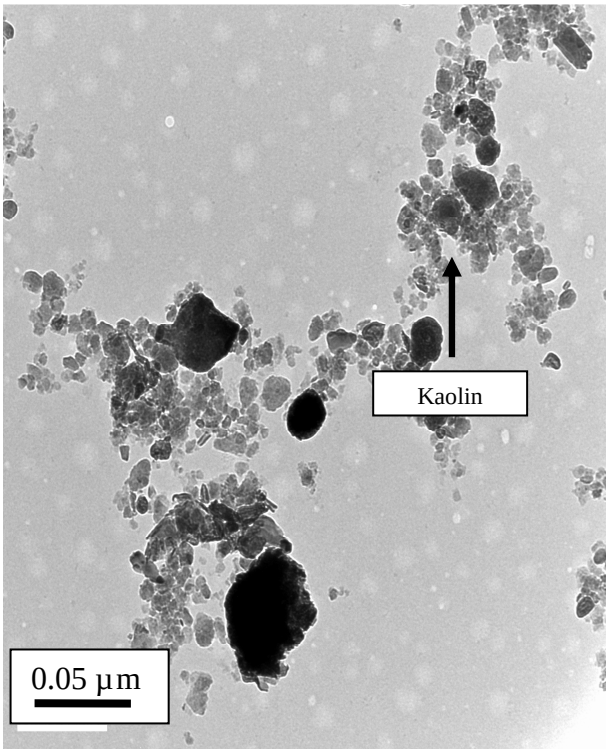

E6 B

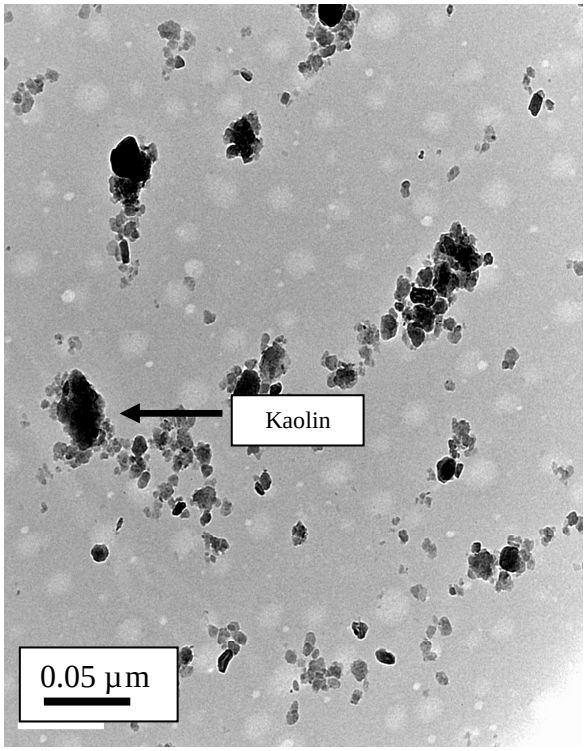

10K A Good

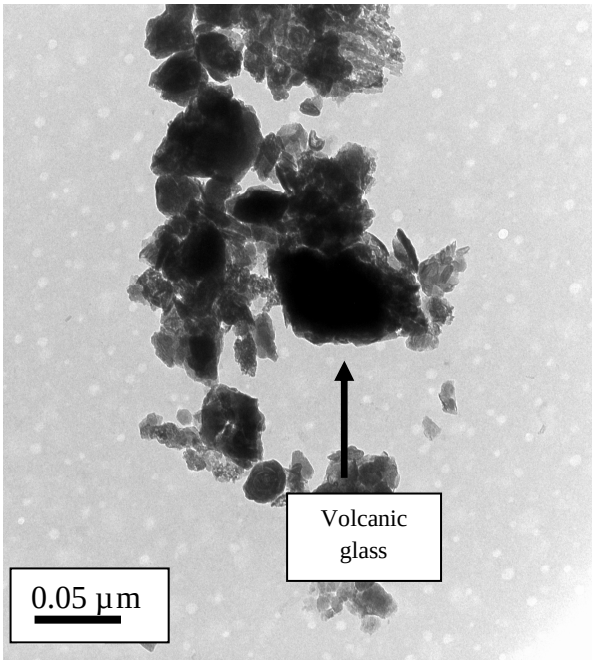

10K B Good

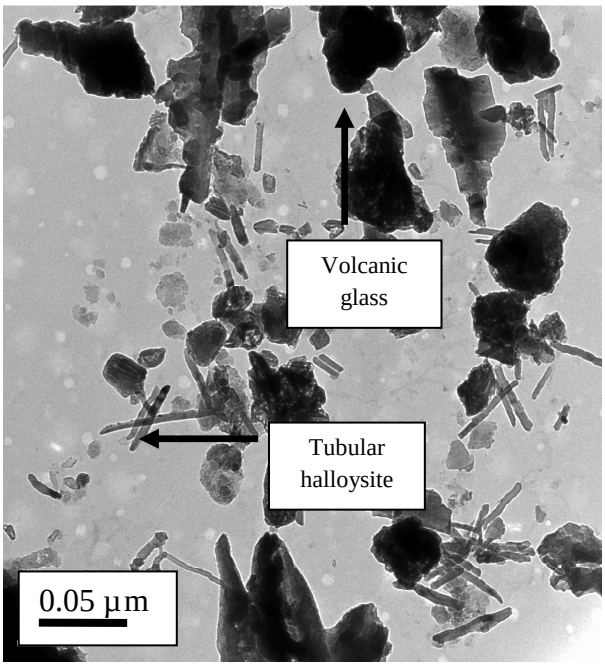

KH29 A **KH29 B**

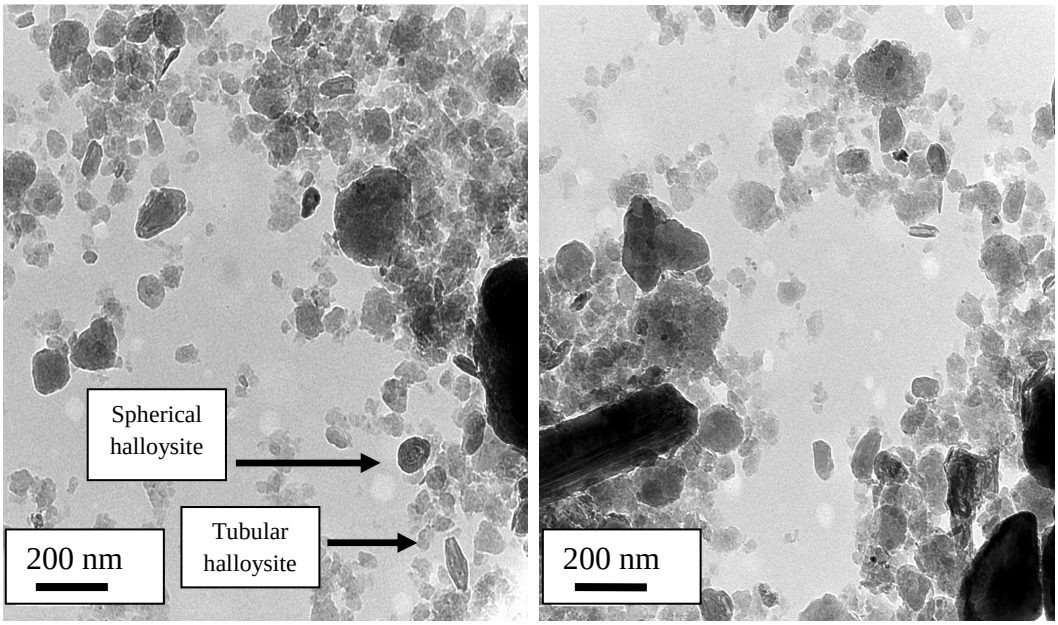

1 A Good **1 B Good**

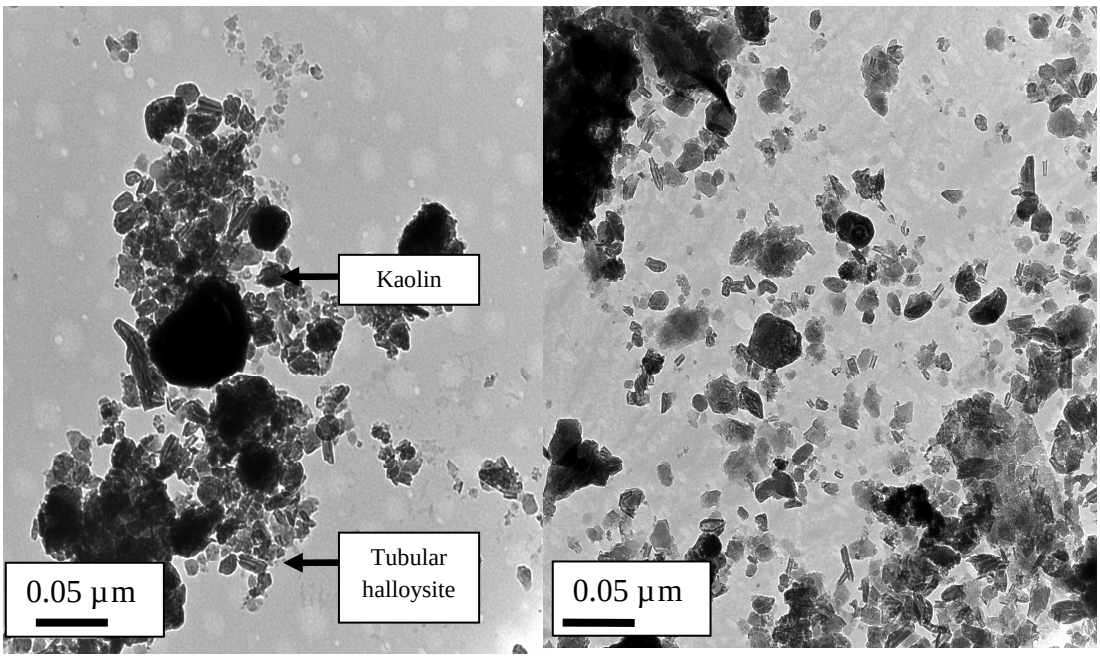

Figure 5.4: Transmission electron microscope images of the R8 ash layer, borehole ash, N65 A and B horizons, E6 A and B horizons, 10K A and B horizons (Good), KH29 A and B horizons, 1 A and B horizons (Good). Scales are indicated on each photomicrograph.

The TEM images indicate that the dominant minerals in TPC soils from all areas of the estate include very small kaolin (<< 0.5 µm) and halloysite. The halloysite is present in both tubular

and spheroidal form. The dominant morphology of halloysite that forms from alteration of feldspars and mica is tubular whereas that forming from volcanic glass has a predominately spheroidal morphology (Adamo *et al*., 2001; Singer *et al*., 2004). A study in Nayarit, Mexico by Gama-Castro *et al*. (2000) found that the dominant crystalline material in soils formed from alluvial pumice parent material is halloysite in both spheroidal and tubular forms. The TEM images also show the presence of volcanic glass clearly in samples from the R8 ash layer and field 10K. Sellitto *et al*. (2010) suggest that fine ash cools rapidly resulting in volcanic glass, while larger particles cool more slowly, resulting in sanidine and mica.

5.2.4 Extractable silica, aluminium and iron

The ranges for the percentages of Si, Al and Fe found in the measured soils from TPC sugar estate for the various selective dissolution methods are presented in Table 5.1. A full table of results for the various selective dissolution methods for all sampled TPC soils is given in Appendix 5.4.

Table 5.1: The range and average (n = 32) of Fe, Al and Si extracted by the acid oxalate, citrate-bicarbonate-dithionite and pyrophosphate methods for the A and B horizons of the sampled soils of TPC sugar estate.

Element	Sample	Acid oxalate (%)		Citrate-bicarbonate-dithionite (%)		Pyrophosphate (%)	
		Range	Average	Range	Average	Range	Average
Fe	A Horizon	0.28 – 1.08	0.51	1.12 – 2.90	1.67	0.00 – 0.08	0.02
	B Horizon	0.20 – 1.00	0.56	0.93 – 3.34	1.75	0.00 – 0.10	0.02
Al	A Horizon	0.16 – 1.07	0.44	0.19 – 3.27	0.99	0.03 – 0.17	0.08
	B Horizon	0.16 – 1.27	0.49	0.46 – 3.13	1.18	0.05 – 0.29	0.11
Si	A Horizon	0.07 – 0.96	0.42	nd*	nd	nd	nd
	B Horizon	0.09 – 0.88	0.52	nd	nd	nd	nd

* nd – not determined

Ferrihydrite (Fe_o x 1.7) (Parfitt *et al*., 1988) contents range between 0.48 and 1.84 % in the A horizon and 0.34 and 1.70 % in the B horizon. With the exception of field 12C Good (1.84 %), the ash layers contain the highest amount of ferrihydrite at 1.97 and 1.62 % for the BH Ash and R8 Ash, respectively (Appendix 5.5). These ferrihydrite levels are relatively low.

Singer *et al*. (2004) also found low ferrihydrite levels (between 0.44 and 3.5 %) in soils developed from basic pyroclastics in the Golan Heights. Gama-Castro *et al*. (2000) found ferrihydrite ranging between 0.20 and 0.51 % in pumiceous, alluvial soils in Nayarit, Mexico and Sellitto *et al*. (2010) found ferrihydrite contents in the range of 0.5 to 1 % in 5 pedons developed from volcanic ash on the Matese Massif in southern Italy. As weathering proceeds in volcanic ash soils the first stage alteration minerals, such as ferrihydrite, are transformed into their second stage alteration minerals (i.e. more crystalline iron oxides) or may be the end product if they are preserved as buried deposits (Nieuwenhuyse *et al*., 2000). Consequently, the low ferrihydrite contents in this study, together with the dominant presence of halloysite (Figure 5.4) in the TPC soils suggest these soils have weathered to some degree from amorphous and short-range order mineralogy to a more crystalline dominated mineralogy. The higher amounts of ferrihydrite in the ash layers may be due to higher initial concentrations in these layers than the surrounding soil, as well as slower weathering rates due to being buried layers within the soil profile.

The greater Fe_o in the soils from the south and west areas, and the lowest Fe_o in the Kahe area (Figure 5.5) indicate that the south and west areas have the highest ferrihydrite levels and have thus either undergone slower weathering rates than the other areas of TPC estate or had higher initial concentrations of amorphous material.

a)

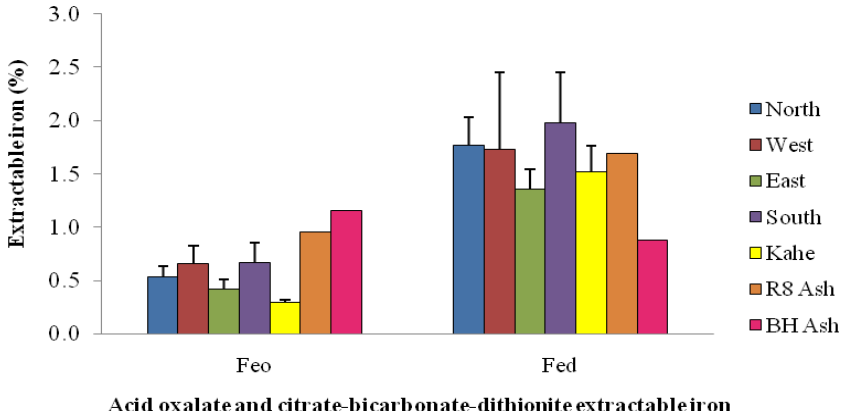

Figure 5.5: Iron extracted by acid oxalate (Fe_o) and citrate-bicarbonate-dithionite (Fe_d) in the a) A horizon and b) B horizon and iron extracted by sodium pyrophosphate (Fe_p) in the c) A horizon and d) B horizon for the north, west, east, south and Kahe areas, and the ash layers (R8 Ash and Borehole Ash (BH Ash)) of TPC sugar estate.

b)

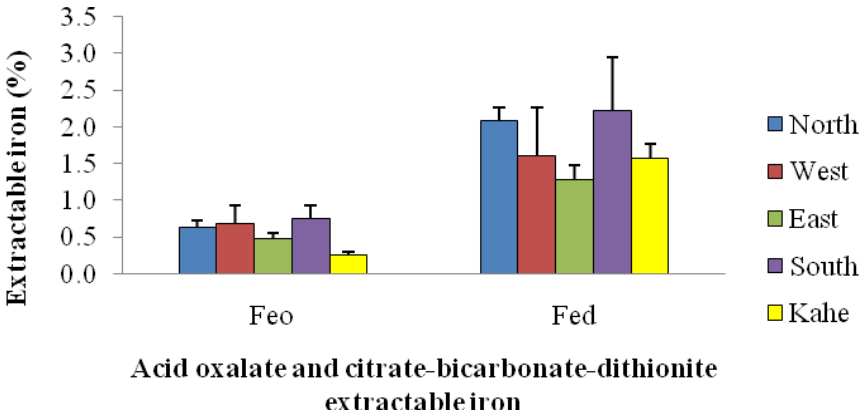

c)

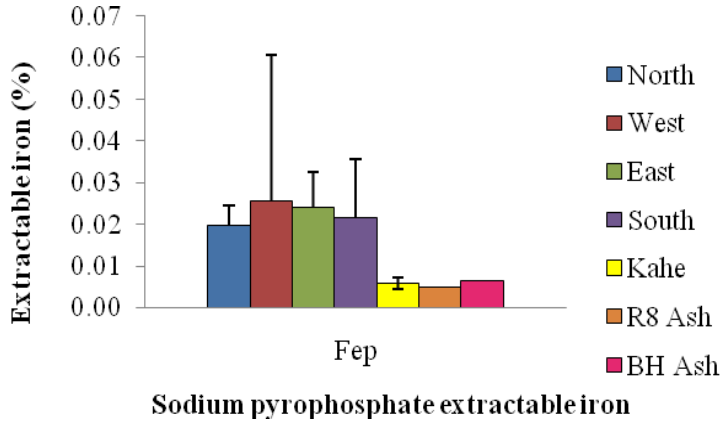

d)

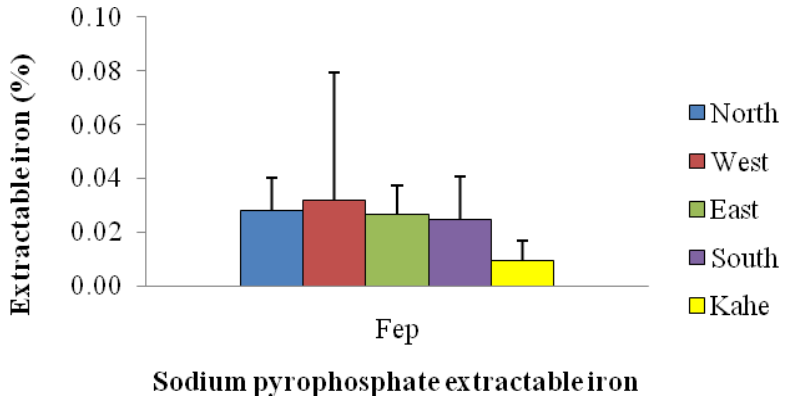

Figure 5.5 continued: Iron extracted by acid oxalate (Fe_o) and citrate-bicarbonate-dithionite (Fe_d) in the a) A horizon and b) B horizon and iron extracted by sodium pyrophosphate (Fe_p) in the c) A horizon and d) B horizon for the north, west, east, south and Kahe areas, and the ash layers (R8 Ash and Borehole Ash (BH Ash)) of TPC sugar estate.

The south and west areas are likely to have received higher initial concentrations of amorphous minerals through alluvial deposits in relation to the other areas of the estate and thus contain higher proportions of amorphous material, such as ferrihydrite and allophane. However, although the allophane content (Si_o x 7.14) (Parfitt and Wilson, 1985) is highest in the BH Ash, similarly to ferrihydrite, the allophane content is highest in the east area (Figure 5.6), rather than the south and west areas as for ferrihydrite.

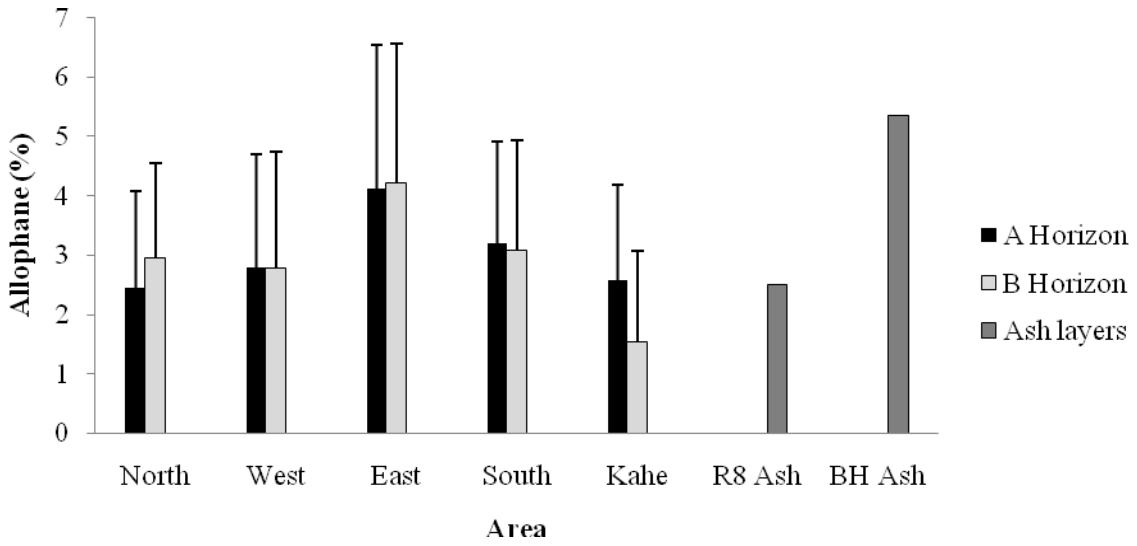

Figure 5.6: Allophane content for the various areas and ash layers of TPC sugar estate for the A and B horizons.

The standard deviation for allophane in all areas is large (Figure 5.6) suggesting an uneven distribution of amorphous material across TPC. This may be due to the nature of the alluvial deposits and buried ash layers. TPC sugar estate is situated over many old river channels which could have deposited more amorphous material in some fields within a particular area. The allophane ranges between 0.52 and 6.84 % in the A horizon and 0.55 and 6.26 % in the B horizon. A full table of allophane results is given in Appendix 5.5. Singer *et al*. (2004) considered allophane levels found in the Golan Heights between 2.5 and 5.3 % to be low. Therefore, as for ferrihydrite in this study, a low content of allophane can be attributed to weathering of volcanic ash minerals to more crystalline minerals, predominately in the form of halloysite. Although the ferrihydrite and allophane contents are low, their presence can play a significant role in the soil properties, such as surface area and related soil characteristics (Gama-Castro *et al*., 2000).

The weathering of amorphous constituents to more crystalline minerals is further supported by the Al_o + ½ Fe_o molar ratios. According to Tsai *et al*. (2010) an Al_o + ½ Fe_o percentage lower than 1 indicates that Al and Fe are present in predominately crystalline forms, whereas a percentage greater than 2 suggests that Fe and Al are in amorphous forms. The IUSS Working Group WRB (2006) uses a percentage of 2 for the sum (Al_o + ½ Fe_o) as the diagnostic limit in defining andic soil properties. For all samples taken from TPC the Al_o + ½ Fe_o percentage is less than 2 (with many less than 1) and as with the ferrihydrite results the highest average values are in the west and south of the estate, and the lowest average values in the Kahe area. The BH Ash has an Al_o + ½ Fe_o percentage of 1.62, close to the threshold value of 2 for defining andic soils. This result corresponds with the high ferrihydrite and allophane content found in the BH Ash (Appendix 5.5).

In summary, the mineralogy of the soils across the TPC sugar estate consists of small quantities of amorphous minerals that are weathering to more crystalline minerals, predominately halloysite and poorly ordered kaolin. This is similar to a study in south western Kenya on six peralkaline volcanic ash profiles where the three least weathered profiles showed morphologies typical of Andisols although they did not meet the criteria to be classified as Andisols. These profiles contained no allophane but were dominated by halloysite (Wielemaker and Wakatsuki, 1984).

The higher quantities of ferrihydrite, allophane and a higher Al_o + ½ Fe_o percentage in the BH Ash indicates that buried ash layers that have been either alluvially or aeolian deposited play a major role in the amount of amorphous material remaining in the soil profiles and may explain the variability in the percentages of amorphous material within the various areas and between fields. Furthermore, more ferrihydrite and a higher Al_o + ½ Fe_o percentage in the south and west areas suggest more amorphous material in these areas which is likely a consequence of greater alluvial deposition of volcanic ash and minerals in these areas of the estate.

5.3 Physical analysis

5.3.1 Final infiltration rate

Infiltration is defined by Schaetzl and Anderson (2005) as "the volume of water entering a specified cross-sectional area of soil per unit time". Overall, the final infiltration rate (FIR) in the south is lower and in Kahe is higher than the other areas of the estate (Table 5.2).

Table 5.2: Final infiltration rates for each area of the TPC estate*.

Area	n	Average final infiltration rate (mm hr^{-1})	Standard deviation
North	6	110	± 49
West	7	138	± 92
East	7	138	± 94
South	6	82	± 70
Kahe	4	210	± 123

* Fields where FIRs were not reached have not been included.

According to Lado and Ben-Hur (2004), the main factor responsible for a decrease in infiltration rate is seal formation on the soil surface. Texture, organic matter content, sodicity and mineralogy contribute to the likelihood of the soil sealing (Lado and Ben-Hur, 2004). Visual observation of many fields in the south showed evidence of calcareous crust formation and surface sealing (Plate 5.2).

Plate 5.2: Surface crust in field R8N (South area).

The south of the TPC estate has the highest sodium adsorption ratio and exchangeable sodium content compared to the other areas of the estate (Sections 5.4.4, 5.4.5 and 5.4.6) and consequently may have greater soil dispersion and clogging of soil pores which results in the formation of a seal on the soil surface and thus the infiltration rate is reduced (Richards, 1954). Visual observation of many fields in the south showed precipitation of salts on the soil surface (Plate 5.3).

Plate 5.3: Precipitated salts on the soil surface in the south area.

In the north for field N66 and in Kahe for field KH4, the FIRs were not recorded as the infiltration rate continuously slowed down (to less than 20 mm hr^{-1} and 10 mm hr^{-1}, respectively). It is speculated that the reason for the FIR not being reached in these fields is due to the addition of water during infiltration measurements which changes the soil from saline-sodic to sodic and thus results in surface sealing as pores are clogged due to increased dispersion. It is suggested that more double ring infiltrometer measurements per field are needed, together with the concentrations of the water soluble cations and electrical conductivity for each measured site to determine if there is any correlation.

In the east for fields D11 and F1S, in the west for field R5N and in the south for fields 10K (Good and Bad), 5^1 (Good and Bad), G2, 19A, $11C^1$ (Good and Bad) and 12 (Good and Bad), FIRs were not recorded as the infiltration rate continuously slowed down to between less than 20 and 90 mm hr^{-1}. However, the apparently relatively high infiltration rate was due to the

soil only absorbing up to 90 mm in an hour and then essentially sealing up. It is likely that this amount of water infiltrated quite rapidly prior to sealing taking place and thereafter infiltration only occurred at an extremely slow rate due to the surface seal. The principal reason for the FIR not being reached in these fields is likely due to the high exchangeable sodium in relation to the other cations (Sections 5.4.4 and 5.4.5) causing soil dispersion which clogs soil pores and creates a surface seal (Walworth, 2006). The rapid introduction of water to infiltrometer rings onto a sodic soil may also contribute to a reduced infiltration rate as soil slaking and dispersion occurs. Further reasons for the FIR not being reached in these fields could be due to saturated soils at the time of the infiltration measurements and the presence of perched water tables. Visual observation indicated that many fields were allowed insufficient time to drain after irrigation (Plate 5.4) and thus the water applied to the soil through the double ring infiltration apparatus is unable to move vertically into the soil, although some lateral movement probably occurred, therefore preventing a FIR measurement.

Plate 5.4: Saturated soil in field D19 (East area).

It is difficult to make any assessment of FIR between the good and bad patches of sugarcane growth. In both the west and the east there was only one field sampled and although in both fields the good patch had a higher FIR than the bad patch it would be necessary to take more measurements to know if this is more widely valid. Furthermore, only one field in the south where infiltration measurements were done on a good and a bad patch reached a FIR, which again indicated a slightly higher FIR for the good patch, although no conclusions can be made without further measurements. A full table of results is given as Appendix 5.6.

Previously on TPC, infiltration rate was measured by Thouvenot (2002), and results indicated a decrease in infiltration rate with increased sodicity. However, often stable infiltration rates were not reached.

5.3.2 Water retention

5.3.2.1 Good and bad patches of cane growth

Fields 1, R^3S, 10K, 12C, 11C, 12 and O^3 were each sampled in an area where the cane was growing well (Good) and in an area where the cane was growing poorly (Bad). There is no trend in the water retention curves for the good and bad patches between fields in either the A or the B horizons (Figure 5.7), with the water retention at the various matric potentials measured sometimes being greater in the good patch, sometimes being greater in the bad patch, or sometimes being similar between the good and bad patches.

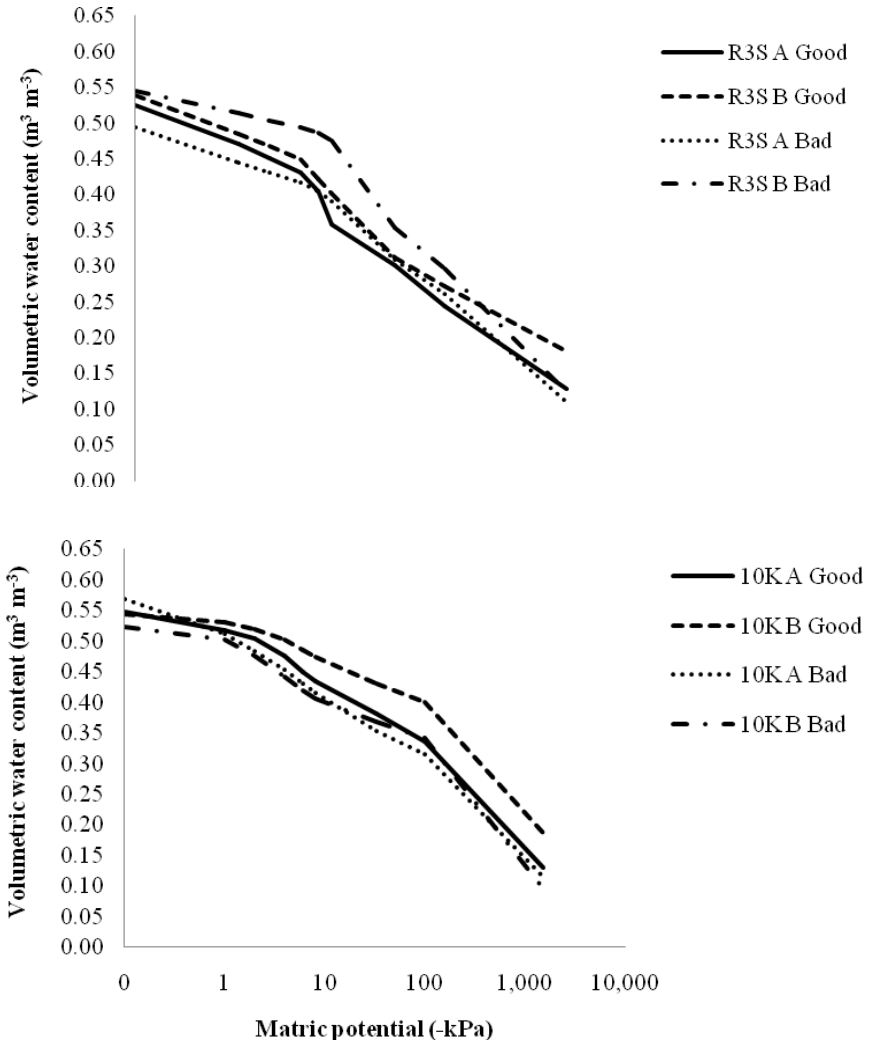

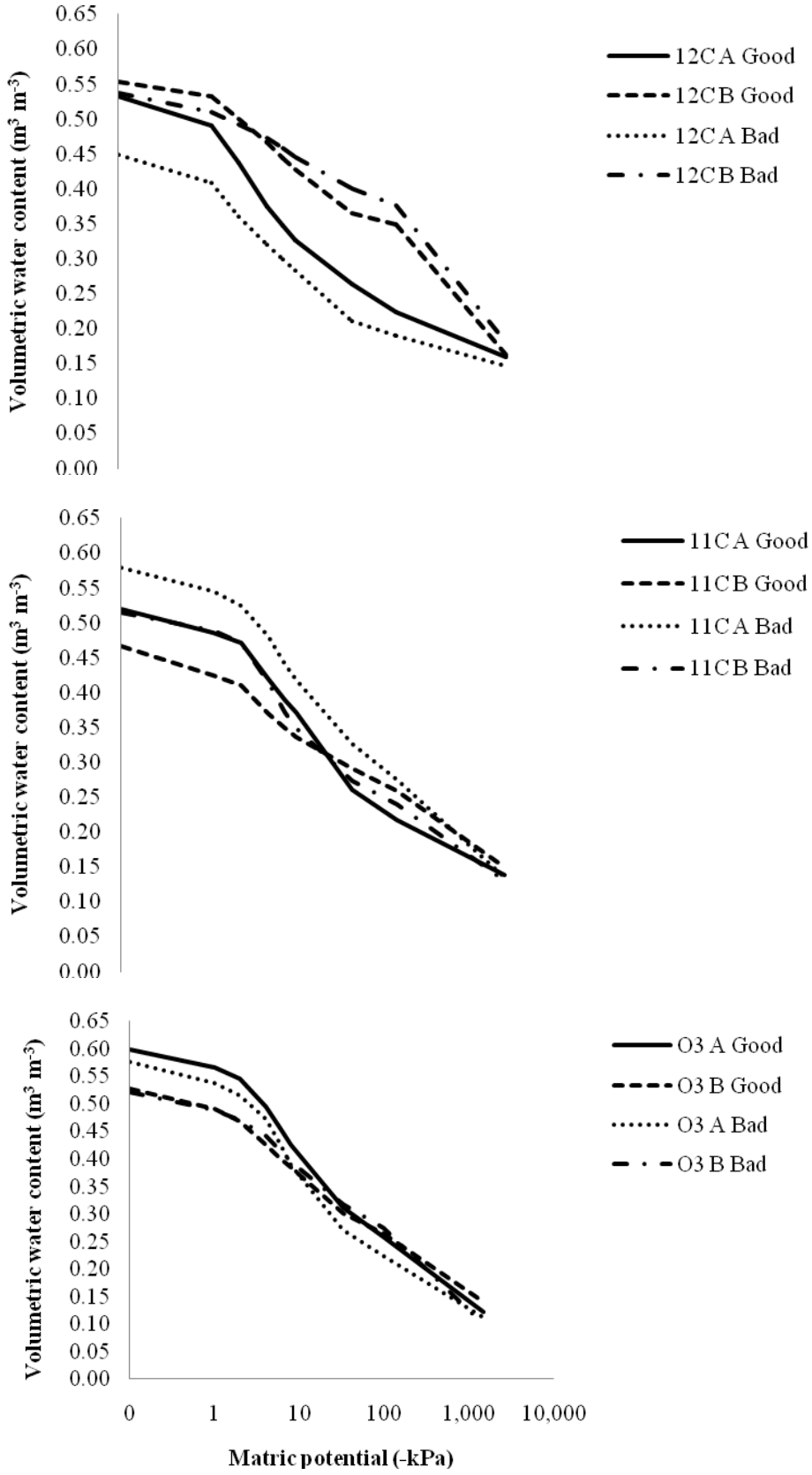
Volumetric water content (m³ m⁻³)
0.65
0.60
0.55
0.50
0.45
0.40
0.35
0.30
0.25
0.20
0.15
0.10
0.05
0.00
12C A Good
12C B Good
12C A Bad
12C B Bad
11C A Good
11C B Good
11C A Bad
11C B Bad
O3 A Good
O3 B Good
O3 A Bad
O3 B Bad
0
1
10
100
1,000
10,000
Matric potential (-kPa)

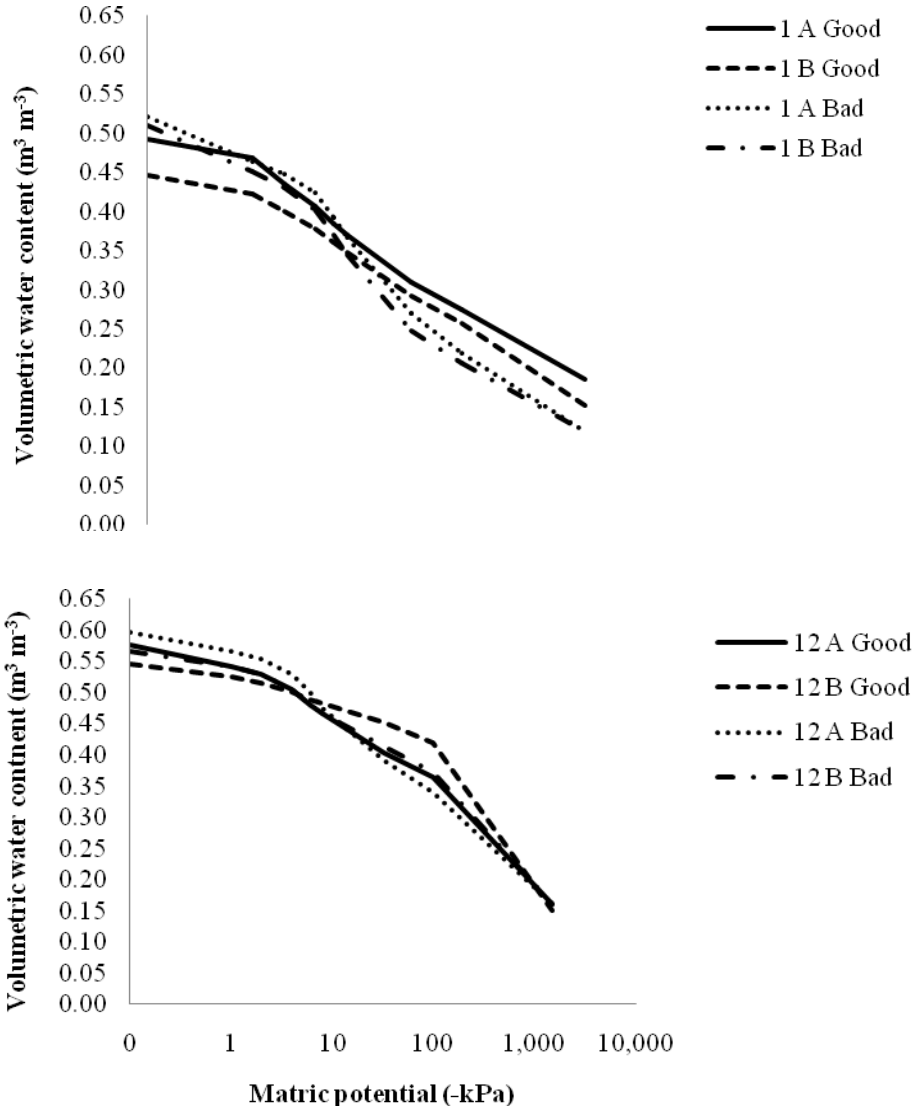

Figure 5.7: Water retentivity curves of a selection of fields with good and bad patches of cane growth.

Paired t-tests between the good and bad patches for the seven fields measured confirm that there are no significant differences between the good and bad patches at all tensions in either the A or B horizon, with all probability values being greater than 0.2. The only exception is at a matric potential of -1500 kPa where the good patch is marginally significantly higher than the bad patch in both the A and B horizon ($p = 0.085$ and 0.080, respectively) (Table 5.3).

Table 5.3: Probability (p = 0.05) from paired t-tests used to compare the water retentivity at various matric potentials, the readily available water (RAW) and the plant available water (PAW) between the good and bad patches of cane growth from both the A and B horizons.

Matric potential and horizon	Probability (p)
0 kPa A	0.987
0 kPa B	0.310
-10 kPa A	0.888
-10 kPa B	0.818
-33 kPa A	0.411
-33 kPa B	0.542
-100 kPa A	0.414
-100 kPa B	0.287
-1500 kPa A	0.085
-1500 kPa B	0.080
RAW A	0.211
RAW B	0.062
PAW A	0.308
PAW B	0.107

This suggests that within a field the water retention of the soil is not being affected by the areas of poorly growing cane and that poor cane growth is not necessarily a consequence of the amount of water retained in the soil. The higher water retention at a matric potential of -1500 kPa in the good patch compared to the bad patch indicates that the good patch has a marginally higher micro-porosity than the bad patch (Figure 5.8).

a)

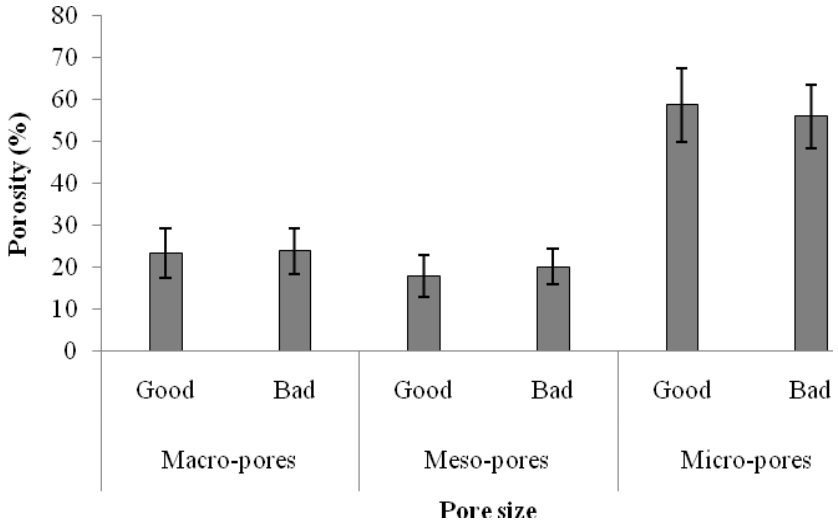

b)

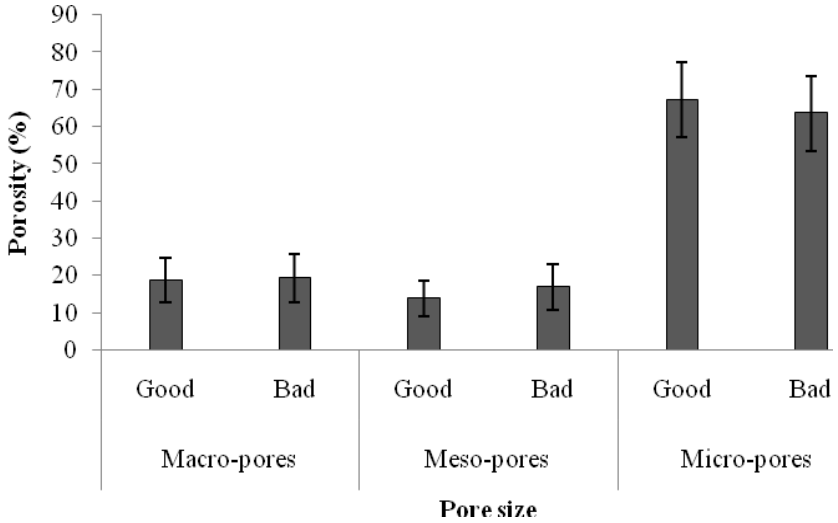

Figure 5.8: The pore size distribution of the good and bad patches of cane growth in the a) A horizon and b) B horizon.

Total porosity is represented by the saturated volumetric water content (Hillel, 1971). Macro-pore space is defined here as the pore space occupied by pores of diameter greater than 30 microns (Johnston, 1973) which retain water at a matric potential between 0 and -10 kPa. Meso-pore space is defined here as the pore space which retains water at a matric potential between -10 kPa and -100 kPa (Hillel, 1971). Therefore, calculation of porosity was done using the volumetric water content at -10 kPa (macro-pores), and between -10 and -100 kPa

(meso-pores) as a percentage of the total porosity. The remaining percentage been attributed to micro-pores.

The dominance of micro-pores corresponds to the presence of allophane, as allophane is essentially a micro-porous material (Paterson, 1977). Allophane has a large specific surface area which allows a high adsorption capacity (Hepper *et al*., 2006). TPC soil clays have high specific surface areas (Section 5.4.8) thus indicating the presence of allophane and explaining the dominance of micro-pores.

Each field's water retention characteristic in the good and bad patch is likely to be the result of a combination of site specific conditions. In circumstances where the good patch has higher RAW than the bad patch, this implies better porosity which is likely a result of better structural stability in the good patch. In circumstances where the bad patch has higher RAW than the good patch, this may be due to increased porosity caused by greater white grub activity in the bad patch, as white grub are more prevalent in the bad patch (visual observation) perhaps because it is easier for the grubs to burrow in areas where the soils have dispersed. Furthermore, the bad patch may have greater RAW due to the slight increase in meso-porosity due to the settling of soil particles into a more compact form due to structural break-down (Figure 5.8).

Another factor which may influence the water retention is the placement of the undisturbed soil core within the field which may result in some soil cores containing more root or animal created pores than other cores. This is likely to affect the observable trend between the good and bad patches in the measured fields.

Paired t-tests between the good and bad patches for RAW and PAW indicate that there is no significant difference in the A horizon for either PAW or RAW, where PAW is defined by the water retained between field capacity (-10 kPa) and wilting point (-1500 kPa) (Nanzyo *et al*., 1993) and RAW is defined by the water retained between -100 kPa and -1500 kPa (Hillel, 1976). However, there is a marginally significantly higher RAW and PAW in the B horizon for the bad patch compared to the good patch (Table 5.3). Greater RAW and PAW in the bad patch can be attributed to the good patch having slightly higher micro-porosity and thus higher water retention at -100 and -1500 kPa. No significant difference in the A horizon between the good and bad patches for PAW and RAW may be due to greater variability in

the macro-porosity of the A horizons which will affect the water retained at saturation. This variability may result from the differing degrees of disturbance on the soil surface when fields have either been recently harvested or planted.

5.3.2.2 Variability within fields

Fields R^3S, P^4N, 10K, N43N, 4D, 12C, 16B, N100KA, 4C and 5D were sampled at more than one site to estimate in-field variability. In all cases the water retentivity measurements from different sites within a field did not exhibit the same trend. However, the standard deviation at the various measured tensions between the replicate sites within a field are generally small (≤ 0.10), with the exception of field 5D B horizon which has a standard deviation of 0.13 at saturation (Table 5.4).

A higher standard deviation at various tensions between sites may be caused if the field is relatively stony or the texture of the soil varies across the field. Some fields (as is the case for field 5D) are situated on an area where there are old river channels and consequently there are areas within the field with a more sandy texture.

Generally, the A horizon either has a higher or similar water retention at the higher matric potentials (0 to -10 kPa) to that of the B horizon. The exceptions are fields N43N, 4D (2.1), 12C (Good and Bad), 12C (2.2), and 5D (2.2), which all have higher water retention at the higher matric potentials in the B horizon compared to the A horizon. Generally, the A horizon will retain greater amounts of water at the higher matric potentials due to a larger proportion of macro-pores compared to the B horizon due to the A horizon generally having more organic matter, animal activity and root channels. The exceptions may be due to the B horizon having a large pore/s caused by a root channel or animal burrow.

In most fields, with the exception of fields R3S (2.1) and P4N (2.4), the B horizon has a higher or similar water retention at -33 and -100 kPa compared to the A horizon. This is likely a result of the B horizon being more compact than the A horizon, with a higher ρb and a greater proportion of meso- and micro-pores. The higher ρb in the B horizon is probably due to the slightly greater clay content in the majority of the measured fields for the B horizon compared to the A horizon (Appendix 5.11). There is a significant ($p < 0.001$) correlation between clay percentage and bulk density in the B horizon ($r = 0.641$) (Appendix

5.20). Figure 5.9 indicates that in all areas the micro-porosity of the B horizon is slightly greater than the A horizon and the meso-porosity in the A and B horizons are similar.

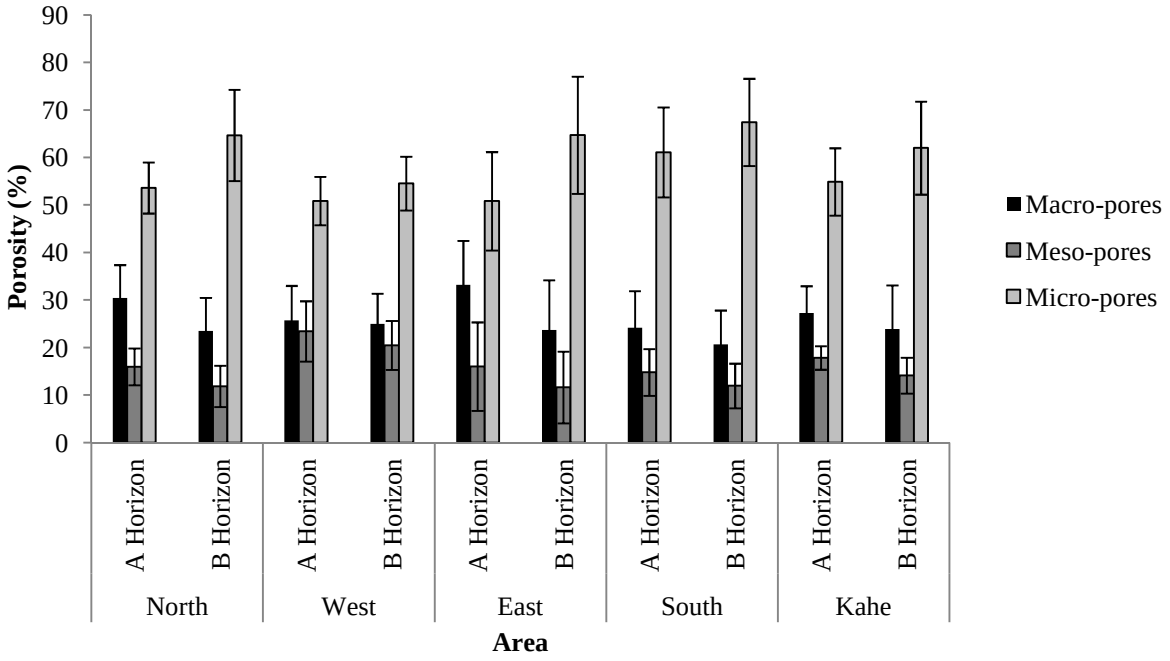

Figure 5.9: Pore size distribution of the A and B horizons for the different areas of TPC sugar estate.

Table 5.4: Volumetric water content (m^3 m^{-3}) at various matric potentials (kPa) for the fields where sampling was done at more than one site.

Field	n	0	±	-1	±	-2	±	-4	±	-6	±	-8	±	-10	±	-33	±	-100	±	-1500 *	±
P4N A	4	0.48	0.08	0.45	0.08	0.42	0.09	0.39	0.11	0.37	0.11	0.34	0.10	0.26	0.03	0.21	0.04	0.16	0.02	0.13	0.02
P4N B	4	0.48	0.05	0.44	0.06	0.41	0.06	0.37	0.07	0.35	0.07	0.33	0.07	0.29	0.04	0.23	0.06	0.20	0.05	0.13	0.03
R3S A	5	0.52	0.03	0.49	0.05	0.47	0.04	0.42	0.03	0.39	0.04	0.37	0.04	0.36	0.06	0.27	0.05	0.22	0.05	0.12	0.01
R3S B	5	0.52	0.03	0.49	0.02	0.47	0.02	0.44	0.04	0.42	0.04	0.40	0.04	0.37	0.01	0.30	0.04	0.25	0.04	0.16	0.02
10K A	4	0.54	0.04	0.50	0.04	0.48	0.04	0.43	0.06	0.40	0.07	0.39	0.07	0.34	0.09	0.32	0.07	0.28	0.07	0.12	0.01
10K B	5	0.51	0.03	0.49	0.03	0.46	0.04	0.42	0.06	0.40	0.07	0.38	0.07	0.33	0.05	0.33	0.07	0.29	0.08	0.14	0.03
N43N A	2	0.50	0.06	0.47	0.06	0.42	0.02	0.37	0.01	0.34	0.01	0.32	0.02	0.32	0.02	0.26	0.01	0.22	0.01	0.12	0.01
N43N B	2	0.50	0.02	0.48	0.01	0.44	0.03	0.41	0.05	0.40	0.06	0.39	0.05	0.39	0.05	0.33	0.05	0.31	0.06	0.13	0.03
4D A	3	0.51	0.04	0.45	0.03	0.41	0.02	0.37	0.03	0.35	0.03	0.34	0.04	0.31	0.03	0.30	0.06	0.26	0.07	0.17	0.00
4D B	3	0.49	0.04	0.44	0.04	0.41	0.04	0.38	0.04	0.36	0.04	0.35	0.04	0.33	0.04	0.33	0.04	0.30	0.04	0.16	0.01
12C A	5	0.52	0.05	0.49	0.06	0.46	0.07	0.43	0.08	0.40	0.08	0.38	0.08	0.42	0.05	0.32	0.08	0.25	0.06	0.17	0.02
12C B	5	0.54	0.01	0.52	0.01	0.50	0.01	0.47	0.01	0.45	0.01	0.44	0.03	0.42	0.04	0.37	0.04	0.33	0.04	0.18	0.01
16B A	2	0.54	0.00	0.51	0.02	0.48	0.03	0.44	0.03	0.41	0.01	0.39	0.01	0.39	0.01	0.31	0.01	0.27	0.01	0.16	0.04
16B B	2	0.50	0.04	0.47	0.03	0.44	0.01	0.41	0.01	0.38	0.02	0.37	0.02	0.37	0.02	0.31	0.03	0.28	0.04	0.15	0.03
N100KA A	3	0.50	0.05	0.46	0.06	0.41	0.08	0.37	0.07	0.34	0.06	0.32	0.05	0.32	0.05	0.25	0.02	0.22	0.01	0.18	0.02
O3 A	2	0.59	0.02	0.55	0.02	0.53	0.02	0.48	0.02	0.44	0.02	0.41	0.02	0.41	0.02	0.29	0.03	0.24	0.02	0.12	0.01
O3 B	2	0.52	0.00	0.49	0.00	0.47	0.00	0.43	0.01	0.41	0.01	0.39	0.01	0.39	0.01	0.31	0.01	0.27	0.01	0.12	0.03
12C A	2	0.59	0.02	0.55	0.02	0.54	0.02	0.52	0.02	0.49	0.02	0.47	0.01	0.47	0.01	0.40	0.01	0.35	0.02	0.16	0.00
12C B	2	0.56	0.01	0.53	0.01	0.52	0.01	0.50	0.00	0.49	0.01	0.47	0.01	0.47	0.01	0.43	0.03	0.40	0.03	0.16	0.01
4C A	2	0.58	0.09	0.55	0.07	0.51	0.03	0.46	0.03	0.45	0.04	0.44	0.05	0.43	0.06	0.38	0.03	0.36	0.03	0.15	0.01
4C B	2	0.52	0.05	0.49	0.02	0.47	0.01	0.42	0.07	0.41	0.08	0.40	0.09	0.40	0.09	0.35	0.07	0.33	0.07	0.16	0.01
5D A	2	0.54	0.07	0.51	0.05	0.48	0.05	0.42	0.04	0.40	0.03	0.38	0.03	0.37	0.02	0.34	0.02	0.32	0.02	0.18	0.03
5D B	2	0.57	0.13	0.52	0.12	0.50	0.11	0.47	0.11	0.46	0.11	0.45	0.10	0.45	0.11	0.44	0.11	0.41	0.12	0.16	0.01

* n = 2 for a matric potential of -1500 kPa for all fields.

5.3.2.3 Water retention across TPC estate

The average volumetric water content and standard deviation at each measured tension between replicates at each sampled site and the trend of the water retention characteristics of each field sampled are presented as Appendix 5.7 and Appendix 5.8, respectively.

Principal component analysis in the A horizon indicates that most of the variation in the ordination was driven by the wet range water contents (0 to – 10 kPa) as they had the greatest correlation with PCA axis 1. The dry range (-1500 kPa) accounted for the least variation, being the most closely associated with ordination axis 2 (Figure 5.10).

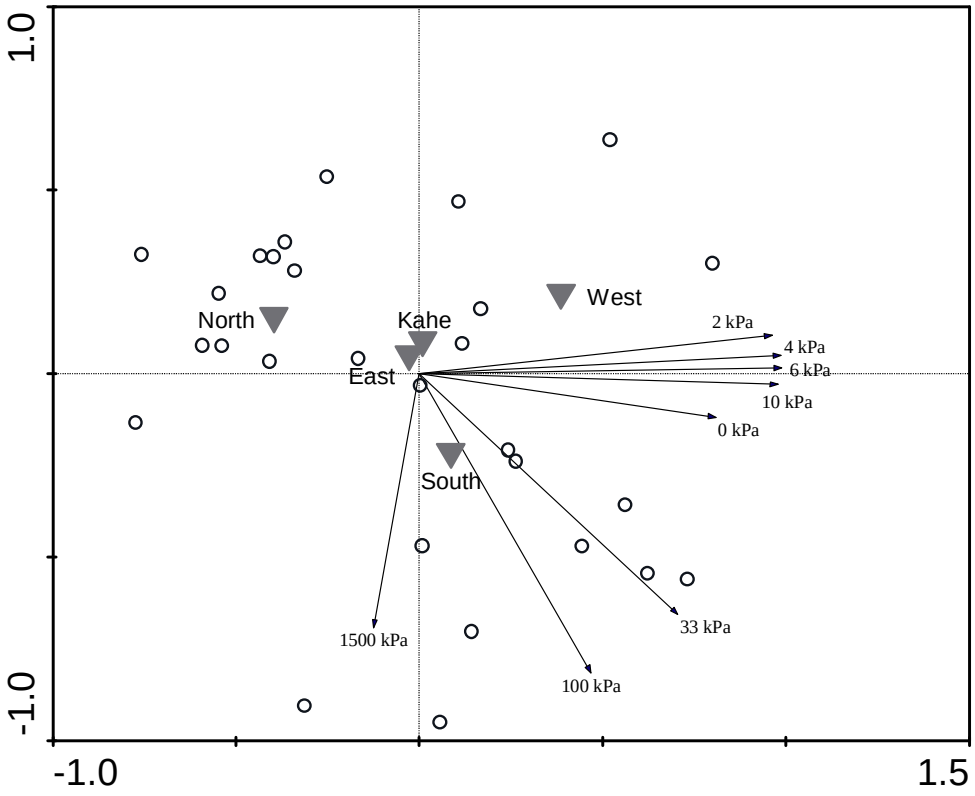

Figure 5.10: Principal component analysis (PCA) of water retention characteristics for the A horizon. Open circles represent each sample point, inverted solid triangles represent the average value for samples collected from the five regions and the vectors represent the magnitude and direction of change for the volumetric water content at various matric potentials (-kPa). Sample point P4N was excluded as an outlier, while some of the measured WRC values are not shown for sake of clarity (-1 and -8 kPa). PCA axis 1 accounted for 68.4 % and PCA axis 2 accounted for 11.8 % of the variation in the data (86.4 % combined).

Figure 5.10 shows that there is a positive correlation between the higher potentials (0 to -10 kPa), but this is considerably weaker for lower potentials (-33 kPa and -100 kPa). At -1500 kPa there is no correlation between the wet range and a weak correlation with -33 kPa and -100 kPa. The average response for each sample location indicates that the south samples had the highest water content in the drier range (-33 kPa, -100 kPa and -1500 kPa), while the western samples tended to have higher wet range water contents. The northern samples typically had the lowest water content over the whole potential range, while east and Kahe were similar. Principal component analysis in the B horizon has a similar pattern with the exception that the north and east have the lowest water retention across the whole range (Figure 5.11).

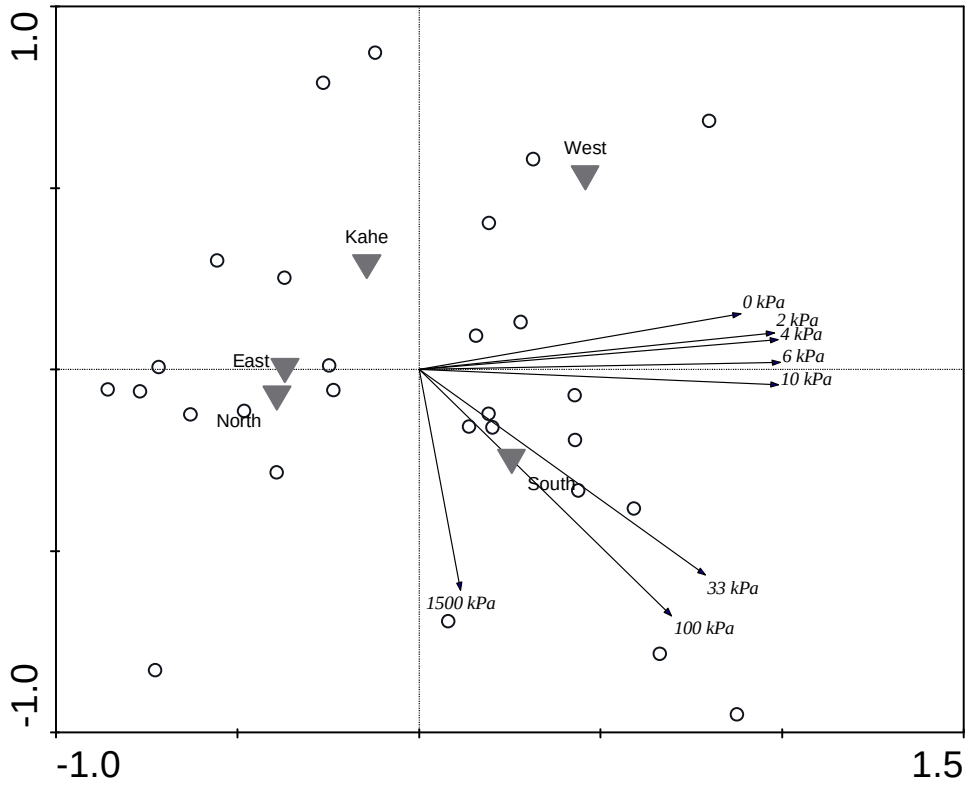

Figure 5.11: Principal component analysis (PCA) of water retention characteristics for the B horizon. Open circles represent each sample point, inverted solid triangles represent the average value for samples collected from the five regions and the vectors represent the magnitude and direction of change for the volumetric water content at various matric potentials (-kPa). Sample point P4N was excluded as an outlier, while some of the measured WRC values are not shown for sake of clarity (-1 and -8 kPa). PCA axis 1 accounted for 72.8 % and PCA axis 2 accounted for 15.9 % of the variation in the data (88.7 % combined).

The reason for higher water retention between -33 kPa and -1500 kPa in the south may be related to greater quantities of amorphous minerals which increase the porosity, whilst the greater water retention in the wet range for the west may be attributed to the higher sand content in this area (Section 5.3.5). Although no correlation was found between any of the measured matric potentials and ferrihydrite or allophane contents (Appendix 5.19), the greater amorphous material in the south of the estate (Section 5.1) is very likely a contributing factor to the higher water retention in this area. Allophane also contributes to high specific surface area which increases the soils water holding capacity (Gama-Castro *et al*., 2000; McDaniel *et al*., 2011).

The soils sampled from TPC have a volumetric water content in the A horizon between 0.22 and 0.48 $m^3 m^{-3}$, 0.15 and 0.40 $m^3 m^{-3}$ and 0.09 and 0.24 $m^3 m^{-3}$ at -10, -33 and -1500 kPa, respectively, and in the B horizon between 0.18 and 0.53 $m^3 m^{-3}$, 0.13 and 0.51 $m^3 m^{-3}$ and 0.09 and 0.20 $m^3 m^{-3}$ at -10, -33 and -1500 kPa, respectively (Appendix 5.7). Gama-Castro *et al*. (2000), who studied volcanic ash soils in the Santiago floodplain of Mexico, found water retention at -33 kPa to be between 0.05 and 0.45 $m^3 m^{-3}$ and at -1500 kPa to be between 0.015 and 0.145 $m^3 m^{-3}$. Values above 0.40 and 0.10 $m^3 m^{-3}$ are considered to be high at -33 and -1500 kPa, respectively (Gama-Castro *et al*., 2000). Johnston (1973) studied the physical properties of soils commonly found in the South African sugar industry and determined the water retention at various tensions for different soil types (Table 5.5).

Table 5.5: Plant available water (PAW), readily available water (RAW) and water content (w w^{-1}) at -10, -33 and -1500 kPa for red, black and grey soils typically found in the South African sugarcane industry (modified from Johnston, 1973).

	Water content (w w^{-1})					
	Red soils		Black soils		Grey soils	
	A Horizon	B Horizon	A Horizon	B Horizon	A Horizon	B Horizon
-10 kPa	8.4 – 32.4	8.4 – 34.0	32.1 – 60.9	30.5 – 52.8	8.6 – 29.1	7.1 – 32.4
-33 kPa	6.0 – 26.6	5.7 – 31.2	31.2 – 55.4	29.4 – 49.7	5.2 – 27.8	3.3 – 30.8
-1500 kPa	2.7 – 23.7	2.3 – 26.3	21.5 – 39.0	23.1 – 37.1	2.2 – 20.6	1.1 – 24.2
PAW	0.85 – 1.60	0.82 – 1.38	1.12 – 2.19	1.0 – 1.66	0.96 – 2.0	0.79 – 1.36
RAW	0.52 – 1.20	0.37 – 0.89	0.33 – 0.79	0.36 – 0.68	0.40 – 1.21	0.35 – 0.84

If an assumption is made that the soils studied by Johnston (1973) have a typical bulk density of 1.2 g cm^{-3} then the volumetric water content range for TPC soils at -10 and -33 kPa is slightly higher than is typical for the red or grey soils sampled by Johnston (1973). At -1500 kPa the volumetric water content range of TPC soils has an upper limit similar to red and grey soils but the lower limit is higher than is commonly found.

In agreement with Gama-Castro *et al*. (2000), it is suggested that the high water retention of the majority of TPC soils at -1500 kPa is primarily due to the high specific surface area created by the very small particle size and the hollow, spherical micro-structure of allophane. Water retention is closely related to the degree of andic character in volcanic ash soils. Armas-Espinel *et al*. (2003) found that as the andic character of a soil decreased there was a decrease in the gravimetric water content. Armas-Espinel *et al*. (2003) attribute high water retention at higher tensions to intra-aggregate voids. At -33 kPa, the majority of TPC soils (89 %) have a volumetric water content between 0.20 and 0.40 m^3 m^{-3}. Samples with a volumetric water content of 0.40 m^3 m^{-3} and above include samples from fields 19A, 15B, 4C, 12C, 12, 10K, 5D. It is interesting to note that all of these fields are situated in the south of the TPC estate, suggesting greater meso-porosity which could be due to higher allophane content in this area. Although the meso-porosity of the soils in the south are not obviously greater than the other areas (Figure 5.9) this could be a case of outliers within the measured fields which affect the average result. A significant correlation ($r = 0.732$ $p < 0.001$) was found between OC and the water retained at a matric potential of -1500 kPa in the A horizon (Appendix 5.20), indicating that the OC is also playing a role in retaining adsorbed water at the lower matric potentials.

Sugar cane ideally requires an air-filled porosity of between 12 and 15 % and a total available moisture content of 15 % or more (Meyer, 2011). In all areas the average PAW is above 15 % and the air-filled porosity is approximately 15 % in the A horizon and slightly less in the B horizon (Table 5.6).

Table 5.6: Readily available water (RAW) and plant available water (PAW) in the A and B horizons for the five areas of TPC sugar estate.

Horizon	Area	RAW	PAW
		……..m^3m^{-3}……..	
A	North	0.09	0.18
	West	0.13	0.21
	East	0.10	0.19
	South	0.10	0.23
	Kahe	0.10	0.21
B	North	0.07	0.20
	West	0.12	0.20
	East	0.07	0.19
	South	0.08	0.24
	Kahe	0.08	0.22

5.3.3 Hydraulic conductivity

Measurements of saturated hydraulic conductivity (K_s) showed high variability between replicate samples from the same site in many of the fields measured (Appendix 5.9). The variability may be attributed to channels being present in some of the cores through white grub activity, root channels or the presence of stones (visual observation). Where channels create greater macro-porosity, the cores with higher K_s should correlate to greater water retention in the wetter range. However, there was no correlation ($r = 0.05$) found between K_s and saturated volumetric water content, suggesting that the variability in the cores was possibly due to boundary flow during K_s measurements. Boundary flow occurs when the soil in the core shrinks with drying and then does not regain its previous volume when it is re-wetted. According to Armas-Espinel *et al.* (2003) soils containing allophane can shrink substantially with drying. This shrinkage results in irreversible changes to the soil's physical properties (Harsh *et al*., 2002). It is therefore speculated that drying the soil cores to a matric potential of -100 kPa before re-saturating the cores and measuring K_s resulted in many cores undergoing shrinkage which resulted in boundary flow and variability in the K_s readings.

As hydraulic conductivity is related to the number, continuity and stability of soil pores (Bhattacharyya *et al*., 2006), it was expected that the K_s would be significantly lower in the

samples which contained higher levels of sodium, which would affect the pore characteristics due to clay dispersion and clogging of soil pores. However, due to the variability in K_s measurements between replicate cores taken from the same site this assumption could not be validated. Amorphous minerals induce soil aggregation and may aid in maintaining the soil structure in soils affected by high sodium (El Swaify *et al*., 1969). However, Armas-Espinel *et al*. (2003) found that the structural deterioration of volcanic ash soils in the Canary Islands irrigated with sodic water was not able to be counter-balanced by the amorphous minerals if Al_o was lower than 3 %, which resulted in very low K_s values (< 8 mm hr^{-1}). As the Al_o content of the measured TPC soils was lower than 3 % (Section 5.2.4) it is speculated that any beneficial aggregating affect of the amorphous material in the soil was likely less than the negative effects of sodium in the soils (Sections 5.4.4, 5.4.5 and 5.4.6).

5.3.4 Bulk density

The average bulk densities between the different areas indicate that the south area has a slightly lower bulk density (ρb) in both the A and B horizon compared to the other areas (Figure 5.12). This may be due to the south area developing a porous soil structure as a result of containing a higher proportion of amorphous material (Broquen *et al*., 2005) (Section 5.2.4) and having higher water soluble and exchangeable sodium concentrations (Sections 5.4.4, 5.4.5 and 5.4.6) than the other areas of the estate.

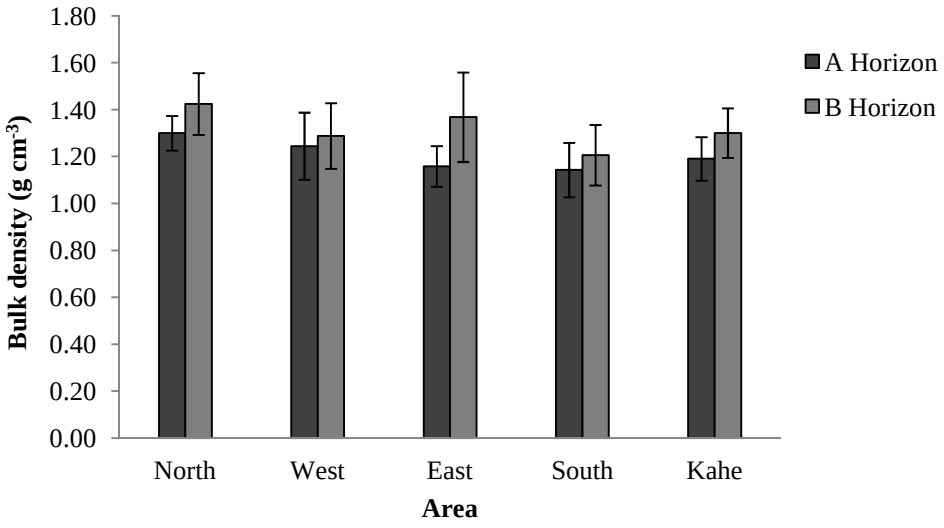

Figure 5.12: Bulk density of the A and B horizons of the various areas within TPC sugar estate.

There is a significant ($p < 0.05$) negative weak correlation between the exchangeable sodium and bulk density in the A horizon ($r = -0.5623$) and B horizon ($r = 0.5215$) (Appendix 5.20). These results suggest an increase in sodium concentration results in a decrease in ρb. Although ρb is not strongly correlated to $Al_o + ½ Fe_o$, allophane or ferrihydrite in the A or B horizons (Appendix 5.19), it is likely that the amorphous material is contributing to a lower ρb. A combination of sodium and amorphous material can lead to the development of "fluffy" soils with low bulk densities (Gama-Castro *et al*., 2000).

In the study by Gama-Castro *et al*. (2000) the ρb was not related to organic carbon (OC) and therefore they attribute the low ρb to the amorphous materials. Similarly, the OC and ρb of the studied TPC soils are not correlated for either the A or B horizon (Appendix 5.20). Although only one sample in the south area qualifies as having an andic soil ρb of below 0.9 g cm^{-3}, almost a third of the sampled soils in the A horizon of the east, south and Kahe area had a ρb below 1.1 (Table 5.7) indicating that these areas are most probably influenced to some extent by amorphous material.

Table 5.7: Percentage of samples within each area of TPC sugar estate with a bulk density of below 1.1 g cm^{-3} for the A and B horizon.

Area	Samples per area with a bulk density below 1.1 g cm^{-3} (%)	
	A Horizon	B Horizon
North	0	0
West	13	6
East	33	0
South	33	17
Kahe	29	0

In general, the ρb of the B horizon is slightly higher than the A horizon in all fields (Appendix 5.10) which is attributed to a greater proportion of smaller pores in the B horizon (Figure 5.9) which allows for a more compact soil. Sites which have higher ρb in the A horizon may be due to greater porosity in the B horizon caused by animal activity and/or root channels.

5.3.5 Particle size distribution

The percentage of sand, silt and clay varies within areas and in general is similar between areas (Figure 5.11).

a)

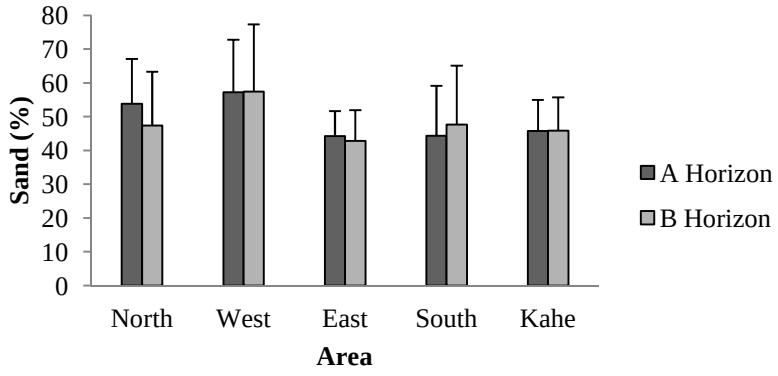

b)

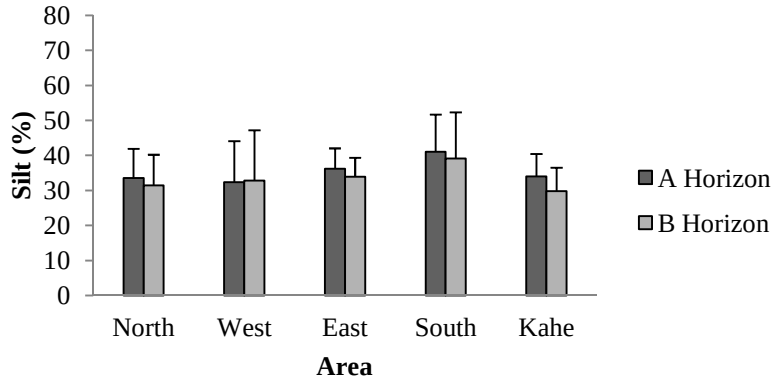

c)

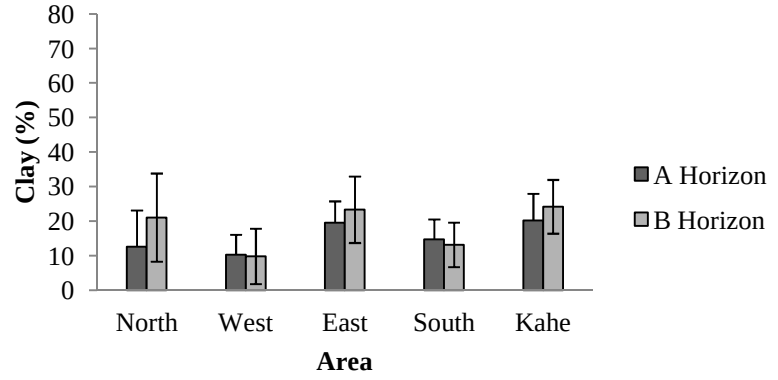

Figure 5.13: The percentage of a) sand, b) silt, and c) clay of the various areas of TPC sugar estate for the A and B horizons.

The average texture for the north, east, south and Kahe in both the A and B horizons is loam, whereas in the west the average texture for the A and B horizons is sandy loam. There were also a number of sandy loam samples in the south. The greater percentage of sand in the west and south areas indicate the alluvial nature of many of these soils. Meyer *et al*. (2009) report four main textural groups, which are related to the parent material, of which about 58 % were sandy loams to loamy sands and about 40 % sandy clay loams. The heavy clay soils found on the volcanic parent material in the far north accounted for less than 1 % and the sandy alluvial soils scattered over the estate accounted for less than 3 %. The sandy and silty alluvial soils were mostly found in the west area, while the medium clay soils formed by a mixture of volcanic parent material and alluvium were found in the north and north east (Meyer *et al*., 2009). This textural distribution is similar to that found in this study. A full table of results is given as Appendix 5.11.

In the A horizon, the north and west areas have a slightly higher sand and lower clay content than the other areas. In the north this may be a result of the shallower soils where there is less soil comprised of deposited material and the soil present is mainly a result of direct weathering from the volcanic parent material. In the west, the coarser soil texture is probably a consequence of the nature of the alluvially deposited material in some fields. The south area has a somewhat finer texture, with a slightly higher silt content than the other areas in the A horizon. This again is likely a result of alluvial deposition in many of these fields. The B horizons of the various areas have a similar proportion of sand, silt and clay to their respective A horizons.

5.3.6 Specific surface area

The dominance of micro-pores in allophane results in soils that contain allophane having high specific surface areas (SSA) and consequently high adsorption capacities (Paterson, 1977). Consequently, soils containing allophane typically have a high water retention even at the low matric potentials (McDaniel *et al*., 2011). Bartoli *et al*. (2007) found that the micro-pore surface area of non-allophanic and allophanic soil horizons ranged from 0 to 110 $m^2\ g^{-1}$ and that this was positively related to the allophane content. The values reported for SSA using nitrogen adsorption techniques vary widely in the literature. Aomine and Otsuka (1968) and Paterson (1977) report values up to 170 $m^2\ g^{-1}$, whereas Lowe (1993) gives values between

400 and 900 m^2 g^{-1} and Brady and Weil (2002) report values between 100 and 1000 m^2 g^{-1}. Table 5.8 presents the SSAs of the measured samples across TPC sugar estate.

Table 5.8: Specific surface area of selected PSU clay (< 2 µm) samples from TPC sugar estate.

Area	Sample	Specific surface area (m^2 g^{-1})
North	N91 A	97.34
	N91 B	113.06
West	P4N A	84.78
	P4N B	144.49
East	B3 A	99.07
	E6 B	102.19
South	12C A Good	91.02
	12C B Good	93.80
	10K A Good	110.84
	10K B Good	116.44
Kahe	KH4 A	126.17
	KH4 B	145.94
	KH29 A	120.39
	KH15 B	115.58

Non-volcanic ash soils, unless smectitic, typically have much lower values than was found across the TPC estate. As no smectitic minerals were found in any of the soils it is concluded that the high SSA is a function of the allophane present in the soil. Hughes *et al*. (2009) studied a variety of soil clays dominated by kaolin minerals and a number of reference kaolins after removal of iron oxides by CBD treatment. The soil clays differed in the proportions and properties of kaolin types and included clays dominated by small kaolinite particles and halloysites. They found that the SSA of the soil kaolins (without allophane impurities) varied from about 40 to 90 m^2 g^{-1} with the highest values in clays from Indonesian soils formed on volcanic tuff dominated (over 90%) by short, tubular halloysite. Given these results and using the lower allophane SSA value reported by Lowe (1993), Table 5.9 has been constructed.

Table 5.9: Hypothetical calculation for clay BET specific surface area at TPC.

Mineral	Assumed BET surface area (m^2 g^{-1})	Assumed percentage of mineral in the clay fraction	Proportion of the clay surface area (m^2 g^{-1})
Allophane	400	5	20
Halloysite (tubular)	80	80	64
Kaolinite (< 0.2 μm)	55	15	8.25
Total			92.25

From Table 5.9 the effect that only small amounts of allophane may have on the SSA of the TPC soils can be seen, whereby 5 % allophane constitutes approximately 22 % of the total SSA. A similar calculation was carried out by Lowe (1993) where he showed that only 1 % of allophane or ferrihydrite accounted for 85 % of the total soil mineral surface area in his hypothetical soil. The total SSA calculated in Table 5.9 may be underestimated compared to the measured values due to the presence of iron oxides in the clays, as removal of iron oxides by CBD was not done prior to analysis. Inclusion of the SSA created by the iron oxides would inflate the BET results (Sei *et al*., 2006). Similarly small amounts of other minerals not considered in Table 5.9 such as illite or HIV would also lead to an underestimation of the true SSA value.

The high SSA values for clay fractions from soils across TPC due to their mineralogy are in agreement with the clay XRD and TEM results, where weak XRD patterns with high backgrounds and the presence of amorphous material in the TEM images also indicate the presence of allophane. Although the soils across the estate are dominated by halloysite and small kaolin particles it is likely that the presence of only small amounts of allophane has a strong influence over their physical and chemical properties. The high adsorption capacity due to the high SSA affects the water holding capacity, especially at the low matric potentials. Although no correlation was found between SSA and the volumetric water content at -1500 kPa (Appendix 5.20), the large amount of water retained at -1500 kPa is considered to be a result of the large adsorption capacity created by the micro-porous allophane in the studied soils.

5.4 Chemical analysis

5.4.1 Organic carbon

In all fields, other than R3S Bad, C2, 11, 7[1] and KH15, the soil OC content is higher in the A horizon than in the B horizon. The average OC is 1.3 and 0.9 % in the A and B horizon, respectively. Appendix 5.12 presents a full table of results.

The ash layers sampled in field R8 and from the borehole in the north both have a very low OC of 0.1 and 0.2 %, respectively. This is due to both these layers being deep within the soil profile and therefore there is little incorporation of organic matter.

Overall, there is little difference in OC between the different areas of TPC in both the A and B horizons (Table 5.10).

Table 5.10: Average soil organic carbon (%) for each area of the TPC estate.

Area	n	A Horizon	B Horizon
North	11	1.4 ± 0.3	0.7 ± 0.2
West	11	1.4 ± 0.5	0.9 ± 0.4
East	14	1.1 ± 0.4	0.6 ± 0.2
South	28	1.5 ± 0.5	1.1 ± 0.8
Kahe	8	1.1 ± 0.3	0.8 ± 0.3

Similarly to the values reported by Meyer *et al*. (2009), OC throughout the majority of the estate ranges between 0.5 and 1.5 % and is thus classified as low (Meyer *et al*., 2009). Some fields have OC ranging between 1.5 and 2.5 % and are classified as moderately low (Meyer *et al*., 2009). Soils with moderately low OC were mostly found in the south area.

Paired t-tests between the good and bad patches of cane growth indicate that in the A horizon the good patches have significantly higher OC than the bad patches ($p = 0.016$) but there is no significant difference between the good and bad patches in the B horizon ($p = 0.335$). The higher OC in the good patches of the A horizon is most probably due to a greater amount of biomass created by the better cane growth, whereas those patches of poorly growing cane are

likely to have less biomass and thus less material contributing to the OC. Practically, there is little difference in OC between the good and bad patches in both the A and B horizon, as in all cases the average organic carbon percentage is low (< 1.5 %), except in the A horizon of the good patches where it is moderately low (Table 5.11).

Table 5.11: Average soil organic carbon (%) for the good and bad patches in the A and B horizons.

	Soil organic carbon (%)
A Horizon Good	1.6
A Horizon Bad	1.3
B Horizon Good	1.0
B Horizon Bad	0.9

5.4.2 pH (H_2O)

The soils in the south area have the highest average pH in both the A and B horizon, followed by the west area (Figure 5.14).

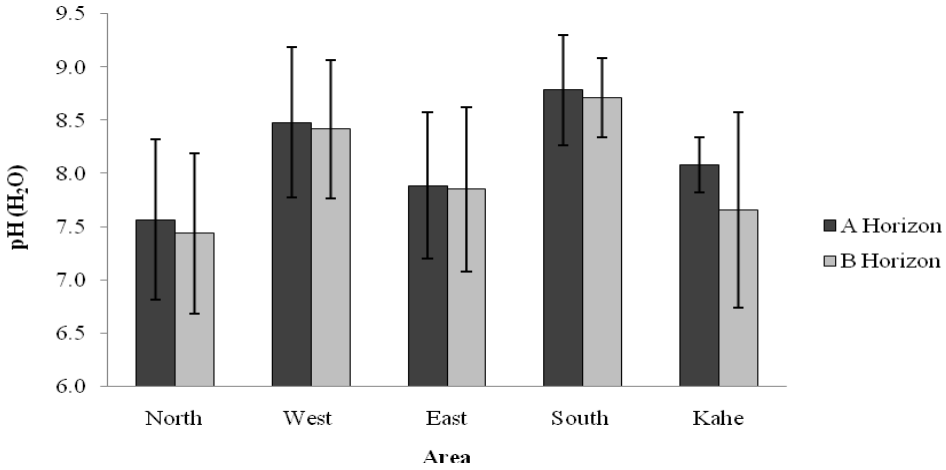

Figure 5.14: pH (H_2O) for the different areas of TPC sugar estate for the A and B horizons.

The lowest pH values are found in the north (Figure 5.12), followed by the fields in the southern part of the north area and east area. The northern section of the Kahe area has pH values similar to those in the east, while the southern section of Kahe has pH values similar to those in the south and west areas of the estate (Appendix 5.13). This follows the same trend

reported by Meyer *et al*. (2009) following the 2004 soil survey carried out on TPC estate. This trend is a combined result of lower pH values in the north possibly caused by higher rainfall in this area (Meyer *et al*., 2009), although there is likely a parent material effect also, as well as higher pH values in the south and west which are caused by higher levels of sodium in the soil (Sections 5.5.4, 5.5.5 and 5.5.6). Exchangeable sodium is unable to compete with H^+ ions as strongly as Ca and Mg on exchange sites and thus a dominance of sodium in the soil means that hydrolysis occurs at a much greater extent with the addition of irrigation and/or rainwater, and consequently soil pH rises (Richards, 1954). Furthermore, soils in the south and west contain appreciable quantities of sodium carbonates which likely undergo alkaline hydrolysis to cause a rise in pH (Richards, 1954).

A significant ($p < 0.05$) correlation was found between exchangeable sodium and pH in both the A and B horizons ($r = 0.848$ and $r = 0.834$, respectively) (Appendix 5.21). The high level of sodium in the south can be attributed to irrigation with poor quality water and surface salt accumulation through capillary rise from perched water tables. The west area is generally irrigated with good quality irrigation water and has a relatively low water table and thus it is likely that the sodicity in the west is due to the low soluble Ca and Mg concentrations in the soil solution in relation to the sodium which results in a high sodium adsorption ratio. Typical pH values for sodic (non-saline) soils range between 8.5 and 10 (Richards, 1954).

It is interesting to note that patchy cane growth was very pronounced in the south and west areas of the TPC estate, and this visual observation is linked to the higher pH values (Table 5.13). Sugarcane can grow in soils with a pH between 5 and 8.5, with the ideal soil pH being 6.5 (www.sugarcanecrops.com/soil_requirement). It is suggested that high pH values related to the high sodium content is the primary cause for the patches of poorly growing cane. The dominance of sodium tends to results in the dispersion of soil particles which then clog soil pores and negatively affect the soils permeability to water and air. Furthermore, although high pH does not directly affect plant growth it frequently results in the lowering of plant nutrient availability (Richard, 1954). Of the seven fields where samples were taken from good and bad patches of sugarcane growth, the pH in the A horizon is higher in the bad patch for fields 12C, 1 and R3S but similar for all other fields. In the B horizon the pH is higher in the bad patch in all fields except R3S and 12C (Table 5.12). Paired t-tests between the good and bad patches of cane growth indicate a marginally significant difference in pH in the A horizon ($p = 0.063$) but no significant difference in the B horizon ($p = 0.313$).

Table 5.12: pH (H_2O) of the fields measured in a patch of poorly growing cane (Bad) and better growing cane (Good) for the A and B horizons.

Field	Good	Bad	Good	Bad
	A Horizon		B Horizon	
O3	8.86	8.85	8.78	9.02
10K	9.00	9.86	8.89	9.40
11C	8.71	8.75	8.80	8.97
12	8.85	8.76	8.88	9.09
12C	8.53	8.94	8.56	8.44
1	8.37	8.77	8.18	8.92
R3S	8.96	9.35	9.06	8.52

pH (H_2O) comparisons between the good and bad patches of cane growth were carried out by TPC laboratory on fields F3 and 16C at two sampling times. The results of the first sampling suggest that the pH is higher in the bad patches than in the good patches, especially in the upper layers. However, results from the second sampling indicate a less clear trend.

The pH measured on the crust sample collected from field 10K is very high (Appendix 5.13), suggesting a high sodium percentage which explains the formation of a crust. The dominance of exchangeable sodium in the top soil causes dispersion of clay particles which results in the soil surface sealing. A number of fields in the south were observed to have surface crusts and it is suggested that further analysis of these fields is necessary in order to determine their impact on soil water relations, particularly infiltration rate (Section 5.3.1).

5.4.3 Electrical conductivity

Figure 5.15 shows that in the A horizon the electrical conductivity of a saturated paste sample (EC_e) of the south area is considerably higher than the other areas of the estate with an average of 276 mS m^{-1}, followed by the west and Kahe areas. In the B horizon the EC_e is similar between areas with the south and Kahe having a slightly greater value than the east, west and north areas. In the A horizon the EC_e is significantly ($p < 0.05$) correlated to the exchangeable sodium ($r = 0.728$) and the exchangeable calcium ($r = 0.671$), whereas in the B

horizon, no correlations between EC_e and the exchangeable cations was found (Appendix 5.21). The very large standard deviations, particularly in the A horizon of the south area, indicate that the EC_e varies greatly between fields within the same area, and in many cases varies considerably within the same field (Appendix 5.14). In the A horizon, fields F1S, L5, R3S (2.1) and R5N have a much larger EC_e than the other fields within their respective areas. Likewise, in the B horizon, fields BO4, KH7, N84, R3S (2.1), R3S (2.3) and R5N have a much larger EC_e than the other fields within their area. In the south area, the EC_e values vary greatly between the measured fields in both the A and B horizon.

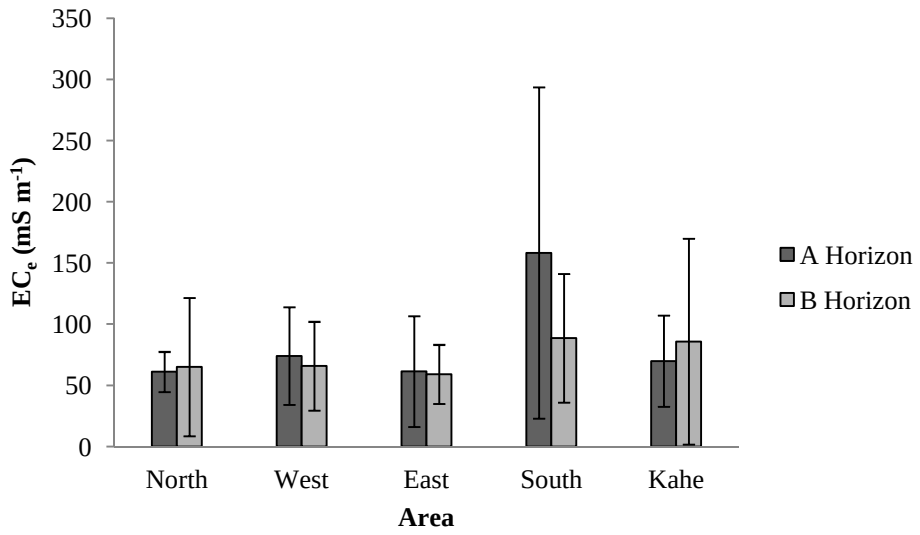

Figure 5.15: Electrical conductivity (ECe) of a saturated paste sample for the various areas of TPC sugar estate in the A and B horizons.

A larger EC_e in the south may be a consequence of higher sodium content present in the south which increases the overall soluble salt content of the soil (Sections 5.4.4, 5.4.5 and 5.4.6). An EC_e of greater than 200 mS m^{-1} indicates a saline soil (Meyer *et al*., 2009) and in the A horizon 9 % of the east area and 24 % of the south area are saline, with the fields with the greatest salinity being in the south. In the B horizon, only fields KH7 and 4D (2.1) can be classified as saline. A considerably higher salinity in the A horizon compared to the B horizon in the south suggests that irrigation with poor quality water in the south, coupled with a high water table, is causing a build-up of salts on the soil surface through capillary rise and surface evaporation. Similarly, previous work done by Leroy (2004) on TPC found the highest average EC_e in the south (n = 21), followed by the west (n = 5) with a considerably higher EC_e in the topsoil compared to the subsoil in the south.

A high level of variability in EC_e within the various areas could be attributed to variable amounts of irrigation water containing sodium being applied over a long period, as well as inherent soil properties differing between fields within the same area.

5.4.4 Water soluble cations of the saturated paste

The water soluble Ca, Mg and K of the saturated paste is similar between the different areas of TPC sugar estate in both the A and B horizons, except for Ca and Mg in Kahe which is slightly greater than the other areas (Figure 5.16). The higher Ca and Mg in Kahe is due to field KH7 (Appendix 5.15) which explains the high standard deviation, especially in the B horizon. The reason for higher Ca and Mg in KH7 is unclear. The water soluble Na of a saturated paste in both the A and B horizons is greatest in the south area, followed by the west (Figure 5.16). The lowest water soluble Na occurs in Kahe for both the A and B horizons. Consequently, the SAR follows the same trend as for the water soluble Na (Figure 5.16). A full table of results is provided as Appendix 5.15.

The south and west areas are situated along the river which is high in basic cations and HCO_3^- (water quality data supplied by TPC). Consequently, alluvial deposition or irrigation with river water could increase the salt concentration of these soils. Increased Na in the south is attributed to a combination of irrigation with poor quality water and insufficient drainage. The higher water soluble Na in the west can be attributed to the irrigation of this area with good quality irrigation water in the presence of carbonates. The excess Ca and Mg are either leached out of the profile or precipitate as Ca and Mg carbonates which results in sodium being the dominant cation in solution (Richards, 1954). Meyer *et al*. (2009) used a critical SAR value of 8 to interpret sodicity as this value represents the average recommended by SASRI for duplex soils (SAR 6) and non-duplex soils (SAR 10). Based on this value, 53 % of the soils in the south can be classified as sodic. The soil sampled from Out 2, F1S in the east, as well as fields R3S Bad and R5N in the west are also classed as sodic. Similarly, previous work carried out by Leroy (2004) on TPC found the highest average SAR in the south (n = 21), and west (n = 5) areas.

a)

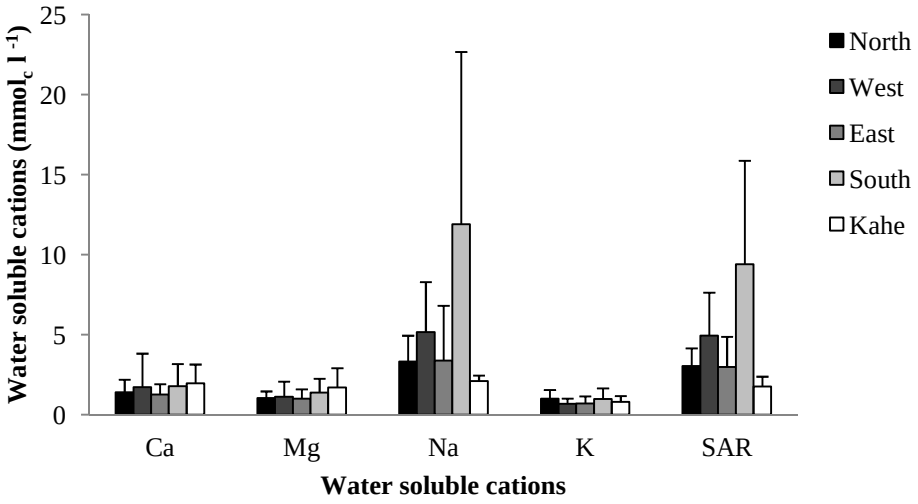

b)

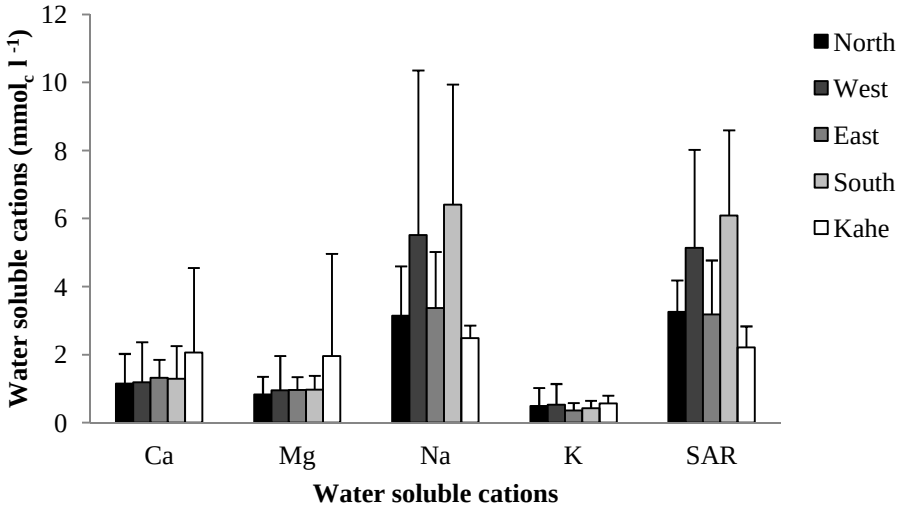

Figure 5.16: Calcium (Ca), magnesium (Mg), sodium (Na), potassium (K) and the sodium adsorption ratio (SAR) for the different areas of TPC sugar estate in the a) A horizon and b) B horizon.

The high standard deviations that exist for the water soluble cations can be attributed to the large variability between fields within a particular area. In the east, the water soluble Na of field F1S is greater than other fields in the east. Samples from fields KH27 and KH7 in Kahe, L5 in the west and 4D in the south have higher water soluble Ca and Mg than the samples taken from the other fields in their respective areas. The south has very variable water soluble Na between sampled fields, with some fields being particularly high. R3S Bad, R3S (2.1) and R5N from the west also have high water soluble Na values (Appendix 5.15). This variability

is probably related to the different fields within an area receiving different amounts and quality of irrigation water, as well as the particular field's inherent soil properties. Variability may be caused by the different fields within an area having variable water table heights which can affect the amount of cations which are dissolved and leached, as well as variable clay and allophane contents.

Fields 10K, 12 and 5^1, indicate that there is a much higher SAR in the poorly growing cane (Bad) compared to the patch of better growing cane (Good), particularly in the A horizon (Table 5.13).

Table 5.13: The sodium adsorption ratio (SAR) of the A and B horizons in good and bad patches of cane growth.

Area	Field	SAR	
		A Horizon	B Horizon
West	R3S Bad	8.72	8.77
	R3S Good	nd*	5.24
East	O^3 Bad	3.08	4.37
	O^3 Good	4.07	3.01
South	1 Bad	4.14	4.79
	1 Good	4.02	3.62
	10K Bad	20.15	10.01
	10K Good	9.99	6.97
	$11C^1$ Bad	2.90	4.04
	$11C^1$ Good	2.23	3.09
	12 Bad	14.52	9.11
	12 Good	5.57	5.14
	12C Bad	7.67	6.47
	12C Good	8.56	4.65
	5^1 Bad	23.87	12.52
	5^1 Good	9.14	9.96

* nd – not determined

Higher SAR values in the bad patches indicate that poor cane growth is at least in part a consequence of high water soluble sodium. As the concentration of exchangeable sodium increases the soil becomes more dispersive and consequently clay particles block soil pores resulting in soils of low permeability which are prone to crust formation. This unfavourable soil structure limits seedling emergence and results in poor soil water and aeration levels for plant growth (Richards, 1954).

5.4.5 Water soluble cations of the soil

The water soluble Mg and K of the soil is similar between the different areas of TPC sugar estate in both the A and B horizons. Calcium is similar between areas in the B horizon but slightly greater in the south and west areas in the A horizon. The Na is highest in the south and west areas in both horizons. In the A horizon the SAR is highest in the south and north, closely followed by the west area, while the SAR in Kahe is substantially lower than the other areas (Figure 5.17). The higher Ca in the south and west prevent the SAR in these areas from being substantially greater than the other areas. In the B horizon the SAR is greatest in the south and west, following the same trend as for Na (Figure 5.17). A full table of results is provided in Appendix 5.16.

a)

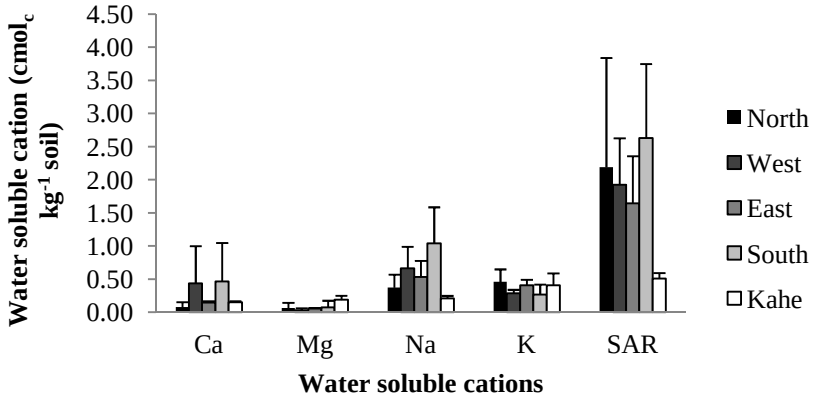

b)

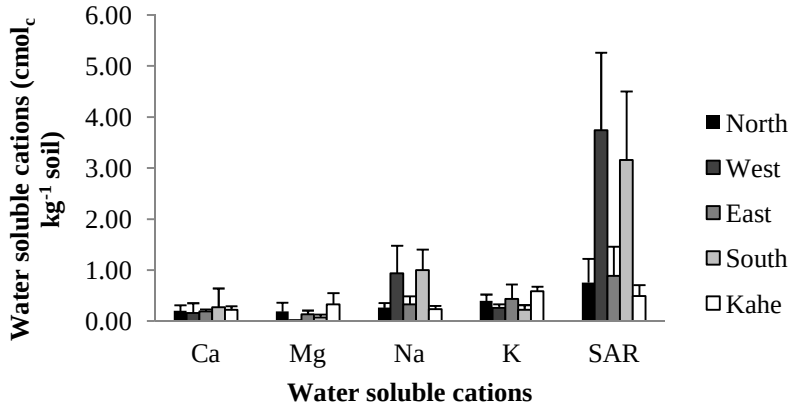

Figure 5.17: Water soluble calcium (Ca), magnesium (Mg), sodium (Na) and potassium (K) and the sodium adsorption ratio (SAR) for the different areas of TPC sugar estate in the a) A horizon and b) B horizon.

5.4.6 Exchangeable cations

The exchangeable Ca, Mg and K are similar between areas with the north having the lowest values in both the A and B horizons (Appendix 5.17). The exchangeable Na is highest in the south and west areas in both the A and B horizons (Figure 5.18) and consequently the sum of exchangeable bases is highest in the south and west areas, followed by Kahe and the east area, with the lowest value for the north area in both horizons (Figure 5.18).

The higher exchangeable Na in the south and west are possibly due to these areas receiving cations through deposition of alluvial material and being irrigated with water high in sodium and bicarbonates, whereas the lower exchangeable cations in the north is likely due to these soils being predominately comprised of cations weathered directly from the acidic parent material as no alluvial material is present.

a)

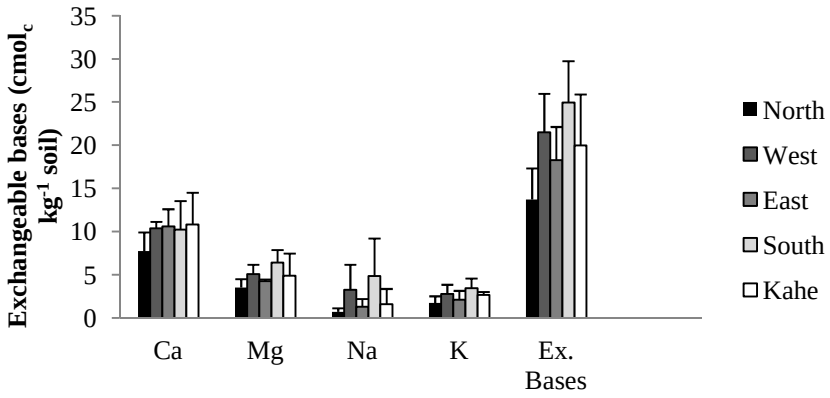

b)

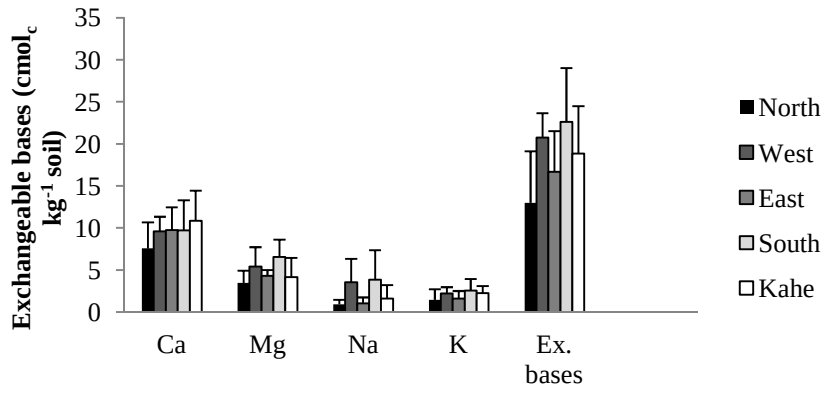

Figure 5.18: Exchangeable calcium (Ca), magnesium (Mg), sodium (Na), potassium (K) and the sum of exchangeable bases (Ex. bases) in the different areas of TPC sugar estate in the a) A horizon and b) B horizon.

Although there is no significant difference ($P \geq 0.05$) between the good and bad patches of sugarcane growth for any of the measured exchangeable bases in either the A or B horizon, fields 5^1 and 10K have considerably higher Ca and lower Na in the patch of better growing cane compared to the patch of poorly growing cane (Appendix 5.17). This suggests that the exchangeable cations are likely to affect cane growth to some degree. However, levels of the various exchangeable cations in the soil may not be the only factor affecting cane growth.

5.4.7 Cation exchange capacity

The cation exchange capacities of TPC sugar estate soils are very similar in both the A and B horizons and between areas with a range between 13.5 and 18.9 $cmol_c\ kg^{-1}$ soil (Figure 5.19). A full table of results is given as Appendix 5.18.

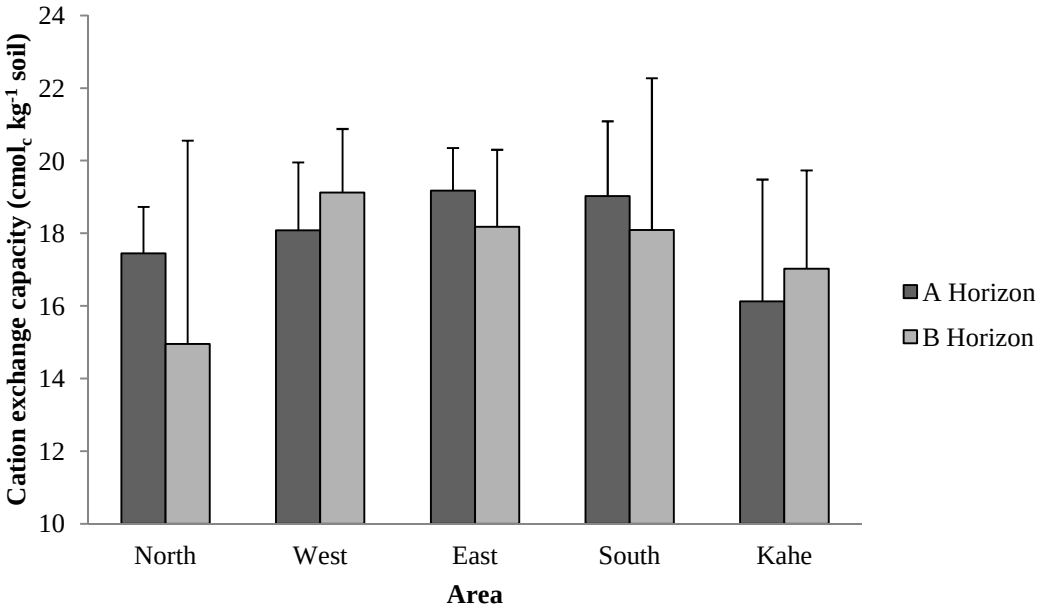

Figure 5.19: Cation exchange capacity in the different areas of TPC sugar estate in the A and B horizons.

This result differs slightly from the cation exchange capacity (CEC) measured by the ammonium acetate method used previously to analyse TPC soils (Meyer *et al*., 2009). The ammonium acetate method indicates a higher CEC in the south and the lowest CEC in the north, and generally the CEC values given for the ammonium acetate method are higher than

those for the $BaCl_2$-TEA method. It is suspected that the reason for the difference in results is that the ammonium acetate CEC results were not corrected for the water soluble fraction. Inclusion of the water soluble fraction into the CEC yields the same trend as that reported when the ammonium acetate method for CEC was used. Furthermore, the $BaCl_2$-TEA method is a more accurate measurement of CEC when soils contain allophane due to the variable charge nature of allophane. The use of $BaCl_2$-TEA buffers the soil pH at 8.2 and therefore limits the effect of pH dependent charge which the ammonium acetate method does not take into account.

The CEC is commonly associated with the amount of OM and clay percentage (Tsai *et al*., 2010). However, no strong correlation was found between CEC and OC or clay percentage (Appendix 5.20). Furthermore, for selected samples collected during the 2004 soil survey at TPC at depths of between 0 and 30 cm, 30 and 60 cm, and 60 and 90 cm, no correlation ($r = -0.18$, 0.13 and 0.12, respectively; $p < 0.05$) was found between CEC and clay content. This suggests that the CEC of TPC soils is primarily due to their volcanic ash content. Maderia *et al*. (2003) found a positive correlation between CEC and OC and CEC with Al_o. Gama-Castro *et al*. (2000) found a positive correlation between CEC and pumice content but no correlation was found between CEC and OC, indicating OC contributes only a small extent to the negative charges on the soil. Although there was no correlation found between CEC and ferrihydrite ($r = 0.17$), or Al_o ($r = 0.23$) or $Al_o + ½ Fe_o$ ($r = 0.33$), the CEC range found for the TPC soils are similar to Hepper *et al*. (2006) who found a CEC ranging between 9.28 and 18.01 $cmol_c\ kg^{-1}$ soil in ash-enriched soils compared to a CEC of between 4.07 and 15.56 $cmol_c\ kg^{-1}$ soil in ash-free soils. Ndayiragije and Delvaux (2003) found a CEC of 11 $cmol_c\ kg^{-1}$ soil on an Andisol with low activity clays (i.e. gibbsite, allophane, kaolinite and hydroxyl Al interlayered 2:1 minerals) from the Island of Basse-Terre, Guadeloupe, in the French West Indies.

CHAPTER 6

GENERAL DISCUSSION, CONCLUSION AND RECOMMENDATIONS

The mineralogy of the soils at TPC sugar estate reflects the influence of past volcanic activity in the area. The weathering of volcanic parent material and previously deposited volcanic ash over the estate result in these soils containing poorly crystalline material as well as more crystalline minerals. Sanidine and a mixture of other K-feldspar minerals have weathered from the volcanic parent material and undergone further weathering to form halloysite and then, in places, gibbsite. The deposition of volcanic ash over the estate has led to the presence of allophane in the soils, although much has presumably weathered to halloysite and kaolin. The co-existence of allophane, halloysite, kaolin and gibbsite suggest that the soils over the estate have weathered at various rates and points towards the alluvial nature of the soils where less weathered material has been periodically deposited over older, more weathered material. The amorphous aluminium, iron and silica extracted by the acid oxalate procedure indicate relatively low concentrations of ferrihydrite and allophane across the estate, as well as an $Al_o + ½ Fe_o$ ratio of less than 2, which is a consequence of these minerals weathering to more crystalline forms. However, the south and west areas have the highest average ferrihydrite content and $Al_o + ½ Fe_o$ ratios. This is likely a consequence of the soils in those areas receiving less weathered material due to alluvial deposition along the Kikuletwa River which is on the western boundary of the estate. The sandy loam texture of many of the soils sampled in the south and west, rather than the loam texture of the majority of soils on the other parts of the estate, indicates that these areas receive a greater contribution of alluvially deposited material. Allophane content is greatest in the east, south and west areas although there is a large standard deviation across all areas which probably reflects the alluvial nature of the soils, as well as uneven ash deposition in the past. Kahe has the lowest ferrihydrite and allophane content of all the areas, suggesting that this area has been least affected by volcanic materials in recent times.

Due to the small particle size and structure of allophane, even small quantities can make a significant contribution to the physical and chemical properties of the soil by increasing the specific surface area. Specific surface area measurements for the soil clays across TPC are relatively high and it is estimated that as little as 5 % allophane can contribute at least 22 % of the total surface area due to allophane being an essentially micro-porous material.

Consequently, in all areas the micro-pores account for the largest percentage of the porosity and the soils have a large adsorption capacity and thus a large cation exchange capacity and water retention capacity, particularly at the higher matric potentials (above -33 kPa).

The water retention results clearly indicate the effects of allophane over the TPC estate. In the south area, the water retained between 0 and -100 kPa is slightly higher than at the other matric potentials and could be a consequence of a higher content of allophane. According to Gama-Castro *et al*. (2000), a volumetric water content above 40 $m^3 m^{-3}$ at -33 kPa is high and many fields in the south meet this requirement, again suggesting the effect of more allophane in this area. At -1500 kPa the water retained in all areas is high, as considered by Gama-Castro *et al*. (2000).

A high water retentivity across TPC generally ensures sufficient plant available water for sugarcane. However, due to the dominance of micro-pores and large adsorption capacities these soils may be prone to an air-filled porosity of less than the ideal for sugarcane of 15 %, especially if soils are over-irrigated. This is particularly relevant in the south and west areas where there seems to be more allophane present.

Although the water retentivity is affected by the mineralogy, variability at the various measured matric potentials across areas and within the same field limits further interpretation. Variability is caused by different pore size distributions which may be caused by textural differences in some fields due to old river channels, stoniness, structural stability of the soil, presence of animal burrows and/or recent soil disturbance such as harvesting. Therefore it is suggested that the water retention at the lower tensions is a function of these variables whilst the water retained at the higher matric potentials is a function of the increased adsorption capacity and micro-porosity created by the presence of allophane and other poorly ordered clay minerals.

Generally, the A horizon retains more water than the B horizon at the lower tensions, while the B horizon retains more water at the higher tensions. This is a consequence of greater macro-porosity in the A horizon and the higher meso- and micro-porosity in the B horizon and its higher bulk density, likely caused by the higher clay percentage. A comparison between the water retention at the various matric potentials for the good and bad patches of cane growth did not indicate any trends and thus cane growth seems to not be affected by the

amount of water retained in the soil. The poor cane growth seems to rather be related to the amount of sodium in the soil.

The patchy cane growth is more prevalent in the south and west areas of the estate. The south area has the highest pH, EC_e and SAR, followed by the west area, as a result of the higher sodium concentrations (exchangeable and soluble) in these areas. In the south, increased sodium concentration is exacerbated by use of poor quality irrigation water and, possibly, strong capillary rise from perched water tables. This increase in sodium is mirrored by somewhat greater amounts of organic carbon (a function probably of reduced microbial activity) than elsewhere on the estate where organic carbon values are low and lower bulk density resulting in 'fluffy' soils due to a combination of the sodium and higher content of allophane. In the west, pH and SAR are high due to the dominance of exchangeable sodium and presence of sodium bicarbonate which increase the rate of hydrolysis with the addition of irrigation and rainwater. The bicarbonate present in the irrigation water causes the Ca and Mg to precipitate whilst Na remains in solution and consequently the SAR increases. The SAR was higher in the poor cane growing areas compared to where cane was growing better, particularly in the A horizon. The high SAR and EC_e in the south, particularly in the A horizon, suggest that salts are brought to the soil surface from the perched water tables through capillary rise action. The presence of allophane, and thus the dominance of micro-pores, enhances such a process.

Sodicity is also the main influencing factor affecting infiltration rate across TPC, rather than the mineralogy. The infiltration rate of TPC soils, especially in the south of the estate, is reduced due to a combination of surface crust development and perched water tables. The dominance of exchangeable sodium in the soils results in soil dispersion and the clogging of soil pores which reduces the soils' porosity and infiltration rate. Capillary rise brings salts to the surface and leads to calcareous crust development. The failure of many of the double ring infiltration measurements to reach final infiltration rate is linked to over-saturated soils and the presence of surface crusts, resulting in the lateral flow of water, rather than vertical flow, during measurements.

Saturated hydraulic conductivity measurements were too variable to allow detailed interpretation. This variability resulted due to a number of cores experiencing boundary flow, likely due to the presence of allophane in the soils. The allophane resulted in irreversible

shrinkage with drying to -100 kPa and thus the soil did not regain its original volume on re-wetting before K_s measurements were done.

6.1 Recommendations and possible future work

The presence of allophane and sodicity over the TPC sugar estate interact to give unique physical and chemical soil properties. In soils of the south and west areas where there is a high content of allophane and sodicity, the sugarcane growth is patchy, suggesting that the beneficial aggregating effect of the allophane is being over-ridden by the presence of the sodium. This study has achieved its aim of giving an overview of the mineralogy, water retention and sodicity across the estate but variability in the results has limited full interpretation. It is recommended that more studies are undertaken on the south and west areas, where the combination of allophane and sodium is particularly important, to better understand these relationships and assist in further management improvements.

It is recommended that to fully understand infiltration rate, alternative methods should be used to assess field water flow such as measurement of unsaturated hydraulic conductivity in the field and the use of water flow modelling. Greater understanding of the effect of sodium on infiltration rate can be achieved by increasing the number of measurements taken for infiltration rate, hydraulic conductivity, EC_e and SAR to allow for accurate correlations between these factors. A focus on the south and west areas for this purpose is recommended. It is also recommended that K_s measurements be taken on undisturbed cores before water retentivity measurements.

Capillary rise should be measured experimentally and/or estimated by water movement modelling and then be related to specific surface area and sodium concentration. Again, it is recommended that for this purpose the focus should be on the south and west areas where a large number of samples should be collected to enable adequate interpretation.

A more in-depth study is required to understand the effect of sodicity on crust formation and infiltration rate, as well as the causes of sodicity and how these problems can be remediated. This can be achieved by focusing on specific problem areas where sodicity can be correlated to other measures such as water quality parameters, water table height, EC_e, cations, pH and SAR. Furthermore, more samples taken from outside the TPC estate should be measured to

assess the influence of TPC's management practices (i.e. irrigation with poor quality water) on the soil physical and chemical properties. This is recommended in the light of the Out 2 sample being sodic, perhaps suggesting that sodicity in the soil is a natural phenomenon and not necessarily a consequence of management practices in some areas.

The remediation of the sodic soils may be achieved with the addition of soluble calcium salts, such as gypsum, to replace the exchangeable sodium (Richards, 1957). Adequate sub-surface drainage is required to ensure that sufficient leaching with good quality irrigation water can occur to remove the build-up of sodium. Sufficient drainage, application of good quality irrigation water, together with the application of gypsum is appropriate management for the removal of sodium in the soil profile and the consequent negative effects it has on the soil physical properties.

REFERENCES

Adamo P., Violante P. and Wilson M.J., 2001. Tubular and spheroidal halloysite in pyroclastic deposits in the area of Roccamonfina volcano (southern Italy). *Geoderma*, 99 (295 – 316).

Amonette J.E., 2002. Methods for determination of mineralogy and environmental availability. *In* Dixon J.B. and Schulze D.G. (Eds.). Soil Mineralogy with Environmental Applications, pg. 153 – 197. Soil Science Society of America. Madison, Wisconsin, USA.

Aomine S. and Otsuka H., 1968. Surface of soil allophanic clays. 9th International Congress of Soil Science Transactions, Volume 1. Adelaide, Australia. 731 – 737.

Armas-Espinel S., Hernández-Moreno J.M., Muñoz-Carpena R. and Regalado C.M., 2003. Physical properties of "sorriba"-cultivated volcanic soils from Tenerife in relation to andic diagnostic parameters. *Geoderma*, 177 (297 – 311).

Avery B.W. and Bascomb C.L., 1974. Soil Survey Laboratory Methods. Rothamsted Experimental Station, Harpenden.

Bamutaze Y., Tenywa M.M., Majoliwa M.J.G., Vanacker V., Bagoora F., Magunda M., Obando J. and Wasige J.E., 2010. Infiltration characteristics of volcanic sloping soils on Mt. Elgon, eastern Uganda. *Catena*, 80 (122 – 130).

Bartoli F., Poulenaud A.J. and Schouller B.E., 2007. Influence of allophane and organic matter contents on surface properties of Andosols. *European Journal of Soil Science*, 58 (450 – 464).

Bates T., 1960. Halloysite and gibbsite formation in Hawaii. *Clays and Clay Minerals*, 9 (315 – 328).

Bhattacharyya R., Prakash V., Kunda S. and Gupta H.S., 2006. Effect of tillage and crop rotation on pore size distribution and soil hydraulic conductivity in sandy clay loam soil of the Indian Himalayas. *Soil and Tillage Research*, 86 (129-140).

Bouwer H., 1986. Intake Rate: Cylinder infiltrometer. *In* Klute A. (Ed.). Methods of soil analysis, ASA Monograph 9, Madison, Wisconsin.

Brady N.C. and Weil R.R., 2002. Elements of nature and properties of soils (13th edition). Prentice Hall, New Jersey.

British Geological Survey, 2000. Groundwater quality: Tanzania. NERC.

Brogna D., 2004. Mapping of salinity and sodicity problems using remote sensing and GIS techniques at TPC Ltd., a sugar cane estate in Tanzania. MSc thesis, Cranfield University, Silsoe.

Broquen P., Lobartini J.C., Candan F. and Falbo G., 2005. Allophane, aluminium, and organic matter accumulation across a bioclimatic sequence of volcanic ash soils of Argentina. *Geoderma*, 129 (167 – 177).

Bühmann C., Fey M.V. and de Villiers J.M., 1985. Aspects of the X-ray identification of swelling clay minerals in soils and sediments. *South African Journal of Science*, 81 (505 – 509).

Carter D.L., Mortland M.M. and Kemper W.D., 1986. Specific surface. *In* Klute A. (Ed.). Methods of soil analysis, Part 1, Agronomy No. 9 (2nd edition), pg. 413 – 423. American Society of Agronomy, Madison, Wisconsin.

Curtin D. and Smillie G.W., 1976. Estimation of components of soil cation exchange capacity from measurements of specific surface and organic matter. *Soil Science Society of America Journal*, 40 (461– 462).

Dorel M., Roger-Estrade J., Manichon H. and Delvaux B., 2000. Porosity and soil water properties of Caribbean volcanic ash soils. *Soil Use and Management*, 16 (133 – 140).

Drouza S., Georgoulias F.A. and Moustakas N.K., 2007. Investigation of soils developed on volcanic materials in Nisyros Island, Greece. *Catena*, 70 (340 – 349).

Egli M., Nater M., Mirabella A., Raimondi S., Plötze M. and Alioth L., 2008. Clay minerals, oxyhydroxide formation, element leaching and humus development in volcanic soils. *Geoderm*a, 143 (101 – 114).

Elgabaly M.M. and Elghamry W.M., 1970. Water permeability and stability of kaolinite systems as influenced by adsorbed cation ratio. *Soil Science*, 110 (107 – 110).

El-Swaify S.A., Swindale L.D. and Uehara G., 1969. Salinity tolerances of certain tropical soils and relationships between sodium ion activities and soil physical properties. Research and Development Progress Report, 419 (1 – 46). United States Department of the Interior.

Fontes J.C., Gonçalves M.C. and Pereira L.S., 2004. Andosols of Terceira, Azores: Measurement and significance of soil hydraulic properties. *Catena*, 56 (145 – 154).

Frenkel H., Goertzen J.O. and Rhoades J.D., 1978. Effects of clay type and content, exchangeable sodium percentage, and electrolyte concentration on clay dispersion and soil hydraulic conductivity. *Soil Science Society of America Journal*, 42 (32 – 39).

Funakawa S., Yoshida H., Watanabe T., Sugihara S., Kilasara M. and Kosaki T., 2012. Soil Fertility Status and its Determining Factors in Tanzania. *In* Hernandez Soriano M.C. (Ed.). Soil Health and Land Use Management, pg. 1 - 15. Available online: http://www.intechopen.com/books/soil-health-and-land-use-management/soil-fertility-status-and-its-determining factors-in-tanzania. Date accessed and verified: 06/03/2013.

Gal M., Arcan L., Shainberg I. and Keren R., 1984. Effect of exchangeable sodium and phosphogypsum on crust structure – scanning electron microscope observations. *Soil Science Society of America Journal*, 48 (872 – 878).

Gama-Castro J.E., Solleiro-Rebolledo E. and Vallejo-Gómez E., 2000. Weathered pumice influence on selected alluvial soil properties in west Nayarit, Mexico. *Soil and Tillage Research*, 55 (143 – 165).

Gee G.W. and Bauder J.W., 1986. Particle size analysis. *In* Klute A (Ed.). Methods of soil analysis, Part 1, Agronomy No. 9 (2nd edition), pg. 383 – 411. American Society of Agronomy, Madison, Wisconsin.

Hardy, Y., 2007. Irrigation and Drainage Master Plan. Concept Document. Unpublished TPC report.

Harsh J., Chorover J. and Nizeyimana E., 2002. Allophane and Imogolite. *In* Dixon J.B. and Schulze D.G. (Eds.). Soil Mineralogy with Environmental Applications, pg. 291 – 322. Soil Science Society of America, Madison, Wisconsin.

Hepper E.N., Buschiazzo D.E., Hevia G.G, Urioste A. and Antón L., 2006. Clay mineralogy, cation exchange capacity and specific surface area of loess soils with different volcanic ash contents. *Geoderma*, 135 (216 – 223).

Hillel D., 1971. *Soil and Water: Physical Principles and Processes*. Academic Press, New York and London.

Hughes J.C., Gilkes R.J. and Hart R.D., 2009. Intercalation of reference and soil kaolins in relation to physico-chemical and structural properties. *Applied Clay Science*, 45 (24 – 35).

Ito T., Shoji S. and Saigusa M., 1991. Classification of volcanic ash soils from Konsen district, Hokkaido according to the last Keys to Soil Taxonomy (1990). *Japanese Journal of Soil Science and Plant Nutrition*, 62 (237 – 247).

IUSS Working Group WRB, 2006. World Reference Base for Soil Resources 2nd edition. World Soil Resources Reports 103. FAO, Rome.

Jager T.J., 1982. Soils of the Serengeti Woodlands, Tanzania. Agricultural Research Reports 912. Centre for Agricultural Publishing and Documentation, Wageningen.

Jalali M., Merikhpour H., Kaledhonkar M.J. and Van Der Zee S.E.A.T.M., 2008. Effects of wastewater irrigation on soil sodicity and nutrient leaching in calcareous soils. *Agricultural Water Management*, 95 (143 – 153).

Johnston M.A., 1973. Physical properties of sugar belt soils with particular reference to moisture release characteristics. *Proceedings of the South African Sugar Technologists' Association* (115 – 119).

Jordán A., Zavala L.M., Nava A.L. and Alanís N., 2009. Occurrence and hydrological effects of water repellency in different soil and land use types in Mexican volcanic highlands. *Catena*, 79 (60 – 71).

Kaufhold S., Ufer K., Kaufhold A., Stucki J.W., Anastácio A.S., Jhan R. and Dohrmann R., 2010. Quantification of allophane from Ecuador. *Clays and Clay Minerals*, 58 (707 – 716).

Klute A. and Dirksen C., 1986. Hydraulic conductivity and diffusivity: Laboratory methods. *In* Klute A. (Ed.). Methods of soil analysis, Part 1, Agronomy No. 9 (2nd edition), pg. 687 – 734. American Society of Agronomy, Madison, Wisconsin.

Lado M. and Ben-Hur M., 2004. Soil mineralogy effects on seal formation, runoff and soil loss. *Applied Clay Science*, 24 (209 – 224).

Leroy L., 2004. Characterisation of vertical profiles at the TPC Ltd. in Tanzania. MSc thesis, Cranfield University, Silsoe.

Levy G.J., 1988. The Effects of Clay Mineralogy and Exchangeable Cations on some of the Hydraulic Properties of Soils. PhD thesis, University of Pretoria, Pretoria.

Lowe D.J., 1993. Teaching clays: from ashes to allophane. *In* Clays: Controlling the Environment. Proceedings of the 10th International Clay Conference, Adelaide, Australia. CSIRO Publishing, Melbourne, Australia, pg. 19 – 23

Madeira M., Auxtero E. and Sousa E., 2003. Cation and anion exchange properties of Andisols from the Azores, Portugal, as determined by the compulsive exchange and the ammonium acetate methods. *Geoderma*, 117 (225 – 241).

McDaniel P.A., Lowe D.J., Arnalds O. and Ping C.L., 2011. Andisols. *In* Li Y. and Sumner M.E. (Eds.). Handbook of Soil Sciences. 2nd edition. Vol. 1: Properties and Processes, pg. 29 - 48. CRC Press, Taylor & Francis, Boca Raton, Florida.

McKeague J.A., 1967. An evaluation of 0.1M pyrophosphate and pyrophosphate–dithionite in comparison with oxalate as extractants of the accumulation products in Podzols and some other soils. *Canadian Journal of Soil Science*, 47 (95 – 99).

McKeague J.A. and Day J.H., 1966. Dithionite and oxalate-extractable Fe and Al as aids in differentiating various classes of soils. *Canadian Journal of Soil Science*, 46 (13 – 22).

Mehra O.P. and Jackson M.L., 1960. Iron oxide removal from soils and clays by a dithionite–citrate system buffered with sodium bicarbonate. Proceedings of the 7th National Conference on Clays and Clay Minerals, Washington DC, pg. 317 – 327.

Meyer J.H., Heathman W., Turner P. and Berjak N., 2009. Final report of a detailed soil survey at TPC estate, Tanzania. Unpublished.

Meyer J.H., 2011. Good practices manual for the cane sugar industry. PGBI Sugar and Bio Energy, Woodmead, Johannesburg.

Moodley M., Johnston M.A., Hughes J.C. and Titshall L.W., 2004. Effects of water treatment residues, lime, gypsum, and polyacrylamide on the water retention and hydraulic conductivity of two contrasting soils under field conditions in KwaZulu-Natal, South Africa. *Australian Journal of Soil Research*, 42 (273 – 282).

Nakagawa T. and Ishiguro M., 1994. Hydraulic conductivity of an allophanic Andisol as affected by solution pH. *Journal of Environmental Quality*, 23 (208 – 210).

Nanzyo M., Dahlgren R.A. and Shoji S., 1993. Chapter 6: Chemical characteristics of volcanic ash soils. *In* Shoji S., Nanzyo M. and Dahlgren R.A. (Eds.). Developments in Soil Science 21: Volcanic Ash Soils: Genesis, Properties and Utilization, pg. 145 – 187. Elsevier Science Publishers, Amsterdam.

Ndayiragije S. and Delvaux B., 2003. Coexsistence of allophane, gibbsite, kaolinite and hydroxyl-Al-interlayered 2:1 clay minerals in a perudic Andosol. *Geoderma*, 117 (203 – 214).

Neall V.E., 2009. Volcanic soils. *In* Verheye W. (Ed). *Land use, land cover and soils science*, 7 (1 – 24). EOLSS with UNESCO, Oxford. Available online: www.eoloss.net, date accessed and verified: 04/08/2012.

Nieuwenhuyse A., Verburg P.S.J. and Jongmans A.G., 2000. Mineralogy of a soil chronosequence on an andesitic lava in humid tropical Costa Rica. *Geoderma*, 98 (61 – 82).

Nonnotte P., Guillou H., Le Gall B., Benoit J.C. and Scaillet S., 2008. "New K-Ar age determinations of Kilimanjaro volcano in the North Tanzanian diverging rift, East Africa". *Journal of Volcanology and Geothermal Research*, 173 (99 – 112).

NSAWC, 1990. The Non-Affiliated Soil Analysis Work Committee, 1990. Handbook of standard soil testing methods for advisory purposes. Soil Science Society of South Africa, Pretoria.

Parfitt R.L., Childs C.W. and Eden D.N., 1988. Ferrihydrite and allophane for Andepts from Hawaii and implications for their classification. *Geoderma*, 41 (223 – 241).

Parfitt R.L. and Wilson A.D., 1985. Estimation of allophane and halloysite in three sequences of volcanic soils, New Zealand. *In* Caldas E.F. and Yaalon D.H. (Eds.), Volcanic soils. Weathering and Landscape Relationships of on Tephras and Basalt. *Catena*, 7 (1 – 8).

Paterson E., 1977. Specific surface area and pore structure of allophanic clay soils. *Clay Minerals,* 12 (1 – 9).

Prado B., Duwig C., Hidalgo C., Gómez D., Yee H., Prat C., Esteves M. and Etchevers J.D., 2007. Characterization, functioning and classification of two volcanic soil profiles under different land uses in Central Mexico. *Geoderma,* 139 (300 – 313).

Richards L.A., 1954. Diagnosis and improvement of saline and alkali soils. U.S Salinity Laboratory, Agricultural Handbook No. 60.

Schaetzl R. and Anderson S., 2005. Soils: Genesis and Geomorphology. Cambridge University Press, New York.

Schulze D.J., 2002. Chapter 1: An introduction to soil mineralogy. *In* Dixon J.B. and Schulze D.G (Eds.). Soil Mineralogy with Environmental Applications, pg. 1 – 35. Soil Science Society of America, Madison, Wisconsin.

Sei J., Morato F., Kra G., Staunton S., Quiquampoix H., Jumas J.C. and Olivier-Fourcade J., 2006. Mineralogical, crystallographic and morphological characteristics of natural kaolins from the Ivory Coast (West Africa). *Journal of African Earth Sciences,* 46 (245 – 252).

Sellitto V.M., Palumbo G., Colombo C., Terribile F. and Schulze D.G., 2010. Formation of volcanic ash soils in the Matese Mountains of southern Italy. 19th World Congress of Soil Science, Soil Solutions for a Changing World. 1 – 6th August 2010, Brisbane, Australia.

Singer A., Zarei M., Lange F.M. and Stahr K., 2004. Halloysite characteristics and formation in northern Golan Heights. *Geoderma,* 123 (279 – 295).

Shoji S., Nanzyo M. and Dahlgren R.A., 1993. Developments in Soil Science 21: Volcanic Ash Soils: Genesis, Properties and Utilization. Elsevier Science Publishers, Amsterdam.

Soil Classification Working Group, 1991. Soil Classification – A Taxonomic System for South Africa. Department of Agricultural Development, Pretoria.

Tan K.H., 2005. Soil sampling, preparation and analysis, 2nd edition. CRC Press, Taylor and Francis Group, Florida.

Thouvenot M., 2002. Understanding the causes of the salinity/sodicity problem at the TPC Ltd. in Tanzania. MSc thesis. Cranfield University, Silsoe.

Tsai C.C., Chen Z.S., Kao C.I., Ottner F., Kao S.J. and Zehetner F., 2010. Pedogenic development of volcanic ash soils along a climosequence in Northern Taiwan. *Geoderma*, 156 (48 – 59).

Vacca A., Adama M., Pigna M. and Violante P., 2003. Genesis of tephra-derived soils from the Roccamonfina volcano, south central Italy. *Soil Science Society of America Journal*, 67 (198 – 207).

Velde B. and Barré P., 2010. Soils, plants and clay minerals. Springer, Berlin, Heidelberg.

Walkley A., 1947. A critical examination of a rapid method for determining organic carbon in soils – Effects and variations in digestion conditions and of inorganic constituents. *Soil Science*, 63 (251 – 264).

Walworth J., 2006. Soil Structure: The Roles of Sodium and Salts. University of Arizona. Available online: http://cals.arizona.edu/pubs/crops/az1414.ppt, date accessed and verified: 06/02/2013.

Watanabe T., Funakawa S. and Kosaki T., 2006. Clay mineralogy and its relationship to soil solution composition in soils from different weathering environments of humid Asia: Japan, Thailand and Indonesia. *Geoderma*, 136 (51 – 63).

Whittig L.D. and Allardice W.R., 1986. Chapter 12: X-ray diffraction techniques. *In* Klute A (Ed.). Methods of soil analysis, Part 1, Agronomy No. 9 (2nd edition). American Society of Agronomy, Madison, Wisconsin.

Wielemaker W.G. and Wakatsuki T., 1984. Properties, weathering and classification of some soils formed in peralkaline volcanic ash in Kenya. *Geoderma*, 32 (21 – 44).

www.sugarcanecrops.com/soil_requirement

APPENDICES

Appendix 4.1: Sample collection summary from a) PSU sites (Undisturbed soil cores and bulk sample from A and B horizons collected), b) non-PSU sites (Undisturbed soil cores and bulk sample from A and B horizons collected), c) bulk sites (Bulk sample collected from A and B horizon, no undisturbed soil cores collected) and d) the two ash layers from the borehole (BH Ash) and field R8 (R8 Ash).

a)

AREA	FIELD	DATE COLLECTED	COMMENT
North	N34N	July 2010	
	N43N	September 2011	On map, it appears as if sample is taken in field N43S, however, this is likely to be a GPS error
	N65	July 2010	
	N91	July 2010	
West	R3S Good	July 2010	
	R3S Bad	July 2010	
	R3S (2.1)	September 2011	
	R3S (2.2)	September 2011	On map, it appears as if sample is taken in field R7, however, this is likely to be a GPS error
	R3S (2.3)	September 2011	
	P4N	July 2010	Appears as if sample is taken in P4S
	P4N (2.1)	September 2011	
	P4N (2.2)	September 2011	
	P4N (2.3)	September 2011	
	P4N (2.4)	September 2011	
	L1S	July 2010	
East	BO4	July 2010	
	E6	July 2010	
	B3	July 2010	
South	12C Good	July 2010	
	12C Bad	July 2010	
	12C (2.1)	September 2011	
	12C (2.2)	September 2011	
	12C (2.3)	September 2011	

Appendix 4.1: Continued

AREA	FIELD	DATE COLLECTED	COMMENT
South	4D	July 2010	
	4D (2.1)	September 2011	
	4D (2.2)	September 2011	
	10K Good	July 2010	
	10K Bad	July 2010	
	10K (2.1)	September 2011	
	10K (2.2)	September 2011	
	10K (2.3)	September 2011	
	17B	July 2010	
	G2	July 2010	
	5[1]	September 2011	
	1 Good	July 2010	
	1 Bad	July 2010	
	16B	July 2010	Appears as if sample taken in field 16[1]
	16B (2.1)	September 2011	
Kahe	KH29	July 2010	On map, it appears as if sample is taken in field KH30, however, this is likely to be a GPS error
	KH15	July 2010	Appears as if sample taken in KH21
	KH4	July 2010	

b)

AREA	FIELD	DATE COLLECTED	COMMENT
North	N51	July 2010	
	N66	July 2010	
	N100KA	July 2010	Appears as if sample taken in N100KE. Cores and bulk sample not collected from the B horizon – too hard.
	N100KA (2.1)	September 2011	
	N100KA (2.2)	September 2011	
West	R5N	July 2010	
	Q4N	July 2010	

Appendix 4.1: Continued.

AREA	FIELD	DATE COLLECTED	COMMENT
West	M1	July 2010	
	K4S	September 2011	Appears as if sample taken in K5 (Not sure if this is a GPS error)
	K5	September 2011	
	N22	July 2010	
East	O[3] Good	July 2010	
	O[3] Bad	July 2010	
	D24	July 2010	
	F1S	July 2010	
	C9	July 2010	
	D11	July 2010	
South	15B	July 2010	
	12 Good	July 2010	
	12 Bad	July 2010	
	5D (2.1)	September 2011	
	5D (2.2)	September 2011	
	4C (2.1)	September 2011	
	4C (2.2)	September 2011	
	11C[1] Good	July 2010	
	11C[1] Bad	July 2010	
	19A	July 2010	On map, it appears as if sample is taken in field 16D, however, this is likely to be a GPS error
Kahe	KH27	September 2011	
	KH19	September 2011	
	KH14	July 2010	
	KH8	September 2011	
Out	Out 1	July 2010	
	Out 2	July 2010	
	Out 3	September 2011	
	Out 4	September 2011	

Appendix 4.1: Continued.

c)

AREA	FIELD	DATE COLLECTED	COMMENT
North	N32N	July 2010	
	N33	July 2010	
	N65	July 2010	
	N72	July 2010	
	N84	July 2010	
West	Q2N	July 2010	
	L3N	July 2010	
	L5	July 2010	
East	E17	July 2010	
	D19	July 2010	
	E10	July 2010	
	B2	July 2010	
	C2	July 2010	
South	13	July 2010	
	18A	July 2010	Bulk sample not collected from the B horizon – too hard.
	7[1]	July 2010	
	G5	July 2010	On map, it appears as if sample is taken in field G4, however, this is likely to be a GPS error
	6D	July 2010	
	4A	July 2010	
	9C	July 2010	
	9	July 2010	
	11	July 2010	
	16[3]	July 2010	
Kahe			Appears as if sample taken in KH18/KH17.
	KH9	July 2010	Bulk sample not collected from the B horizon – too hard.
	KH7	July 2010	Appears as if sample taken in KH8

Appendix 4.1: Continued.

d)

AREA	FIELD	DATE COLLECTED	COMMENT
South	R8 Ash	July 2010	
North	BH Ash	July 2010	

Appendix 4.2: Map of sample points taken over TPC estate

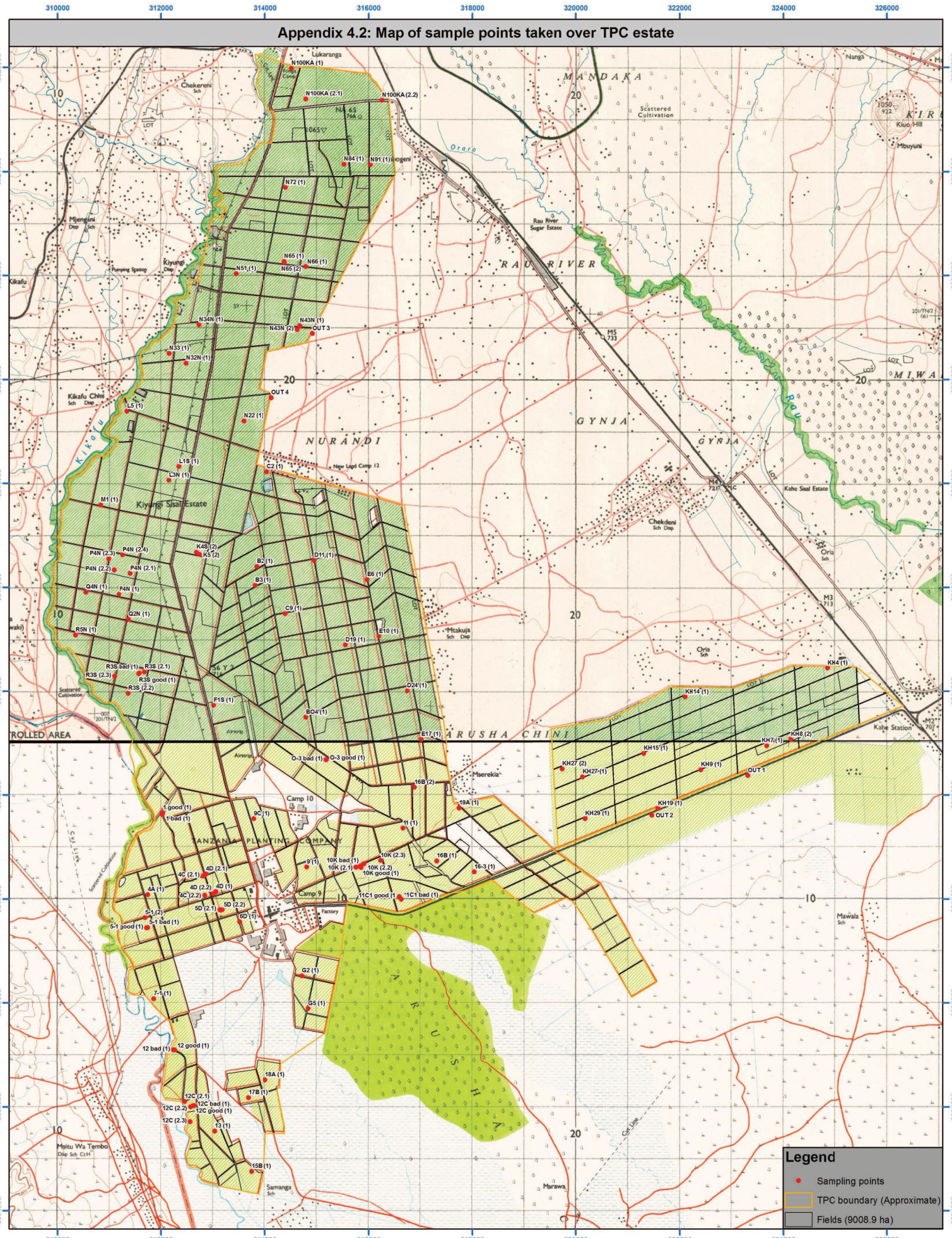

Mapping, layout and printng by:

S3 Technologies Spatial Systems Solutions
Tel: (033) 342 3681 Fax: (033) 342 3696 email: admin@s3.co.za

For Terri Taylor

Date of print: March, 2013

TPC LIMITED

Appendix 5.2: X-ray diffraction patterns of random powder samples of the sand fraction from the A and B horizon for specimens N91, N65 and N34N (North), L1S (West), E6 (East), 17B and G2 (South), KH4 and KH29 (Kahe), and R8 Ash and BH Ash (Ash layers).

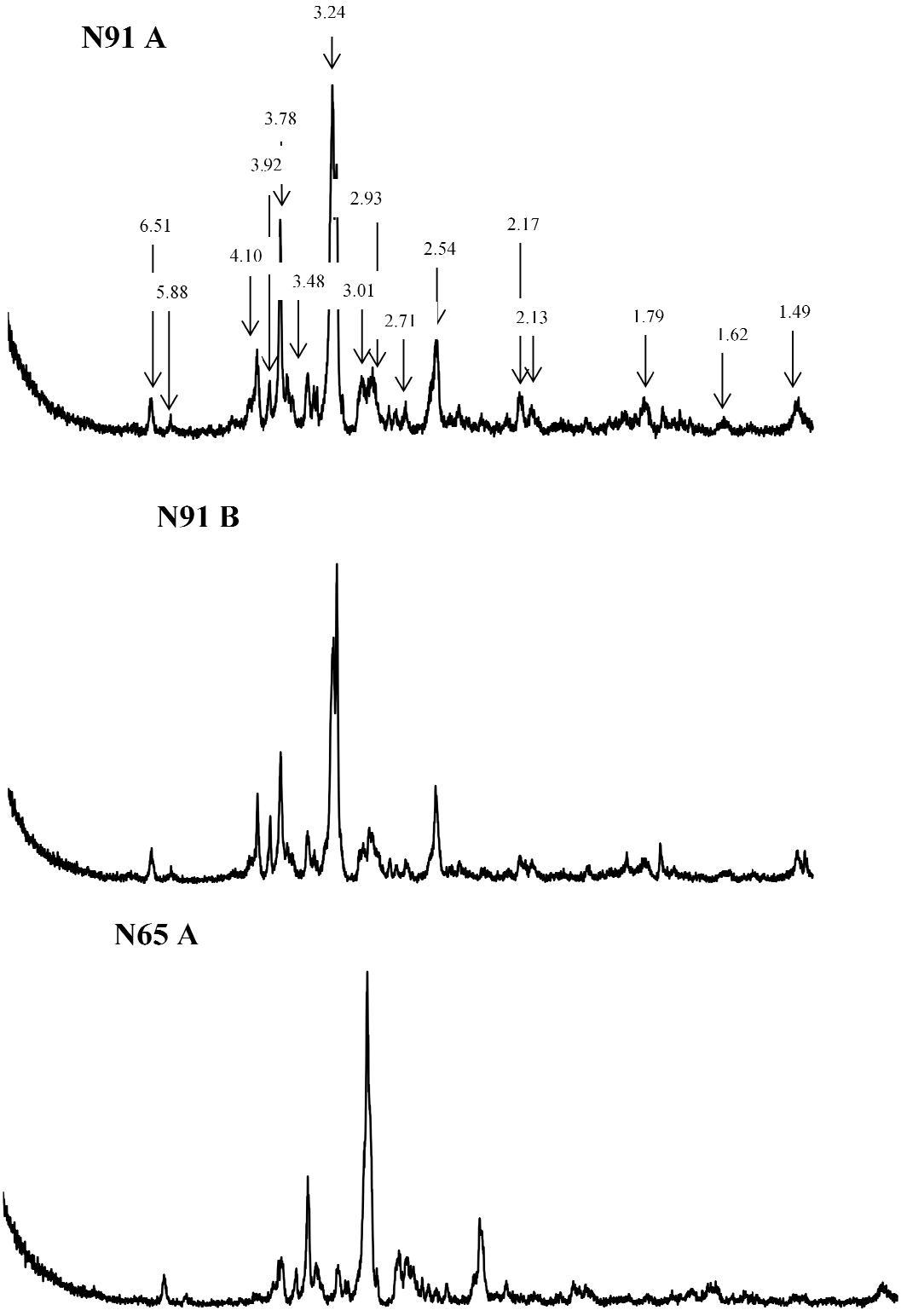

N65 B

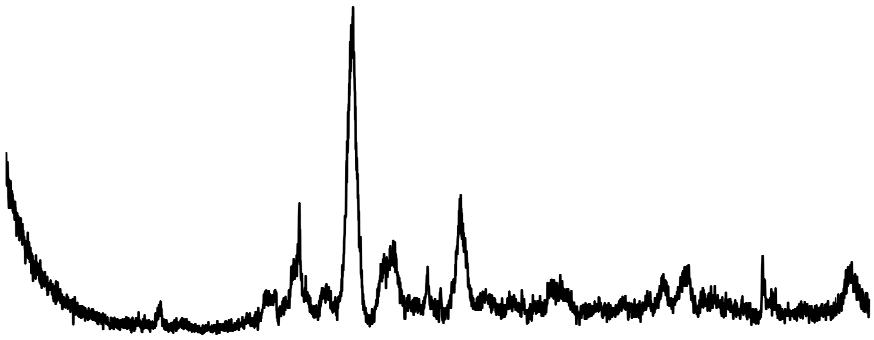

N34N A

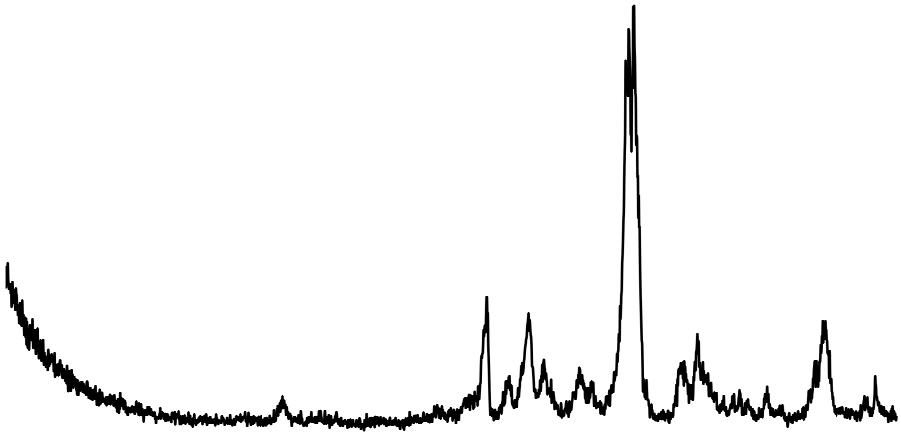

N34N B

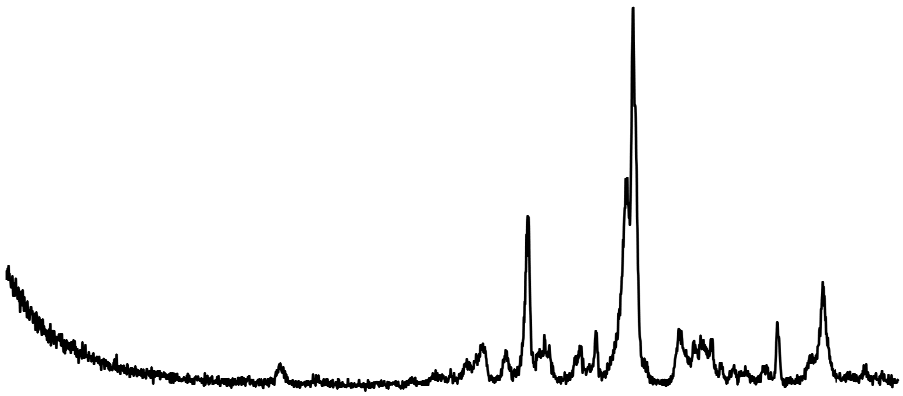

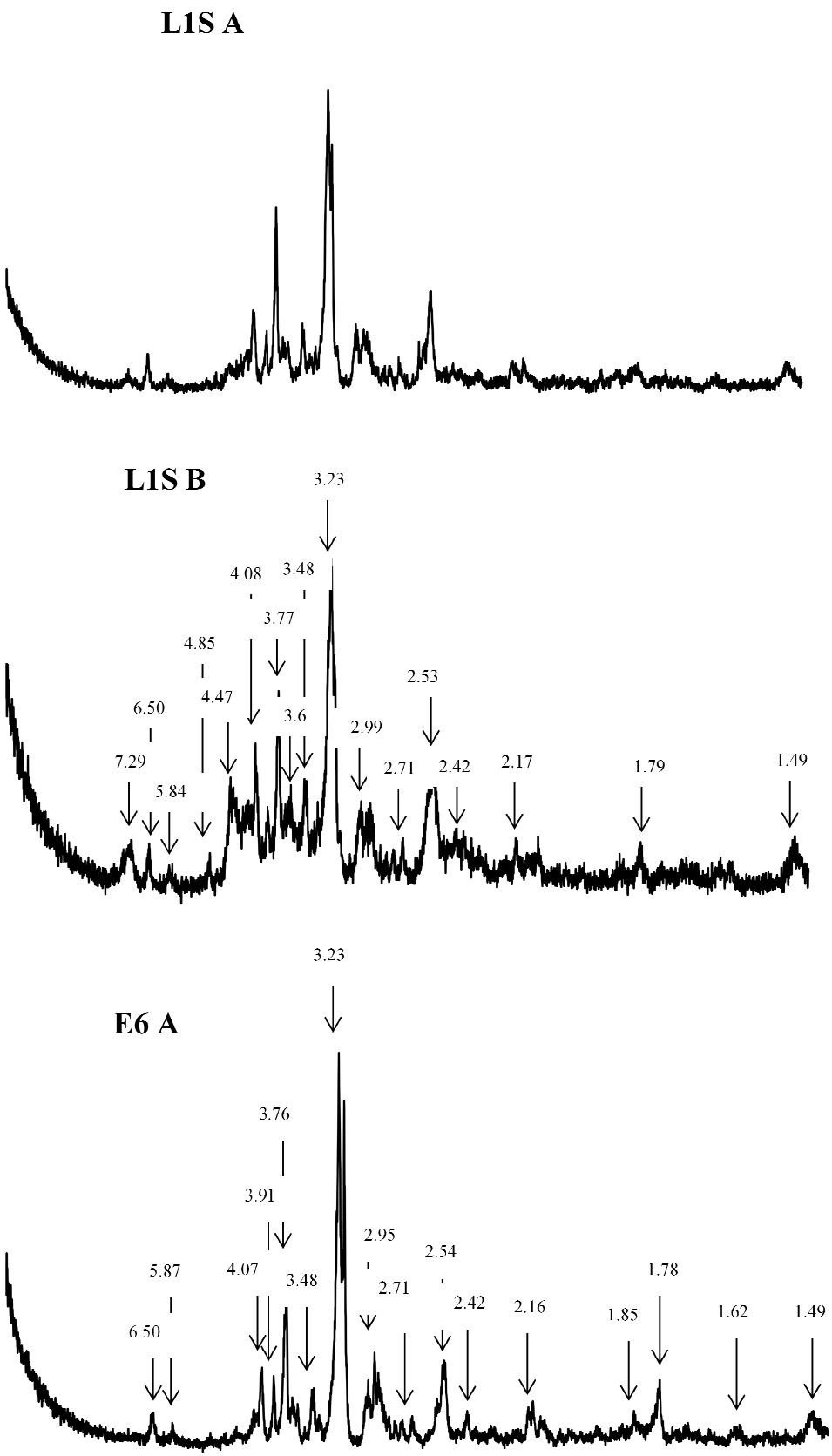
L1S A
L1S B
3.23
4.08
3.48
3.77
4.85
2.53
4.47
6.50
3.6
2.99
7.29
2.71
2.42
2.17
1.79
1.49
5.84
E6 A
3.23
3.76
3.91
2.95
2.54
5.87
4.07
3.48
1.78
2.71
2.42
2.16
1.85
1.62
1.49
6.50

E6 B

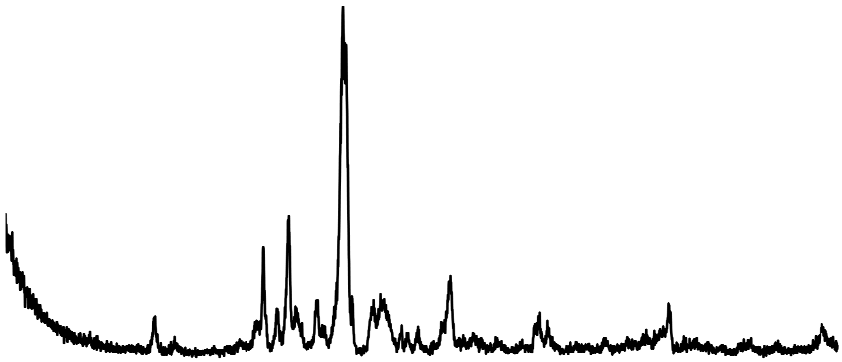

17B A

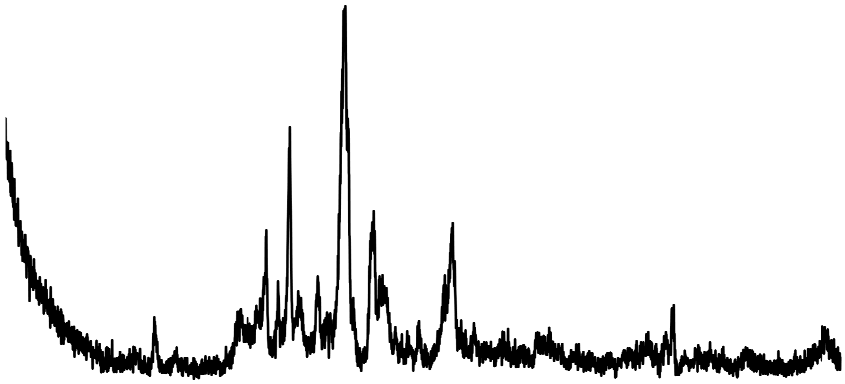

17B B

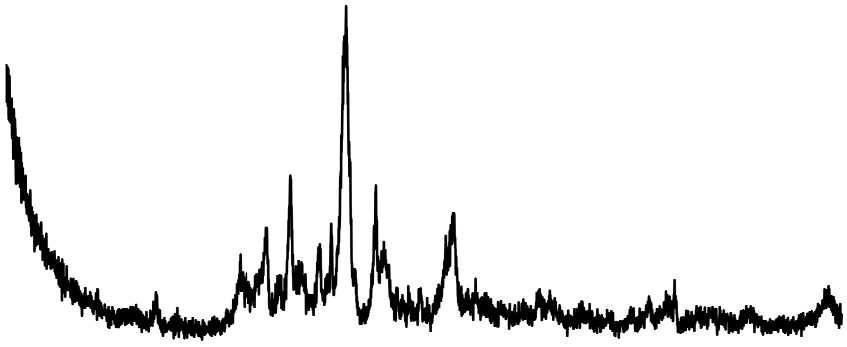

G2 A

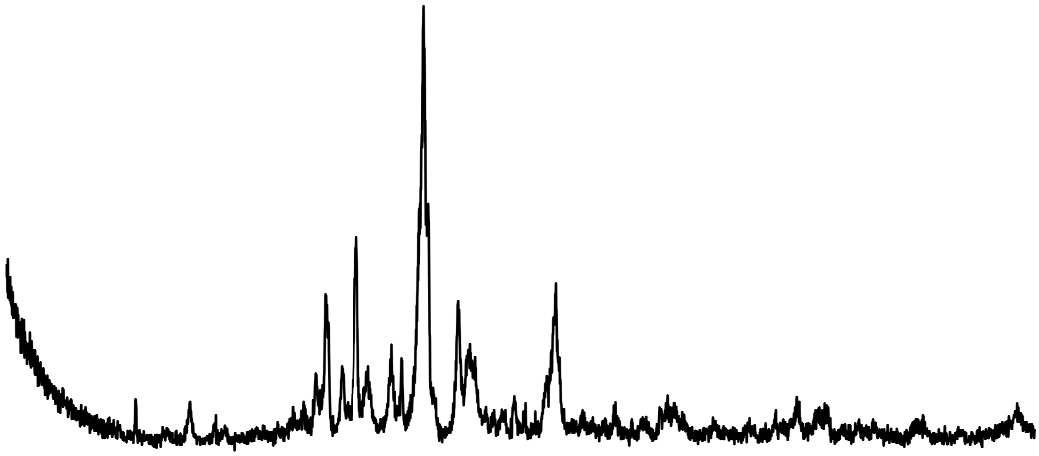

G2 B

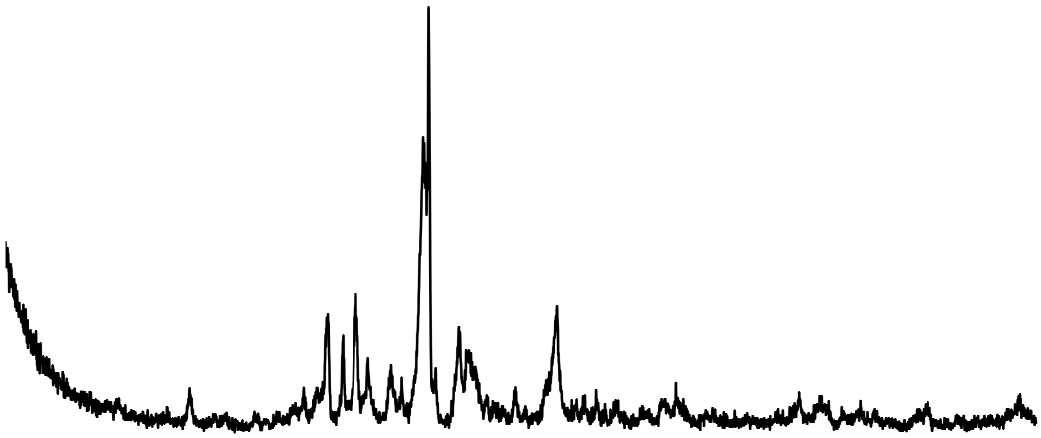

KH4 A

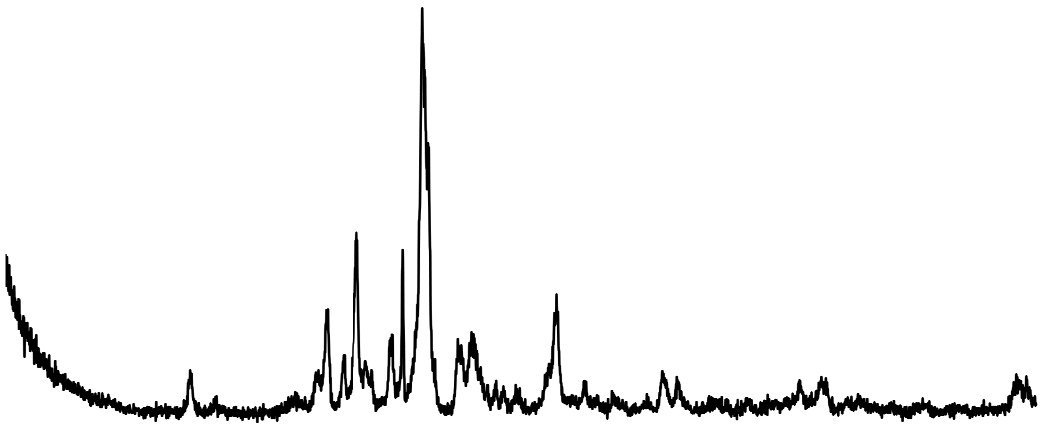

KH4 B

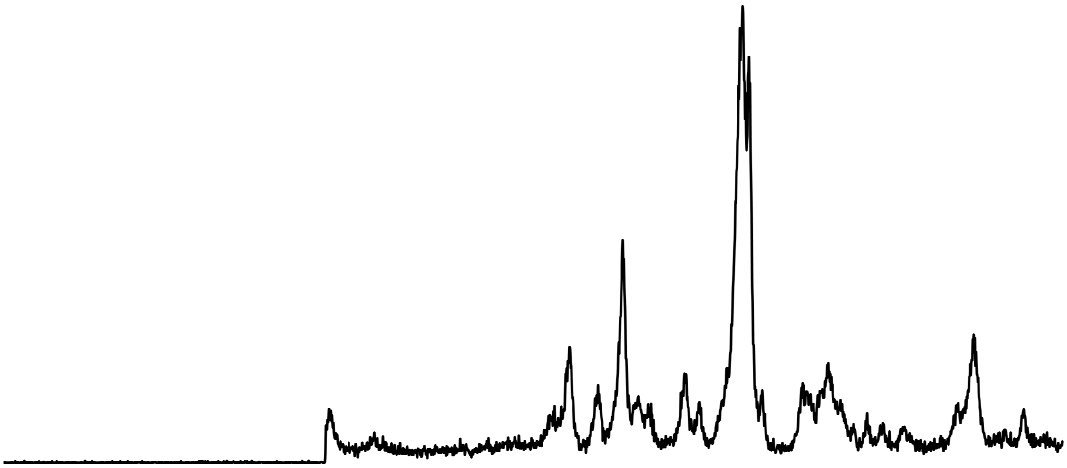

KH29 A

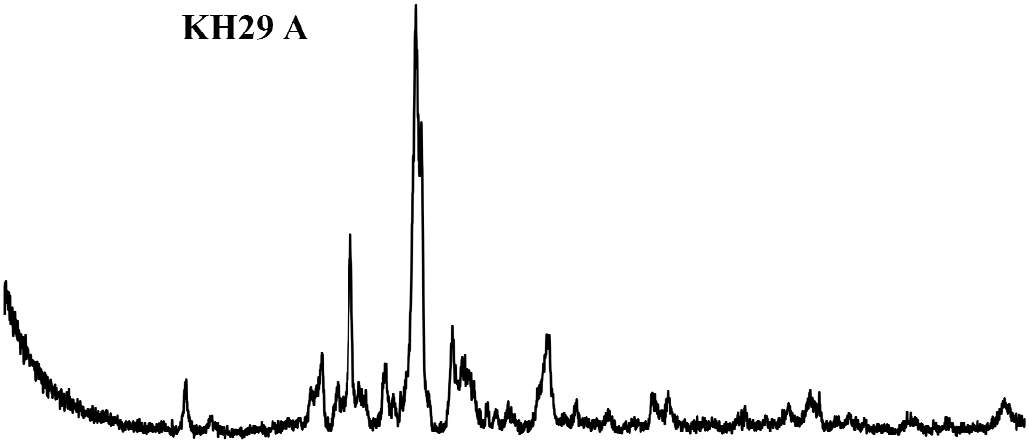

KH29 B

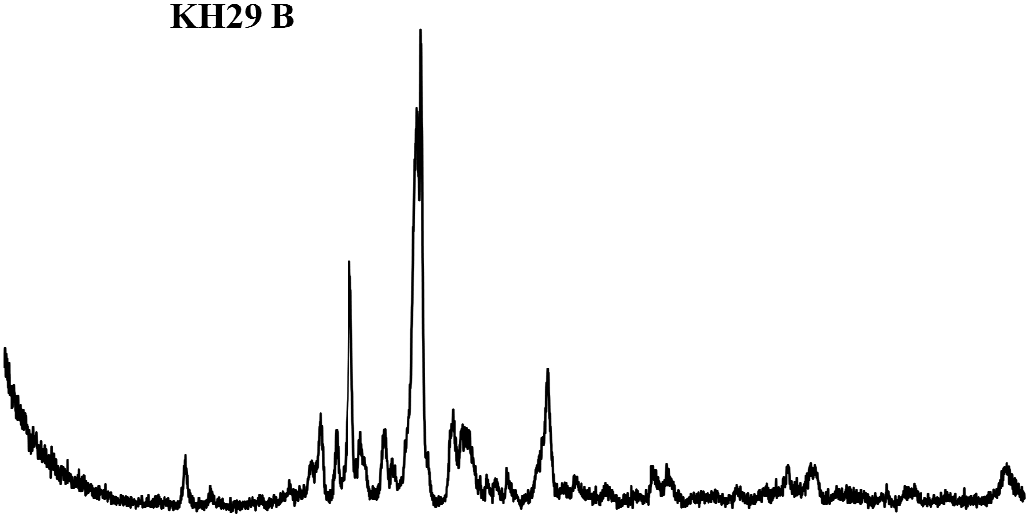

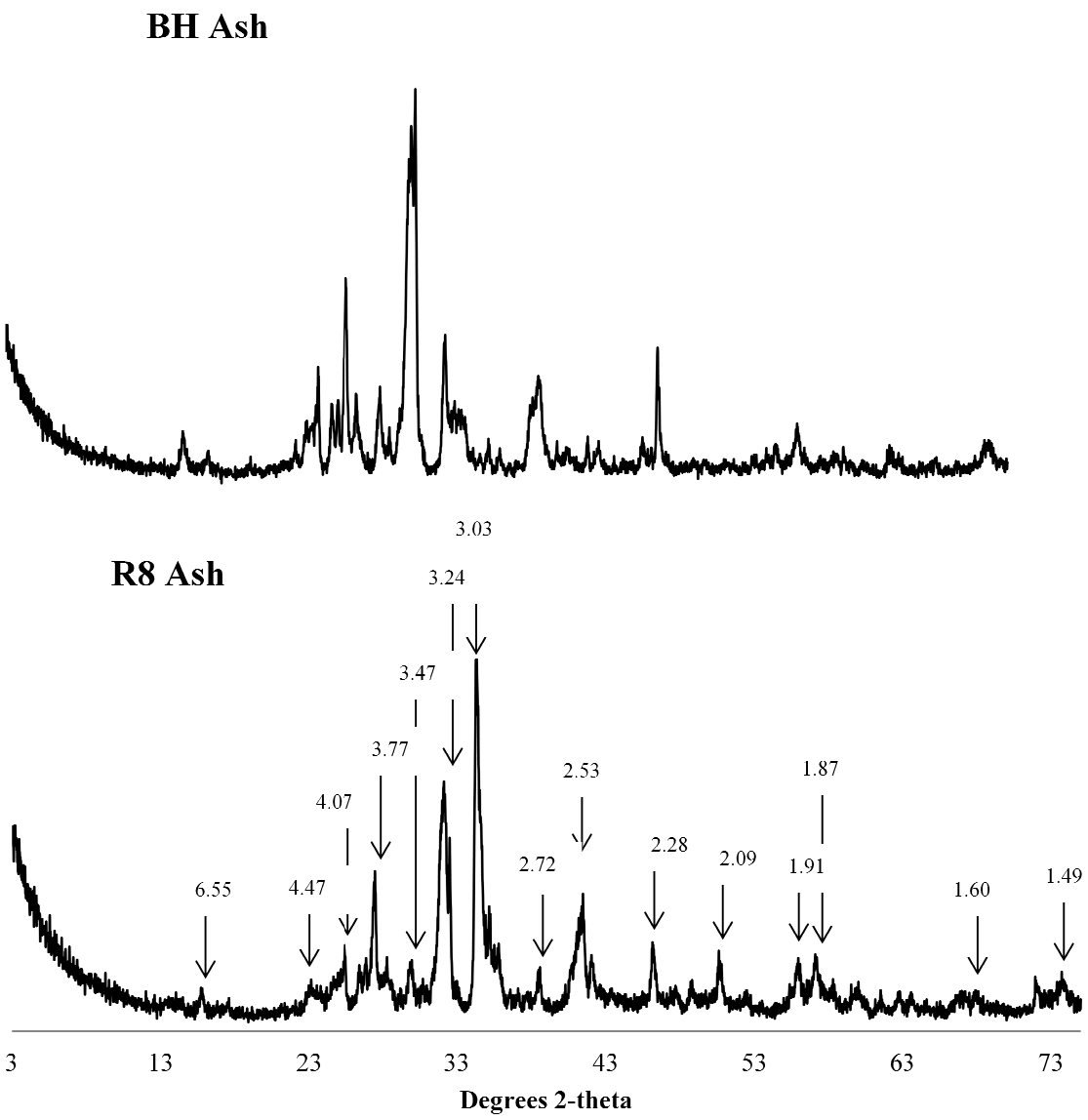
BH Ash
3.03
R8 Ash
3.24
3.47
3.77
4.07
2.53
1.87
6.55
4.47
2.72
2.28
2.09
1.91
1.60
1.49
3
13
23
33
43
53
63
73
Degrees 2-theta

Appendix 5.4: Acid oxalate extractable Fe, Al and Si (Fe_o, Al_o, Si_o), citrate-bicarbonate-dithionite extractable Fe and Al (Fe_d, Al_d) and sodium pyrophosphate extractable Fe and Al (Fe_p, Al_p) for TPC soil samples in the A horizon (A) and B horizon (B).

AREA	FIELD	Fe (%)						Al (%)						Si (%)	
		Fe_o		Fe_d		Fe_p		Al_o		Al_d		Al_p		Si_o	
		A	B	A	B	A	B	A	B	A	B	A	B	A	B
North	N 91	0.52	0.50	1.63	2.38	0.02	0.03	0.18	0.18	1.63	2.38	0.09	0.16	0.09	0.09
	N 65	0.52	0.68	1.60	2.19	0.02	0.04	0.21	0.26	1.60	2.19	0.07	0.17	0.47	0.50
	N 43 N	0.34	0.53	1.68	2.06	nd*	nd	0.18	0.20	1.68	2.06	nd	nd	0.08	0.10
	N 34 N	0.62	0.54	1.44	2.04	0.01	0.02	0.40	0.38	1.44	2.04	0.08	0.10	0.62	0.61
	N66	0.57	0.74	1.96	1.95	nd	nd	0.23	0.30	1.96	1.95	nd	nd	0.45	0.51
	N72	0.65	0.68	1.84	1.83	nd	nd	0.24	0.30	1.84	1.83	nd	nd	0.55	0.52
	N51	0.52	0.73	2.22	nd	nd	nd	0.27	0.35	2.22	nd	nd	nd	0.13	0.57
	AVERAGE	**0.53**	**0.63**	**1.77**	**2.08**	**0.02**	**0.03**	**0.24**	**0.28**	**1.77**	**2.08**	**0.08**	**0.14**	**0.34**	**0.41**
	Std Dev	**0.10**	**0.10**	**0.26**	**0.19**	**0.00**	**0.01**	**0.08**	**0.07**	**0.26**	**0.19**	**0.01**	**0.03**	**0.23**	**0.22**
West	L 1 S	0.89	0.97	2.78	2.55	0.08	0.10	0.50	0.77	2.78	2.55	0.17	0.29	0.19	0.24
	P 4 N	0.66	0.81	1.30	1.53	0.02	0.01	0.49	0.70	1.30	1.53	0.06	0.09	0.78	0.80
	R 3 S Good	0.49	0.49	1.58	1.04	0.00	0.00	0.72	0.77	1.58	1.04	0.06	0.05	0.29	0.28
	R 3 S Bad	0.59	0.47	1.27	1.31	0.01	0.01	0.76	0.64	1.27	1.31	0.06	0.07	0.31	0.24
	AVERAGE	**0.66**	**0.69**	**1.73**	**1.61**	**0.03**	**0.03**	**0.62**	**0.72**	**1.73**	**1.61**	**0.09**	**0.13**	**0.39**	**0.39**
	Std Dev	**0.17**	**0.25**	**0.72**	**0.66**	**0.04**	**0.05**	**0.14**	**0.06**	**0.72**	**0.66**	**0.06**	**0.11**	**0.27**	**0.27**
East	B 3	0.51	0.47	1.33	1.39	0.03	0.04	0.28	0.27	1.33	1.39	0.10	0.13	0.47	0.45
	E 6	0.34	0.38	1.58	0.93	0.03	0.02	0.16	0.18	1.58	0.93	0.07	0.08	0.07	0.08
	O3 Good	0.49	0.46	1.13	1.28	nd	nd	0.66	0.64	1.13	1.28	nd	nd	0.96	0.82
	O3 Bad	0.44	0.60	1.50	1.39	nd	nd	0.64	0.75	1.50	1.39	nd	nd	0.80	0.87
	B O 4	0.31	0.47	1.22	1.37	0.02	0.02	0.42	0.48	1.22	1.37	0.07	0.10	0.59	0.73
	AVERAGE	**0.42**	**0.48**	**1.35**	**1.27**	**0.02**	**0.03**	**0.43**	**0.46**	**1.35**	**1.27**	**0.08**	**0.10**	**0.58**	**0.59**
	Std Dev	**0.09**	**0.08**	**0.19**	**0.20**	**0.01**	**0.01**	**0.22**	**0.24**	**0.19**	**0.20**	**0.02**	**0.02**	**0.34**	**0.33**
South	16 B	0.65	0.80	2.08	2.43	0.02	0.04	0.37	0.40	2.08	2.43	0.08	0.11	0.16	0.17
	10 K Good	0.65	0.70	1.84	1.93	0.01	0.01	0.79	0.76	1.84	1.93	0.05	0.08	0.25	0.29
	10 K Bad	0.58	0.80	1.54	1.72	0.00	0.01	0.77	0.80	1.54	1.72	0.04	0.09	0.27	0.30
	10 K Crust	0.58	nd	1.93	nd	nd	nd	0.71	nd	1.93	nd	0.03	nd	0.30	nd
	4 D	0.52	0.78	2.01	2.30	0.02	0.03	0.50	0.53	2.01	2.30	0.08	0.10	0.84	0.88
	5^1 Good	0.80	0.79	nd	nd	nd	nd	1.07	1.27	nd	nd	nd	nd	0.48	0.52
	5^1 Bad	0.66	0.80	nd	nd	nd	nd	0.94	0.98	nd	nd	nd	nd	0.49	0.43
	12 C Good	1.08	0.92	2.44	3.14	0.04	0.04	0.86	0.77	2.44	3.14	0.11	0.12	0.41	0.36
	12 C Bad	0.80	0.87	2.33	3.34	0.04	0.04	0.72	0.76	2.33	3.34	0.09	0.12	0.31	0.33
	1 Good	0.83	1.00	2.90	2.67	0.02	0.03	0.78	0.83	2.90	2.67	0.13	0.15	0.32	0.32
	1 Bad	0.71	0.71	1.77	2.18	0.01	0.01	0.66	0.79	1.77	2.18	0.08	0.08	0.34	0.40
	17 B	0.46	0.53	1.77	1.48	0.02	0.03	0.46	0.47	1.77	1.48	0.09	0.11	0.78	0.75
	G 2	0.34	0.30	1.12	1.00	0.02	0.01	0.95	1.04	1.12	1.00	0.08	0.07	0.88	0.85
	AVERAGE	**0.66**	**0.75**	**1.98**	**2.22**	**0.02**	**0.02**	**0.74**	**0.78**	**1.98**	**2.22**	**0.08**	**0.10**	**0.45**	**0.47**
	Std Dev	**0.19**	**0.18**	**0.47**	**0.72**	**0.01**	**0.02**	**0.20**	**0.24**	**0.47**	**0.72**	**0.03**	**0.02**	**0.24**	**0.23**

Appendix 5.4: Continued.

AREA	FIELD	Fe (%)						Al (%)						Si (%)	
		Fe_o		Fe_d		Fe_p		Al_o		Al_d		Al_p		Si_o	
		A	B	A	B	A	B	A	B	A	B	A	B	A	B
Kahe	KH 4	0.31	0.27	1.76	1.78	0.01	0.02	0.21	0.18	1.76	1.78	0.06	0.08	0.53	0.46
	KH 15	0.31	0.30	1.27	1.39	0.00	0.01	0.19	0.20	1.27	1.39	0.06	0.06	0.10	0.10
	KH 29	0.28	0.20	1.53	1.52	0.01	0.00	0.19	0.16	1.53	1.52	0.05	0.05	0.45	0.09
	AVERAGE	**0.30**	**0.26**	**1.52**	**1.56**	**0.01**	**0.01**	**0.19**	**0.18**	**1.52**	**1.56**	**0.06**	**0.07**	**0.36**	**0.22**
	Std Dev	**0.02**	**0.05**	**0.24**	**0.20**	**0.00**	**0.01**	**0.01**	**0.02**	**0.24**	**0.20**	**0.01**	**0.02**	**0.23**	**0.22**
South	R8 Ash	0.96	nd	1.70	nd	0.01	nd	0.69	nd	1.70	nd	0.05	nd	0.35	nd
North	BH Ash	1.16	nd	0.88	nd	0.01	nd	1.05	nd	0.88	nd	0.04	nd	0.75	nd

* Not determined

Appendix 5.5: Amount of ferrihydrite, allophane and Al_o + ½ Fe_o in soils from TPC sugar estate from the A horizon (A) and B horizon (B).

		Ferrihydrite (%)		Allophane (%)		$Al_o + {}^1/_2\ Fe_o$	
AREA	FIELD	A	B	A	B	A	B
North	N 91	0.89	0.84	0.66	0.64	0.44	0.43
	N 65	0.88	1.15	3.35	3.59	0.47	0.60
	N 43 N	0.58	0.91	0.59	0.69	0.35	0.47
	N 34 N	1.06	0.92	4.42	4.32	0.71	0.65
	N66	0.96	1.25	3.21	3.66	0.51	0.67
	N51	0.88	1.23	0.94	4.06	0.53	0.72
	N72	1.11	1.15	3.89	3.74	0.57	0.64
	AVERAGE	**0.91**	**1.07**	**2.44**	**2.96**	**0.51**	**0.60**
	Std Dev	**0.17**	**0.17**	**1.65**	**1.58**	**0.11**	**0.11**
West	L 1 S	1.51	1.66	1.34	1.70	0.94	1.26
	P 4 N	1.12	1.38	5.58	5.71	0.82	1.11
	R 3 S Good	0.84	0.82	2.09	1.98	0.97	1.01
	R 3 S Bad	1.00	0.80	2.18	1.72	1.05	0.88
	AVERAGE	**1.12**	**1.17**	**2.80**	**2.78**	**0.95**	**1.06**
	Std Dev	**0.29**	**0.42**	**1.89**	**1.96**	**0.09**	**0.16**
East	B 3	0.86	0.80	3.37	3.19	0.53	0.50
	E 6	0.57	0.65	0.52	0.55	0.33	0.37
	B O 4	0.53	0.80	4.19	5.23	0.58	0.72
	O3 Good	0.83	0.78	6.84	5.85	0.90	0.87
	O3 Bad	0.75	1.02	5.70	6.21	0.86	1.05
	AVERAGE	**0.71**	**0.81**	**4.13**	**4.21**	**0.64**	**0.70**
	Std Dev	**0.15**	**0.13**	**2.42**	**2.35**	**0.24**	**0.28**
South	16 B	1.10	1.37	1.14	1.19	0.69	0.80
	10 K Good	1.10	1.19	1.81	2.10	1.11	1.11
	10 K Bad	0.98	1.37	1.92	2.11	1.05	1.21
	10 K Crust	0.99		2.13		1.00	0.00
	4 D	0.88	1.33	5.97	6.26	0.76	0.93
	5^1 Good	1.35	1.35	3.46	3.74	1.47	1.67
	5^1 Bad	1.12	1.36	3.49	3.08	1.27	1.38
	12 C Good	1.83	1.56	2.95	2.58	1.40	1.23
	12 C Bad	1.37	1.47	2.18	2.36	1.12	1.19
	1 Good	1.41	1.70	2.26	2.31	1.19	1.33
	1 Bad	1.21	1.20	2.44	2.87	1.02	1.14

Appendix 5.5: Continued.

AREA	FIELD	Ferrihydrite (%) A	Ferrihydrite (%) B	Allophane (%) A	Allophane (%) B	$Al_o + {}^1/_2\ Fe_o$ A	$Al_o + {}^1/_2\ Fe_o$ B
	17 B	0.79	0.89	5.58	5.37	0.69	0.73
	G 2	0.57	0.52	6.30	6.05	1.11	1.19
	AVERAGE	**1.13**	**1.28**	**3.20**	**3.33**	**1.07**	**1.16**
	Std Dev	**0.32**	**0.31**	**1.70**	**1.67**	**0.24**	**0.40**
Kahe	KH 4	0.52	0.47	3.78	3.31	0.36	0.32
	KH 15	0.53	0.50	0.74	0.69	0.34	0.34
	KH 29	0.47	0.34	3.21	0.61	0.32	0.26
	AVERAGE	**0.51**	**0.44**	**2.57**	**1.54**	**0.34**	**0.31**
	Std Dev	**0.03**	**0.09**	**1.62**	**1.54**	**0.02**	**0.04**
South	R8 Ash	1.62		2.51		1.17	
North	BH Ash	1.97		5.36		1.62	

Appendix 5.6: Final infiltration rate (mm hr^{-1}) of measured fields across TPC sugar estate.

AREA	FIELD	FINAL INFILTRATION RATE (mm hr^{-1})	FIELD OBSERVATIONS
North	N 91	40	
	N 65	126	
	N 43 N	98	
	N 34 N	87	
	N 100 KA	124	
	N 66	19	Deep, dry but kept slowing down
	N 51	187	Wet layer at 70cm - slows down
West	L 1 S	149	
	P 4 N	96	
	R 3 S Good	90	
	R 3 S Bad	17	
	N 22	119	
	M 1	190	
	Q 4 N	306	
	R 5 N	53	Slow
East	B 3	89	Saturation reached
	E 6	88	
	B O 4	201	
	D 11	31	Slowing down
	C 9	42	
	F 1 S	90	Slowing down, surface sealing
	D 24	318	
	O 3 Good	137	
	O 3 Bad	91	
South	16 B	59	
	10 K Good	41	Slowing down
	10 K Bad	53	Slowing down
	4 D	119	Saturation reached
	5^{1} Good	50	Slowing down
	5^{1} Bad	52	Slowing down
	12 C Good	18	
	12 C Bad	15	
	17 B	199	
	G 2	49	Slowing down, surface sealing
	19 A	40	Slowing down
	11 C^{1} Good	59	Slowing down
	11 C^{1} Bad	61	Slowing down
	12 Good	20	Slowing down
	12 Bad	60	Slowing down
	15 B	79	

Appendix 5.6: Continued.

AREA	FIELD	FINAL INFILTRATION RATE (mm hr-1)	FIELD OBSERVATIONS
Kahe	KH 4	14	Slowing down
	KH 15	171	
	KH 29	85	
	KH 19	207	
	KH 14	379	
Out	Out 1	118	Slowing down
	Out 2	50	

Appendix 5.7: The volumetric water content (m^3 m^{-3}) for the A horizon (A) and B horizon (B) at each measured matric potential (kPa) at each sampled site across TPC sugar estate.

AREA	FIELD			MATRIC POTENTIAL (kPa)									
			n	0	-1	-2	-4	-6	-8	-10	-33	-100	-1500
North	N34N A	Average	3	0.45	0.44	0.44	0.42	0.39	0.37	0.37	0.30	0.26	0.14
		Std dev	3	0.02	0.02	0.02	0.02	0.02	0.02	0.02	0.01	0.01	
	N34N B	Average	3	0.42	0.39	0.37	0.36	0.33	0.32	0.32	0.29	0.26	0.14
		Std dev	3	0.01	0.01	0.01	0.02	0.02	0.02	0.02	0.02	0.02	
	N65 A	Average	3	0.50	0.44	0.39	0.35	0.32	0.31	0.31	0.25	0.22	0.11
		Std dev	3	0.01	0.02	0.02	0.02	0.02	0.02	0.02	0.02	0.02	
	N65 B	Average	3	0.43	0.39	0.36	0.34	0.32	0.31	0.31	0.27	0.23	0.11
		Std dev	3	0.02	0.02	0.02	0.02	0.01	0.02	0.02	0.02	0.01	
	N91 A	Average	3	0.45	0.39	0.37	0.34	0.32	0.31	0.31	0.25	0.23	0.11
		Std dev	3	0.01	0.00	0.00	0.00	0.00	0.00	0.00	0.00	0.00	
	N91 B	Average	3	0.45	0.40	0.38	0.35	0.34	0.33	0.33	0.30	0.28	0.14
		Std dev	3	0.02	0.02	0.02	0.02	0.01	0.01	0.01	0.01	0.00	
	N43N A	Average	3	0.46	0.43	0.41	0.36	0.33	0.31	0.31	0.25	0.21	0.12
		Std dev	3	0.05	0.05	0.05	0.05	0.05	0.05	0.05	0.05	0.05	
	N43N B	Average	3	0.51	0.48	0.46	0.45	0.43	0.42	0.42	0.37	0.35	0.11
		Std dev	3	0.04	0.05	0.05	0.05	0.05	0.05	0.05	0.05	0.05	
	N43N A (2.1)	Average	3	0.54	0.51	0.44	0.38	0.35	0.33	0.32	0.27	0.23	0.12
		Std dev	3	0.03	0.03	0.05	0.04	0.03	0.03	0.03	0.02	0.01	
	N43N B (2.1)	Average	3	0.49	0.47	0.42	0.38	0.36	0.35	0.34	0.29	0.26	0.15
		Std dev	3	0.05	0.05	0.04	0.04	0.04	0.04	0.04	0.05	0.04	
	N66 A	Average	3	0.47	0.41	0.39	0.35	0.33	0.32	0.32	0.26	0.26	0.11
		Std dev	3	0.03	0.03	0.03	0.03	0.03	0.02	0.02	0.03	0.06	
	N66 B	Average	3	0.37	0.34	0.34	0.33	0.32	0.32	0.32	0.30	0.27	0.10
		Std dev	3	0.03	0.02	0.01	0.01	0.01	0.01	0.01	0.01	0.01	
	N51 A	Average	3	0.47	0.40	0.35	0.32	0.31	0.30	0.30	0.26	0.24	0.11
		Std dev	3	0.06	0.05	0.03	0.01	0.01	0.01	0.01	0.01	0.01	
	N51 B	Average	3	0.44	0.39	0.34	0.31	0.30	0.29	0.29	0.26	0.23	0.13
		Std dev	3	0.01	0.02	0.02	0.02	0.02	0.02	0.02	0.02	0.01	
	N100KA A	Average	3	0.46	0.40	0.33	0.30	0.28	0.27	0.27	0.24	0.22	0.15
		Std dev	3	0.01	0.00	0.01	0.01	0.01	0.01	0.01	0.01	0.01	
	N100KA A (2.1)	Average	3	0.56	0.52	0.49	0.44	0.40	0.38	0.36	0.28	0.23	0.20
		Std dev	3	0.01	0.00	0.02	0.04	0.05	0.05	0.05	0.04	0.01	
	N100KA B (2.1)	Average	3	0.53	0.50	0.47	0.41	0.36	0.35	0.33	0.25	0.23	0.15
		Std dev	3										
	N100KA A (2.2)	Average	3	0.49	0.45	0.41	0.37	0.34	0.32	0.31	0.24	0.21	0.18
		Std dev	3	0.02	0.00	0.02	0.05	0.05	0.05	0.04	0.01	0.01	
West	P4N A	Average	3	0.60	0.56	0.55	0.53	0.51	0.48	0.48	0.27	0.19	0.10
		Std dev	3	0.03	0.02	0.01	0.01	0.01	0.01	0.01	0.04	0.00	
	P4N B	Average	3	0.56	0.53	0.50	0.49	0.46	0.44	0.44	0.28	0.23	0.12
		Std dev	3	0.02	0.01	0.01	0.01	0.01	0.01	0.01	0.03	0.01	
	P4N A (2.1)	Average	3	0.44	0.38	0.33	0.28	0.26	0.25	0.23	0.19	0.16	0.16
		Std dev	3	0.00	0.00	0.00	0.01	0.01	0.01	0.01	0.02	0.02	
	P4N B (2.1)	Average	3	0.44	0.39	0.35	0.30	0.28	0.27	0.26	0.20	0.17	0.16
		Std dev	3	0.06	0.06	0.05	0.05	0.05	0.04	0.04	0.04	0.03	

Appendix 5.7: Continued.

AREA	FIELD		MATRIC POTENTIAL (kPa)										
			n	0	-1	-2	-4	-6	-8	-10	-33	-100	-1500
West	P4N A (2.2)	Average	3	0.45	0.43	0.42	0.41	0.39	0.34	0.30	0.19	0.13	0.13
		Std dev	3	0.03	0.03	0.02	0.01	0.00	0.01	0.01	0.01	0.00	
	P4N B (2.2)	Average	3	0.42	0.39	0.38	0.35	0.32	0.28	0.25	0.16	0.12	0.14
		Std dev	3	0.03	0.03	0.03	0.02	0.01	0.00	0.00	0.00	0.00	
	P4N B (2.3)	Average	3	0.49	0.44	0.40	0.36	0.33	0.32	0.30	0.25	0.20	0.20
		Std dev	3	0.01	0.02	0.01	0.01	0.01	0.01	0.01	0.01	0.00	
	P4N A (2.4)	Average	3	0.45	0.41	0.39	0.34	0.31	0.28	0.27	0.21	0.17	0.14
		Std dev	3	0.02	0.02	0.02	0.00	0.00	0.00	0.00	0.00	0.00	
	P4N B (2.4)	Average	3	0.47	0.43	0.41	0.37	0.36	0.34	0.33	0.29	0.26	0.14
		Std dev	3	0.00	0.00	0.00	0.00	0.00	0.00	0.00	0.00	0.00	
	R3S A Good	Average	2	0.52	0.47	0.45	0.43	0.41	0.36	0.36	0.30	0.24	0.13
		Std dev	2	0.01	0.01	0.00	0.00	0.01	0.04	0.04	0.02	0.00	
	R3S B Good	Average	2	0.54	0.48	0.47	0.45	0.42	0.40	0.40	0.31	0.27	0.18
		Std dev	2	0.02	0.02	0.01	0.01	0.00	0.00	0.00	0.00	0.01	
	R3S A Bad	Average	2	0.49	0.44	0.43	0.42	0.40	0.39	0.39	0.31	0.26	0.11
		Std dev	2	0.02	0.01	0.00	0.00	0.00	0.00	0.00	0.02	0.02	
	R3S B Bad	Average	2	0.55	0.51	0.50	0.49	0.49	0.47	0.47	0.35	0.30	0.12
		Std dev	2	0.01	0.02	0.02	0.02	0.02	0.01	0.01	0.00	0.00	
	R3S A (2.1)	Average	3	0.51	0.51	0.49	0.47	0.45	0.44	0.42	0.30	0.26	0.13
		Std dev	3	0.03	0.04	0.03	0.02	0.01	0.01	0.01	0.03	0.02	
	R3S B (2.1)	Average	3	0.53	0.51	0.48	0.42	0.40	0.39	0.38	0.30	0.23	0.14
		Std dev	3	0.01	0.01	0.00	0.01	0.01	0.01	0.01	0.01	0.04	
	R3S A (2.2)	Average	3	0.49	0.46	0.43	0.38	0.36	0.34	0.33	0.23	0.16	0.13
		Std dev	3	0.05	0.04	0.03	0.03	0.03	0.03	0.03	0.02	0.01	
	R3S B (2.2)	Average	3	0.49	0.48	0.44	0.39	0.38	0.37	0.36	0.30	0.25	0.17
		Std dev	3	0.03	0.03	0.03	0.02	0.02	0.02	0.01	0.01	0.00	
	R3S A (2.3)	Average	3	0.57	0.56	0.53	0.40	0.35	0.33	0.32	0.21	0.18	0.12
		Std dev	3	0.03	0.03	0.02	0.01	0.00	0.00	0.00	0.02	0.02	
	R3S B (2.3)	Average	3	0.49	0.48	0.46	0.42	0.40	0.39	0.38	0.25	0.20	0.17
		Std dev	3	0.03	0.02	0.02	0.01	0.01	0.01	0.01	0.00	0.02	
	L1S A	Average	3	0.60	0.51	0.45	0.41	0.38	0.35	0.35	0.32	0.30	0.17
		Std dev	3	0.03	0.02	0.01	0.01	0.01	0.03	0.03	0.01	0.01	
	L1S B	Average	3	0.52	0.48	0.46	0.43	0.40	0.38	0.38	0.30	0.29	0.15
		Std dev	3	0.00	0.00	0.01	0.01	0.01	0.01	0.01	0.01	0.00	
	N22 A	Average	3	0.45	0.42	0.41	0.38	0.37	0.36	0.36	0.31	0.27	0.13
		Std dev	3	0.00	0.01	0.01	0.02	0.02	0.02	0.02	0.02	0.01	
	N22 B	Average	3	0.40	0.37	0.36	0.34	0.34	0.33	0.33	0.30	0.28	0.14
		Std dev	3	0.01	0.01	0.01	0.02	0.02	0.02	0.02	0.01	0.01	
	M1 A	Average	3	0.53	0.46	0.44	0.41	0.39	0.38	0.38	0.34	0.30	0.16
		Std dev	3	0.01	0.00	0.01	0.01	0.01	0.01	0.01	0.01	0.01	
	M1 B	Average	3	0.44	0.41	0.39	0.37	0.36	0.35	0.35	0.29	0.25	0.16
		Std dev	3	0.05	0.06	0.06	0.06	0.07	0.07	0.07	0.08	0.07	
	K4S A	Average	3	0.49	0.47	0.45	0.39	0.38	0.37	0.37	0.32	0.28	0.17
		Std dev	3	0.03	0.02	0.02	0.00	0.00	0.00	0.00	0.00	0.01	
	K4S B	Average	3	0.54	0.51	0.48	0.39	0.37	0.36	0.36	0.30	0.27	0.18
		Std dev	3	0.01	0.01	0.01	0.01	0.01	0.01	0.01	0.00	0.02	

Appendix 5.7: Continued.

AREA	FIELD		MATRIC POTENTIAL (kPa)										
			n	0	-1	-2	-4	-6	-8	-10	-33	-100	-1500
West	K5 A	Average	3	0.41	0.38	0.35	0.30	0.26	0.23	0.22	0.15	0.12	0.09
		Std dev	3	0.01	0.01	0.01	0.01	0.01	0.01	0.01	0.00	0.00	
	K5 B	Average	3	0.37	0.33	0.30	0.25	0.22	0.19	0.18	0.13	0.11	0.14
		Std dev	3										
	Q4N A	Average	3	0.49	0.46	0.44	0.38	0.33	0.30	0.30	0.21	0.17	0.10
		Std dev	3	0.01	0.02	0.02	0.02	0.02	0.02	0.02	0.01	0.01	
	Q4N B	Average	3	0.47	0.41	0.35	0.27	0.23	0.21	0.21	0.16	0.13	0.10
		Std dev	3	0.02	0.01	0.05	0.06	0.05	0.04	0.04	0.02	0.01	
	R5N A	Average	3	0.55	0.51	0.50	0.47	0.44	0.42	0.42	0.32	0.27	0.13
		Std dev	3	0.02	0.02	0.02	0.00	0.00	0.00	0.00	0.01	0.00	
	R5N B	Average	3	0.52	0.50	0.49	0.46	0.44	0.42	0.42	0.36	0.32	0.18
		Std dev	3	0.01	0.01	0.00	0.01	0.01	0.00	0.00	0.01	0.00	
East	E6 A	Average	3	0.49	0.43	0.40	0.36	0.32	0.32	0.32	0.25	0.22	0.11
		Std dev	3	0.01	0.02	0.01	0.01	0.01	0.00	0.00	0.01	0.01	
	E6 B	Average	3	0.40	0.36	0.32	0.30	0.29	0.28	0.28	0.25	0.24	0.12
		Std dev	3	0.03	0.02	0.01	0.00	0.00	0.00	0.00	0.01	0.01	
	BO4 A	Average	3	0.52	0.42	0.39	0.36	0.35	0.34	0.34	0.31	0.28	0.21
		Std dev	3	0.01	0.03	0.03	0.02	0.02	0.02	0.02	0.01	0.01	
	BO4 B	Average	3	0.40	0.38	0.36	0.32	0.30	0.29	0.29	0.25	0.22	0.16
		Std dev	3	0.02	0.01	0.01	0.01	0.01	0.01	0.01	0.01	0.01	
	C9 A	Average	3	0.49	0.40	0.33	0.30	0.28	0.27	0.27	0.23	0.21	0.14
		Std dev	3	0.01	0.01	0.01	0.01	0.01	0.00	0.00	0.01	0.01	
	C9 B	Average	3	0.41	0.34	0.30	0.28	0.28	0.27	0.27	0.25	0.24	0.12
		Std dev	3	0.00	0.02	0.01	0.01	0.01	0.01	0.01	0.01	0.01	
	D24 A	Average	3	0.58	0.47	0.43	0.38	0.35	0.32	0.32	0.26	0.24	0.14
		Std dev	3	0.01	0.00	0.01	0.02	0.02	0.02	0.02	0.01	0.02	
	D24 B	Average	3	0.48	0.44	0.44	0.42	0.40	0.39	0.39	0.35	0.33	0.17
		Std dev	3	0.04	0.03	0.03	0.02	0.02	0.02	0.02	0.01	0.02	
	D11 A	Average	3	0.50	0.44	0.41	0.37	0.34	0.32	0.32	0.25	0.23	0.16
		Std dev	3	0.03	0.02	0.01	0.01	0.01	0.01	0.01	0.01	0.01	
	D11 B	Average	3	0.44	0.39	0.38	0.36	0.35	0.33	0.33	0.29	0.27	0.18
		Std dev	3	0.02	0.02	0.02	0.02	0.02	0.02	0.02	0.02	0.02	
	O3 A Good	Average	3	0.60	0.57	0.55	0.49	0.45	0.42	0.42	0.31	0.26	0.12
		Std dev	3	0.03	0.03	0.04	0.04	0.04	0.03	0.03	0.03	0.02	
	O3 B Good	Average	3	0.53	0.49	0.47	0.43	0.40	0.38	0.38	0.30	0.26	0.14
		Std dev	3	0.02	0.03	0.03	0.04	0.04	0.04	0.04	0.03	0.03	
	O3 A Bad	Average	3	0.58	0.54	0.52	0.47	0.43	0.39	0.39	0.27	0.22	0.11
		Std dev	3	0.01	0.01	0.01	0.01	0.01	0.00	0.00	0.01	0.00	
	O3 B Bad	Average	3	0.52	0.49	0.47	0.44	0.42	0.40	0.40	0.32	0.27	0.10
		Std dev	3	0.00	0.00	0.01	0.01	0.00	0.00	0.00	0.01	0.00	
	F1S A	Average	3	0.53	0.50	0.47	0.43	0.40	0.39	0.39	0.31	0.27	0.17
		Std dev	3	0.01	0.01	0.00	0.00	0.00	0.00	0.00	0.00	0.00	
	F1S B	Average	3	0.51	0.48	0.46	0.45	0.44	0.43	0.43	0.38	0.36	0.18
		Std dev	3	0.00	0.01	0.01	0.01	0.01	0.01	0.01	0.01	0.01	

Appendix 5.7: Continued.

AREA	FIELD			MATRIC POTENTIAL (kPa)									
			n	0	-1	-2	-4	-6	-8	-10	-33	-100	-1500
East	B3 A	Average	3	0.50	0.40	0.35	0.31	0.29	0.28	0.28	0.23	0.21	0.18
		Std dev	3	0.04	0.04	0.03	0.02	0.01	0.01	0.01	0.01	0.01	
	B3 B	Average	3	0.45	0.35	0.33	0.31	0.30	0.30	0.30	0.29	0.27	0.20
		Std dev	3	0.01	0.01	0.01	0.01	0.01	0.01	0.01	0.01	0.01	
South	12 A Good	Average	2	0.58	0.54	0.53	0.50	0.48	0.47	0.47	0.40	0.36	0.16
		Std dev	2	0.01	0.01	0.01	0.01	0.02	0.01	0.01	0.01	0.01	
	12 B Good	Average	2	0.55	0.53	0.52	0.50	0.49	0.48	0.48	0.45	0.42	0.15
		Std dev	2	0.04	0.03	0.03	0.02	0.02	0.03	0.03	0.02	0.02	
	12 A Bad	Average	2	0.60	0.57	0.56	0.53	0.50	0.48	0.48	0.39	0.34	0.16
		Std dev	2	0.01	0.00	0.00	0.03	0.03	0.03	0.03	0.02	0.02	
	12 B Bad	Average	2	0.57	0.54	0.53	0.50	0.48	0.47	0.47	0.41	0.37	0.16
		Std dev	2	0.02	0.02	0.01	0.01	0.00	0.00	0.00	0.01	0.01	
	4C A (2.1)	Average	3	0.51	0.50	0.49	0.48	0.48	0.48	0.47	0.40	0.39	0.14
		Std dev	3	0.03	0.02	0.03	0.03	0.03	0.02	0.03	0.02	0.01	
	4C B (2.1)	Average	3	0.48	0.48	0.47	0.47	0.47	0.46	0.46	0.40	0.38	0.16
		Std dev	3										
	4C A (2.2)	Average	3	0.64	0.60	0.53	0.44	0.42	0.40	0.39	0.36	0.34	0.16
		Std dev	3	0.03	0.00	0.01	0.00	0.00	0.00	0.00	0.01	0.01	
	4C B (2.2)	Average	3	0.55	0.51	0.46	0.37	0.36	0.34	0.33	0.30	0.28	0.17
		Std dev	3	0.10	0.11	0.11	0.11	0.10	0.10	0.10	0.10	0.10	
	5D A (2.1)	Average	3	0.49	0.48	0.44	0.39	0.38	0.36	0.35	0.33	0.30	0.15
		Std dev	3	0.09	0.08	0.07	0.06	0.06	0.05	0.05	0.06	0.06	
	5D B (2.1)	Average	3	0.47	0.44	0.42	0.40	0.39	0.38	0.38	0.36	0.32	0.16
		Std dev	3	0.01	0.02	0.02	0.02	0.02	0.02	0.02	0.02	0.04	
	5D A (2.2)	Average	3	0.59	0.54	0.51	0.45	0.42	0.40	0.39	0.36	0.33	0.20
		Std dev	3	0.01	0.02	0.03	0.05	0.04	0.03	0.03	0.02	0.01	
	5D B (2.2)	Average	3	0.66	0.61	0.58	0.55	0.54	0.53	0.53	0.51	0.49	0.17
		Std dev	3										
	5 A	Average	3	0.48	0.45	0.41	0.32	0.31	0.30	0.29	0.25	0.21	0.15
		Std dev	3	0.09	0.10	0.11	0.11	0.11	0.11	0.11	0.11	0.12	
	5 B	Average	3	0.47	0.44	0.41	0.36	0.35	0.34	0.34	0.30	0.29	0.11
		Std dev	3	0.00	0.01	0.02	0.03	0.03	0.03	0.03	0.04	0.04	
	1 A Good	Average	2	0.49	0.47	0.43	0.41	0.38	0.37	0.37	0.31	0.27	0.19
		Std dev	2	0.02	0.01	0.01	0.02	0.02	0.02	0.02	0.01	0.00	
	1 B Good	Average	2	0.45	0.42	0.40	0.38	0.36	0.35	0.35	0.29	0.26	0.15
		Std dev	2	0.02	0.01	0.00	0.00	0.00	0.00	0.00	0.01	0.00	
	1 A Bad	Average	2	0.52	0.46	0.45	0.42	0.39	0.37	0.37	0.27	0.22	0.12
		Std dev	2	0.00	0.01	0.01	0.01	0.01	0.00	0.00	0.01	0.01	
	1 B Bad	Average	2	0.51	0.45	0.43	0.40	0.37	0.35	0.35	0.25	0.21	0.12
		Std dev	2	0.04	0.02	0.02	0.02	0.01	0.02	0.02	0.00	0.00	
	G2 A	Average	3	0.53	0.48	0.47	0.45	0.41	0.40	0.40	0.30	0.25	0.20
		Std dev	3	0.02	0.02	0.02	0.02	0.02	0.02	0.02	0.02	0.01	
	G2 B	Average	3	0.49	0.45	0.43	0.42	0.40	0.39	0.39	0.34	0.32	0.12
		Std dev	3	0.00	0.01	0.01	0.01	0.02	0.02	0.02	0.02	0.01	
	17B A	Average	3	0.57	0.50	0.47	0.44	0.42	0.40	0.40	0.35	0.31	0.13
		Std dev	3	0.01	0.01	0.02	0.03	0.03	0.03	0.03	0.01	0.02	

Appendix 5.7: Continued.

AREA	FIELD			MATRIC POTENTIAL (kPa)									
			n	0	-1	-2	-4	-6	-8	-10	-33	-100	-1500
South	17B B	Average	3	0.51	0.48	0.47	0.46	0.43	0.42	0.42	0.38	0.34	0.14
		Std dev	3	0.00	0.02	0.03	0.03	0.03	0.03	0.03	0.01	0.03	
	10K A Good	Average	2	0.55	0.52	0.51	0.48	0.45	0.43	0.43	0.38	0.34	0.13
		Std dev	2	0.05	0.04	0.04	0.03	0.02	0.02	0.02	0.03	0.02	
	10K B Good	Average	2	0.54	0.53	0.52	0.50	0.49	0.47	0.47	0.43	0.40	0.19
		Std dev	2	0.01	0.01	0.01	0.01	0.01	0.01	0.01	0.03	0.00	
	10K A Bad	Average	2	0.57	0.51	0.48	0.45	0.43	0.41	0.41	0.35	0.32	0.12
		Std dev	2	0.01	0.01	0.02	0.01	0.01	0.01	0.01	0.01	0.01	
	10K B Bad	Average	2	0.52	0.50	0.48	0.44	0.42	0.41	0.41	0.37	0.34	0.10
		Std dev	2	0.02	0.05	0.05	0.04	0.04	0.04	0.04	0.04	0.02	
	10K A (2.1)	Average	3	0.55	0.53	0.51	0.47	0.43	0.41	0.40	0.33	0.27	0.13
		Std dev	3										
	10K B (2.1)	Average	3	0.51	0.49	0.47	0.43	0.40	0.39	0.37	0.32	0.28	0.15
		Std dev	3	0.01	0.02	0.02	0.02	0.02	0.02	0.02	0.02	0.02	
	10K B (2.2)	Average	3	0.49	0.47	0.44	0.41	0.37	0.36	0.35	0.29	0.24	0.13
		Std dev	3										
	10K A (2.3)	Average	3	0.48	0.45	0.42	0.34	0.30	0.29	0.28	0.23	0.19	0.11
		Std dev	3	0.04	0.03	0.03	0.03	0.03	0.03	0.03	0.03	0.01	
	10K B (2.3)	Average	3	0.46	0.44	0.40	0.34	0.30	0.29	0.28	0.24	0.20	0.13
		Std dev	3	0.00	0.00	0.00	0.01	0.01	0.01	0.01	0.00	0.00	
	4D A	Average	3	0.53	0.45	0.42	0.40	0.38	0.37	0.37	0.35	0.33	0.17
		Std dev	3	0.01	0.03	0.03	0.04	0.04	0.04	0.04	0.04	0.05	
	4D B	Average	3	0.50	0.44	0.42	0.40	0.39	0.38	0.38	0.37	0.34	0.15
		Std dev	3	0.01	0.01	0.01	0.00	0.01	0.01	0.01	0.01	0.00	
	4D A (2.1)	Average	3	0.47	0.43	0.39	0.34	0.32	0.29	0.28	0.23	0.19	0.17
		Std dev	3	0.03	0.02	0.02	0.02	0.02	0.02	0.02	0.02	0.03	
	4D B (2.1)	Average	3	0.52	0.48	0.44	0.40	0.38	0.37	0.36	0.34	0.31	0.16
		Std dev	3	0.01	0.01	0.00	0.00	0.00	0.00	0.00	0.00	0.00	
	4D A (2.2)	Average	3	0.55	0.48	0.43	0.37	0.36	0.34	0.33	0.30	0.28	0.17
		Std dev	3	0.03	0.00	0.00	0.00	0.01	0.00	0.00	0.01	0.01	
	4D B (2.2)	Average	3	0.45	0.40	0.36	0.33	0.32	0.31	0.30	0.28	0.25	0.18
		Std dev	3	0.01	0.01	0.01	0.00	0.00	0.00	0.00	0.01	0.02	
	12C A Good	Average	2	0.53	0.49	0.44	0.38	0.35	0.33	0.33	0.26	0.22	0.16
		Std dev	2	0.13	0.11	0.10	0.12	0.12	0.12	0.12	0.13	0.12	
	12C B Good	Average	2	0.55	0.53	0.50	0.47	0.44	0.43	0.43	0.37	0.35	0.16
		Std dev	2	0.02	0.02	0.02	0.02	0.02	0.02	0.02	0.04	0.02	
	12C A Bad	Average	2	0.45	0.41	0.36	0.32	0.30	0.28	0.28	0.21	0.19	0.15
		Std dev	2	0.14	0.13	0.13	0.13	0.13	0.13	0.13	0.10	0.12	
	12C B Bad	Average	2	0.54	0.51	0.49	0.47	0.46	0.45	0.45	0.40	0.38	0.18
		Std dev	2	0.01	0.01	0.00	0.00	0.00	0.00	0.00	0.00	0.01	
	12C A (2.1)	Average	3	0.57	0.55	0.54	0.52	0.49	0.48	0.47	0.41	0.34	0.16
		Std dev	3	0.06	0.06	0.05	0.05	0.06	0.06	0.06	0.06	0.06	
	12C B (2.1)	Average	3	0.54	0.53	0.51	0.49	0.47	0.46	0.46	0.42	0.36	0.19
		Std dev	3	0.00	0.00	0.00	0.00	0.00	0.00	0.00	0.01	0.02	
	12C A (2.2)	Average	3	0.50	0.48	0.46	0.43	0.39	0.38	0.37	0.31	0.25	0.20
		Std dev	3	0.07	0.07	0.08	0.10	0.09	0.09	0.09	0.09	0.07	

Appendix 5.7: Continued.

AREA	FIELD			MATRIC POTENTIAL (kPa)									
			n	0	-1	-2	-4	-6	-8	-10	-33	-100	-1500
South	12C B (2.2)	Average	3	0.52	0.50	0.49	0.48	0.46	0.44	0.43	0.37	0.33	0.18
		Std dev	3	0.01	0.01	0.01	0.01	0.01	0.01	0.01	0.01	0.01	
	12C A (2.3)	Average	3	0.56	0.53	0.52	0.49	0.46	0.45	0.43	0.39	0.25	0.20
		Std dev	3	0.05	0.05	0.05	0.05	0.04	0.04	0.04	0.02	0.02	
	12C B (2.3)	Average	3	0.55	0.53	0.51	0.46	0.43	0.39	0.38	0.31	0.26	0.19
		Std dev	3	0.01	0.00	0.01	0.01	0.02	0.01	0.01	0.01	0.00	
	15B A	Average	3	0.54	0.50	0.49	0.47	0.46	0.45	0.45	0.42	0.40	0.24
		Std dev	3	0.02	0.01	0.01	0.03	0.03	0.03	0.03	0.01	0.03	
	15B B	Average	3	0.52	0.47	0.46	0.44	0.43	0.43	0.43	0.40	0.37	0.23
		Std dev	3	0.01	0.03	0.03	0.03	0.03	0.03	0.03	0.04	0.03	
	11C A Good	Average	2	0.52	0.49	0.47	0.42	0.39	0.37	0.37	0.26	0.22	0.14
		Std dev	2	0.00	0.02	0.02	0.01	0.00	0.00	0.00	0.05	0.06	
	11C B Good	Average	2	0.47	0.43	0.41	0.37	0.35	0.34	0.34	0.29	0.26	0.15
		Std dev	2	0.07	0.05	0.05	0.03	0.02	0.01	0.01	0.00	0.01	
	11C A Bad	Average	2	0.58	0.55	0.53	0.48	0.44	0.42	0.42	0.33	0.28	0.14
		Std dev	2	0.01	0.00	0.00	0.00	0.00	0.00	0.00	0.00	0.01	
	11C B Bad	Average	2	0.51	0.49	0.47	0.42	0.37	0.35	0.35	0.27	0.24	0.13
		Std dev	2										
	16B A	Average	3	0.54	0.50	0.46	0.42	0.40	0.38	0.38	0.31	0.28	0.14
		Std dev	3	0.02	0.02	0.02	0.02	0.02	0.02	0.02	0.02	0.02	
	16B B	Average	3	0.53	0.49	0.45	0.41	0.40	0.38	0.38	0.34	0.31	0.13
		Std dev	3	0.01	0.01	0.01	0.01	0.01	0.01	0.01	0.01	0.01	
	16B A (2.1)	Average	3	0.54	0.52	0.50	0.46	0.41	0.40	0.38	0.30	0.26	0.19
		Std dev	3	0.02	0.02	0.02	0.02	0.03	0.03	0.03	0.04	0.03	
	16B B (2.1)	Average	3	0.47	0.45	0.43	0.40	0.36	0.35	0.34	0.29	0.25	0.17
		Std dev	3										
	19A A	Average	3	0.49	0.45	0.44	0.43	0.43	0.43	0.43	0.40	0.38	nd*
		Std dev		0.01	0.01	0.01	0.01	0.01	0.01	0.01	0.01	0.01	
	19A B	Average	3	0.47	0.39	0.38	0.37	0.36	0.35	0.35	0.30	0.28	nd
		Std dev	3	0.01	0.01	0.01	0.01	0.01	0.01	0.01	0.01	0.01	
Kahe	KH4 A	Average	3	0.53	0.51	0.49	0.47	0.45	0.43	0.43	0.37	0.32	0.15
		Std dev	3	0.02	0.02	0.02	0.02	0.02	0.01	0.01	0.01	0.01	
	KH4 B	Average	3	0.45	0.44	0.43	0.43	0.42	0.41	0.41	0.35	0.32	0.13
		Std dev	3	0.03	0.02	0.02	0.02	0.02	0.01	0.01	0.03	0.02	
	KH15 A	Average	3	0.47	0.43	0.39	0.36	0.34	0.33	0.33	0.25	0.23	0.12
		Std dev	3	0.01	0.01	0.01	0.01	0.01	0.01	0.01	0.03	0.02	
	KH15 B	Average	3	0.49	0.43	0.39	0.36	0.34	0.32	0.32	0.27	0.23	0.14
		Std dev	3	0.01	0.02	0.03	0.02	0.02	0.02	0.02	0.01	0.01	
	KH19 A	Average	3	0.49	0.44	0.40	0.35	0.33	0.30	0.30	0.22	0.18	0.13
		Std dev	3	0.03	0.05	0.06	0.05	0.05	0.05	0.05	0.02	0.02	
	KH19 B	Average	3	0.46	0.42	0.39	0.36	0.33	0.31	0.31	0.25	0.22	0.12
		Std dev	3	0.01	0.03	0.02	0.02	0.01	0.01	0.01	0.01	0.00	
	KH8 A	Average	3	0.51	0.48	0.43	0.39	0.37	0.36	0.34	0.28	0.25	0.13
		Std dev	3	0.08	0.07	0.05	0.05	0.04	0.04	0.03	0.01	0.01	
	KH8 B	Average	3	0.32	0.37	0.36	0.35	0.34	0.34	0.33	0.30	0.28	0.14
		Std dev	3	0.02	0.00	0.00	0.00	0.00	0.00	0.00	0.00	0.01	

Appendix 5.7: Continued.

AREA	FIELD		MATRIC POTENTIAL (kPa)										
			n	0	-1	-2	-4	-6	-8	-10	-33	-100	-1500
Kahe	KH27 A	Average	3	0.57	0.54	0.49	0.43	0.39	0.38	0.36	0.29	0.26	0.19
		Std dev	3	0.03	0.04	0.04	0.03	0.03	0.03	0.03	0.03	0.03	
	KH27 B	Average	3	0.58	0.56	0.52	0.48	0.45	0.42	0.43	0.38	0.36	0.18
		Std dev	3	0.10	0.10	0.10	0.11	0.11	0.14	0.11	0.11	0.11	
	KH14 A	Average	3	0.51	0.48	0.43	0.39	0.36	0.35	0.35	0.28	0.26	0.17
		Std dev	3	0.02	0.03	0.01	0.01	0.01	0.01	0.01	0.01	0.01	
	KH14 B	Average	3	0.53	0.46	0.41	0.38	0.36	0.35	0.35	0.31	0.29	0.16
		Std dev	3	0.02	0.03	0.03	0.02	0.02	0.02	0.02	0.01	0.01	
	KH29 A	Average	3	0.47	0.43	0.41	0.38	0.35	0.33	0.33	0.26	0.21	0.10
		Std dev	3	0.01	0.01	0.02	0.02	0.01	0.01	0.01	0.01	0.01	
	KH29 B	Average	3	0.48	0.44	0.41	0.38	0.35	0.33	0.33	0.26	0.22	0.09
		Std dev	3	0.01	0.01	0.02	0.02	0.02	0.02	0.02	0.01	0.01	
Out	Out 1 A	Average	3	0.52	0.48	0.47	0.43	0.40	0.36	0.36	0.29	0.24	0.12
		Std dev	3	0.02	0.02	0.02	0.02	0.02	0.04	0.04	0.03	0.01	
	Out 1 B	Average	3	0.50	0.45	0.42	0.35	0.32	0.31	0.31	0.23	0.22	0.11
		Std dev	3	0.01	0.01	0.01	0.01	0.00	0.01	0.01	0.02	0.01	
	Out 2 A	Average	3	0.50	0.46	0.43	0.39	0.37	0.35	0.35	0.28	0.23	0.13
		Std dev	3	0.02	0.01	0.01	0.00	0.00	0.00	0.00	0.00	0.00	
	Out 2 B	Average	3	0.43	0.41	0.38	0.36	0.34	0.33	0.33	0.26	0.24	0.11
		Std dev	3	0.01	0.01	0.01	0.00	0.00	0.00	0.00	0.00	0.00	
	Out 3 A	Average	3	0.43	0.41	0.39	0.32	0.30	0.30	0.29	0.22	0.18	0.12
		Std dev	3	0.06	0.05	0.05	0.01	0.01	0.01	0.01	0.02	0.01	
	Out 4 A	Average	3	0.43	0.40	0.37	0.32	0.29	0.26	0.24	0.18	0.14	0.14
		Std dev	3	0.00	0.01	0.02	0.02	0.02	0.02	0.02	0.01	0.01	
	Out 4 B	Average	3	0.42	0.36	0.31	0.26	0.24	0.22	0.21	0.17	0.13	0.12
		Std dev	3	0.04	0.04	0.02	0.01	0.01	0.01	0.01	0.01	0.02	

* Not determined

Appendix 5.8: Trends in water retention characteristics for each sampled site.

Notes:

- A difference in volumetric water content of less than or equal to 0.03 m^3 m^{-3} is considered as similar volumetric water contents and thus only differences greater than 0.03 m^3m^{-3} are discussed.
- For most replicate samples from one site within a field the standard deviation between samples at each measured tension did not exceed 0.06 m^3 m^{-3}. The highest standard deviation was 0.10 m^3 m^{-3}. The higher standard deviations exist in the lower tension range, as well as in some fields which are relatively stony. This is expected as the water content at the higher matric potentials is dependent on the macro-porosity which may be variable due to cracks and animal and root channels. Stony fields influence the variability of the water retention as each undisturbed soil core collected from a single site is likely to have different proportion and size of stones within the soil collected which affects the volume and weight of the soil collected which are used in the determination of the water content.

North:

Field N34N (A vs B) – A horizon is higher than B horizon between 0 and -8 kPa. At -33, -100 and -1500 kPa the water content of the A and B horizon is similar.

Field N65 (A vs B) – A horizon is higher than B horizon between -1 and -4 kPa. At all other higher tensions the water content between the A and B horizon is similar.

Field N91 (A vs B) – The A and B horizons are similar between sat and- 8 kPa. At -33, -100 and -1500 kPa the B horizon is higher than the A horizon.

Field N43N (A vs B) – B horizon is higher at all tensions except 1500 kPa. At 1500 kPa A and B horizon is similar.

Field N43N (2.1) (A vs B) – A horizon is slightly higher at 0 and -1 kPa. At all other higher tensions the A and B horizon are similar.

Field N66 (A vs B) – A horizon is higher than B horizon between 0 and -2 kPa. The A and B horizon are similar at all other higher tensions.

Appendix 5.8: Continued.

Field N51 (A vs B) – A slightly higher than B at 0 kPa. At all other higher tensions both the A and B horizon are similar.

Field N100KA (A vs B) – No B horizon so no comparison can be done.

Field N100KA (2.1) (A vs B) – A horizon is slightly higher than B horizon at all tensions.

Field N100KA (2.2) (A vs B) – No B horizon so no comparison can be done.

West:

Field P4N (A vs B) – A horizon is higher between 0 and -10 kPa but the B horizon is slightly higher at -33, -100 and -1500 kPa.

Field P4N (2.1) (A vs B) – The A and B horizon have a similar water content at all tensions.

P4N (2.2) (A vs B) – A horizon is slightly higher between 0 and -33 kPa. At -100 and -1500 kPa the water content is similar in the A and B horizon.

Field P4N (2.3) (A vs B) – No A horizon so nothing to compare.

Field P4N (2.4) (A vs B) – B horizon has slightly higher water content between 0 and -100 kPa. At -1500 kPa the water content is similar between the A and B horizon.

Field R3S (Good and Bad) – A Good is slightly higher than A Bad at 0 and -1 kPa and similar at higher tensions. B Bad is slightly higher than B Good at all tensions except -1500 kPa, where B Good is slightly higher than B Bad.

Field R3S (A vs B) – B horizon is slightly higher than A horizon at all tensions in Good and Bad patch. Differences are greater in Bad patch.

Field R3S (2.1) (A vs B) – A horizon is slightly higher than B horizon between -4 and -100 kPa, at all other tensions the water content is similar.

Appendix 5.8: Continued.

Field R3S (2.2) (A vs B) – B horizon is slightly higher than A horizon between -8 and -1500 kPa, at all other lower tensions the water content is similar.

Field R3S (2.3) (A vs B) – A horizon is higher than B horizon between 0 and -2 kPa but B horizon is higher than A horizon at all other higher tensions

Field L1S (A vs B) – A horizon is higher than the B horizon at 0 and -1 kPa. At all other higher tensions the A and B horizon are similar.

Field N22 (A vs B) – A horizon is higher than B horizon between 0 and -8 kPa. At-33, -100 and -1500 both horizons are similar.

Field M1 (A vs B) – A horizon is higher than B horizon at all tensions except -1500 kPa. At -1500 kPa both horizons are similar.

Field K5 (A vs B) – A horizon is higher than B horizon between 0 and -10 kPa. B horizon is higher than A horizon at -1500 kPa. At -33 and -100 kPa the water content of both horizons is similar.

Field K4S (A vs B) – B horizon is higher between 0 and -2 kPa. At all other higher tensions the water content of both horizons is similar.

Field Q4N (A vs B) – A horizon is higher than B horizon at all tensions except -1500 kPa. At -1500 kPa both horizons are similar.

Field R5N (A vs B) – A horizon is higher than B horizon at 0 kPa. B horizon is higher than A horizon at -33, -100 and -1500 kPa. At all other tensions both horizons are similar.

East:

Field E6 (A vs B) – A horizon is higher than B horizon between 0 and -8 kPa but at -33, -100 and -1500 kPa the water retention between the A and B horizons is similar.

Field BO4 (A vs B) – A horizon is higher than B horizon at all tensions.

Appendix 5.8: Continued.

Field C9 (A vs B) – A horizon is higher than B horizon between 0 and -2 kPa. At all other higher tensions the A and B horizon are similar.

Field D24 (A vs B) – A horizon is higher than B horizon at 0 and -1 kPa. At all other tensions the B horizon is higher than the A horizon.

Field D11 (A vs B) – A horizon is higher than B horizon between 0 and -2 kPa. B horizon is higher than A horizon at -33, -100 and -1500 kPa. At all other tensions the water content in both horizons is similar.

Field O3 (Good and Bad) – The Good patch is slightly higher than the Bad patch in the A horizon at all tensions except -1500 kPa. At -1500 kPa both horizons are similar. The Good and Bad patch of the B horizon are similar at all tensions except -1500 kPa. At -1500 kPa the Good patch is slightly higher than the Bad patch in the B horizon.

Field O3 (A vs B) – The A is higher than B in Good patch between 0 and -8 kPa. At -33, -100 and -1500 kPa both horizons are similar. A horizon is higher than B in Bad patch between 0 and -6 kPa. At -33 and -100 kPa the B horizon is higher than the A horizon in Bad patch. At all other tensions in Bad patch both horizons are similar.

Field F1S (A vs B) – B horizon is higher than A horizon between -6 and -100 kPa. At all other tensions both horizons are similar.

Field B3 (A vs B) – A horizon is higher than B horizon at 0 and -1 kPa. At -33 and -100 kPa the B horizon is higher than the A. At all other tensions both horizons are similar.

South:

Field 12 (Good and Bad) – Bad is slightly higher than Good in A horizon between 0 and -4 kPa. At all other higher tensions the Good and Bad patch of the A horizon are similar. The Good patch is slightly higher than the Bad patch in the B horizon at -33 and -100 kPa. At all other tensions the water content is similar.

Appendix 5.8: Continued.

Field 12 (A vs B) – The B horizon is higher than the A horizon in the Good patch at -33 and -100 kPa. At all other tensions the water content is similar. The water content of the A and B horizon in the bad patch are similar at all tensions.

Field 4C (2.1) (A vs B) – The A and B horizon are similar at all tensions.

Field 4C (2.2) (A vs B) – A horizon is higher than B horizon at all tensions except -1500 kPa. At -1500 kPa the water content for both horizons is similar.

Field 5D (2.1) (A vs B) – The A and B horizon are similar at all tensions.

Field 5D (2.2) (A vs B) – B horizon is higher at all tensions except -1500 kPa. At -1500 kPa the water content for both horizons is similar.

Field 5 (A vs B) – B horizon is higher than A horizon between -4 and -100 kPa. At all other tensions the water content of both horizons is similar.

Field 1 (Good and Bad) - A Bad slightly higher than A Good at 0 kPa but A Good slightly higher at -33, -100 and -1500 kPa. Similarly, B Bad slightly higher at 0 kPa and lower tensions than B Good but B Good slightly higher at -33, -100 and -1500 kPa.

Field 1 (A vs B) – A horizon of both Good and Bad patch is slightly higher than B horizon. Difference is greater in A horizon.

Field G2 (A vs B) – A horizon is slightly higher than B horizon between 0 and -8 kPa but at -33 and -100 kPa the B horizon is higher. At -1500 kpa the A horizon is higher than the B horizon.

Field 17B (A vs B) – A horizon is higher at 0 kPa but at -33 and -100 the B horizon is slightly higher. At all other tensions the water content is similar.

Field 10K (Good and Bad) – The Good and Bad patch have similar water contents at all tensions in the A horizon. The Good patch of the B horizon has higher water content at all tensions compared to the Bad patch.

Appendix 5.8: Continued.

Field 10K (A vs B) – B horizon is higher between -8 and -1500 kPa than A horizon in Good patch. At all other lower tensions the A and B horizon are similar. A horizon has higher water retention than B horizon at 0 kPa in bad patch. At all other higher tensions the water content between the A and B horizon in the bad patch is similar.

Field 10K (2.1) (A vs B) – A horizon is higher than B horizon between 0 and -10 kPa. At -33, -100 and -1500 kPa the water content is similar.

Field 10K (2.2) (A vs B) – No reps are valid for A horizon so no comparison can be made.

Field 10K (2.3) (A vs B) – A and B horizon are similar at all tensions.

Field 4D (A vs B) – The A and B horizon are similar at all tensions.

Field 4D (2.1) (A vs B) – B horizon is higher than A horizon at all tensions except -1500 kPa. At -1500 kPa the A and B horizon are similar.

Field 4D (2.2) (A vs B) – A horizon is higher than B horizon between 0 and -10 kPa. At -33, -100 and -1500 kPa the A and B horizon are similar.

Field 12C (Good and Bad) – Good is higher than Bad in A horizon at all tensions except -1500 kPa. At -1500 kPa the water content is similar between Good and Bad in the A horizon. The Good and Bad in the B horizon is similar at all water contents.

Field 12C (A vs B) – B horizon is higher than A horizon in Good and Bad patch at all tensions except -1500 kPa. At -1500 kPa the water content is similar.

Field 12C (2.1) (A vs B) – A horizon is slightly higher than B horizon between 0 and -10 kPa. At -33, -100 and -1500 kPa the B horizon is slightly higher than the A horizon.

Field 12C (2.2) (A vs B) – B horizon is higher than A horizon at all tensions except -1500 kPa. At -1500 kPa the A and B horizon are similar.

Field 12C (2.3) (A vs B) – A horizon is higher than B horizon between -4 and -33 kPa. At all other tensions the A and B horizon are similar.

Appendix 5.8: Continued.

The standard deviations for most of the 12C samples are high. This is very likely due to the soil being very stony.

Field 15 B (A vs B) – A and B horizon are similar at all tensions.

Field 11C (Good and Bad) – The Bad patch is higher than the Good patch in the A horizon at all tensions except -1500 kPa. At -1500 kPa the Good and Bad patch in the A horizon are similar. The Bad patch is higher than the Good patch in the B horizon between 0 and -8 kPa. At all other higher tensions the Good patch is slightly higher than the Bad patch in the B horizon.

Field 11C (A vs B) – A horizon is higher than B horizon in the Good patch between 0 and -8 kPa. At -33 and -100 kPa the B horizon is higher than the A horizon and at -1500 kPa both horizons are similar. A horizon is higher than the B horizon at all tensions in the Bad patch except -1500 kPa. At -1500 kPa the A and B horizons in the Bad patch are similar.

Field 16B (A vs B) – The A and B horizon are similar at all tensions.

Field 16B (2.1) (A vs B) – A horizon is higher than B horizon between 0 and -10 kPa. At -33, -100 and -1500 kPa the A and B horizon are similar.

Field 19A (A vs B) – A horizon is higher than B horizon at all tensions.

Kahe:

Field KH4 (A vs B) – A horizon is higher than B horizon between 0 and -6 kPa. At all other higher tensions the water content is similar between the A and B horizon.

Field KH15 (A vs B) – The A and B horizon are similar at all tensions.

Field KH19 (A vs B) – A horizon is slightly higher than B at 0 and -1 kPa. B horizon is slightly higher than the A horizon at -33 and -100 kPa. At all other tensions A and B horizon are similar.

Field KH8 (A vs B) – A horizon is higher than B horizon between 0 and -6 kPa. At all other higher tensions the water content for both horizons are similar.

Appendix 5.8: Continued.

Field KH27 (A vs B) – B horizon is higher than A horizon between -4 and -100 kPa. At all other tensions the water content of both horizons are similar.

Field KH14 (A vs B) – Both horizons are similar at all tensions.

Field KH29 (A vs B) – Both horizons are similar at all tensions.

Out:

Out 1 (A vs B) – A horizon is higher than B horizon between 0 and -33 kPa. At -100 and -1500 kPa the water content is similar.

Out 2 (A vs B) – A horizon is higher than B horizon between 0 and -4 kPa. At all other higher tensions the water content is similar.

Out 3 (A vs B) – No B horizon collected so no comparison can be made.

Out 4 (A vs B) – A horizon is higher than B horizon between -1 and -10 kPa. At all other tensions the water content of both horizons is similar.

Appendix 5.9: Saturated hydraulic conductivity (K_s) of undisturbed soil cores from the A and B horizons for TPC sugar estate.

AREA	SAMPLE	K_s (mm hr^{-1})	SAMPLE	K_s (mm hr^{-1})
	A Horizon		B Horizon	
North	N100KA A1	1502.60		
	N100KA A2	433.44		
	N100KA A3	724.33		
	N100KA A1 (2.1)	76.05	N100KA B1 (2.1)	21.73
	N100KA A2 (2.1)	92.35		
	N100KA A1 (2.2)	21.73		
	N100KA A2 (2.2)	173.84		
	N34N A1	25.38	N34N B1	28.20
	N34N A2	225.57	N34N B2	28.20
	N34N A3	29.61	N34N B3	26.43
	N65 A1	606.63	N65 B1	235.41
	N65 A2	316.90	N65 B2	48.89
	N65 A3	199.19	N65 B3	76.96
			N91 B1	48.89
	N43N A1	169.18	N43N B1	14.10
	N43N A2	105.74	N43N B2	17.62
	N43N A3	50.75	N43N B3	16.92
	N43N A1	38.03	N43N B1	59.76
	N43N A2	29.88	N43N B2	54.32
	N66 A1	76.05		
	N66 A2	135.81		
	N66 A3	537.82		
	N51 A1	253.52	N51 B1	36.22
	N51 A2	235.41	N51 B2	27.16
	N51 A3	362.17	N51 B3	54.32
West	R3S A1 Good	97.23	R3S B1 Good	32.59
	R3S A2 Good	39.42	R3S B2 Good	38.03
	R3S A1 Bad	27.16	R3S B1 Bad	16.30
	R3S A2 Bad	6.79		
	R3S A1 (2.1)	29.88	R3S B1 (2.1)	40.74
	R3S A2 (2.1)	16.30	R3S B2 (2.1)	38.03
	R3S A1 (2.2)	97.78	R3S B1 (2.2)	43.46
	R3S A2 (2.2)	97.78		
	R3S A1 (2.3)	287.92		
	R3S A2 (2.3)	124.95	R3S B2 (2.3)	54.32
	P4N A1	208.25		
	P4N A2	190.14		
	P4N A3	208.25		
	P4N A1 (2.1)	201.00	P4N B1 (2.1)	108.65
			P4N B2 (2.1)	54.32

Appendix 5.9: Continued.

AREA	SAMPLE	K_s (mm hr^{-1})	SAMPLE	K_s (mm hr^{-1})
	A Horizon		B Horizon	
West	P4N A1 (2.2)	86.92	P4N B1 (2.2)	114.08
	P4N A2 (2.2)	217.30	P4N B2 (2.2)	81.49
			P4N B1 (2.3)	59.76
			P4N B2 (2.3)	363.98
	P4N A1 (2.4)	59.76	P4N B1 (2.4)	27.16
	P4N A2 (2.4)	162.97	P4N B2 (2.4)	244.46
	L1S A1	230.88	L1S B1	298.79
	L1S A2	298.79	L1S B2	99.60
	L1S A3	122.23	L1S B3	54.32
	N22 A1	93.05		
	N22 A2	8.46	N22 B2	21.15
	N22 A3	4.23	N22 B3	33.84
	M1 A1	67.91	M1 B1	18.11
	M1 A2	525.14	M1 B2	21.73
	M1 A3	94.62	M1 B3	16.30
	Q4N A1	147.17	Q4N B1	421.02
			Q4N B2	1113.66
	Q4N A3	190.14		
	R5N A1	155.08	R5N B1	304.52
	R5N A2	162.13	R5N B2	59.21
	R5N A3	140.98	R5N B3	114.20
	K4S A1	54.32	K4S B1	84.20
	K4S A2	35.31	K4S B2	92.35
	K5 A1	385.71		
	K5 A2	217.30	K5 B1	260.76
East			E6 B1	92.35
	E6 A2	43.46	E6 B2	65.19
	E6 A3	40.74	E6 B3	2.72
			BO4 B1	206.43
			BO4 B2	fast
			BO4 B3	86.92
	D24 A1	624.74		
	D24 A2	353.11	D24 B2	0.00
			D24 B3	40.74
	D11 A1	199.19	D11 B1	18.11
	D11 A2	135.81	D11 B2	5.43
	D11 A3	67.91	D11 B3	8.15
	C9 A1	258.04	C9 B1	389.33
	C9 A2	312.37	C9 B2	362.17
	C9 A3	226.35	C9 B3	50.30
	O3 A1 Good	27.16	O3 B1 Good	90.54

Appendix 5.9: Continued.

AREA	SAMPLE	Ks (mm hr^{-1})	SAMPLE	Ks (mm hr^{-1})
	A Horizon		B Horizon	
East	O3 A2 Good	226.35	O3 B2 Good	36.22
	O3 A1 Bad	67.91	O3 B1 Bad	18.11
	O3 A2 Bad	72.43	O3 B2 Bad	27.16
	F1S A1	16.30	F1S B1	10.86
	F1S A2	21.73	F1S B2	2.72
	F1S A3	5.43	F1S B3	2.72
	B3 A1	81.49	B3 B1	45.27
	B3 A2	393.86	B3 B2	90.54
	B3 A3	312.37	B3 B3	72.43
South	1 A1 Good	59.76	1 B1 Good	260.76
	1 A2 Good	54.32	1 B2 Good	27.16
	1 A1 Bad	86.92	1 B1 Bad	84.20
	1 A2 Bad	86.92	1 B2 Bad	86.92
	G2 A1	63.44	G2 B1	33.84
	G2 A2	42.29	G2 B2	42.29
	G2 A3	77.54	G2 B3	25.38
	17B A1	108.65	17B B1	36.22
	17B A2	72.43	17B B2	54.32
	17B A3	307.84	17B B3	54.32
	10K A1 Good	63.38	10K B1 Good	144.87
	10K A2 Good	16.30	10K B2 Good	126.76
	10K A1 Bad	45.27	10K B1 Bad	58.85
	10K A2 Bad	45.27	10K B2 Bad	62.47
	10K A1 (2.1)	30.97	10K B1 (2.1)	30.97
	10K A2 (2.1)	48.89	10K B2 (2.1)	56.77
	10K A1 (2.2)	54.32	10K B1 (2.2)	38.03
	10K A1 (2.3)	157.54	10K B1 (2.3)	113.54
	10K A2 (2.3)	216.76	10K B2 (2.3)	92.35
	4D A1	36.22	4D B1	65.19
	4D A2	211.87	4D B2	38.03
	4D A3	228.16	4D B3	97.78
	4D A1 (2.1)	271.62	4D B1 (2.1)	651.90
	4D A2 (2.1)	152.11	4D B2 (2.1)	532.38
	4D A1 (2.2)	2716.24	4D B1 (2.2)	440.03
	4D A2 (2.2)	2716.24	4D B2 (2.2)	2716.24
	12C A1 Good	108.65	12C B1 Good	54.32
	12C A2 Good	153.92	12C B2 Good	103.22
	12C A1 Bad	90.54	12C B1 Bad	5.43
	12C A2 Bad	9.05	12C B2 Bad	27.16
	12C A1 (2.1)	21.73	12C B1 (2.1)	65.19

Appendix 5.9: Continued.

AREA	SAMPLE	Ks (mm hr^{-1})	SAMPLE	Ks (mm hr^{-1})
	A Horizon		B Horizon	
South	12C A2 (2.1)	16.30	12C B2 (2.1)	27.16
	12C A1 (2.2)	43.46	12C B1 (2.2)	2.72
	12C A2 (2.2)	27.16	12C B2 (2.2)	2.72
	12C A1 (2.3)	38.03	12C B1 (2.3)	54.32
	12C A2 (2.3)	54.32	12C B2 (2.3)	81.49
	15B A1	244.46	15B B1	27.16
	15B A2	13.58	15B B2	1.36
	15B A3	2.72	15B B3	199.19
	11C A1 Good	325.95	11C B1 Good	63.38
	11C A2 Good	135.81	11C B2 Good	162.97
	11C A1 Bad	43.46	11C B1 Bad	59.76
	11C A2 Bad	40.74	11C B2 Bad	54.32
	16B A1	135.81	16B B1	95.07
	16B A2	181.08	16B B2	135.81
	16B A3	190.14	16B B3	190.14
	16B A1 (2.1)	16.30		
	16B A2 (2.1)	119.51	16B B1 (2.1)	27.16
			19A B1	119.83
	19A A2	7.05	19A B2	35.25
	19A A3	197.37	19A B3	70.49
	12 A1 Good	15.77	12 B1 Good	8.15
	12 A2 Good	27.16	12 B2 Good	24.45
	12 A1 Bad	22.64	12 B1 Bad	8.15
	12 A2 Bad	172.03		
	5^{1} A1	65.19		
	51 A2	73.34	5^{1} B2	54.32
	4C A1 (2.1)	16.73	4C B1 (2.1)	12.55
	4C A2 (2.1)	12.55		
	4C A1 (2.2)	794.50	4C B1 (2.2)	Fast
	4C A2 (2.2)	684.49	4C B2 (2.2)	Fast
	5D A1 (2.1)	611.15	5D B1 (2.1)	108.65
	5D A2 (2.1)	516.09	5D B2 (2.1)	244.46
	5D A1 (2.2)	380.27		
	5D A2 (2.2)	285.21	5D B2 (2.2)	624.74
Kahe	KH4 A1	22.64	KH4 B1	slow
	KH4 A2	22.64	KH4 B2	slow
	KH4 A3	4.53	KH4 B3	slow
	KH15 A1	92.35	KH15 B1	92.35
	KH15 A2	65.19	KH15 B2	65.19
	KH15 A3	65.19	KH15 B3	54.32

Appendix 5.9: Continued.

AREA	SAMPLE	Ks (mm hr^{-1})	SAMPLE	Ks (mm hr^{-1})
	A Horizon		B Horizon	
Kahe	KH19 A1	234.38	KH19 B1	38.77
	KH19 A2	105.74	KH19 B2	38.77
	KH19 A3	109.65	KH19 B3	42.29
	KH14 A1	162.13	KH14 B1	35.95
	KH14 A2	91.64	KH14 B2	177.64
	KH14 A3	98.69	KH14 B3	46.52
	KH29 A1	5.43	KH29 B1	37.65
	KH29 A2	10.76	KH29 B2	45.27
	KH29 A3	16.30	KH29 B3	389.33
	KH27 A1	29.88	KH27 B1	32.59
	KH27 A2	10.86	KH27 B2	92.35
	KH8 A1	10.86	KH8 B1	5.43
	KH8 A2	65.19	KH8 B2	2.72
Out	Out 1 A1	63.44	Out 1 B1	91.64
	Out 1 A2	79.30	Out 1 B2	84.59
	Out 1 A3	42.29	Out 1 B3	28.20
	Out 2 A1	70.49	Out 2 B1	19.38
	Out 2 A2	59.21	Out 2 B2	18.36
	Out 2 A3	77.54	Out 2 B3	21.15
	Out 3 A1	141.24		
	Out 3 A2	16.30		
	Out 4 A1	54.32	Out 4 B1	217.30
	Out 4 A2	116.80	Out 4 B2	108.65

Appendix 5.10: Bulk density of soil samples from TPC sugar estate for the A and B horizon.

		Bulk density (g cm^{-3})	
AREA	SAMPLE	A Horizon	B Horizon
North	N34N	1.27	1.34
	N65	1.24	1.49
	N91	1.48	1.44
	N43N	1.24	1.37
	N43N	1.28	1.38
	N66	1.27	1.71
	N51	1.32	1.39
	N100KA	1.28	
	N100KA (2.1)	1.26	1.28
	N100KA (2.2)	1.36	
West	R3S Good	1.24	1.14
	R3S Bad	1.38	1.32
	R3S (2.1)	1.41	1.33
	R3S (2.2)	1.07	1.23
	R3S (2.3)	1.16	1.26
	P4N	1.14	1.22
	P4N (2.1)	1.15	1.41
	P4N (2.2)	1.43	1.43
	P4N (2.3)		1.08
	P4N (2.4)	1.48	1.52
	L1S	1.12	1.18
	N22	1.38	1.53
	M1	1.19	1.21
	Q4N	1.33	1.33
	R5N	0.98	1.16
	K4S	1.20	1.11
	K5	1.27	1.43
East	E6	1.31	1.46
	BO4	1.13	1.32
	D24	1.08	1.61
	D11	1.29	1.71
	C9	1.17	1.33
	O3 Good	1.18	1.13
	O3 Bad	1.07	1.20
	F1S	1.08	1.26
	B3	1.11	1.28
South	1 Good	1.17	1.32
	1 Bad	1.24	1.16
	G2	1.15	1.26
	17B	1.13	1.24

Appendix 5.10: Continued.

AREA	SAMPLE	Bulk density (g cm^{-3}) A Horizon	B Horizon
South	10K Good	1.10	1.08
	10K Bad	0.98	1.10
	10K (2.1)	1.04	1.15
	10K (2.2)	1.03	1.11
	10K (2.3)	1.17	1.25
	4D	1.16	1.21
	4D (2.1)	1.16	1.19
	4D (2.2)	1.02	1.21
	12C Good	1.17	1.12
	12C Bad	1.12	1.23
	12C (2.1)	1.18	1.15
	12C (2.2)	1.16	1.19
	12C (2.3)	1.16	1.10
	15B	1.21	1.22
	11C Good	1.10	1.27
	11C Bad	1.00	1.20
	16B	1.13	1.11
	16B (2.1)	1.25	1.46
	19A	1.48	1.44
	12 Good	1.13	1.22
	12 Bad	1.08	1.13
	4C (2.1)	1.36	1.49
	4C (2.2)	0.85	0.91
	5D (2.1)	1.18	1.34
	5D (2.2)	1.09	0.99
	5	1.28	1.36
Kahe	KH4	1.24	1.48
	KH15	1.28	1.20
	KH19	1.09	1.27
	KH14	1.10	1.23
	KH29	1.33	1.31
	KH8	1.19	1.41
	KH27	1.12	1.21
Out	Out 1	1.20	1.26
	Out 2	1.23	1.37
	Out 3	1.35	
	Out 4	1.20	1.29

Appendix 5.11: Particle size distribution of sampled fields across TPC sugar estate.

AREA	SAMPLE	Coarse sand	Medium sand	Fine sand	Very fine sand	Sand	Coarse silt	Fine silt	Silt	Clay	Coarse sand	Medium sand	Fine sand	Very fine sand	Sand	Coarse silt	Fine silt	Silt	Clay
		A Horizon									B Horizon								
North	N100KA	9	6	8	5	27	10	24	34	39									
	N100KA (2.1)	9	17	25	12	63	13	19	31	5	20	25	22	11	79	4	12	16	5
	N100KA (2.2)	11	13	27	12	63	13	20	33	4									
	N32N	2	4	14	16	36	17	27	45	19	3	7	14	16	40	26	24	50	10
	N33	8	7	18	14	47	16	21	37	16	4	7	21	15	48	16	4	20	32
	N34N		59			59	8	22	30	11		45			45	7	28	35	20
	N43N		64			64	8	19	27	9		45			45	11	24	35	20
	N43N (2.1)	23	19	18	7	67	9	21	30	2	20	16	13	8	57	7	19	26	17
	N51	8	13	21	12	54	13	22	35	11	4	10	20	11	46	12	23	35	19
	N65		62			62	9	20	28	9		50			50	9	21	30	20
	N66	9	8	14	8	39	13	46	58	3	6	6	12	9	33	14	27	40	26
	N72	29	16	15	6	66	11	17	28	7	15	15	14	9	53	13	20	33	14
	N84		41			41	9	24	33	26		15			15	3	32	35	50
	N91		48			48	10	18	28	24		37			37	9	19	28	35
	Average	**27**	**12**	**18**	**10**	**54**	**11**	**22**	**34**	**13**	**22**	**13**	**17**	**11**	**47**	**11**	**21**	**31**	**21**
	Std. dev	**22**	**6**	**6**	**4**	**13**	**3**	**7**	**8**	**11**	**17**	**7**	**4**	**3**	**16**	**6**	**7**	**9**	**13**
West	K4S	14	15	19	11	59	15	23	38	3	14	16	29	9	67	10	21	31	2
	K5	26	14	27	10	77	10	11	21	2	25	28	31	7	91	3	3	6	4
	L1S		48			48	10	25	35	17		52			52	9	25	34	14
	L3N	21	18	19	8	66	11	13	24	10	24	15	17	8	63	13	14	27	10
	L5	6	6	10	7	30	23	31	54	16	5	7	8	10	30	24	24	48	22
	M1	16	4	10	8	38	18	33	51	11	3	4	5	5	17	23	46	69	14
	N22	8	8	13	9	38	14	26	41	22	6	5	11	8	31	11	27	38	31

Appendix 5.11: Continued.

AREA	SAMPLE	Coarse sand	Medium sand	Fine sand	Very fine sand	Sand	Coarse silt	Fine silt	Silt	Clay	Coarse sand	Medium sand	Fine sand	Very fine sand	Sand	Coarse silt	Fine silt	Silt	Clay
						A Horizon									B Horizon				
West	P4N		67			67	9	14	23	10		56			56	15	22	37	7
	P4N (2.1)	13	22	20	15	70	10	17	27	3	21	20	23	12	76	11	12	23	1
	P4N (2.2)	14	15	29	16	74	6	11	17	9	13	14	38	15	80	10	8	19	2
	P4N (2.3)										9	14	17	8	48	15	27	42	10
	P4N (2.4)	21	21	24	8	75	3	17	20	5	14	15	24	14	68	13	19	32	0
	Q2N	4	9	20	14	48	18	23	41	11	1	9	38	15	63	13	16	29	8
	Q4N	23	30	19	5	78	4	11	15	7	21	31	24	7	83	4	5	9	8
	R3S (2.1)	12	15	14	13	53	13	25	39	8	8	13	25	13	59	14	21	35	6
	R3S (2.2)	9	10	27	11	57	13	20	32	10	8	10	22	12	52	15	23	38	10
	R3S (2.3)	8	15	30	15	68	11	16	28	4	6	11	32	16	65	14	17	31	4
	R3S Bad		55			55	12	17	29	16		65			65	11	14	25	10
	R3S Good		59			59	14	16	30	11		63			63	13	15	28	9
	R5N	4	5	11	9	28	19	32	51	20	4	4	7	6	21	16	39	55	24
	Average	**23**	**14**	**19**	**11**	**57**	**12**	**20**	**32**	**10**	**21**	**14**	**22**	**10**	**57**	**13**	**20**	**33**	**10**
	Std. dev	**20**	**7**	**7**	**3**	**16**	**5**	**7**	**12**	**6**	**21**	**8**	**10**	**4**	**20**	**5**	**10**	**14**	**8**
East	B2	9	7	9	6	31	13	29	41	27	10	8	9	6	33	9	24	33	34
	B3		46			46	8	27	35	19		38			38	10	29	39	23
	BO4		60			60	6	21	27	13		60			60	7	20	27	13
	BO4 (2.1)	16	14	13	7	50	11	27	38	12	15	18	20	7	60	7	19	26	14
	C2	11	10	15	10	46	11	24	35	19	9	8	12	8	37	9	26	35	28
	C9	11	10	13	9	42	12	26	37	21	10	8	11	8	36	10	27	37	26
	D11	13	11	12	7	43	12	23	35	23	16	12	11	6	45	8	21	29	27
	D19	13	11	12	8	45	13	22	35	20	14	10	12	9	45	11	21	32	24

Appendix 5.11: Continued.

AREA	SAMPLE	Coarse sand	Medium sand	Fine sand	Very fine sand	Sand	Coarse silt	Fine silt	Silt	Clay	Coarse sand	Medium sand	Fine sand	Very fine sand	Sand	Coarse silt	Fine silt	Silt	Clay
		A Horizon									B Horizon								
East	D24	12	9	10	5	35	13	20	33	32	12	7	7	4	30	7	22	29	41
	E10	10	10	13	7	40	14	19	33	27	11	8	9	6	34	12	19	31	35
	E17	13	12	13	9	46	11	25	36	18	13	10	11	7	40	10	25	35	25
	E6		46			46	11	20	31	23		42			42	10	20	30	28
	F1S	3	4	15	11	33	22	31	53	13	8	8	13	12	41	20	24	44	15
	O3 Bad	4	8	27	14	53	13	20	33	14	6	11	24	7	49	17	24	41	10
	O3 Good	3	6	25	13	48	17	23	41	11	4	8	27	12	52	17	23	40	8
	Average	**18**	**9**	**15**	**9**	**44**	**12**	**24**	**36**	**20**	**18**	**10**	**14**	**8**	**43**	**11**	**23**	**34**	**23**
	Std. dev	**18**	**3**	**6**	**3**	**7**	**4**	**4**	**6**	**6**	**16**	**3**	**6**	**3**	**9**	**4**	**3**	**5**	**10**
South	1 Bad		54			54	12	24	36	10		67			67	15	9	24	9
	1 Good		63			63	14	15	30	7		64			64	12	15	27	9
	10K (2.1)	4	7	17	8	35	15	36	51	14	7	15	23	8	53	16	26	42	4
	10K (2.2)	6	12	22	11	51	9	30	39	10									
	10K (2.3)	13	14	25	10	61	8	22	30	9	12	15	28	12	67	8	16	24	9
	10K Bad		53			53	12	25	38	9		62			62	9	22	31	7
	10K Good		29			29	12	41	53	18		35			35	8	41	49	16
	10K Crust Bad		49			49	18	22	40	11									
	11	7	10	19	11	47	13	28	41	12	3	6	20	14	43	21	27	48	9
	11C Bad	4	5	15	12	35	19	27	45	19	7	14	34	10	65	8	15	23	12
	11C Good	15	10	15	10	49	12	23	35	16	22	12	15	8	56	9	18	27	16
	12 Bad	3	5	15	13	36	16	28	44	20	3	5	15	10	33	18	31	49	18
	12 Good	4	4	12	10	29	17	31	48	22	1	2	3	5	10	27	45	72	18
	12C (2.1)	6	4	12	9	31	15	36	52	17	28	22	13	7	70	7	23	30	0

Appendix 5.11: Continued.

AREA	SAMPLE	Coarse sand	Medium sand	Fine sand	Very fine sand	Sand	Coarse silt	Fine silt	Silt	Clay	Coarse sand	Medium sand	Fine sand	Very fine sand	Sand	Coarse silt	Fine silt	Silt	Clay
		A Horizon									B Horizon								
South	12C (2.2)	3	4	7	6	20	13	44	57	23	1	2	6	5	14	38	25	63	23
	12C (2.3)	4	6	17	13	39	18	34	52	9	10	7	14	11	42	15	35	50	8
	12C Bad		42			42	13	29	42	16		53			53	6	27	33	14
	12C Good		49			49	7	29	36	15		60			60	8	22	30	10
	13	4	4	5	5	18	13	42	55	27	6	4	5	5	20	13	41	54	26
	15B	5	6	8	6	25	18	34	52	23	11	7	10	6	34	13	30	43	23
	16 (3)	26	14	13	8	61	11	20	31	8	23	13	16	6	58	13	16	29	13
	16B		63			63	5	18	23	14		58			58	14	15	29	13
	16B (2.1)	16	16	20	11	63	5	17	22	15	15	11	15	12	53	12	16	28	19
	17B		54			54	15	15	30	16		56			56	10	19	29	15
	18A	13	8	13	9	44	13	23	35	21									
	4A	19	12	20	11	62	17	14	32	6	17	11	21	10	60	15	17	32	8
	4C (2.1)	10	5	6	6	27	5	42	47	26	14	8	9	7	38	12	40	52	10
	4C (2.2)	7	5	6	3	21	6	51	57	21	5	6	7	5	23	12	42	54	24
	4D		44			44	8	31	39	17		37			37	5	35	40	23
	4D (2.1)	17	9	10	5	41	4	41	45	14	17	12	17	6	52	9	26	35	13
	4D (2.2)	6	6	10	6	28	19	35	54	18	10	12	15	6	42	11	36	47	12
	5 (1) Bad	16	8	11	6	40	14	30	44	16	12	7	10	6	36	13	29	42	22
	5 (1) Good	18	10	10	6	45	13	26	39	16	17	6	8	6	36	13	32	45	19
	5 (1)	20	16	18	10	64	11	23	34	2	27	19	22	11	79	8	12	20	0
	5D (2.1)	19	18	15	16	68	6	18	24	8	13	8	14	12	47	13	29	42	11
	5D (2.2)	11	15	16	5	47	12	33	45	8	10	13	17	5	45	13	32	45	10
	6D	10	8	12	9	39	15	26	41	19	20	19	15	8	62	14	15	29	9

Appendix 5.11: Continued.

AREA	SAMPLE	Coarse sand	Medium sand	Fine sand	Very fine sand	Sand	Coarse silt	Fine silt	Silt	Clay	Coarse sand	Medium sand	Fine sand	Very fine sand	Sand	Coarse silt	Fine silt	Silt	Clay
		A Horizon									B Horizon								
South	7(1)	1	1	3	6	11	28	40	68	21	0	0	1	4	5	27	47	74	21
	9	11	12	19	11	52	15	20	35	13	8	6	13	11	39	18	26	44	17
	9C	7	7	15	11	40	24	24	48	12	19	10	13	12	55	14	22	36	9
	G2		68			68	9	18	27	5		66			66	8	18	26	8
	G5	30	12	13	8	63	6	19	25	12	26	16	15	8	65	9	19	28	7
	Average	**22**	**9**	**13**	**9**	**44**	**13**	**28**	**41**	**15**	**24**	**10**	**14**	**8**	**48**	**13**	**26**	**39**	**13**
	Std. dev	**20**	**4**	**5**	**3**	**15**	**5**	**9**	**11**	**6**	**21**	**5**	**7**	**3**	**18**	**6**	**10**	**13**	**6**
Kahe	KH14	12	8	11	10	41	14	15	29	30	21	15	15	6	57	3	10	13	30
	KH15		52			52	8	21	29	19		43			43	8	23	31	26
	KH19	15	9	13	7	44	11	27	38	18	11	8	13	7	40	11	24	35	25
	KH27	8	3	12	7	30	11	26	37	34	6	6	8	8	28	10	24	34	38
	KH27 (2.1)	8	8	15	9	40	12	23	35	25	7	11	19	9	46	11	21	32	22
	KH29		57			57	7	23	30	13		53			53	8	25	33	14
	KH4		50			50	8	26	34	16		39			39	7	27	34	27
	KH7	25	15	14	7	61	11	14	25	14	23	17	13	7	60	14	14	28	12
	KH8	9	11	12	10	42	16	32	48	10	12	10	15	9	46	5	25	30	24
	KH9	13	9	10	8	40	11	25	37	23									
	Average	**25**	**9**	**13**	**8**	**46**	**11**	**23**	**34**	**20**	**24**	**11**	**14**	**8**	**46**	**9**	**21**	**30**	**24**
	Std. dev	**20**	**4**	**2**	**1**	**9**	**3**	**5**	**6**	**8**	**17**	**4**	**4**	**1**	**10**	**3**	**6**	**7**	**8**
Ash layers	BH Ash		89			89	1	6	7	4									
	R8 Ash		12			12	15	57	72	16									

Appendix 5.11: Continued.

AREA	SAMPLE	Coarse sand	Medium sand	Fine sand	Very fine sand	Sand	Coarse silt	Fine silt	Silt	Clay	Coarse sand	Medium sand	Fine sand	Very fine sand	Sand	Coarse silt	Fine silt	Silt	Clay
		A Horizon									B Horizon								
Out	Out 1										18	12	14	6	49	9	22	31	20
	Out 2	13	17	22	9	62	10	17	27	11	8	10	17	7	42	10	28	38	20
	Out 3	18	15	23	13	69	6	23	29	2									
	Out 4	9	11	19	10	49	17	31	48	3	8	11	18	9	46	21	29	50	4

Appendix 5.12: Soil organic carbon (%) from the A and B horizons of fields sampled at TPC sugar estate.

AREA	FIELD	A HORIZON	B HORIZON
North	N 91	0.8	0.4
	N 65	1.5	0.8
	N 43 N	1.6	0.9
	N 34 N	1.5	0.5
	N 100 KA	0.9	
	N 66	1.4	0.9
	N 51	1.2	0.8
	N 84	1.7	0.8
	N 72	1.1	0.6
	N 33	1.6	0.9
	N 32 N	1.4	0.7
	Average	**1.4**	**0.7**
	Std dev	**0.3**	**0.2**
West	L 1 S	2.5	1.2
	P 4 N	1.3	0.6
	R 3 S Good	1.1	0.7
	R 3 S Bad	0.8	1.4
	N 22	1.4	0.7
	M 1	1.5	1.2
	Q 4 N	0.8	0.3
	R 5 N	2.2	1.5
	L 5	1.3	1.1
	L 3 N	1.0	0.7
	Q 2 N	1.1	0.3
	Average	**1.4**	**0.9**
	Std dev	**0.5**	**0.4**
East	B 3	1.2	0.9
	E 6	1.0	0.5
	B O 4	2.1	0.9
	D 11	1.0	0.3
	C 9	1.0	0.4
	F 1 S	0.8	0.6
	D 24	1.2	0.3
	O 3 Good	1.1	0.8
	O 3 Bad	1.1	0.9
	C 2	0.2	0.6
	B 2	1.2	0.4
	E 10	1.1	0.5

Appendix 5.12: Continued.

AREA	FIELD	A HORIZON	B HORIZON
East	D 19	1.0	0.6
	E 17	0.9	0.6
	Average	**1.1**	**0.6**
	Std dev	**0.4**	**0.2**
South	16 B	1.5	1.5
	10 K Good	1.6	0.7
	10 K Bad	1.1	0.3
	4 D	1.9	1.4
	5^1 Good	1.4	0.9
	5^1 Bad	1.1	0.5
	12 C Good	2.2	2.0
	12 C Bad	2.0	1.8
	17 B	1.2	1.6
	G 2	2.3	1.0
	19 A	0.4	0.4
	11 C^1 Good	1.7	0.8
	11 C^1 Bad	1.6	0.5
	12 Good	2.1	1.1
	12 Bad	1.9	1.1
	1 Good	1.6	1.3
	1 Bad	0.7	0.5
	15 B	1.8	1.3
	9	1.1	1.6
	9 C	1.2	0.6
	11	1.1	4.0
	163	1.9	0.5
	6 D	2.0	0.7
	4 A	1.2	0.3
	7(1)	1.4	1.6
	13	2.5	2.1
	18 A	1.1	
	G 5	1.7	1.0
	Average	**1.5**	**1.1**
	Std dev	**0.5**	**0.8**
Kahe	KH 4	1.6	1.0
	KH 15	0.6	0.7
	KH 29	0.6	0.4
	KH 19	1.1	0.6
	KH 14	1.1	0.7

Appendix 5.12: Continued.

AREA	FIELD	A HORIZON	B HORIZON
	KH 27	1.2	1.2
	KH 9	1.2	
	KH 7	0.9	0.6
	Average	**1.1**	**0.8**
	Std dev	**0.3**	**0.3**
Out	Out 1	1.5	0.6
	Out 2	0.7	0.3
South	10 K Crust	0.9	
North	BH Ash	0.1	
South	R8 Ash	0.2	

Appendix 5.13: pH (H_2O) in the A and B horizons of the sampled fields across TPC sugar estate.

AREA	FIELD	A HORIZON	B HORIZON
North	N100KA	7.24	
	N100KA (2.1)	6.27	5.53
	N100KA (2.2)	6.10	
	N91	7.42	7.41
	N84	7.68	7.23
	N72	7.09	7.76
	N65	7.27	7.11
	N65 (2.1)	7.66	7.27
	N66	7.55	7.63
	N51	7.31	7.30
	N43N	8.40	8.22
	N34N	8.33	7.83
	N33	8.70	8.26
	N32N	8.39	8.38
	Average	**7.53**	**7.49**
	Std dev	**0.76**	**0.76**
West	L1S	7.35	7.22
	P4N	8.63	8.92
	P4N (2.1)	8.83	8.12
	P4N (2.2)	8.72	8.85
	P4N (2.3)		8.57
	P4N (2.4)	8.63	8.57
	R3S Good	8.96	9.06
	R3S Bad	9.35	8.52
	R3S (2.1)	9.25	9.10
	R3S (2.2)	9.10	9.02
	R3S (2.3)	8.65	8.78
	Q4N	8.82	9.00
	R5N	9.18	9.16
	M1	7.99	7.81
	L5	7.25	7.69
	L3N	7.78	7.61
	Q2N	9.10	8.89
	K5	7.61	7.61
	K4S	7.46	7.47
	Average	**8.48**	**8.42**
	Std dev	**0.71**	**0.65**
East	B3	7.31	7.32
	B2	7.20	7.19
	C2	7.22	7.05
	D11	7.51	7.05
	D19	7.52	7.38

Appendix 5.13: Continued.

AREA	FIELD	A HORIZON	B HORIZON
East	D24	7.81	8.35
	E6	7.29	7.31
	E10	7.74	7.60
	E17	7.18	7.29
	BO4	8.48	8.12
	BO4 (2.1)	8.88	8.55
	C9	7.61	7.43
	F1S	8.85	9.35
	O3 Good	8.86	8.78
	O3 Bad	8.85	9.02
	Average	**7.89**	**7.85**
	Std dev	**0.69**	**0.77**
South	15B	9.08	9.06
	16 B	7.03	7.58
	16B (2.1)	8.06	8.46
	10 K Good	9.00	8.89
	10 K Bad	9.86	9.40
	10K (2.1)	8.79	8.86
	10K (2.2)	9.07	8.99
	10K (2.3)	8.38	8.44
	4C (2.1)	9.09	8.78
	4C (2.2)	9.06	8.96
	4 D	8.75	8.56
	4D (2.1)	8.37	8.25
	4D (2.2)	8.63	8.33
	5D (2.1)	8.52	8.39
	5D (2.2)	8.80	8.28
	6D	9.19	9.17
	5[1]	9.02	8.82
	11C Good	8.71	8.80
	11C Bad	8.75	8.97
	12 Good	8.85	8.88
	12 Bad	8.76	9.09
	12 C Good	8.53	8.56
	12 C Bad	8.94	8.44
	12C (2.1)	8.61	8.58
	12C (2.2)	8.25	8.36
	12C (2.3)	8.28	8.67
	1 Good	8.37	8.18
	1 Bad	8.77	8.92
	17 B	8.94	8.61

Appendix 5.13: Continued.

AREA	FIELD	A HORIZON	B HORIZON
South	G 2	8.65	9.19
	G 5	8.44	8.24
	9C	8.44	8.46
	9	9.35	8.90
	11	9.01	8.98
	16^3	8.87	8.85
	4A	9.28	9.25
	7^1	10.32	9.13
	13	9.00	8.81
	Average	**8.78**	**8.71**
	Std dev	**0.52**	**0.37**
Kahe	KH 4	8.27	7.64
	KH7	7.88	5.92
	KH8	8.50	9.04
	KH9	8.25	
	KH14	8.00	7.00
	KH 15	8.11	7.92
	KH27	7.97	7.80
	KH27 (2.1)	7.60	7.65
	KH29	8.17	8.32
	Average	**8.08**	**7.66**
	Std dev	**0.26**	**0.92**
Ash layers	BH Ash	9.04	
	R8 Ash	10.40	
Out	OUT 1	8.18	7.71
	OUT 2	7.41	6.79
	OUT 3	7.74	
	OUT 4	6.27	6.34
South	10 K Crust	10.06	

Appendix 5.14: Electrical conductivity of a saturated paste sample for TPC sugar estate fields in the A and B horizons.

AREA	SAMPLE	A Horizon	B Horizon
North	N100KA	46	
	N100KA (2.1)	46	40
	N100KA (2.2)	99	
	N32N	82	49
	N33	63	43
	N34N	58	
	N43N	71	49
	N51	44	43
	N65	53	38
	N66	48	
	N72	60	
	N84	62	193
	Average	**61**	**65**
	Std. dev	**16**	**57**
West	K4S	38	38
	K5	32	26
	L3N	47	38
	L5	159	45
	M1	37	33
	N22	41	45
	P4N (2.1)	71	62
	P4N (2.2)	48	59
	P4N (2.3)	72	
	P4N (2.4)	63	75
	Q2N	81	62
	Q4N	55	53
	R3S (2.1)	149	104
	R3S (2.2)	92	73
	R3S (2.3)	70	109
	R5N	130	164
	Average	**74**	**66**
	Std. dev	**40**	**36**
East	B2	48	51
	BO4	71	117
	C2	47	84
	C9	37	46
	D11	34	24
	D19	44	50
	D24	44	45
	E10	49	51
	E17	34	36

Appendix 5.14: Continued.

AREA	SAMPLE	A Horizon	B Horizon
East	F1S	200	83
	O3 Bad	60	67
	O3 Good	68	55
	Average	**61**	**59**
	Std. dev	**45**	**24**
South	11	108	90
	13	112	96
	51	67	63
	71	120	47
	163	88	85
	10K (2.1)	614	131
	10K (2.2)	472	78
	10K (2.3)	57	46
	11	138	126
	11C1 Bad	63	51
	11C1 Good	54	56
	12 Bad	303	88
	12 Good	85	58
	12C (2.1)	71	63
	12C (2.2)	209	63
	12C (2.3)	187	63
	15B	129	101
	16B	55	55
	4A	105	76
	4C (2.1)	136	94
	4C (2.2)	120	115
	4D (2.1)	378	314
	4D (2.2)	71	70
	5D (2.1)	73	67
	5D (2.2)	245	182
	6D	127	85
	9	275	87
	9C	58	59
	G5	69	58
	Average	**158**	**89**
	Std. dev	**135**	**53**
Kahe	KH14	42	48
	KH19	60	46
	KH27	47	57
	KH7	150	236

Appendix 5.14: Continued.

AREA	SAMPLE	A Horizon	B Horizon
Kahe	KH8	48	42
	KH9	72	
	Average	70	86
	Std. dev	37	84
Out	OUT 3	69	
	OUT 4	82	52

Appendix 5.15: Water soluble cations and the sodium adsorption ratio (SAR) of a saturated paste for the A horizon (A) and B horizon (B) of sampled fields across TPC sugar estate.

AREA	SAMPLE	Ca^{2+} ($mmol_c\ l^{-1}$)		Mg^{2+} ($mmol_c\ l^{-1}$)		Na^{+} ($mmol_c\ l^{-1}$)		K^{+} ($mmol_c\ l^{-1}$)		SAR	
		A	B	A	B	A	B	A	B	A	B
North	N100KA	0.88		0.73		2.24		0.67		2.49	
	N100KA (2.1)	1.19	0.96	0.74	0.67	1.58	1.54	0.72	0.40	1.61	1.70
	N100KA (2.2)	3.02		1.68		1.59		2.35		1.04	
	N32N	1.10	0.59	1.11	0.53	4.45	3.21	0.99	0.36	4.24	4.30
	N33	0.80	0.43	0.80	0.44	3.62	2.65	0.60	0.22	4.05	4.02
	N34N	1.37	1.02	1.07	0.87	4.17	3.27	0.82	0.25	3.77	3.37
	N43N Rep 1	1.14	1.03	0.79	0.72	3.95	2.58	1.02	0.20	4.02	2.76
	N43N Rep 2	2.26	1.10	1.75	0.83	7.04	4.17	1.75	0.56	4.97	4.25
	N51	0.87	0.89	0.67	0.65	2.17	2.34	0.81	0.34	2.48	2.67
	N65	0.87	0.91	0.64	0.63	2.54	2.05	0.75	0.23	2.93	2.33
	N66	1.13		0.94		2.60		0.45		2.56	
	N72	0.87		0.89		3.09		0.47		3.30	
	N84 Rep 1	3.29		1.99		6.29		1.82		3.87	
	N91	1.45		1.05		1.97		1.18		1.76	
West	K4S	0.74	0.72	0.47	0.49	2.09	1.86	0.52	0.63	2.68	2.40
	K5	0.71	0.62	0.50	0.43	1.70	1.42	0.16	0.11	2.18	1.96
	L1S	1.43	0.80	1.15	0.56	2.81	2.07	1.31	0.31	2.48	2.51
	L3N	0.68	0.56	0.62	0.55	2.17	1.93	0.62	0.25	2.68	2.60
	L5 Rep 1	8.47		3.84		3.71		1.38		1.49	
	L5 Rep 2	7.48	0.70	3.92	0.66	3.19	2.14	1.42	0.53	1.34	2.59
	M1	0.66	0.68	0.56	0.51	2.27	2.17	0.51	0.14	2.91	2.82
	N22	0.80	0.86	0.62	0.68	2.29	2.85	0.60		2.73	3.25
	P4N	1.49	0.81	1.09	0.73	4.16	4.46	0.63	0.27	3.66	5.07
	P4N (2.1)	0.96	0.95	0.88	0.80	5.44	4.27	0.64	0.36	5.67	4.56
	P4N (2.2)	0.68	0.86	0.55	0.69	3.68	4.85	0.33	0.32	4.68	5.52
	P4N (2.3)	0.90		0.77		5.89		0.31		6.45	
	P4N (2.4)	0.85	0.79	0.76	0.61	4.75	5.67	0.46	0.34	5.30	6.80
	Q2N Rep 1	0.97		0.84		7.23		0.59		7.61	
	Q2N Rep 2	0.94	0.87	0.87	0.53	5.77	4.75	0.50	0.32	6.05	5.67
	Q4N	1.09	0.91	0.78	0.59	3.99	4.04	0.49	0.40	4.13	4.66
	R3S (2.1)	1.75	1.63	1.31	1.27	12.03	6.90	0.93	0.43	9.74	5.73
	R3S (2.2)	1.17	1.04	0.98	0.79	7.12	5.81	0.52	0.33	6.87	6.08
	R3S (2.3)	1.06	1.29	0.87	1.01	5.36	7.78	0.55	0.77	5.45	7.26
	R3S Bad	1.90	5.93	1.31	4.99	11.04	20.48	0.84	2.87	8.72	8.77
	R3S Good		1.20		1.19		5.73		0.48		5.24
	R5N	1.29	1.36	1.05	1.06	11.68	15.54	1.00	0.67	10.79	14.12
East	B3	1.04	1.21	0.73	0.92	1.88	2.59	0.42	0.27	2.00	2.52
	BO4	2.89	1.62	2.53	1.27	4.73	3.75	1.59	0.39	2.87	3.12
	BO4 (2.1)	1.12	2.51	0.88	1.83	3.63	6.05	1.79	1.05	3.63	4.11

Appendix 5.15: Continued.

AREA	SAMPLE	Ca^{2+} ($mmol_c\ l^{-1}$)		Mg^{2+} ($mmol_c\ l^{-1}$)		Na^{+} ($mmol_c\ l^{-1}$)		K^{+} ($mmol_c\ l^{-1}$)		SAR	
		A	B	A	B	A	B	A	B	A	B
East	C2 Rep 1	0.90	2.04	0.72	1.41	2.52	3.99	0.65	0.19	2.80	3.04
	C2 Rep 2	0.79	1.98	0.72	1.52	2.01	3.71	0.59	0.16	2.31	2.80
	C9	0.96	1.13	0.66	0.80	2.00	2.81	0.28	0.17	2.22	2.86
	D11	0.87	0.71	0.64	0.46	1.69	1.21	0.37	0.27	1.95	1.59
	D19	0.78	0.99	0.72	0.77	1.91	2.30	0.52	0.27	2.20	2.45
	D24	1.24	1.16	0.93	0.83	1.79	2.47	0.72	0.29	1.72	2.47
	E10	0.75	0.88	0.68	0.85	2.28	2.32	0.56	0.31	2.69	2.49
	E17 Rep 1	0.80	0.81	0.66	0.60	1.56	2.12	0.37	0.22	1.83	2.53
	E17 Rep 2	0.90	0.82	0.83	0.70	1.77	1.81	0.32	0.23	1.90	2.07
	E6	1.20		0.97		2.74		0.50		2.63	
	F1S	2.80	0.90	2.43	0.66	15.68	7.36	1.35	0.47	9.69	8.33
	O3 Bad	1.62	1.40	1.10	0.91	3.59	4.69	0.61	0.53	3.08	4.37
	O3 Good	1.45	1.56	0.91	0.93	4.41	3.36	0.73	0.51	4.07	3.01
South	9	2.23	1.53	1.55	1.19	22.58	5.24	2.19	0.73	16.42	4.49
	11 Rep 1	1.16	0.80	0.84	0.54	8.23	7.76	0.16	0.61	8.23	9.47
	11 Rep 2	1.61	1.43	1.23	1.22	9.42	8.41	0.83	0.14	7.91	7.31
	13 Rep 1	0.61	0.94	0.41	0.59	7.64	2.02	0.60	0.60	10.69	2.30
	13 Rep 1	1.10	1.08	1.37	0.87	9.23	6.94	0.78	0.47	8.31	7.03
	51	1.08	0.98	0.84	0.72	4.31	3.95	0.36	0.24	4.41	4.28
	71 Rep 1	0.43	0.99	0.26	0.91	12.15	2.52	0.19	0.89	20.63	2.58
	163	1.27	1.34	0.99	1.07	5.25	5.41	0.87	0.26	4.94	4.93
	1 Bad	1.01	1.01	0.81	0.77	3.94	4.52	0.44	0.31	4.14	4.79
	1 Good	1.17	1.04	1.14	0.76	4.32	3.44	0.43	0.19	4.02	3.62
	10K (2.1)	5.69	1.23	4.16	0.99	53.20	10.34	3.40	0.60	23.97	9.81
	10K (2.2)	2.59	1.08	1.67	0.81	33.54	5.88	1.78	0.41	22.98	6.05
	10K (2.3)	1.08	1.05	0.96	0.84	3.38	2.69	0.42	0.30	3.35	2.76
	10K Bad A	2.51	0.99	0.74	0.73	25.69	9.28	1.13	0.48	20.15	10.01
	10K Crust	2.54		1.35		39.48		1.55		28.33	
	10K Good	1.34	1.34	0.63	0.91	9.91	7.40	0.73	0.28	9.99	6.97
	11C1 Bad	1.66	1.21	1.15	0.62	3.43	3.87	0.63	0.22	2.90	4.04
	11C1 Good	1.64	1.60	1.30	1.02	2.71	3.54	0.37	0.25	2.23	3.09
	12 Bad	2.91	0.98	2.61	0.72	24.14	8.41	1.81	0.18	14.52	9.11
	12 Good	1.32	0.94	1.17	0.65	6.22	4.59	0.64	0.10	5.57	5.14
	12C (2.1)	1.16	0.70	1.03	0.53	4.47	5.18	0.91	0.25	4.27	6.59
	12C (2.2)	2.77	1.20	2.67	1.28	12.57	3.37	1.94	0.43	7.62	3.03
	12C (2.3)	2.56	0.84	2.58	0.72	9.30	4.26	2.20	0.44	5.80	4.83
	12C Bad	1.53	0.94	1.19	0.83	8.94	6.09	1.34	0.79	7.67	6.47
	12C Good	1.41	2.09	1.37	2.01	10.07	6.66	1.63	0.82	8.56	4.65
	15B	1.76	1.34	1.77	1.14	10.08	8.75	0.84	0.45	7.58	7.86
	16B	3.26	1.61	2.82	1.43	5.68	4.13	1.51	0.50	3.25	3.35
	16B (2.1)	0.94	0.93	0.76	0.81	3.80	3.68	0.40	0.30	4.12	3.95

Appendix 5.15: Continued.

AREA	SAMPLE	Ca^{2+} ($mmol_c\ l^{-1}$)		Mg^{2+} ($mmol_c\ l^{-1}$)		Na^{+} ($mmol_c\ l^{-1}$)		K^{+} ($mmol_c\ l^{-1}$)		SAR	
		A	B	A	B	A	B	A	B	A	B
South	17B	1.06	1.30	1.12	1.07	10.01	6.63	0.65	0.52	9.59	6.08
	4A Rep 1	0.46	1.07	0.53	0.85	6.12	9.59	0.29	1.01	8.70	9.80
	4A Rep 2	1.18	0.83	0.90	0.72	7.75	5.51	0.59	0.26	7.60	6.27
	4C (2.1)	1.14	0.92	0.78	0.69	10.81	6.80	0.47	0.26	11.03	7.59
	4C (2.2)	0.94	1.18	0.71	0.81	9.29	8.97	1.12	0.49	10.21	8.99
	4D	1.44	1.27	1.44	1.01	6.57	5.46	0.57	0.17	5.47	5.12
	4D (2.1)	8.63	7.10	4.55	2.62	25.46	21.63	1.51	0.75	9.92	9.81
	4D (2.2)	0.93	1.00	0.71	0.82	4.63	5.00	0.32	0.37	5.11	5.24
	51 Bad	1.49	1.20	1.55	1.29	29.40	13.97	1.01	0.44	23.87	12.52
	51 Good	1.27	0.84	1.32	0.94	10.40	9.39	0.55	0.29	9.14	9.96
	5D (2.1)	0.96	0.77	0.77	0.62	5.33	4.74	0.37	0.16	5.74	5.68
	5D (2.2)	2.48	2.33	1.93	1.96	17.47	11.34	0.82	0.63	11.77	7.75
	6D	1.35	0.91	1.13	0.75	9.39	6.00	0.86	0.30	8.43	6.58
	9C	1.45	1.18	1.25	0.97	2.53	3.20	0.47	0.30	2.17	3.09
	G2	1.70	1.38	1.36	1.11	11.69	5.96	2.33	0.68	9.45	5.34
	G5	1.45	1.04	1.28	0.87	3.41	3.26	0.84	0.28	2.92	3.34
Kahe	KH14	1.25	1.25	1.00	0.98	1.66	2.91	0.60	0.18	1.57	2.75
	KH15	1.18	1.28	0.85	0.97	1.79	2.25	0.69	0.72	1.77	2.12
	KH19	1.89	1.14	1.53	0.76	2.05	2.16	1.18	0.85	1.57	2.22
	KH27 Rep 1	3.82	0.95	3.29	0.72	1.83	2.68	1.17	0.40	0.97	2.94
	KH27 Rep 2	0.91	1.12	0.79	0.95	2.07	2.76	0.47	0.47	2.24	2.72
	KH29	1.57	1.14	1.12	0.82	2.33	2.00	0.79	0.57	2.01	2.03
	KH4	1.64	1.37	1.51	1.05	2.24	2.16	0.76	0.50	1.78	1.96
	KH7	4.34	8.22	4.36	9.40	2.50	2.94	1.44	0.85	1.20	0.99
	KH8	0.90		0.57		2.75		0.15		3.20	
	KH9	2.12		1.98		1.89		0.80		1.32	
Out	OUT 1	3.94	13.58	3.65	10.70	3.51	10.73	5.13	5.52	1.80	3.08
	OUT 2	2.10	1.21	1.01	0.71	14.85	16.23	2.00	1.11	11.91	16.55
	OUT 3	1.25		0.90		2.90		1.28		2.79	
	OUT 4	2.31	1.35	1.39	0.85	1.30	1.26	2.08	1.06	0.95	1.20

Appendix 5.16: Water soluble cations (Ca, Mg, Na and K) and the sodium adsorption ratio (SAR) of the A horizon (A) and B horizon (B) of sampled fields across TPC sugar estate.

AREA	SAMPLE	Ca ($cmol_c\ kg^{-1}$ soil)		Mg ($cmol_c\ kg^{-1}$ soil)		Na ($cmol_c\ kg^{-1}$ soil)		K ($cmol_c\ kg^{-1}$ soil)		SAR	
		A	B	A	B	A	B	A	B	A	B
North	N34N	0.06	0.30	0.02	0.35	0.52	0.36	0.42	0.51	2.64	0.62
	N65	0.01	0.08	0.02	0.00	0.44	0.26	0.30	0.26	3.57	1.27
	N91	0.16	0.22	0.16	0.21	0.15	0.17	0.67	0.43	0.36	0.37
	Average	**0.08**	**0.20**	**0.06**	**0.19**	**0.37**	**0.26**	**0.46**	**0.40**	**2.19**	**0.76**
	Std dev	**0.07**	**0.11**	**0.08**	**0.17**	**0.20**	**0.09**	**0.19**	**0.13**	**1.65**	**0.46**
West	L1S	0.05	0.03	0.02	0.02	0.33	0.31	0.34	0.24	1.82	1.99
	P4N	0.04	0.01	0.02	0.02	0.49	0.65	0.31	0.19	2.94	5.34
	R3S Bad	0.40	0.44	0.02	0.02	0.74	1.42	0.29	0.36	1.62	3.00
	R3S Good	1.25	0.16	0.08	0.02	1.08	1.36	0.21	0.26	1.33	4.63
	Average	**0.43**	**0.16**	**0.03**	**0.02**	**0.66**	**0.94**	**0.29**	**0.26**	**1.93**	**3.74**
	Std dev	**0.57**	**0.19**	**0.03**	**0.00**	**0.33**	**0.54**	**0.05**	**0.07**	**0.70**	**1.52**
East	B3	0.14	0.24	0.07	0.15	0.76	0.29	0.50	0.32	2.33	0.67
	BO4	0.17	0.16	0.06	0.06	0.57	0.51	0.34	0.22	1.70	1.54
	E6	0.12	0.17	0.06	0.20	0.27	0.19	0.38	0.76	0.90	0.45
	Average	0.14	0.19	0.06	0.14	0.53	0.33	0.41	0.43	1.64	0.88
	Std dev	0.02	0.04	0.01	0.07	0.25	0.16	0.09	0.29	0.71	0.58
South	1 Bad	0.05	0.01	0.02	0.02	0.54	0.55	0.14	0.31	2.94	5.00
	1 Good	0.08	0.72	0.02	0.03	0.54	1.49	0.25	0.24	2.49	2.42
	10K Bad	1.45	0.13	0.06	0.15	1.69	1.73	0.05	0.15	1.94	4.60
	10K Good	1.09	0.11	0.01	0.02	1.72	0.95	0.36	0.36	2.32	3.83
	10K Crust	1.53		0.11		1.72		0.20		1.90	
	12C Bad	0.07	0.09	0.02	0.02	1.02	1.12	0.22	0.29	4.80	4.95
	12C Good	0.09	0.10	0.02	0.02	0.73	0.74	0.25	0.16	3.25	3.03
	16B	0.23	0.11	0.23	0.09	0.16	0.49	0.63	0.25	0.34	1.57
	17B	0.18	0.14	0.30	0.16	1.45	0.78	0.30	0.27	2.94	2.01
	4D	0.15	0.14	0.05	0.08	1.14	0.84	0.39	0.17	3.57	2.55
	G2	0.19	1.16	0.00	0.13	0.74	1.29	0.14	0.05	2.42	1.60
	Average	0.46	0.27	0.08	0.07	1.04	1.00	0.27	0.22	2.63	3.16
	Std dev	0.59	0.37	0.10	0.06	0.55	0.40	0.16	0.09	1.12	1.35
Kahe	KH15	0.16	0.20	0.19	0.22	0.17	0.19	0.62	0.66	0.41	0.41
	KH29	0.14	0.16	0.13	0.19	0.21	0.31	0.28	0.48	0.57	0.74
	KH4	0.17	0.30	0.25	0.59	0.25	0.22	0.32	0.61	0.55	0.32
	Average	0.15	0.22	0.19	0.33	0.21	0.24	0.41	0.58	0.51	0.49
	Std dev	0.01	0.08	0.06	0.22	0.04	0.06	0.18	0.09	0.09	0.22
North	BH Ash	0.01		0.02		0.49		0.14		4.25	
South	R8 Ash	0.00		0.02		1.74		0.60		17.45	

Appendix 5.17: Exchangeable Ca, Mg, Na, K and the sum of exchangeable bases (Ex. bases) in the A horizon (A) and B horizon B of sampled fields across TPC sugar estate.

AREA	SAMPLE	Ca ($cmol_c\ kg^{-1}$ soil)		Mg ($cmol_c\ kg^{-1}$ soil)		Na ($cmol_c\ kg^{-1}$ soil)		K ($cmol_c\ kg^{-1}$ soil)		Ex. bases ($cmol_c\ kg^{-1}$ soil)	
		A	B	A	B	A	B	A	B	A	B
North	N51	6.45	6.72	3.04	2.73	1.08	1.08	3.11	1.66	13.68	12.19
	N72	8.09	6.78	2.85	2.30	1.05	1.39	1.28	0.68	13.27	11.15
	N66	7.87		3.37		0.85		1.33		13.41	
	N34N	11.10	13.71	4.90	6.37	0.91	1.05	2.43	4.16	19.33	25.30
	N43N	9.81	7.81	4.91	4.23	0.79	0.79	1.67	1.25	17.18	14.07
	N91	5.48	6.02	2.71	2.68	0.02	0.07	1.57	0.53	9.78	9.31
	N65	5.40	8.29	2.97	3.56	0.22	0.52	0.76	0.96	9.35	13.33
	Average	**7.74**	**7.56**	**3.53**	**3.45**	**0.70**	**0.93**	**1.74**	**1.44**	**13.71**	**12.99**
	Std dev	**2.16**	**3.11**	**0.96**	**1.47**	**0.41**	**0.52**	**0.79**	**1.26**	**3.61**	**6.12**
West	L1S	11.29	8.41	4.59	3.56	7.49	7.72	4.12	3.24	27.49	22.95
	P4N	9.68	8.45	3.86	3.67	1.39	2.41	1.87	2.00	16.80	16.54
	R3S Good	10.72	9.41	6.34	8.46	1.29	1.99	3.18	2.14	21.52	22.00
	R3S Bad	9.81	12.10	5.52	5.93	2.85	2.05	2.01	1.48	20.19	21.56
	Average	**10.38**	**9.59**	**5.08**	**5.41**	**3.25**	**3.54**	**2.79**	**2.22**	**21.50**	**20.76**
	Std dev	**0.76**	**1.74**	**1.08**	**2.31**	**2.91**	**2.79**	**1.06**	**0.74**	**4.46**	**2.87**
East	O3 Good	12.90	11.79	4.52	4.22	2.26	1.70	3.47	2.24	23.15	19.94
	O3 Bad	11.66	11.92	4.22	4.87	1.76	1.72	2.82	2.66	20.47	21.18
	BO4	10.44	11.47	4.36	5.10	1.85	1.11	1.98	1.74	18.63	19.42
	E6	7.52	6.81	4.26	3.87	0.37	0.33	1.12	0.62	13.28	11.63
	B3	10.47	6.73	3.94	3.42	0.28	0.25	1.09	0.80	15.77	11.20
	Average	**10.60**	**9.74**	**4.26**	**4.29**	**1.30**	**1.02**	**2.10**	**1.61**	**18.26**	**16.67**
	Std dev	**2.00**	**2.72**	**0.21**	**0.70**	**0.91**	**0.71**	**1.05**	**0.89**	**3.87**	**4.85**
South	5 Good	12.00	11.88	7.71	8.06	7.03	10.20	4.20	4.01	30.94	34.14
	5 Bad	7.10	5.39	5.91	7.45	14.87	11.27	5.70	4.72	33.58	28.83
	17B	9.37	10.92	8.69	7.49	4.78	3.38	4.12	3.66	26.95	25.45
	10K Good	12.36	10.59	5.68	4.60	4.45	4.45	4.14	1.12	26.63	20.77
	10K Bad	6.23	4.58	3.89	7.74	11.97	7.05	4.58	3.69	26.67	23.07
	1 Good	6.47	11.93	4.45	6.18	3.06	1.62	3.48	1.91	17.45	21.63
	1 Bad		7.95		4.47		1.83		3.35		17.60
	G2	13.56	7.77	6.98	9.20	1.41	3.33	2.67	3.84	24.62	24.13
	16B	12.56	13.00	6.81	8.52	0.63	0.79	1.84	1.42	21.84	23.73
	12C Good	13.37	12.99	6.88	7.01	1.97	1.48	2.46	1.62	24.68	23.10
	12C Bad	13.55	14.00	7.23	6.93	2.78	1.54	3.68	2.15	27.24	24.63
	4D	13.42	12.22	7.08	5.96	1.98	2.26	2.29	0.49	24.78	20.94
	Average	**10.91**	**9.72**	**6.48**	**6.54**	**4.99**	**3.82**	**3.56**	**2.56**	**25.94**	**22.63**
	Std dev	**3.02**	**3.58**	**1.40**	**2.06**	**4.58**	**3.53**	**1.15**	**1.36**	**4.25**	**6.40**

Appendix 5.17: Continued.

AREA	SAMPLE	Ca ($cmol_c\ kg^{-1}$ soil)		Mg ($cmol_c\ kg^{-1}$ soil)		Na ($cmol_c\ kg^{-1}$ soil)		K ($cmol_c\ kg^{-1}$ soil)		Ex. bases ($cmol_c\ kg^{-1}$ soil)	
Kahe	KH29	7.91	7.94	3.07	2.56	0.77	1.00	2.29	1.47	14.04	12.97
	KH15	9.66	9.77	3.73	3.12	3.63	3.41	3.03	3.11	20.05	19.41
	KH4	14.94	14.85	7.84	6.76	0.42	0.39	2.67	2.17	47.87	24.18
	Average	**10.84**	**10.85**	**4.88**	**4.15**	**1.61**	**1.60**	**2.66**	**2.25**	**27.32**	**18.85**
	Std dev	**3.66**	**3.58**	**2.58**	**2.28**	**1.76**	**1.60**	**0.37**	**0.83**	**18.05**	**5.62**
South	**10K Crust**		**4.10**		**2.07**		**16.42**		**5.07**		**23.57**

Appendix 5.18: Cation exchange capacity (CEC) of the A horizon (A) and B horizon (B) of measured fields across TPC sugar estate.

AREA	SAMPLE	CEC ($cmol_c$ kg^{-1} soil)	
		A	B
North	N51	18.71	16.76
	N72	17.97	16.17
	N66	18.86	17.47
	N66 (rep 2)	15.35	nd*
	N65	16.47	16.37
	N91	15.17	15.31
	N34N	18.27	18.86
	N34N (rep 2)	18.86	nd
	N43N	18.43	17.37
West	P4N	15.50	16.50
	L1S	18.94	18.94
	R3S Good	18.49	18.79
	R3S Bad	18.32	18.75
East	E6	17.47	15.95
	B3	18.94	18.86
	BO4	18.40	15.81
	O3 Good	18.94	19.11
	O3 Bad	18.94	18.94
South	5 Good	18.94	18.94
	5 Bad	18.94	18.94
	5 Bad (rep 2)	16.76	nd
	G2	18.97	17.64
	16B	18.82	18.94
	17B	18.94	18.94
	1 Good	13.57	18.94
	1 Bad	15.16	13.51
	1 Bad (rep 2)	17.15	nd
	10K Crust	15.40	
	10K Good	18.94	18.94
	10K Bad	18.94	18.40
	12C Bad	18.79	18.94
	12C Good	18.82	18.94
	4D	18.90	18.82
Kahe	KH4	18.86	18.75
	KH29	15.33	14.71
	KH29 (rep 2)	13.08	nd
	KH15	14.18	16.36

* Not determined

Appendix 5.19: Correlations (r value) between amorphous mineral content of the soils from TPC sugar estate and other measured soil properties in the a.) A horizon and b.) B horizon

a.)

n				
	Alo + 1/2 Feo	0.232	-	
	P-value	0.194	-	
	Ferrihydrite	-0.088	0.514	-
	P-value	0.627	0.002	-
33	Sand	0.258	0.082	-0.046
	P-value	0.148	0.650	0.802
	Silt	-0.134	0.072	0.125
	P-value	0.459	0.692	0.488
	Clay	-0.355	-0.346	-0.155
	P-value	0.043	0.048	0.388
30	OC	0.135	-0.150	-0.234
	P-value	0.476	0.428	0.214
	Bulk density	-0.371	-0.464	-0.219
	P-value	0.062	0.017	0.282
	PAW	0.262	0.346	0.184
	P-value	0.196	0.084	0.368
	RAW	0.407	0.301	0.060
	P-value	0.039	0.136	0.770
	0 kPa	0.483	0.528	0.289
26	P-value	0.012	0.006	0.152
	100 kPa	0.105	0.332	0.203
	P-value	0.609	0.098	0.319
	10 kPa	0.499	0.580	0.230
	P-value	0.009	0.002	0.258
	1500 kPa	0.277	0.245	0.011
	P-value	0.171	0.228	0.957
	33 kPa	0.249	0.502	0.210
	P-value	0.221	0.009	0.303
	pH	0.945	0.662	-0.715
7	P-value	0.001	0.106	0.071
	EC	0.721	0.554	-0.661
	P-value	0.067	0.197	0.106
7	SSA	-0.186	-0.383	-0.787
	P-value	0.724	0.454	0.063
		Allophane	Alo + 1/2 Feo	Ferrihydrite

b.)

n				
30	Alo + 1/2 Feo	0.270	-	
	P-value	0.150	-	
	Ferrihydrite	0.055	0.706	-
	P-value	0.772	<0.001	-
	Sand	0.059	0.610	0.219
	P-value	0.757	<0.001	0.246
	Silt	0.244	-0.125	0.060
	P-value	0.194	0.510	0.754
	Clay	-0.277	-0.761	-0.345
	P-value	0.139	<0.001	0.062
29	OC	0.123	0.369	0.386
	P-value	0.527	0.049	0.039
28	Bulk density	-0.052	-0.573	-0.242
	P-value	0.793	0.001	0.215
	PAW	0.043	0.374	0.139
	P-value	0.828	0.050	0.482
	RAW	0.101	0.291	-0.004
	P-value	0.609	0.133	0.984
	0 kPa	-0.032	0.537	0.253
	P-value	0.873	0.003	0.194
	100 kPa	-0.030	0.328	0.255
	P-value	0.879	0.089	0.191
	10 kPa	0.044	0.506	0.230
	P-value	0.826	0.006	0.238
	1500 kPa	-0.004	0.226	0.172
	P-value	0.985	0.248	0.383
	33 kPa	0.007	0.357	0.226
	P-value	0.970	0.063	0.248
7	SSA	0.684	-0.116	-0.209
	P-value	0.090	0.805	0.653
7	pH	0.506	0.575	-0.681
	P-value	0.247	0.177	0.092
	EC	0.388	0.212	-0.511
	P-value	0.390	0.649	0.242
		Allophane	Alo + 1/2 Feo	Ferrihydrite

Appendix 5.20: Correlations (r value) between water retention characteristics and other measured soil properties in the a.) A horizon and b.) B horizon

a.)

n												
	0 kPa	-										
	P-value	-										
	10 kPa	0.734	-									
	P-value	<0.001	-									
	33 kPa	0.667	0.884	-								
	P-value	<0.001	<0.001	-								
	100 kPa	0.604	0.778	0.954	-							
	P-value	<0.001	<0.001	<0.001	-							
	1500 kPa	0.236	0.214	0.411	0.410	-						
	P-value	0.044	0.069	<0.001	<0.001	-						
73	PAW	0.599	0.870	0.658	0.554	-0.295	-					
	P-value	<0.001	<0.001	<0.001	<0.001	0.011	-					
	RAW	0.242	0.395	-0.039	-0.270	-0.272	0.523					
	P-value	0.039	<0.001	0.741	0.021	0.020	<0.001	-				
	Sand	-0.394	-0.417	-0.548	-0.574	-0.325	-0.244	0.200	-			
	P-value	<0.001	<0.001	<0.001	<0.001	0.005	0.037	0.090	-			
	Silt	0.345	0.407	0.534	0.518	0.314	0.240	-0.133	-0.851	-		
	P-value	0.003	<0.001	<0.001	<0.001	0.007	0.041	0.262	<0.001	-		
	Clay	0.269	0.229	0.304	0.374	0.186	0.130	-0.196	-0.716	0.244	-	
	P-value	0.022	0.052	0.009	0.001	0.115	0.274	0.097	<0.001	0.037	-	
	pH	0.298	0.425	0.352	0.312	0.049	0.420	0.218	-0.183	0.157	0.140	-
44	P-value	0.050	0.004	0.019	0.040	0.754	0.005	0.156	0.235	0.308	0.366	-
	EC	0.190	0.306	0.312	0.235	0.207	0.216	0.138	-0.336	0.416	0.076	0.284
	P-value	0.216	0.043	0.039	0.125	0.177	0.160	0.373	0.026	0.005	0.626	0.062

Appendix 5.20: Continued

	Ca	0.334	0.323	0.319	0.228	0.459	0.028	0.140	-0.172	0.131	0.108			-					
	P-value	0.083	0.093	0.098	0.244	0.014	0.887	0.478	0.383	0.506	0.586			-					
	Mg	0.249	0.307	0.479	0.410	0.401	0.045	-0.036	-0.045	0.002	0.093			0.729	-				
	P-value	0.201	0.112	0.010	0.030	0.034	0.822	0.858	0.821	0.994	0.640			<0.001	-				
28	Na	0.442	0.315	0.469	0.494	0.039	0.240	-0.100	-0.176	0.217	-0.023			-0.071	0.071	-			
	P-value	0.019	0.102	0.012	0.008	0.842	0.220	0.611	0.371	0.267	0.909			0.719	0.719	-			
	K	0.413	0.398	0.527	0.501	0.114	0.269	-0.019	-0.211	0.263	-0.027			0.223	0.340	0.760	-		
	P-value	0.029	0.036	0.004	0.007	0.565	0.166	0.922	0.282	0.177	0.890			0.254	0.077	<0.001	-		
	CEC	0.347	0.123	0.369	0.372	0.284	-0.046	-0.195	-0.236	0.249	0.033			0.582	0.540	0.189	0.235	-	
	P-value	0.071	0.533	0.054	0.052	0.143	0.816	0.321	0.227	0.202	0.866			0.001	0.003	0.336	0.228	-	
	OC	0.283	0.123	0.396	0.444	0.732	-0.297	-0.244	0.120	0.029	-0.251			0.446	0.366	0.115	0.135	0.444	-
	P-value	0.161	0.550	0.046	0.023	<0.001	0.141	0.230	0.561	0.888	0.216			0.022	0.066	0.576	0.511	0.023	-
26	Bulk density	-0.727	-0.454	-0.468	-0.389	-0.393	-0.161	-0.129	-0.012	-0.145	0.236			-0.357	-0.302	-0.562	-0.469	-0.439	-0.432	-
	P-value	<0.001	0.020	0.016	0.049	0.047	0.432	0.531	0.955	0.481	0.245			0.073	0.135	0.003	0.016	0.025	0.028	-
7	SSA	-0.304	-0.038	0.532	0.635	0.200	-0.102	-0.506	-0.321	0.394	0.005			0.483	0.570	0.050	0.478	0.239	0.102	0.131
	P-value	0.558	0.943	0.278	0.176	0.704	0.848	0.306	0.535	0.440	0.992			0.332	0.237	0.925	0.338	0.648	0.847	0.805
		0 kPa	10 kPa	33 kPa	100 kPa	1500 kPa	PAW	RAW	Sand	Silt	Clay	pH	EC	K	Mg	Na	Ca	CEC	OC	Bulk density

Appendix 5.20: Continued

b.)

n												
	0 kPa	-										
	P-value	-										
	10 kPa	0.730	-									
	P-value	<0.001	-									
	33 kPa	0.615	0.925	-								
	P-value	<0.001	<0.001	-								
	100 kPa	0.570	0.879	0.986	-							
	P-value	<0.001	<0.001	<0.001	-							
	1500 kPa	0.366	0.423	0.482	0.458	-						
	P-value	0.002	<0.001	<0.001	<0.001	-						
72	PAW	0.627	0.898	0.787	0.748	-0.019	-					
	P-value	<0.001	<0.001	<0.001	<0.001	0.872	-					
	RAW	0.284	0.187	-0.182	-0.303	-0.099	0.254	-				
	P-value	0.016	0.115	0.126	0.010	0.409	0.031	-				
	Sand	-0.069	-0.356	-0.468	-0.474	-0.347	-0.224	0.265	-			
	P-value	0.564	0.002	<0.001	<0.001	0.003	0.059	0.024	-			
	Silt	0.232	0.446	0.489	0.449	0.377	0.309	-0.033	-0.825	-		
	P-value	0.050	<0.001	<0.001	<0.001	0.001	0.008	0.781	<0.001	-		
	Clay	-0.175	0.052	0.193	0.255	0.130	-0.006	-0.423	-0.688	0.158	-	
	P-value	0.142	0.667	0.104	0.031	0.277	0.959	<0.001	<0.001	0.185	-	
	pH	0.289	0.386	0.316	0.263	0.155	0.380	0.267	-0.135	0.258	-0.126	-
42	P-value	0.064	0.012	0.042	0.092	0.327	0.013	0.087	0.396	0.099	0.428	-
	EC	0.381	0.316	0.339	0.325	0.309	0.224	-0.068	-0.126	0.213	-0.073	0.305	-
	P-value	0.013	0.042	0.028	0.036	0.047	0.153	0.670	0.428	0.175	0.645	0.050	-

Appendix 5.20: Continued

	Ca	0.215	0.390	0.350	0.299	0.313	0.224	0.165	0.083	0.070	-0.164			-						
	P-value	0.272	0.040	0.068	0.123	0.105	0.251	0.401	0.676	0.724	0.403			-						
	Mg	0.393	0.590	0.687	0.673	0.336	0.403	-0.037	0.201	-0.076	-0.205			0.633	-					
	P-value	0.038	<0.001	<0.001	<0.001	0.080	0.034	0.853	0.306	0.702	0.296			<0.001	-					
	Na	0.438	0.379	0.319	0.309	0.012	0.352	0.135	0.238	0.100	-0.394			-0.196	0.100	-				
	P-value	0.020	0.047	0.098	0.109	0.952	0.066	0.493	0.222	0.614	0.038			0.318	0.614	-				
	K	0.213	0.154	0.025	-0.013	-0.153	0.216	0.235	0.464	-0.225	-0.452			0.097	0.220	0.540	-			
28	P-value	0.276	0.434	0.898	0.947	0.436	0.269	0.228	0.013	0.250	0.016			0.624	0.262	0.003	-			
	CEC	0.336	0.521	0.642	0.641	0.389	0.313	-0.093	-0.035	0.361	-0.226			0.526	0.572	0.264	0.127	-		
	P-value	0.080	0.004	<0.001	<0.001	0.041	0.105	0.638	0.861	0.059	0.249			0.004	0.002	0.174	0.518	-		
	OC	0.314	0.432	0.517	0.521	0.319	0.261	-0.064	0.209	-0.097	-0.207			0.633	0.467	-0.006	-0.044	0.577	-	
	P-value	0.103	0.022	0.005	0.005	0.098	0.179	0.748	0.287	0.623	0.291			<0.001	0.012	0.975	0.822	0.001	-	
	Bulk denity	-0.816	-0.499	-0.355	-0.317	-0.332	-0.318	-0.295	-0.449	-0.056	0.641			-0.196	-0.331	-0.522	-0.351	-0.305	-0.180	-
	P-value	<0.001	0.007	0.064	0.100	0.084	0.099	0.127	0.017	0.778	<0.001			0.318	0.085	0.004	0.067	0.114	0.360	-
7	SSA	0.095	0.350	-0.042	-0.155	-0.414	0.564	0.663	-0.113	0.294	-0.100			0.400	0.155	0.042	0.243	0.058	-0.326	0.235
	P-value	0.840	0.442	0.929	0.740	0.356	0.188	0.105	0.809	0.522	0.831			0.374	0.741	0.929	0.599	0.901	0.475	0.612
		0 kPa	10 kPa	33 kPa	100 kPa	1500 kPa	PAW	RAW	Sand	Silt	Clay	pH	EC	K	Mg	Na	Ca	CEC	OC	Bulk density

Appendix 5.21: Correlations (r value) between pH and electrical conductivity (EC) of the soils from TPC sugar estate with exchangeable cations in the a.) A horizon and b.) B horizon (n = 7)

a.)

pH	0.476	-0.271	0.848	0.474	0.328	
P-value	0.281	0.557	0.016	0.283	0.473	
EC	0.260	0.158	0.728	0.671	0.370	0.777
P-value	0.574	0.735	0.063	0.099	0.414	0.040
	K	Mg	Na	Ca	CEC	pH

b.)

pH	0.816	0.044	0.834	0.515	0.558	
P-value	0.025	0.926	0.020	0.237	0.193	
EC	0.318	0.241	0.274	0.484	-0.288	0.339
P-value	0.486	0.604	0.553	0.271	0.532	0.457
	K	Mg	Na	Ca	CEC	pH

Appendix 5.1: X-ray diffraction patterns with labelled peaks (Å) of oriented clay samples treated with magnesium (Mg) and potassium (K) and analysed as air-dry samples (AD), heated at 550^{o}C (Htd) and analysed after treatment with ethylene glycol (EG) and glycerol (Gly) for the A and B horizons of selected fields from the a) north, b) west, c) east, d) south, e) Kahe areas and f) the ash layers of TPC sugar estate.

a)

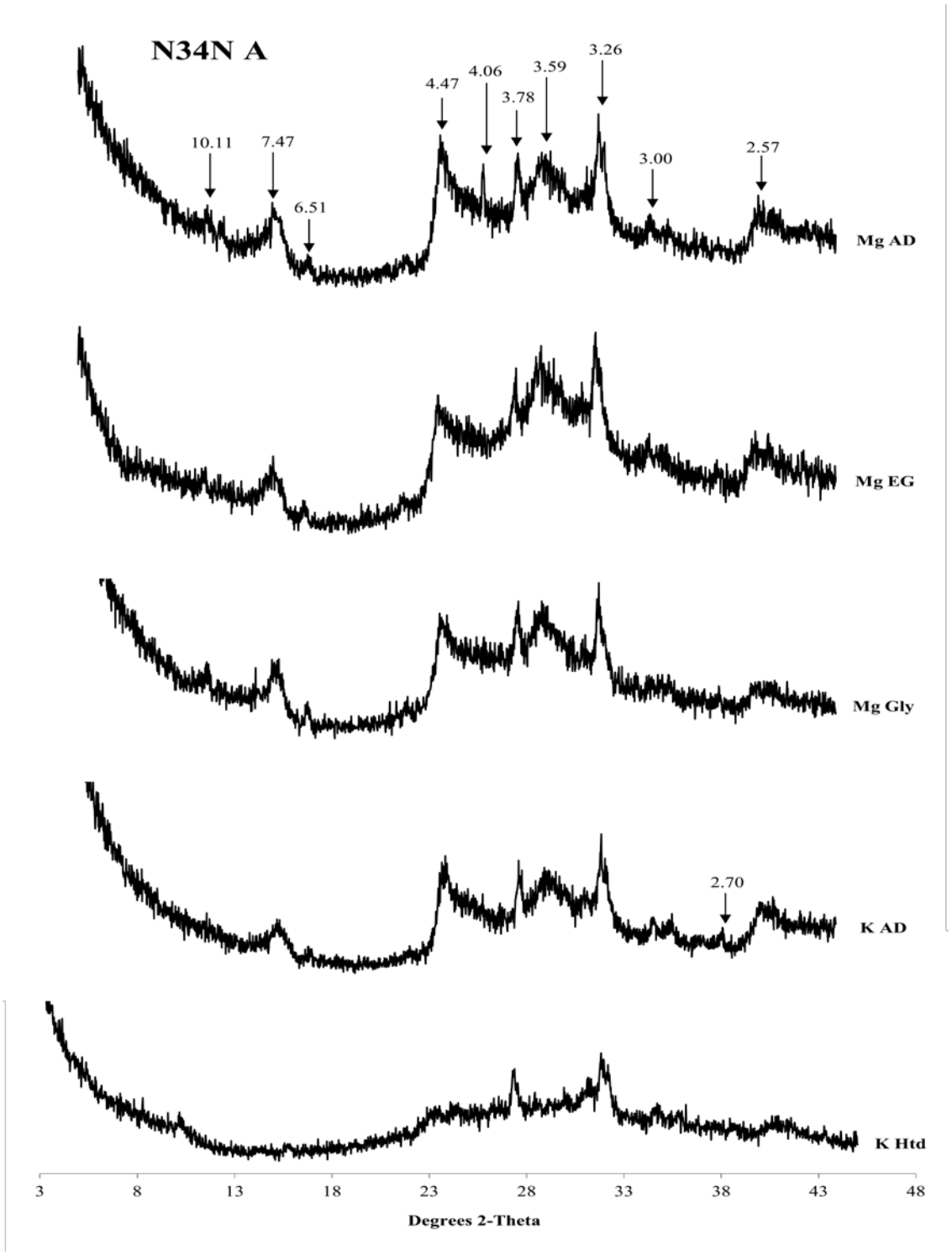

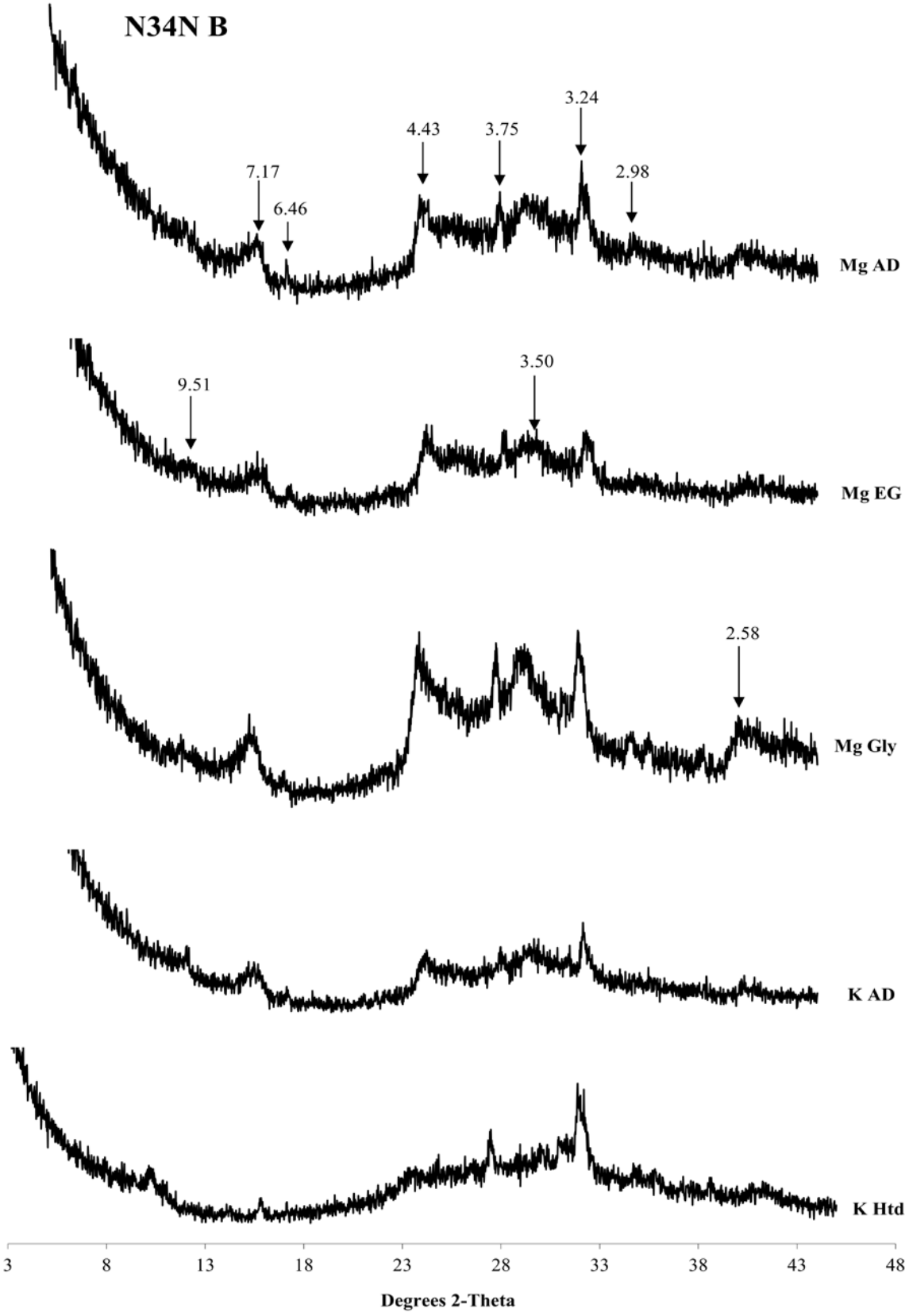
N34N B
3.24
4.43
3.75
7.17
2.98
6.46
Mg AD
3.50
9.51
Mg EG
2.58
Mg Gly
K AD
K Htd
3
8
13
18
23
28
33
38
43
48
Degrees 2-Theta

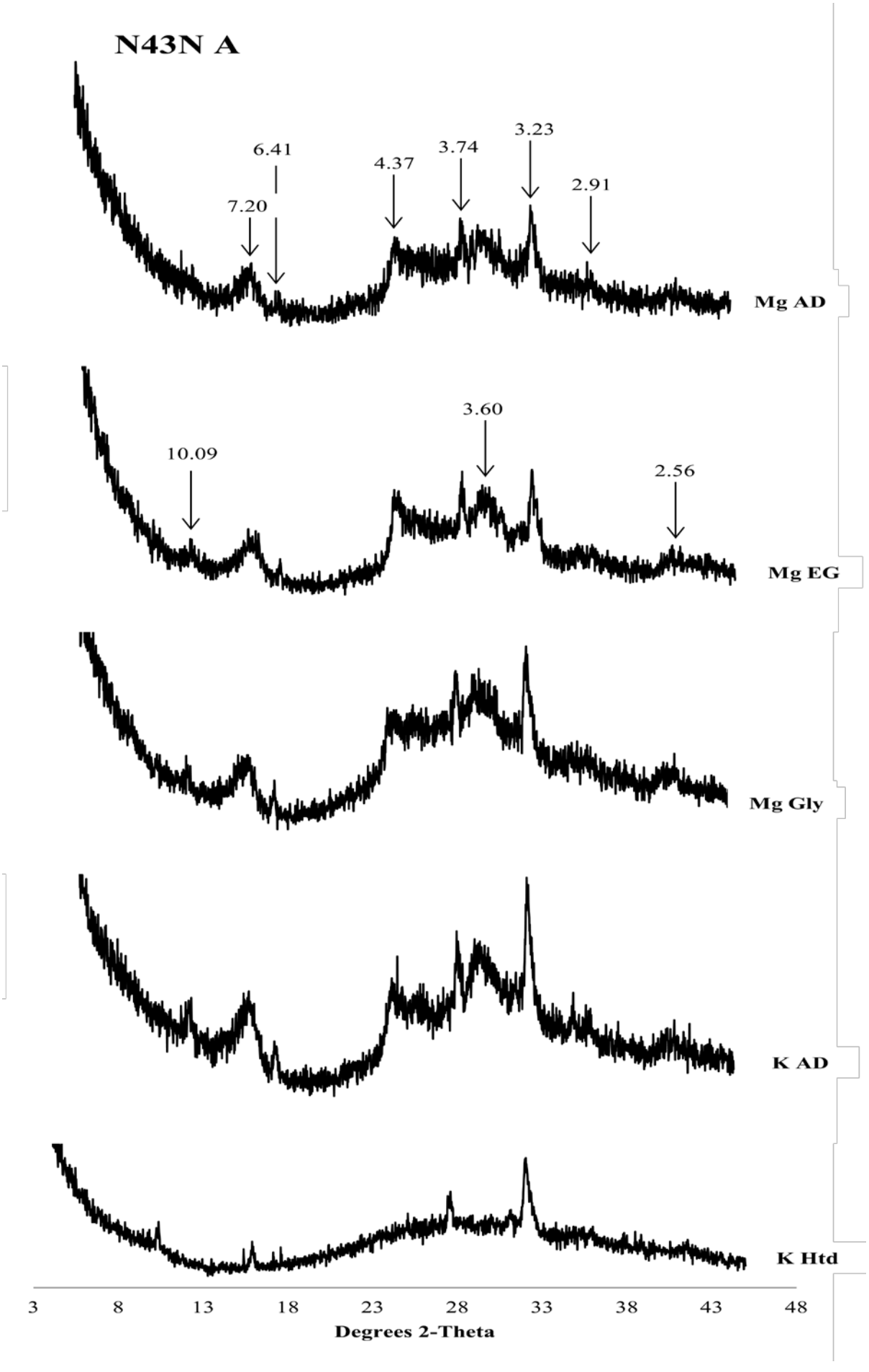
N43N A
6.41
7.20
4.37
3.74
3.23
2.91
Mg AD
10.09
3.60
2.56
Mg EG
Mg Gly
K AD
K Htd
3
8
13
18
23
28
33
38
43
48
Degrees 2-Theta

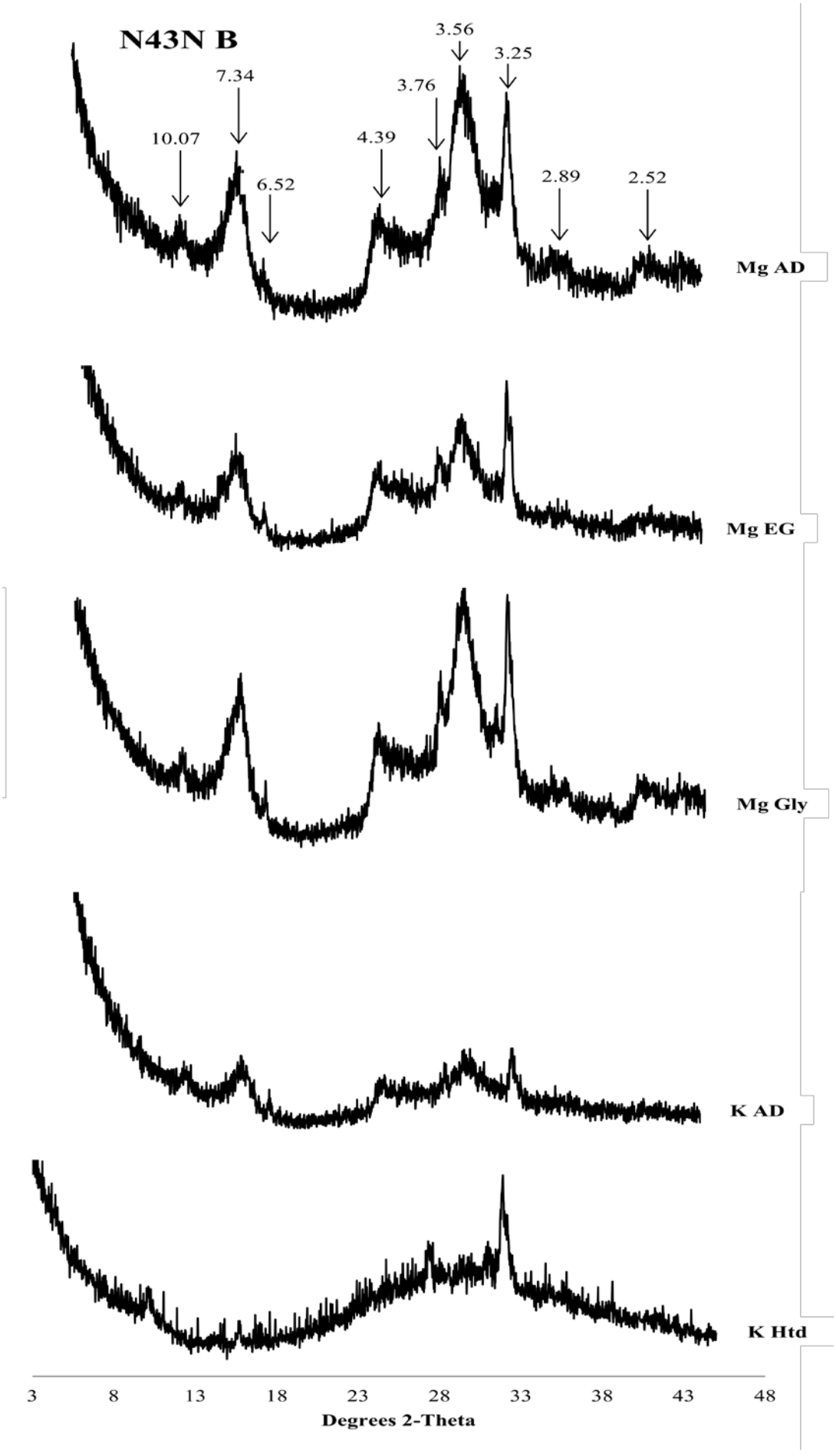
N43N B
10.07
7.34
6.52
4.39
3.76
3.56
3.25
2.89
2.52
Mg AD
Mg EG
Mg Gly
K AD
K Htd
3
8
13
18
23
28
33
38
43
48
Degrees 2-Theta

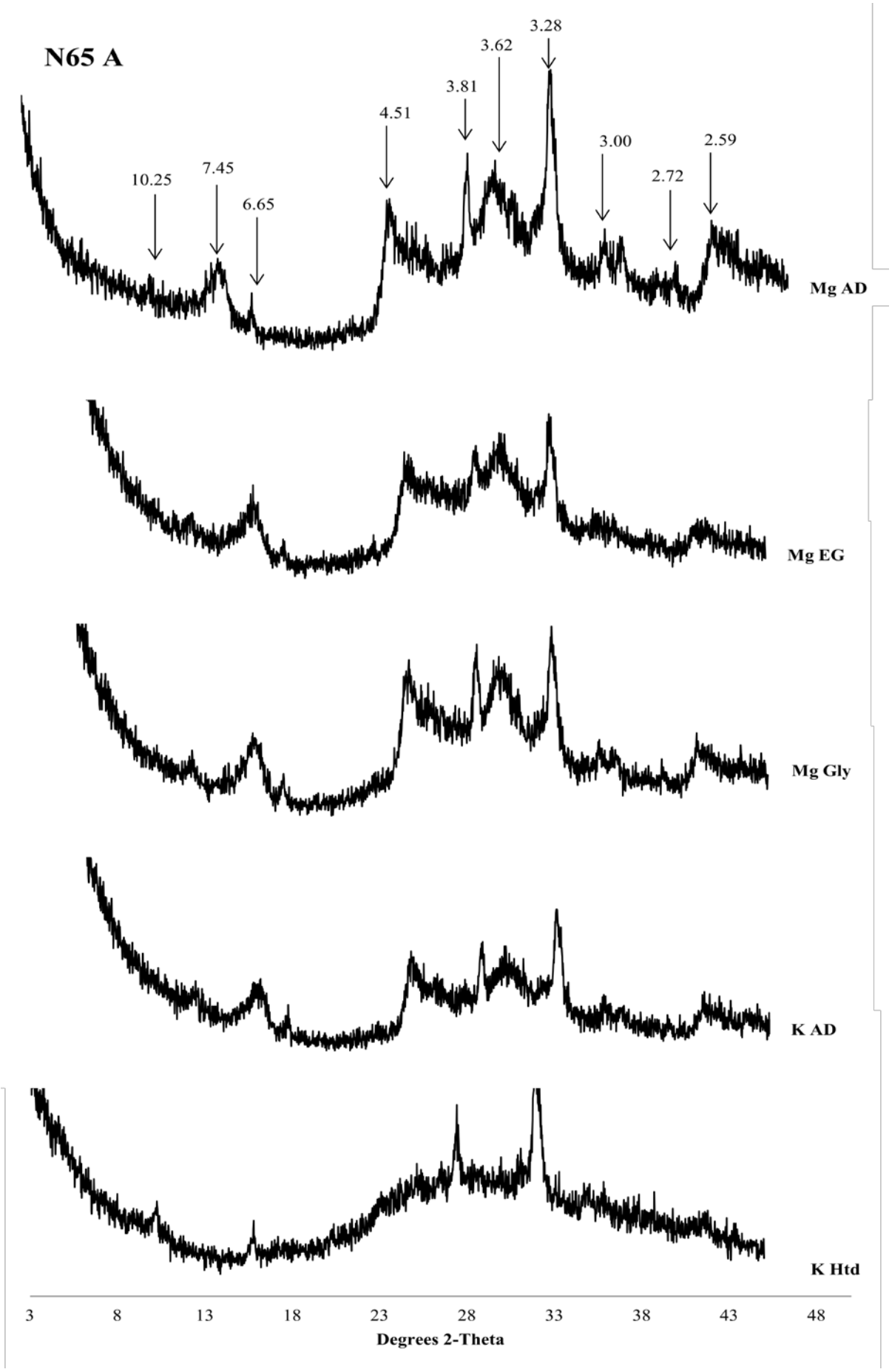
N65 A
10.25
7.45
6.65
4.51
3.81
3.62
3.28
3.00
2.72
2.59
Mg AD
Mg EG
Mg Gly
K AD
K Htd
3
8
13
18
23
28
33
38
43
48
Degrees 2-Theta

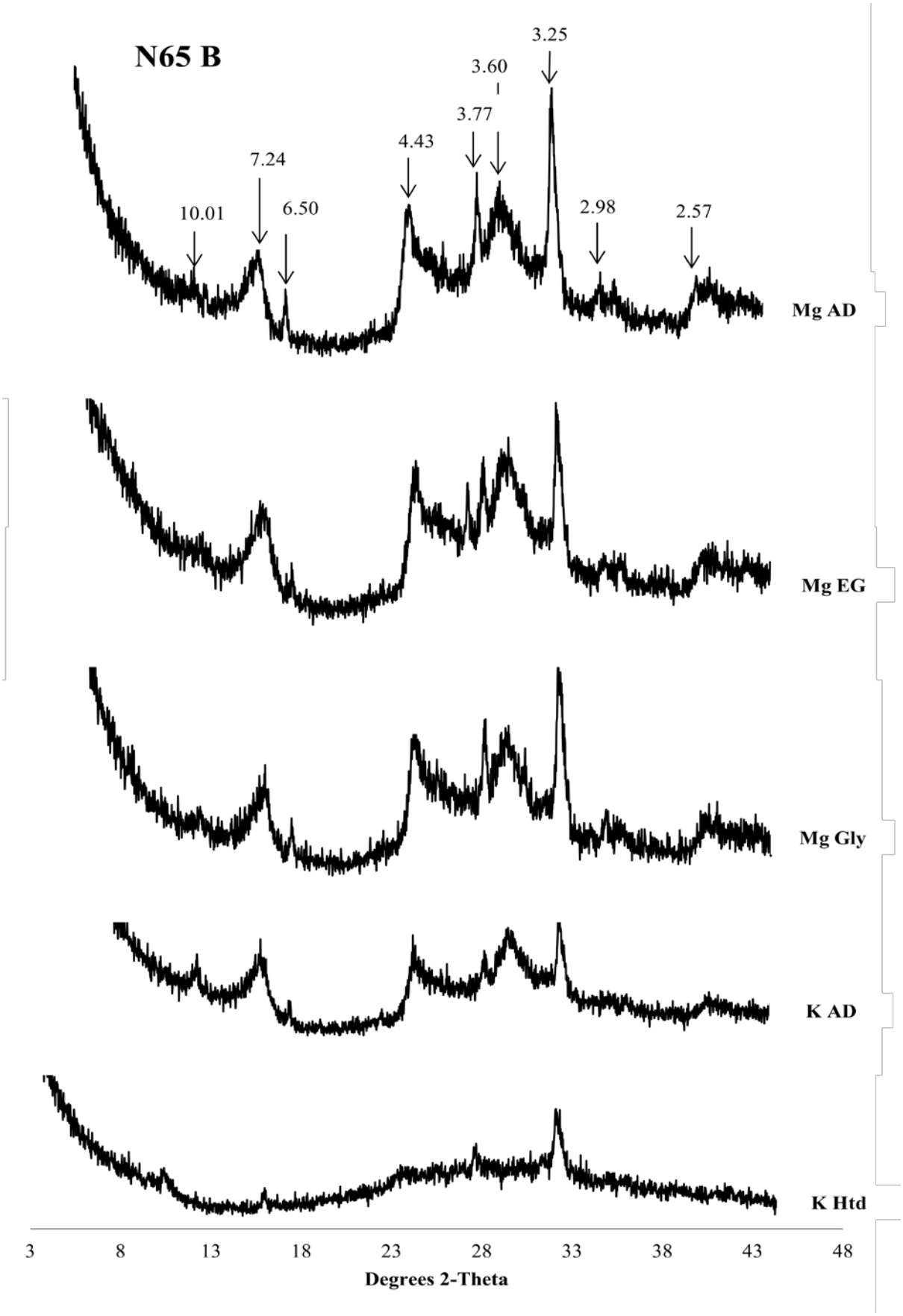
N65 B
10.01
7.24
6.50
4.43
3.77
3.60
3.25
2.98
2.57
Mg AD
Mg EG
Mg Gly
K AD
K Htd
3
8
13
18
23
28
33
38
43
48
Degrees 2-Theta

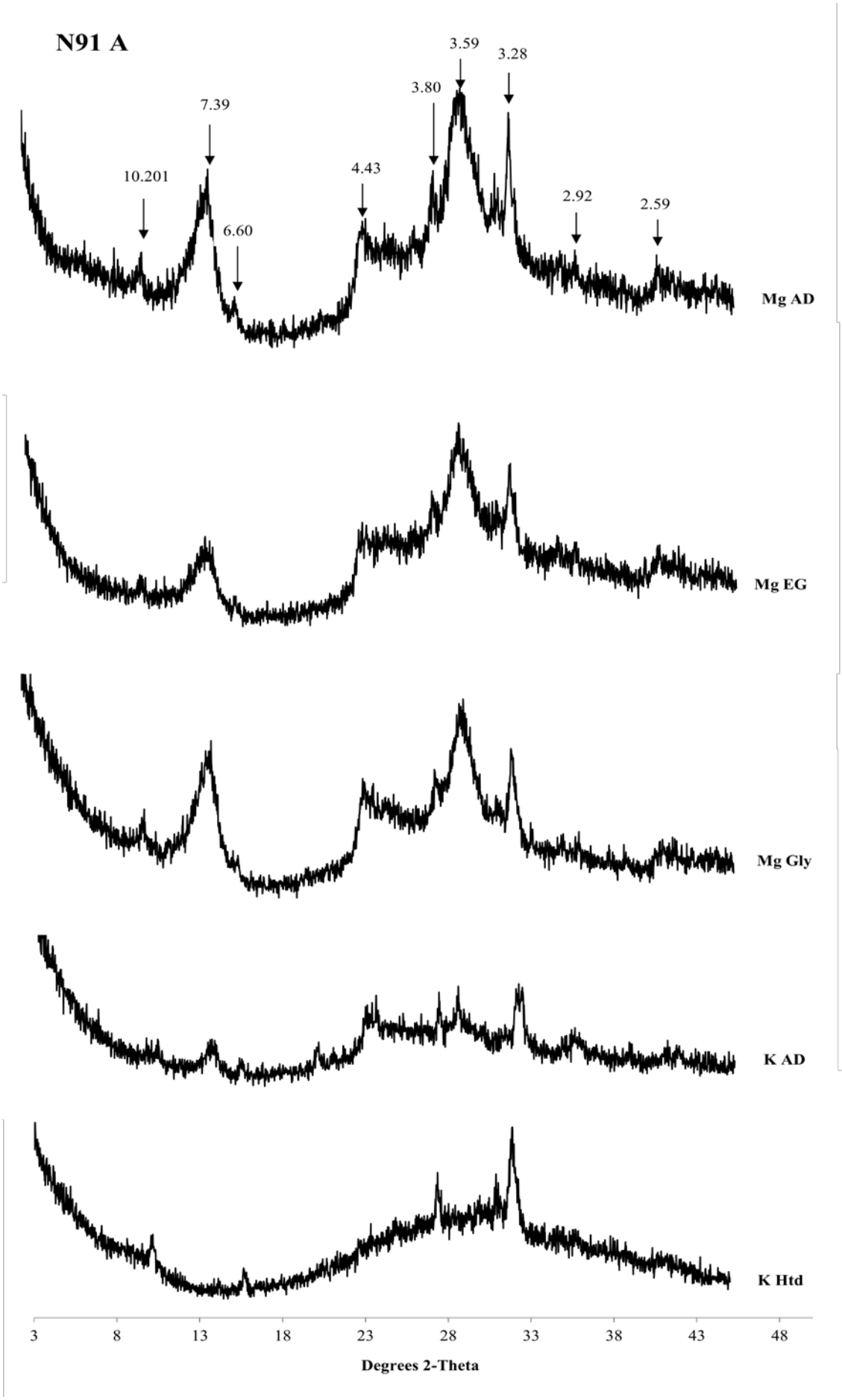
N91 A
10.201
7.39
6.60
4.43
3.80
3.59
3.28
2.92
2.59
Mg AD
Mg EG
Mg Gly
K AD
K Htd
3
8
13
18
23
28
33
38
43
48
Degrees 2-Theta

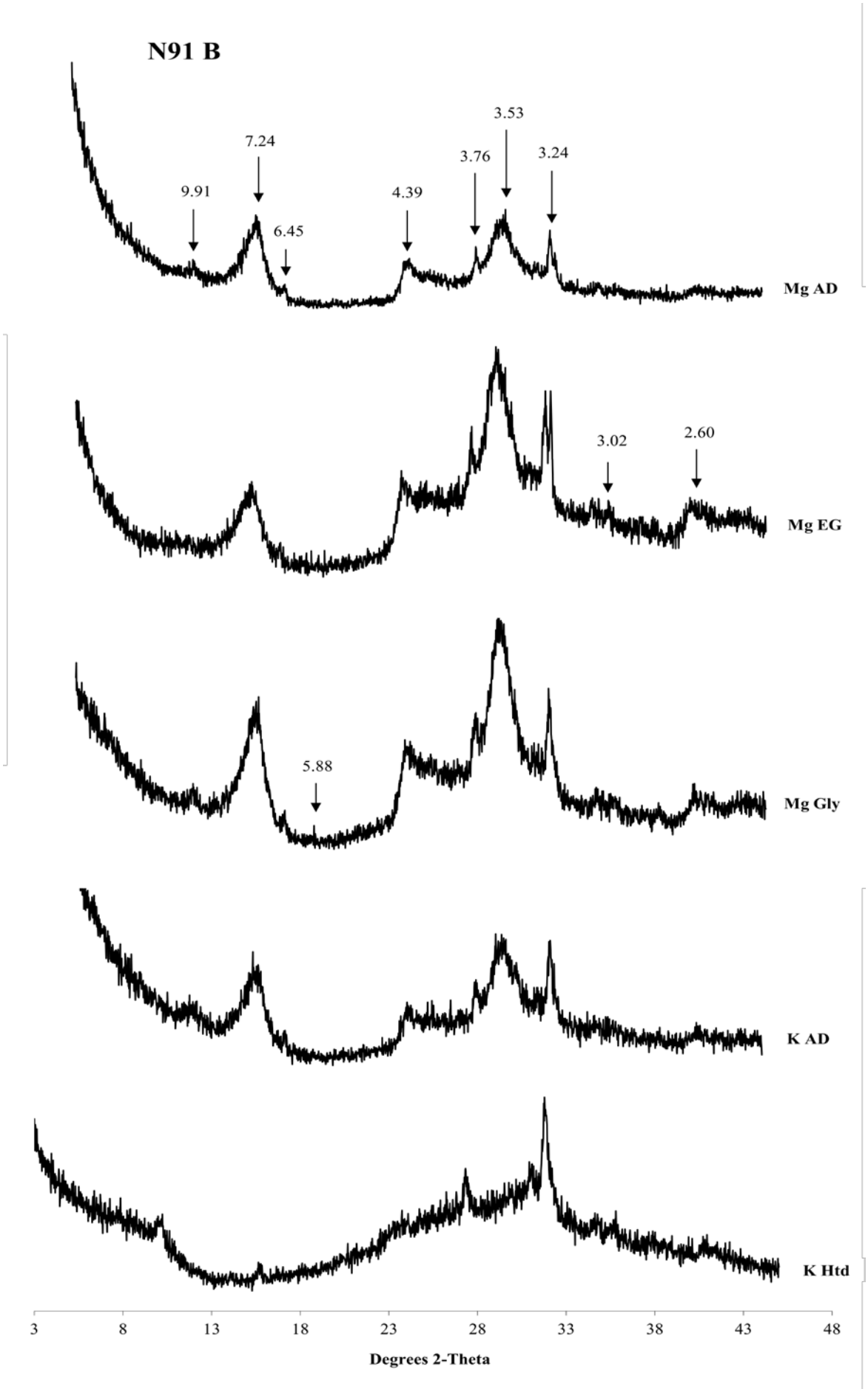
N91 B
9.91
7.24
6.45
4.39
3.76
3.53
3.24
Mg AD
3.02
2.60
Mg EG
5.88
Mg Gly
K AD
K Htd
3
8
13
18
23
28
33
38
43
48
Degrees 2-Theta

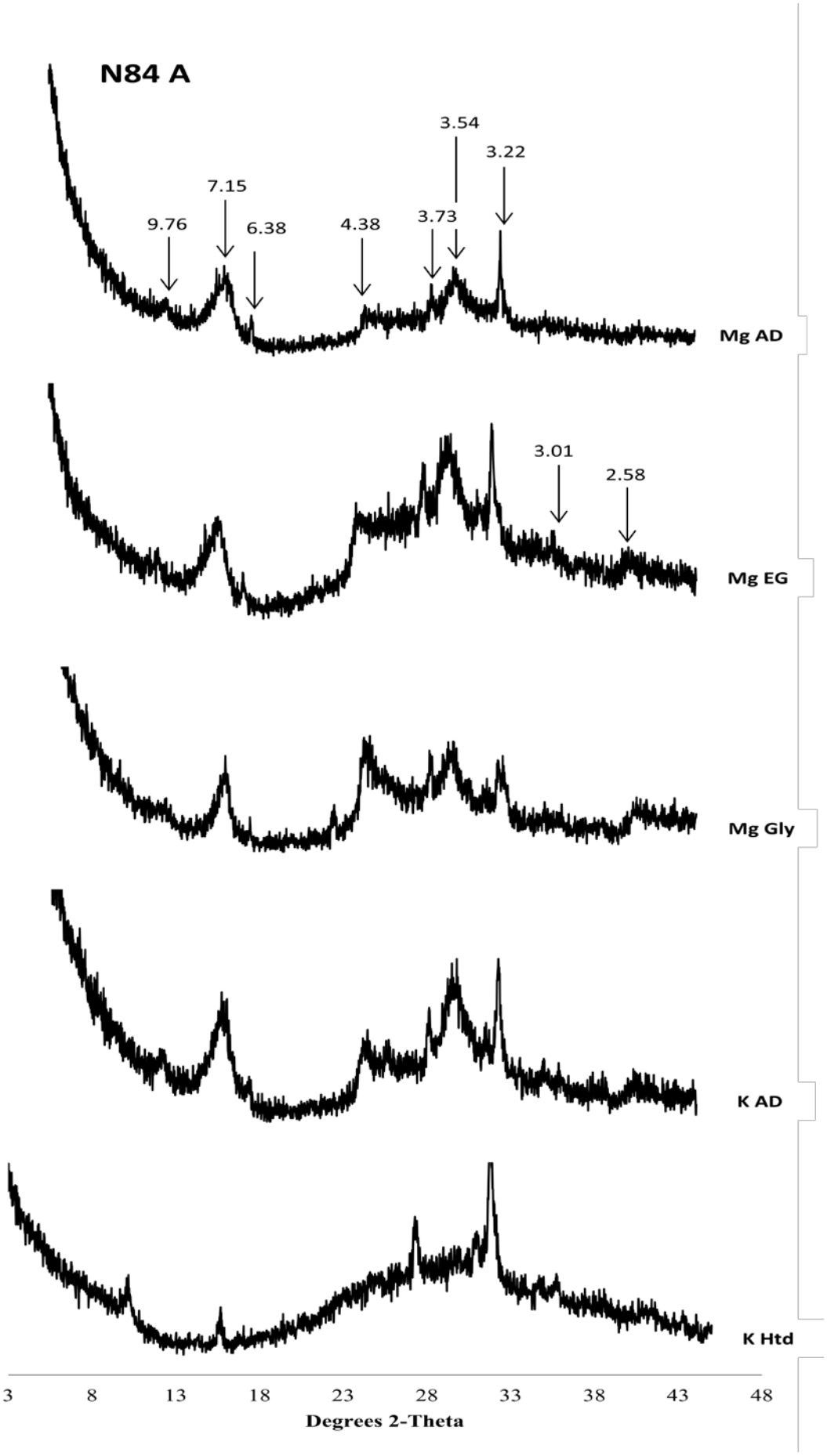
N84 A
9.76
7.15
6.38
4.38
3.73
3.54
3.22
Mg AD
3.01
2.58
Mg EG
Mg Gly
K AD
K Htd
3
8
13
18
23
28
33
38
43
48
Degrees 2-Theta

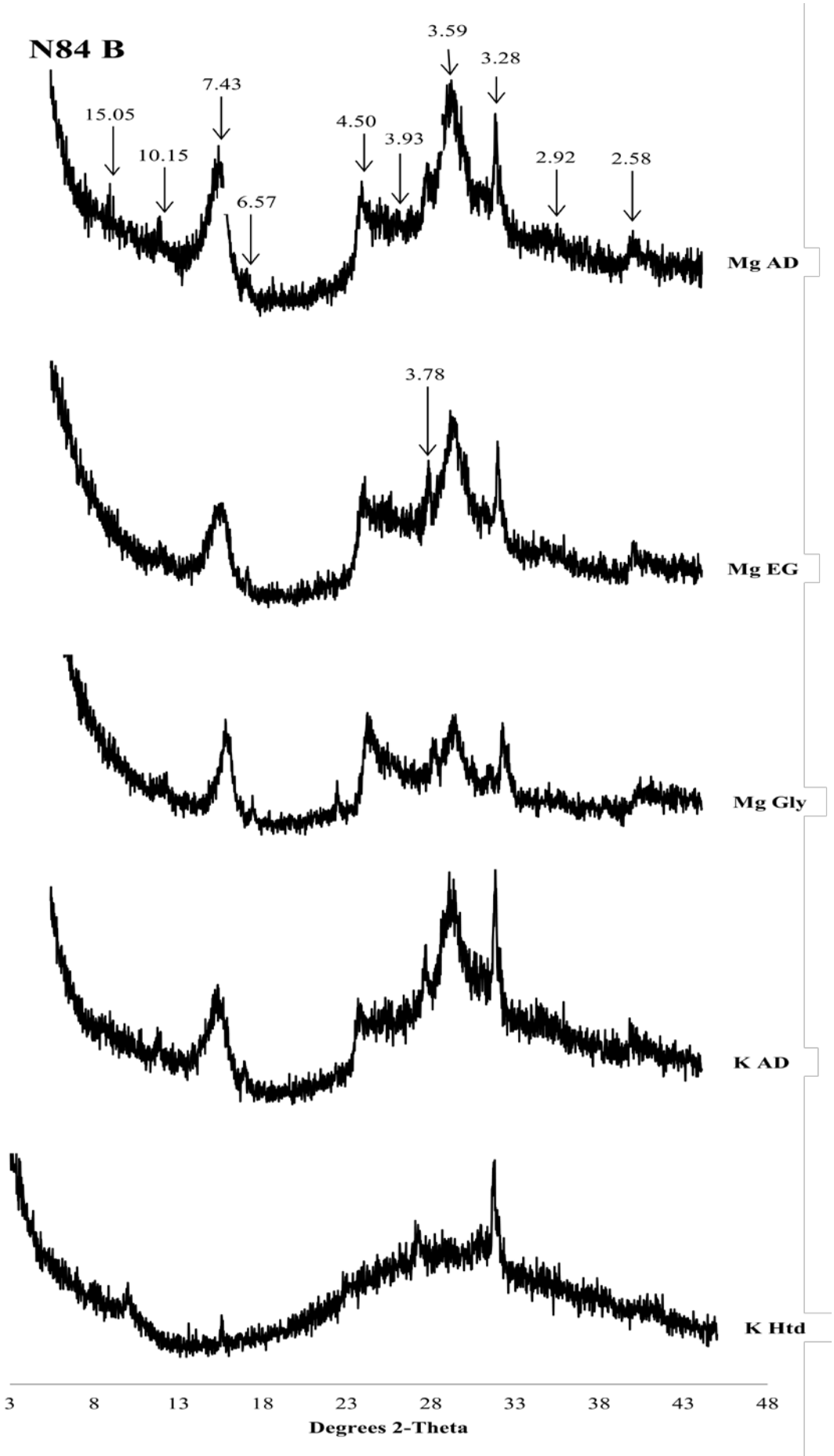
N84 B
15.05
10.15
7.43
6.57
4.50
3.93
3.59
3.28
2.92
2.58
Mg AD
3.78
Mg EG
Mg Gly
K AD
K Htd
3
8
13
18
23
28
33
38
43
48
Degrees 2-Theta

b)

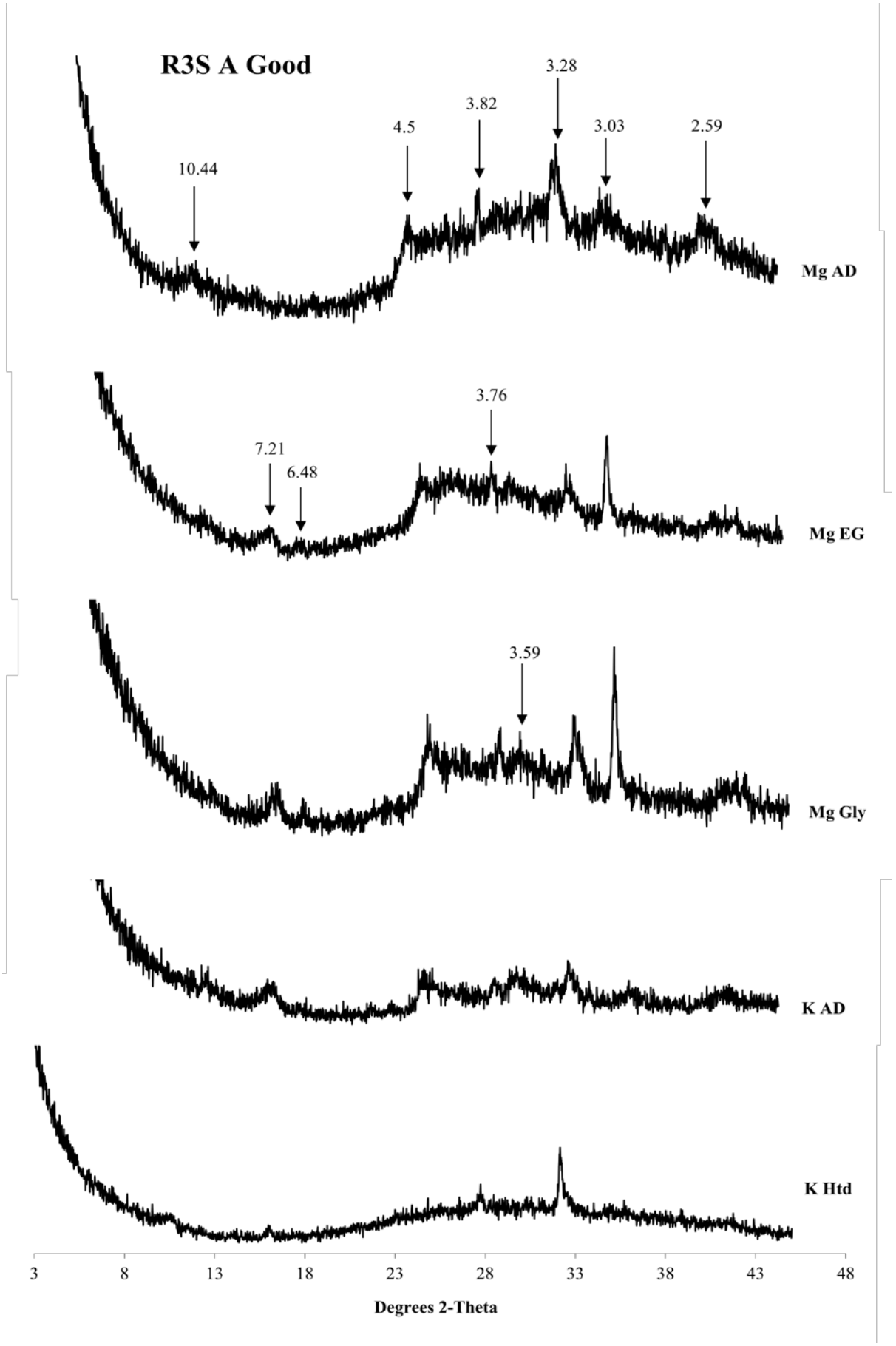
R3S A Good
10.44
4.5
3.82
3.28
3.03
2.59
Mg AD
7.21
6.48
3.76
Mg EG
3.59
Mg Gly
K AD
K Htd
3
8
13
18
23
28
33
38
43
48
Degrees 2-Theta

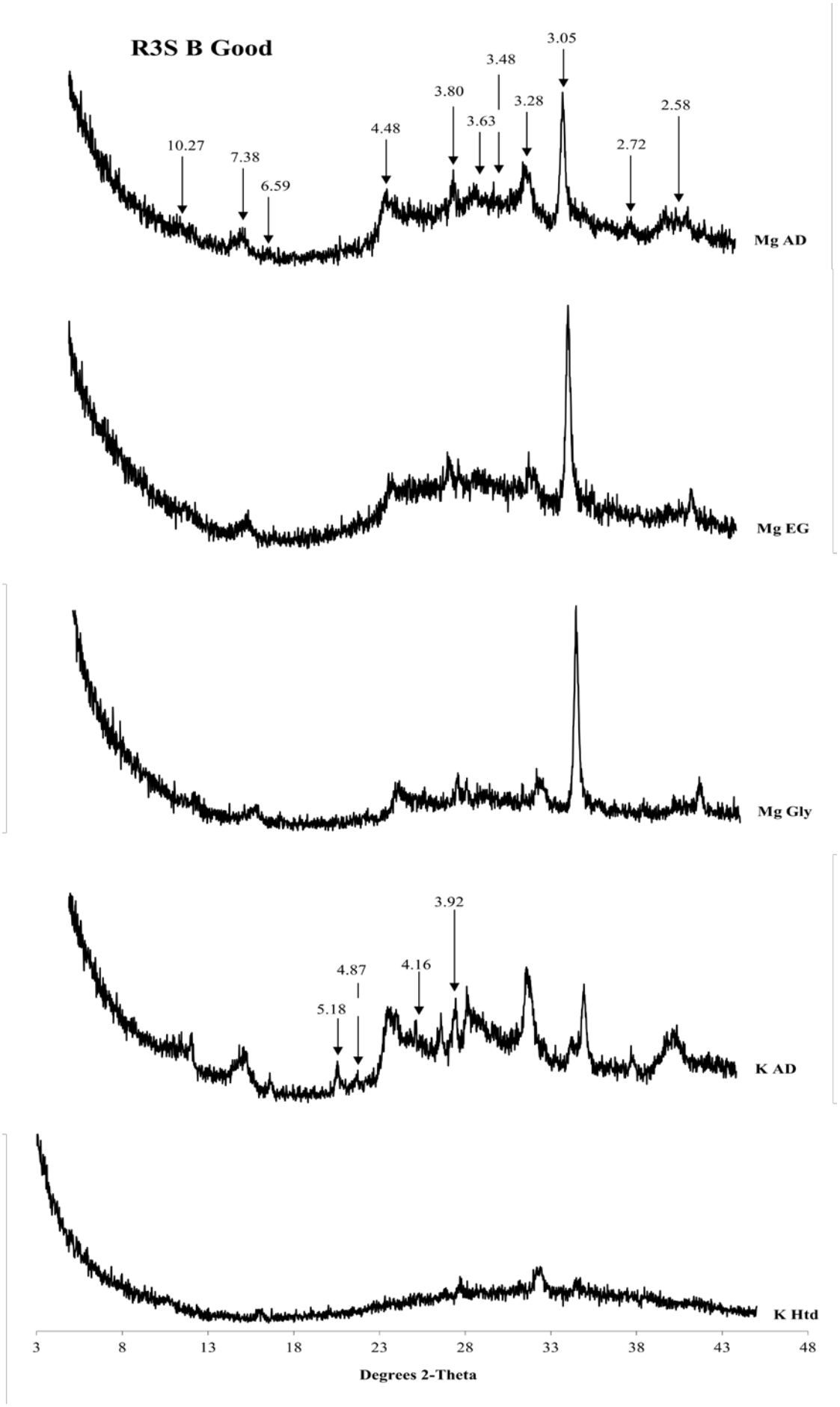
R3S B Good
10.27
7.38
6.59
4.48
3.80
3.63
3.48
3.28
3.05
2.72
2.58
Mg AD
Mg EG
Mg Gly
5.18
4.87
4.16
3.92
K AD
K Htd
3
8
13
18
23
28
33
38
43
48
Degrees 2-Theta

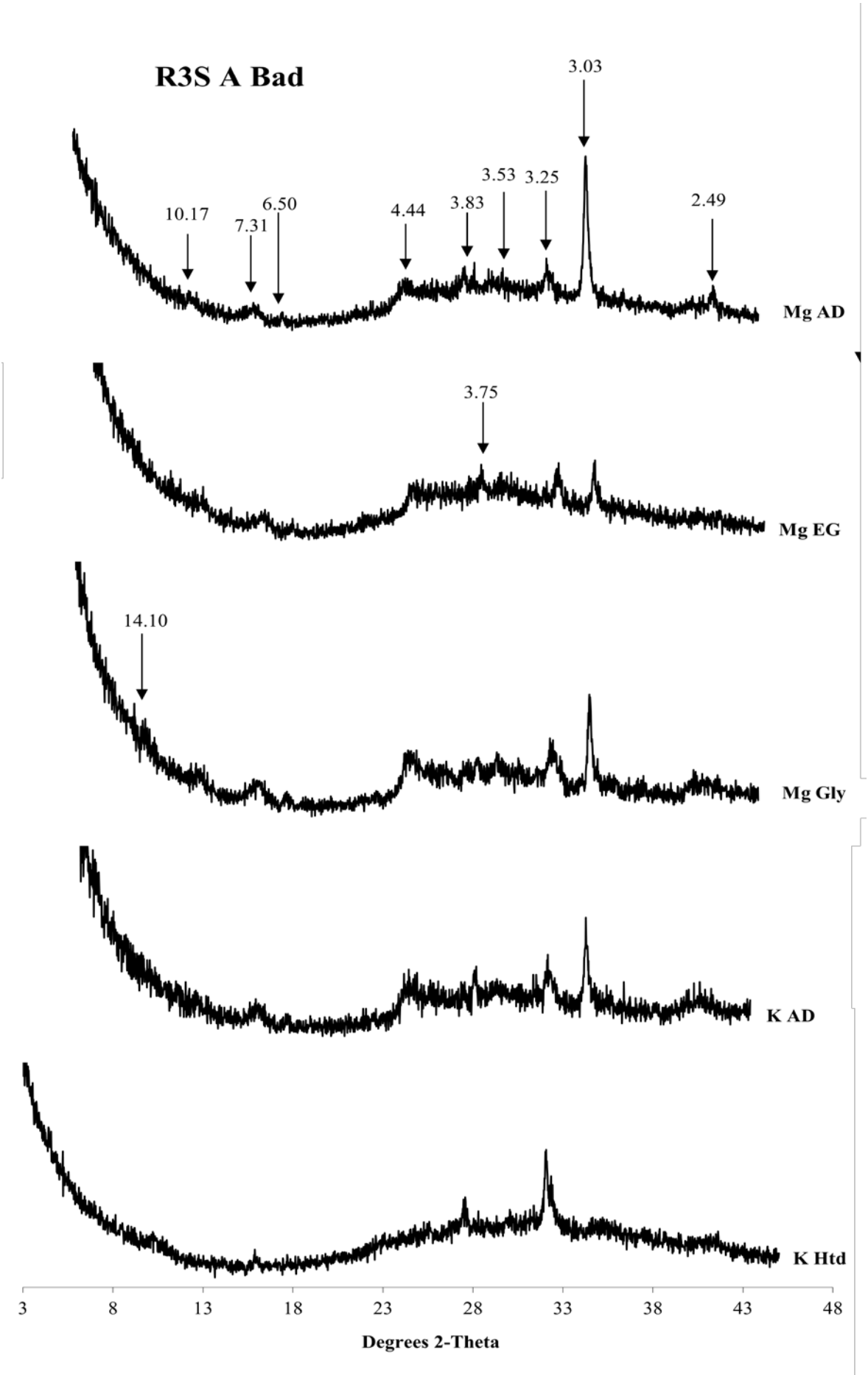
R3S A Bad
3.03
10.17
7.31
6.50
4.44
3.83
3.53
3.25
2.49
Mg AD
3.75
Mg EG
14.10
Mg Gly
K AD
K Htd
3
8
13
18
23
28
33
38
43
48
Degrees 2-Theta

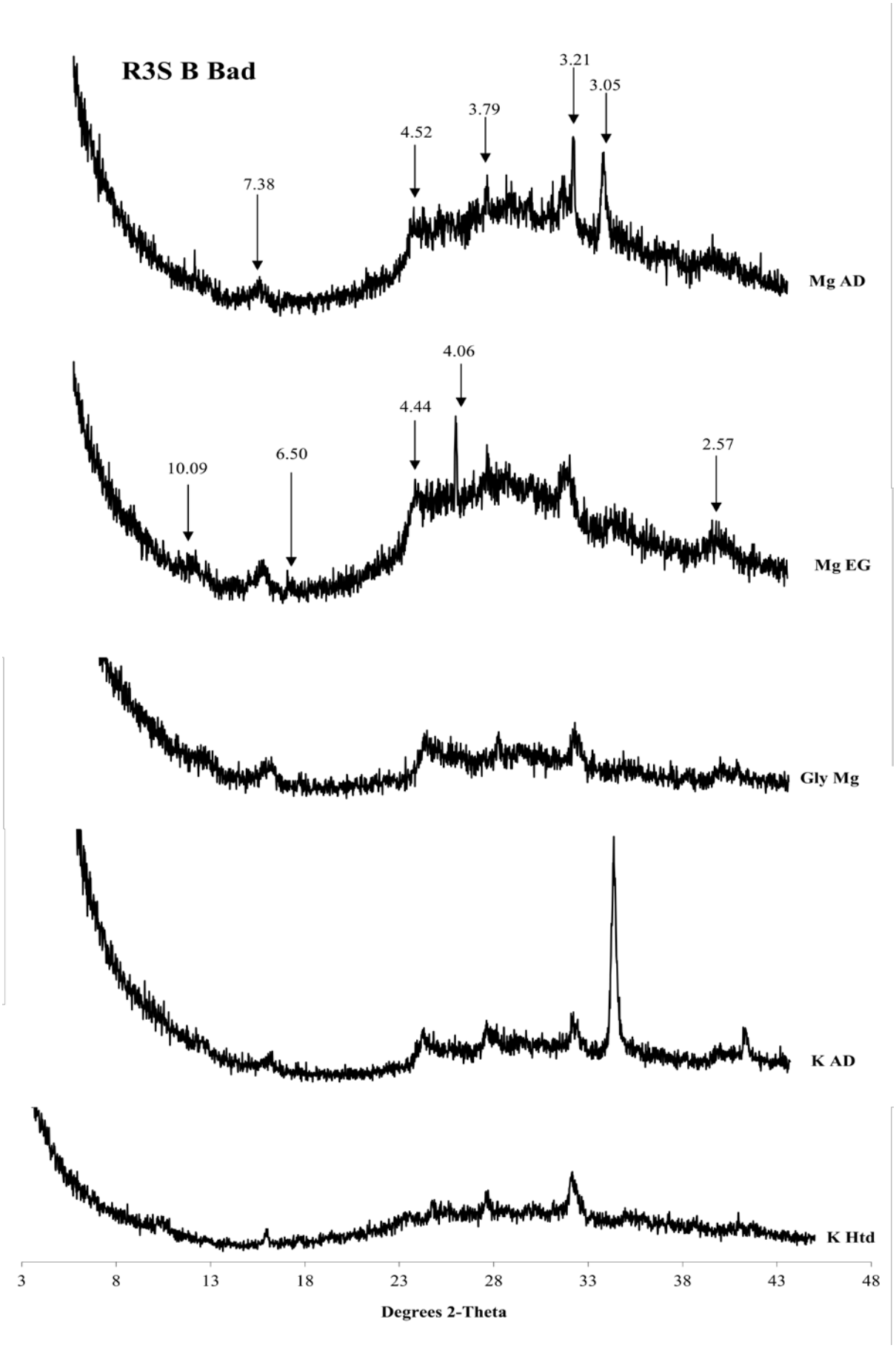
R3S B Bad
3.21
3.05
3.79
4.52
7.38
Mg AD
4.06
4.44
10.09
6.50
2.57
Mg EG
Gly Mg
K AD
K Htd
3
8
13
18
23
28
33
38
43
48
Degrees 2-Theta

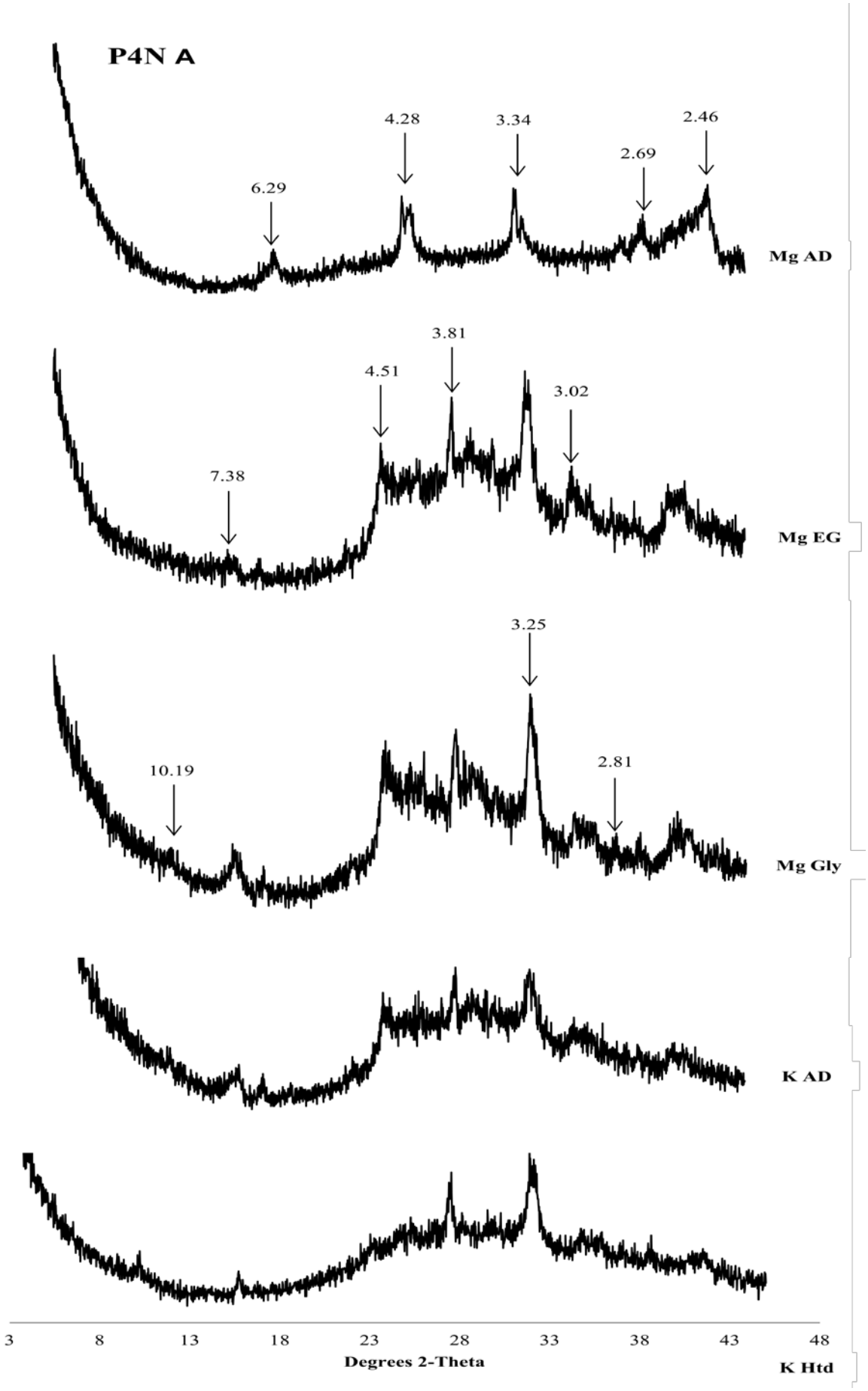
P4N A
6.29
4.28
3.34
2.69
2.46
Mg AD
7.38
4.51
3.81
3.02
Mg EG
10.19
3.25
2.81
Mg Gly
K AD
K Htd
3
8
13
18
23
28
33
38
43
48
Degrees 2-Theta

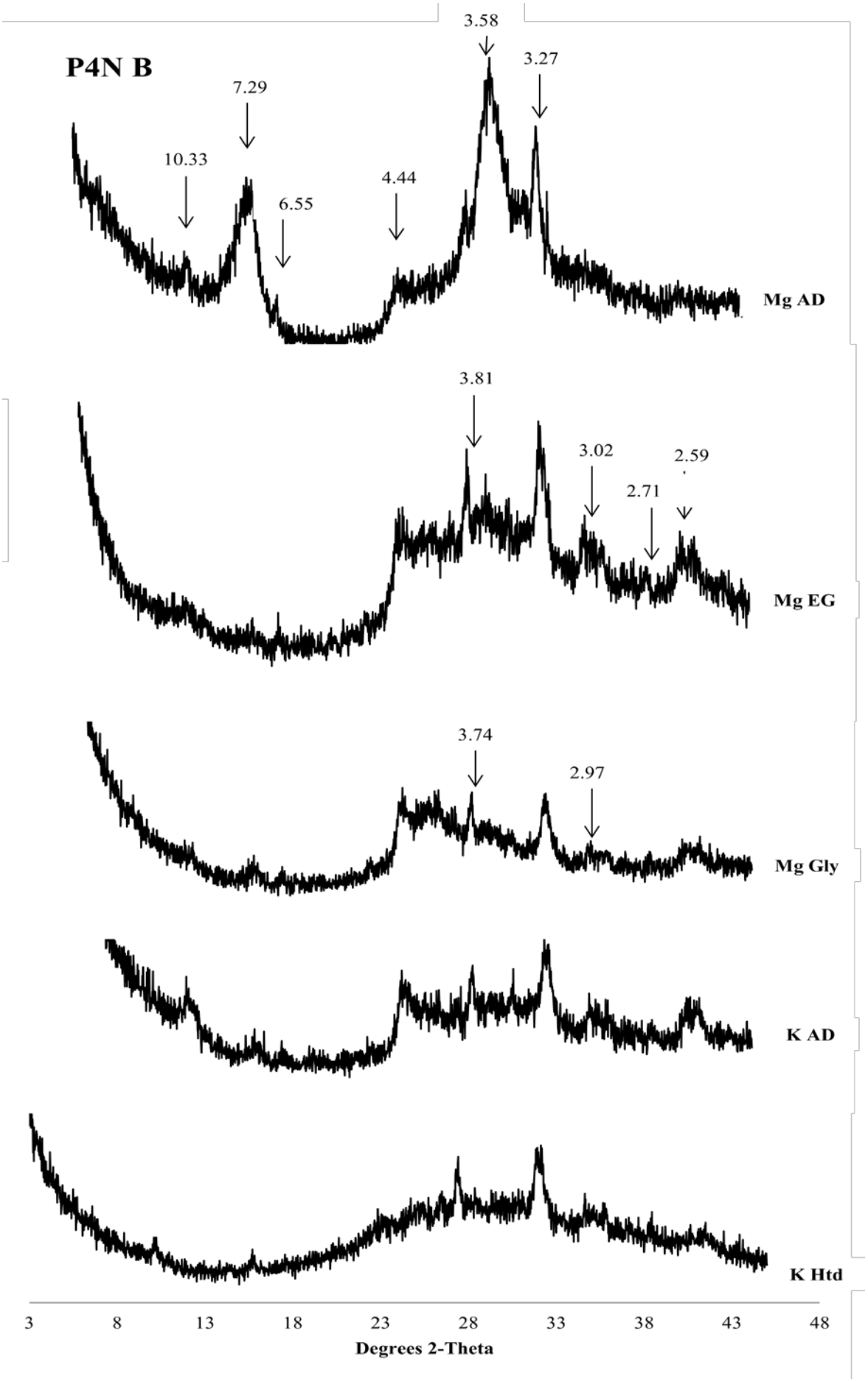
P4N B
3.58
3.27
7.29
10.33
4.44
6.55
Mg AD
3.81
3.02
2.59
2.71
Mg EG
3.74
2.97
Mg Gly
K AD
K Htd
3
8
13
18
23
28
33
38
43
48
Degrees 2-Theta

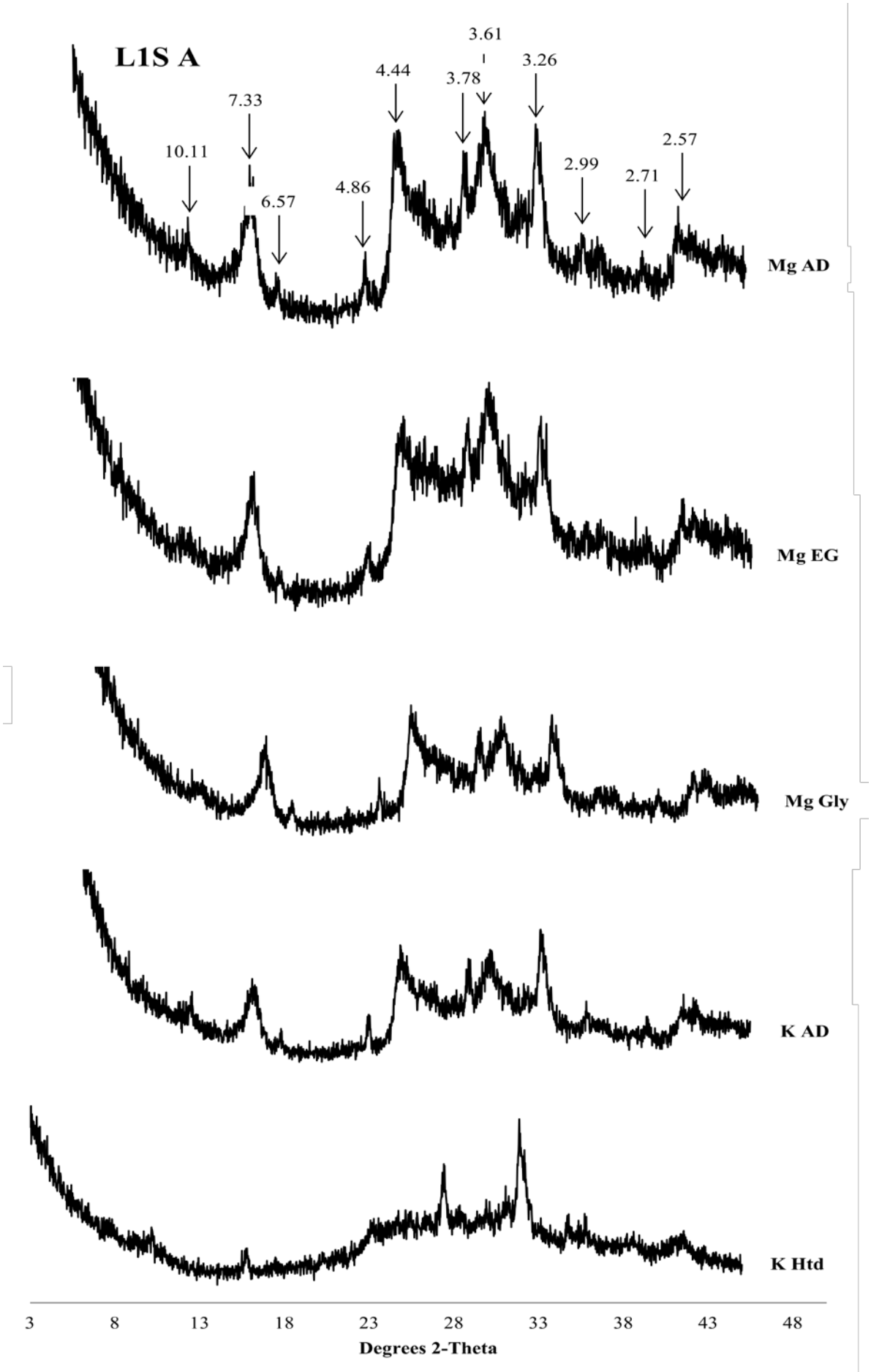
L1S A
10.11
7.33
6.57
4.86
4.44
3.78
3.61
3.26
2.99
2.71
2.57
Mg AD
Mg EG
Mg Gly
K AD
K Htd
3
8
13
18
23
28
33
38
43
48
Degrees 2-Theta

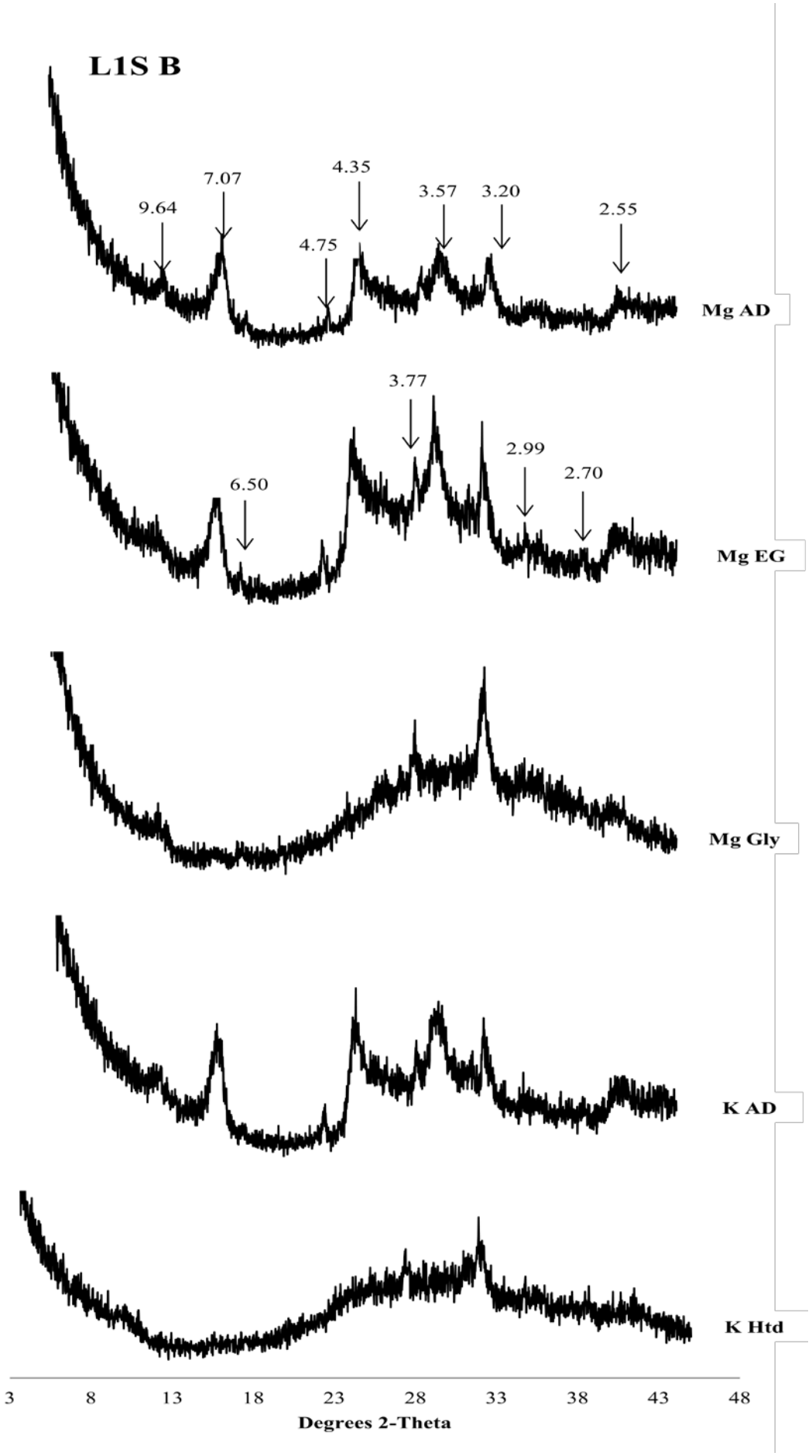
L1S B
9.64
7.07
4.75
4.35
3.57
3.20
2.55
Mg AD
6.50
3.77
2.99
2.70
Mg EG
Mg Gly
K AD
K Htd
3
8
13
18
23
28
33
38
43
48
Degrees 2-Theta

c)

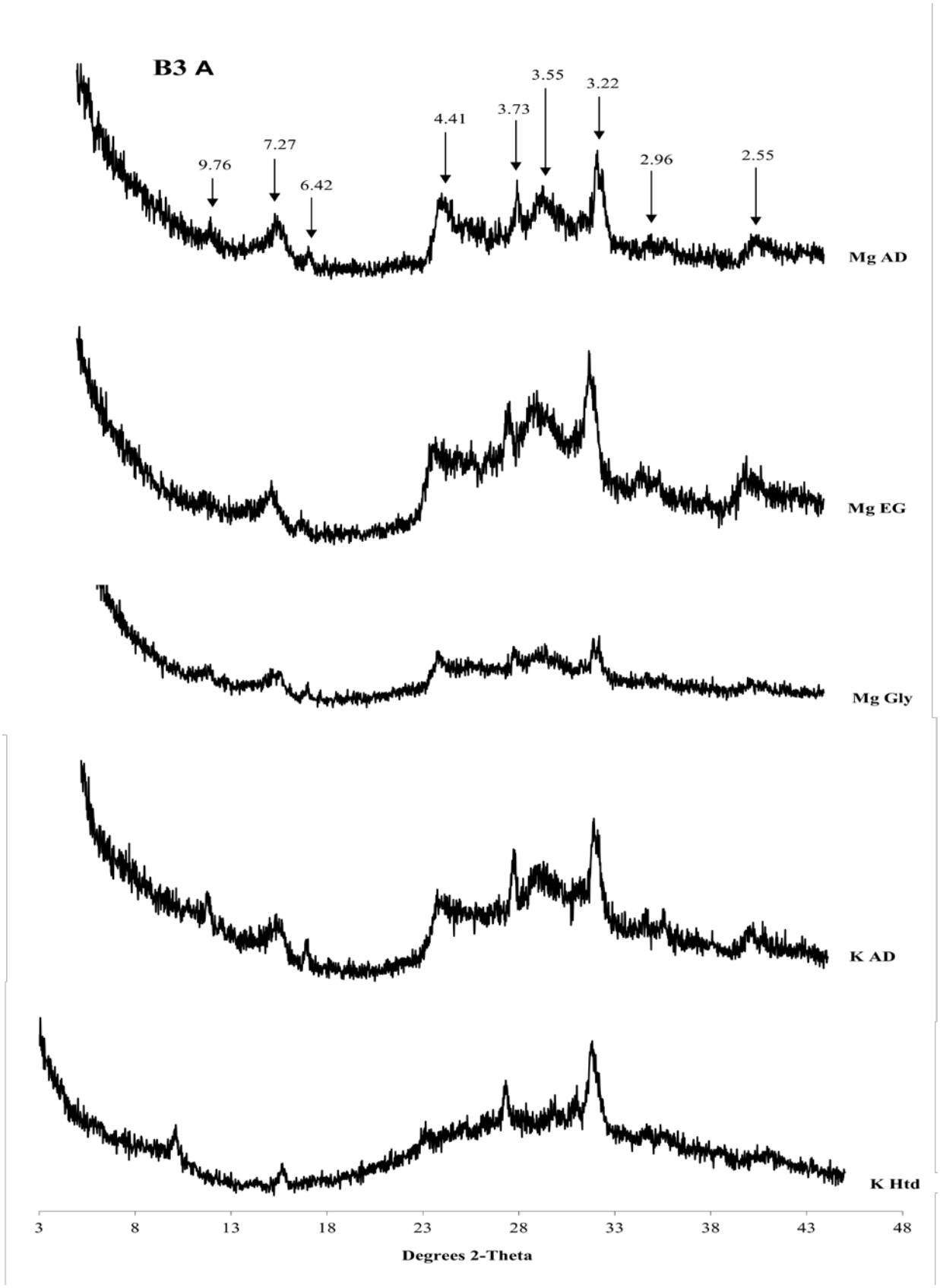
B3 A
9.76
7.27
6.42
4.41
3.73
3.55
3.22
2.96
2.55
Mg AD
Mg EG
Mg Gly
K AD
K Htd
3
8
13
18
23
28
33
38
43
48
Degrees 2-Theta

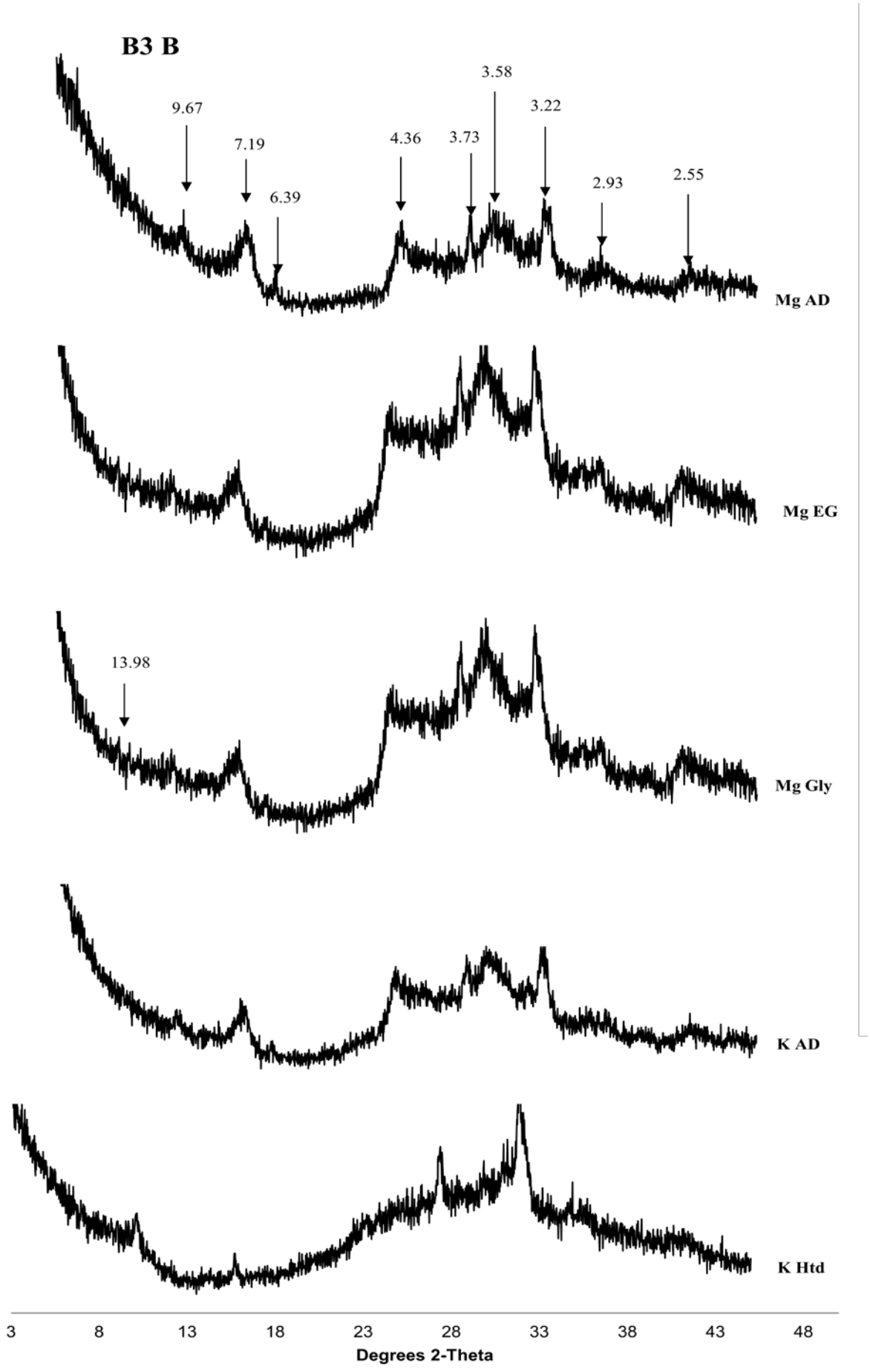
B3 B
9.67
7.19
6.39
4.36
3.73
3.58
3.22
2.93
2.55
Mg AD
Mg EG
13.98
Mg Gly
K AD
K Htd
3
8
13
18
23
28
33
38
43
48
Degrees 2-Theta

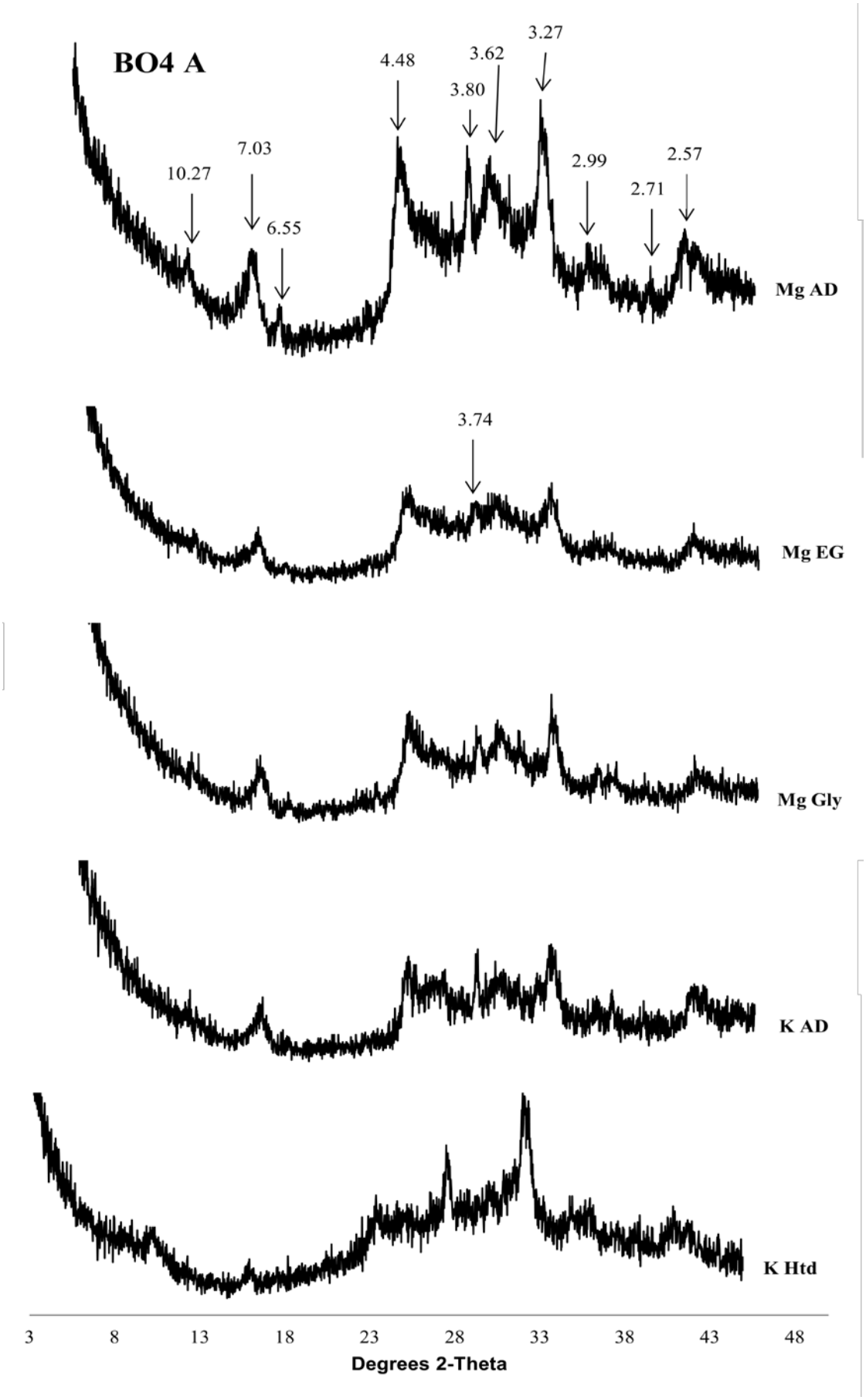
BO4 A
10.27
7.03
6.55
4.48
3.80
3.62
3.27
2.99
2.71
2.57
Mg AD
3.74
Mg EG
Mg Gly
K AD
K Htd
3
8
13
18
23
28
33
38
43
48
Degrees 2-Theta

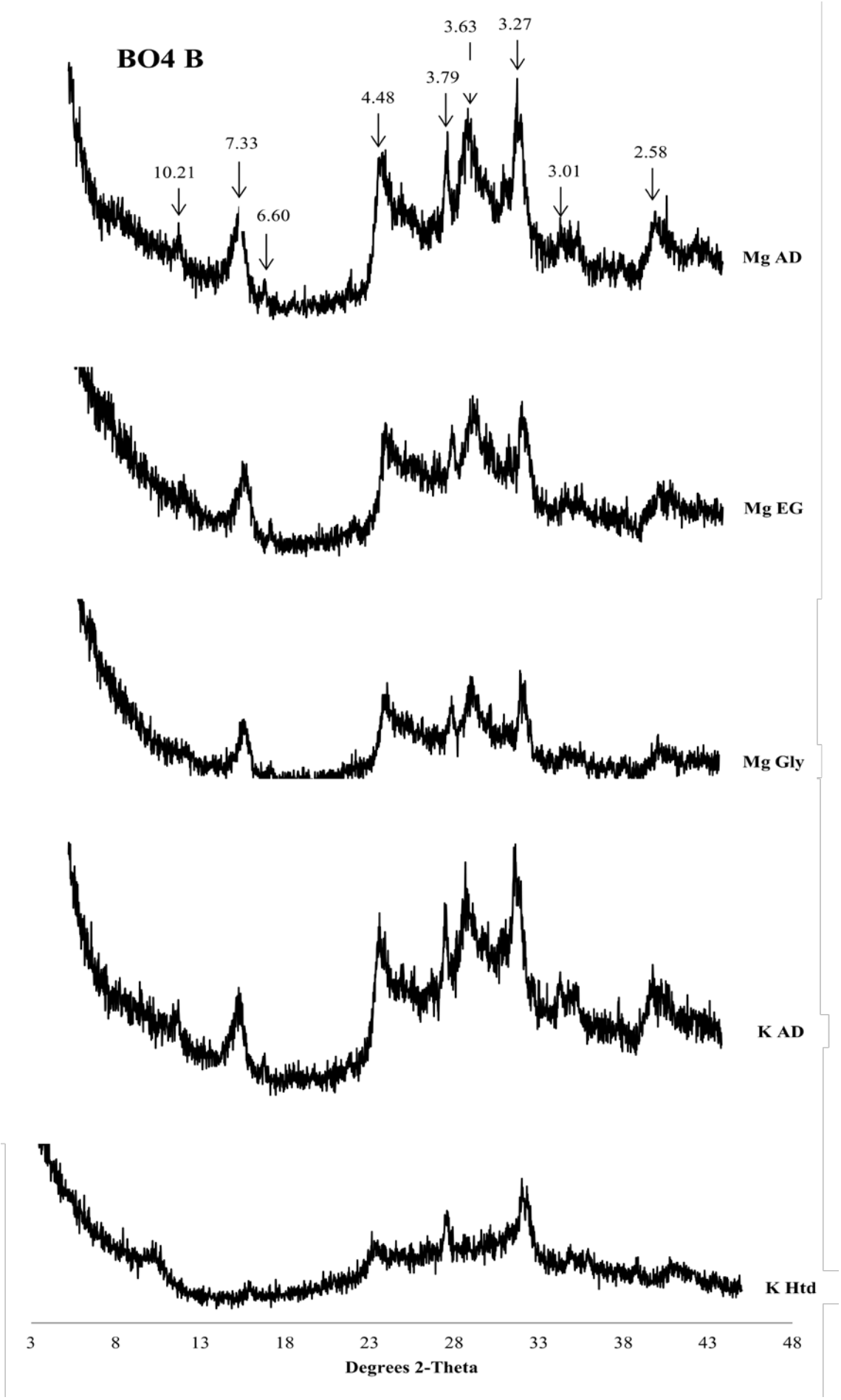
BO4 B
10.21
7.33
6.60
4.48
3.79
3.63
3.27
3.01
2.58
Mg AD
Mg EG
Mg Gly
K AD
K Htd
3
8
13
18
23
28
33
38
43
48
Degrees 2-Theta

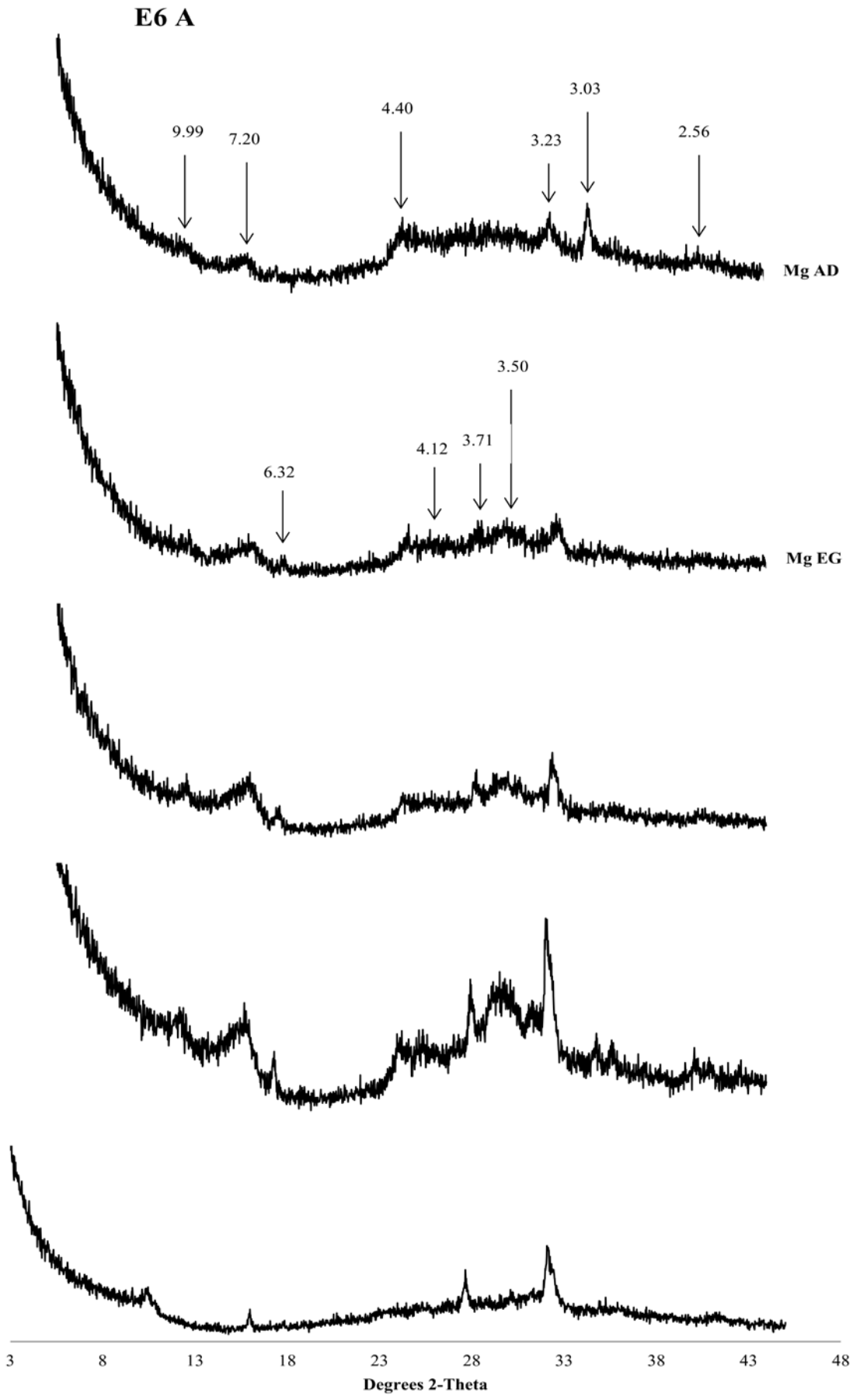
E6 A
9.99
7.20
4.40
3.23
3.03
2.56
Mg AD
6.32
4.12
3.71
3.50
Mg EG
3
8
13
18
23
28
33
38
43
48
Degrees 2-Theta

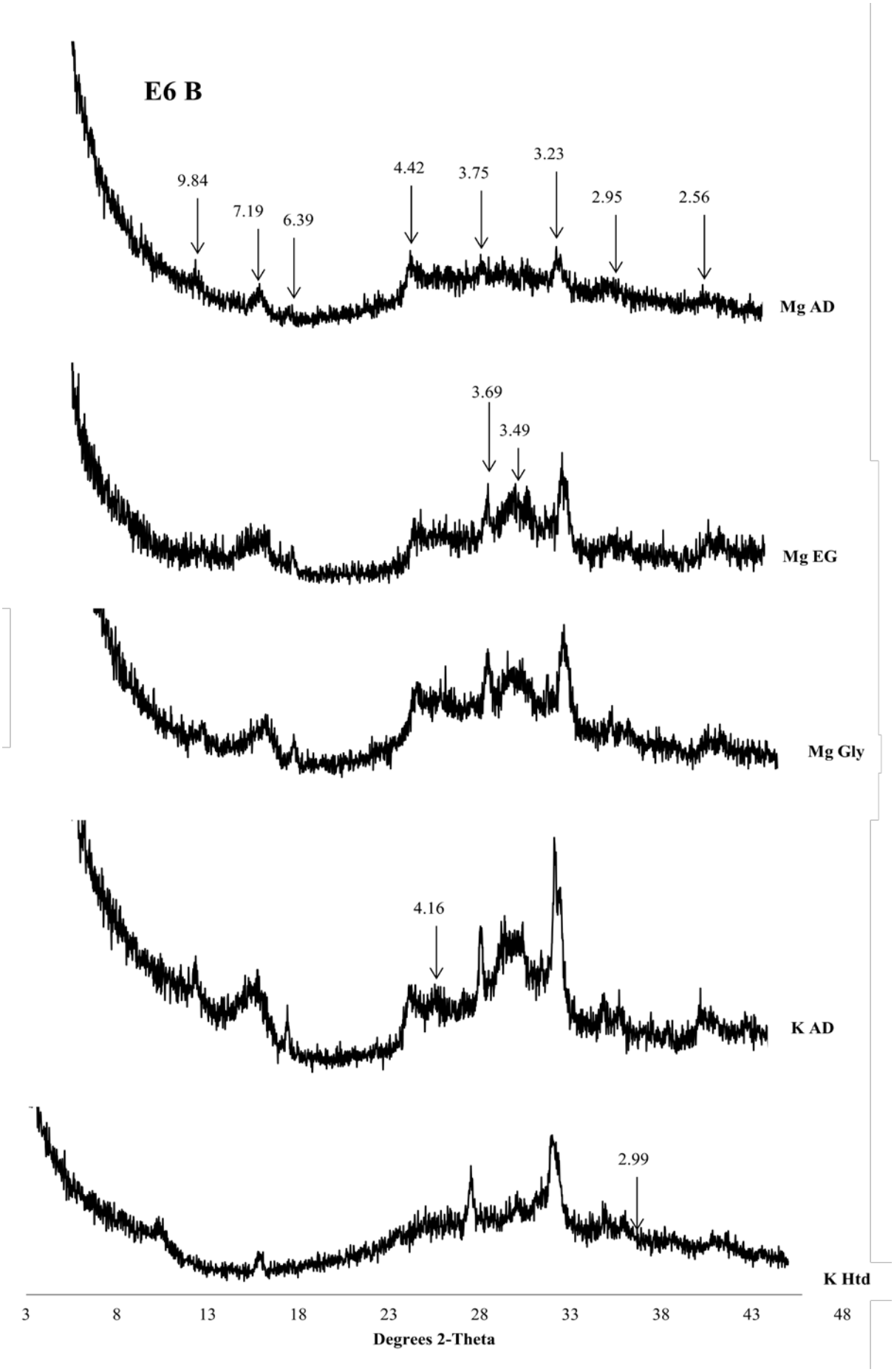
E6 B
9.84
7.19
6.39
4.42
3.75
3.23
2.95
2.56
Mg AD
3.69
3.49
Mg EG
Mg Gly
4.16
K AD
2.99
K Htd
3
8
13
18
23
28
33
38
43
48
Degrees 2-Theta

d)

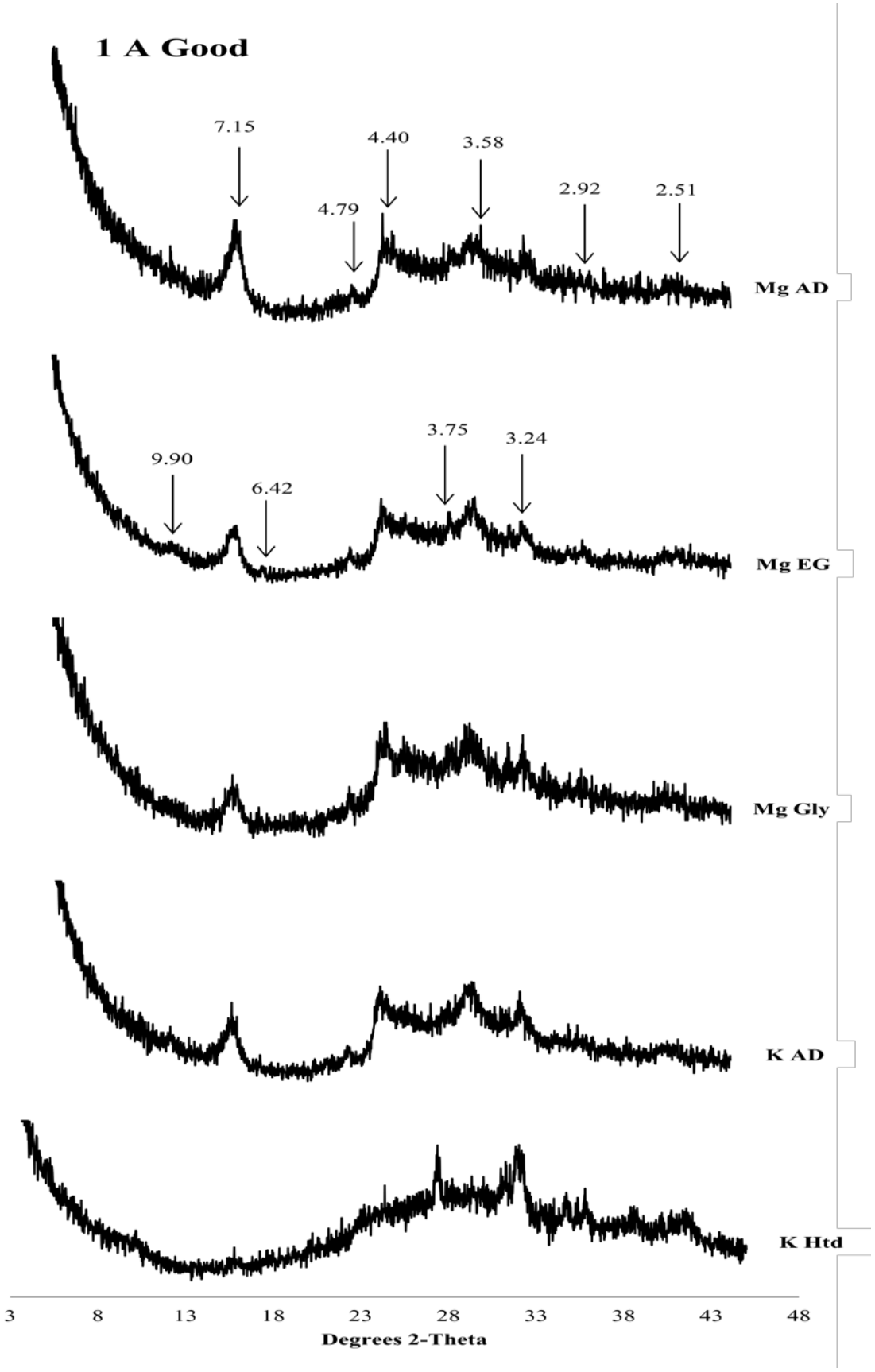
1 A Good
7.15
4.40
3.58
4.79
2.92
2.51
Mg AD
9.90
6.42
3.75
3.24
Mg EG
Mg Gly
K AD
K Htd
3
8
13
18
23
28
33
38
43
48
Degrees 2-Theta

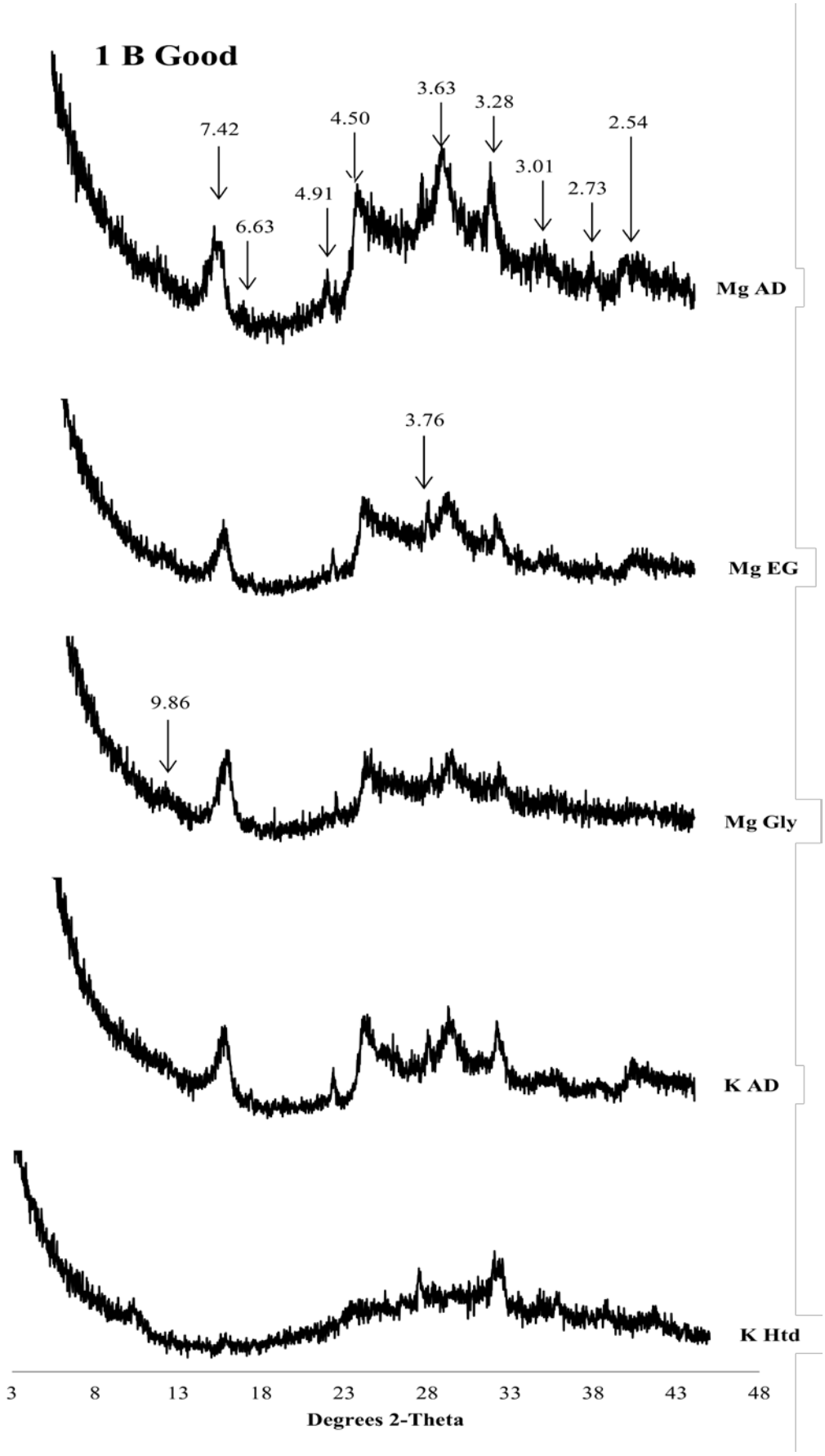
1 B Good
7.42
6.63
4.91
4.50
3.63
3.28
3.01
2.73
2.54
Mg AD
3.76
Mg EG
9.86
Mg Gly
K AD
K Htd
3
8
13
18
23
28
33
38
43
48
Degrees 2-Theta

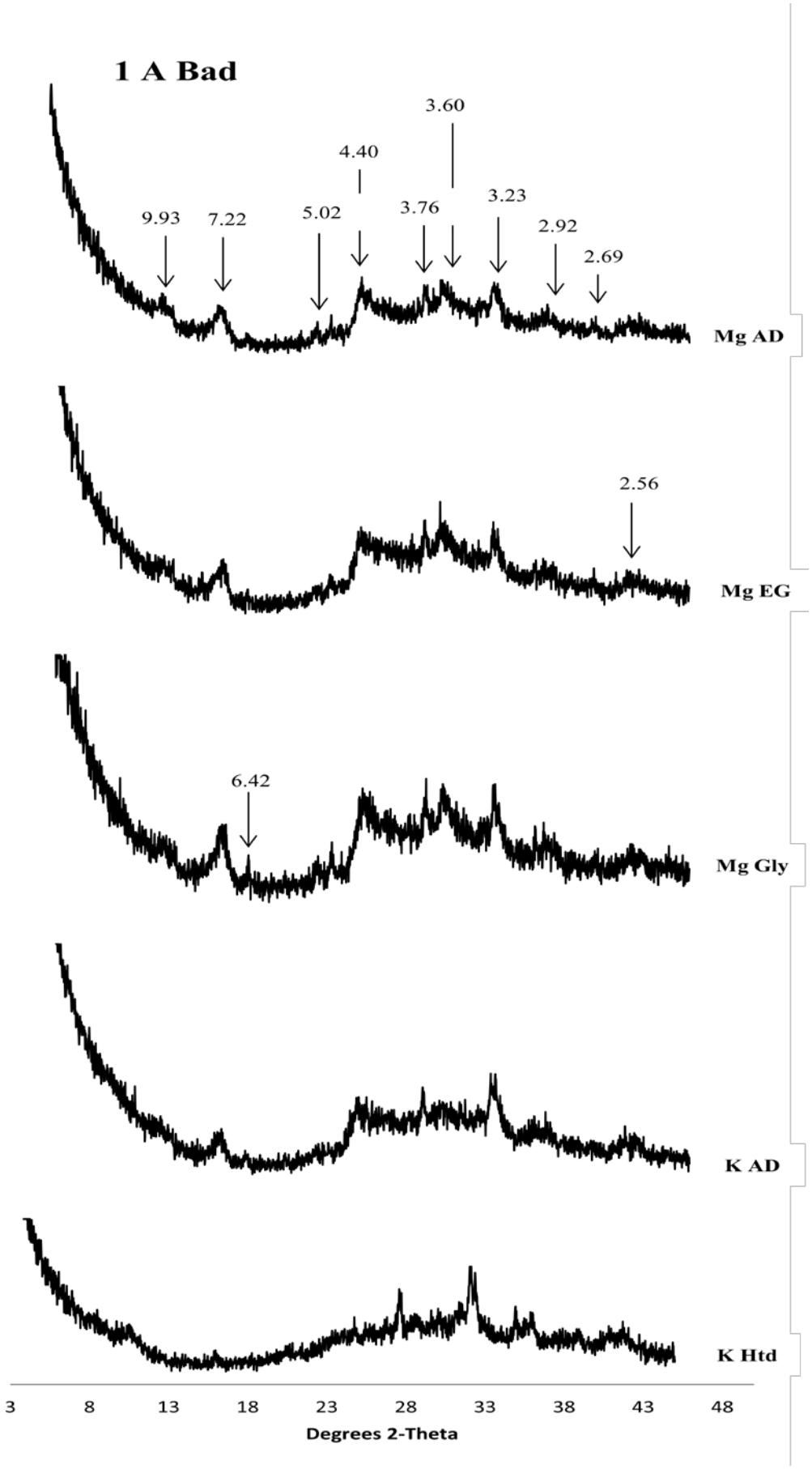
1 A Bad
3.60
4.40
9.93
7.22
5.02
3.76
3.23
2.92
2.69
Mg AD
2.56
Mg EG
6.42
Mg Gly
K AD
K Htd
3
8
13
18
23
28
33
38
43
48
Degrees 2-Theta

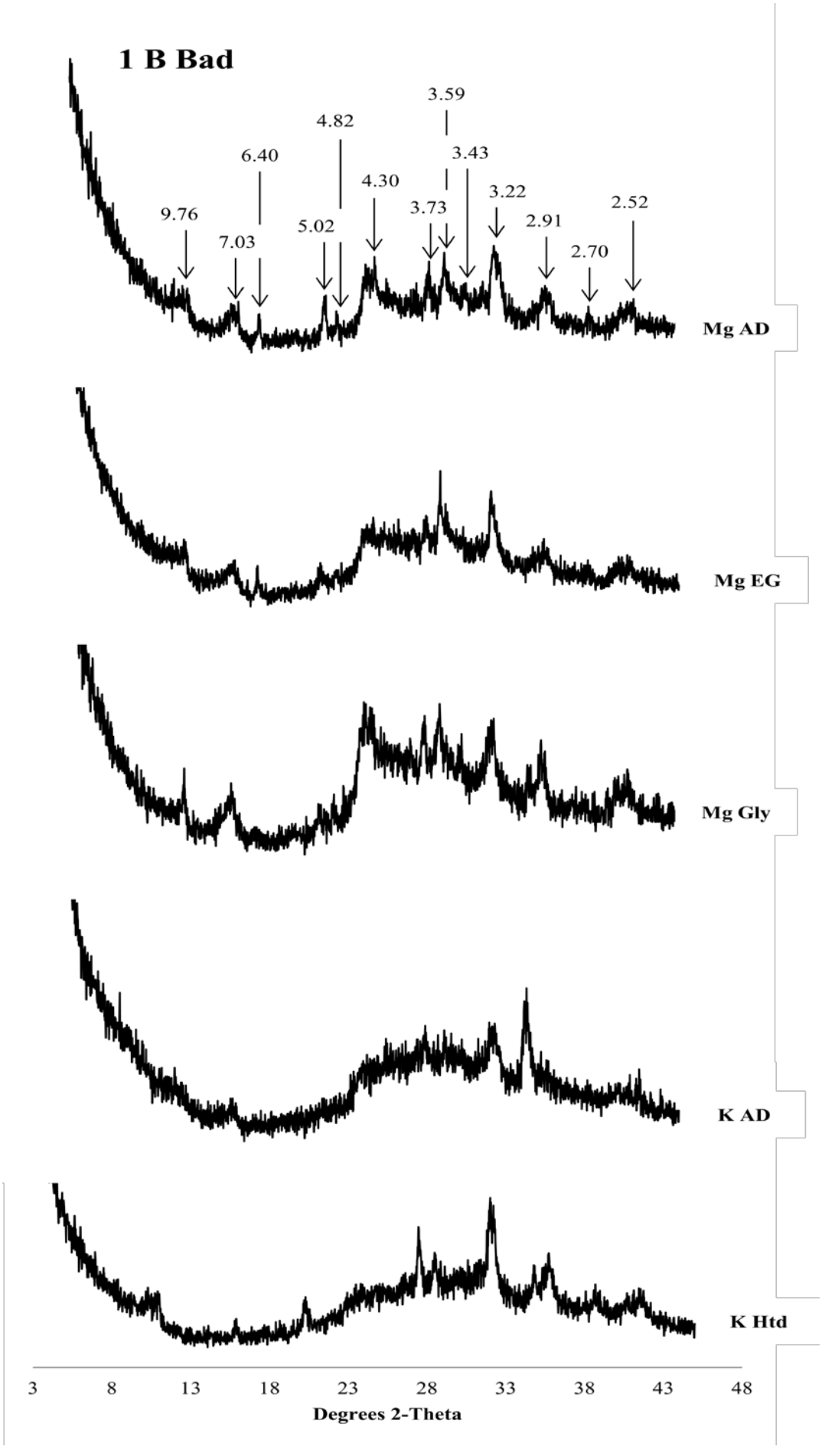
1 B Bad
9.76
7.03
6.40
5.02
4.82
4.30
3.73
3.59
3.43
3.22
2.91
2.70
2.52
Mg AD
Mg EG
Mg Gly
K AD
K Htd
3
8
13
18
23
28
33
38
43
48
Degrees 2-Theta

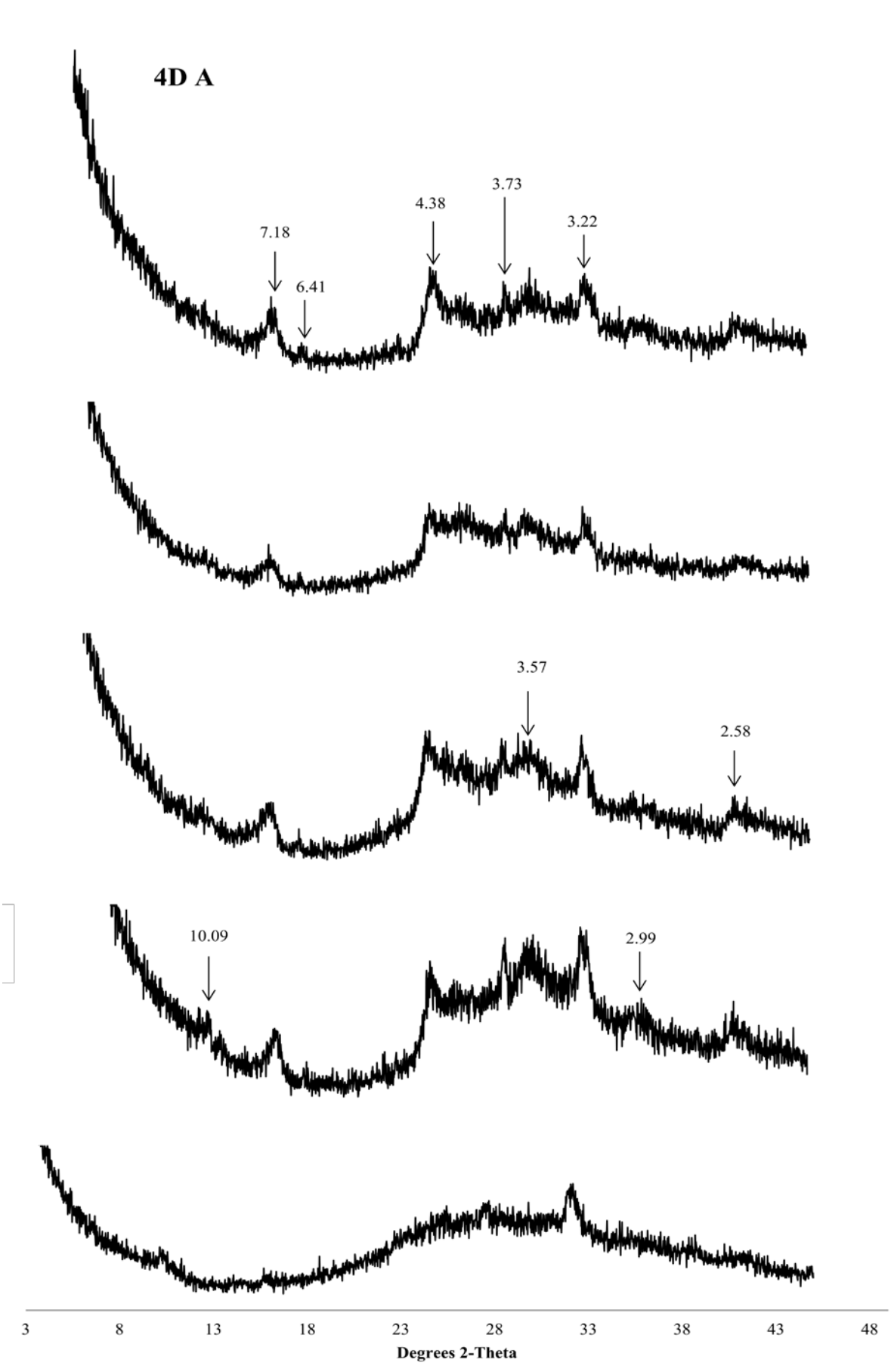
4D A
7.18
6.41
4.38
3.73
3.22
3.57
2.58
10.09
2.99
3
8
13
18
23
28
33
38
43
48
Degrees 2-Theta

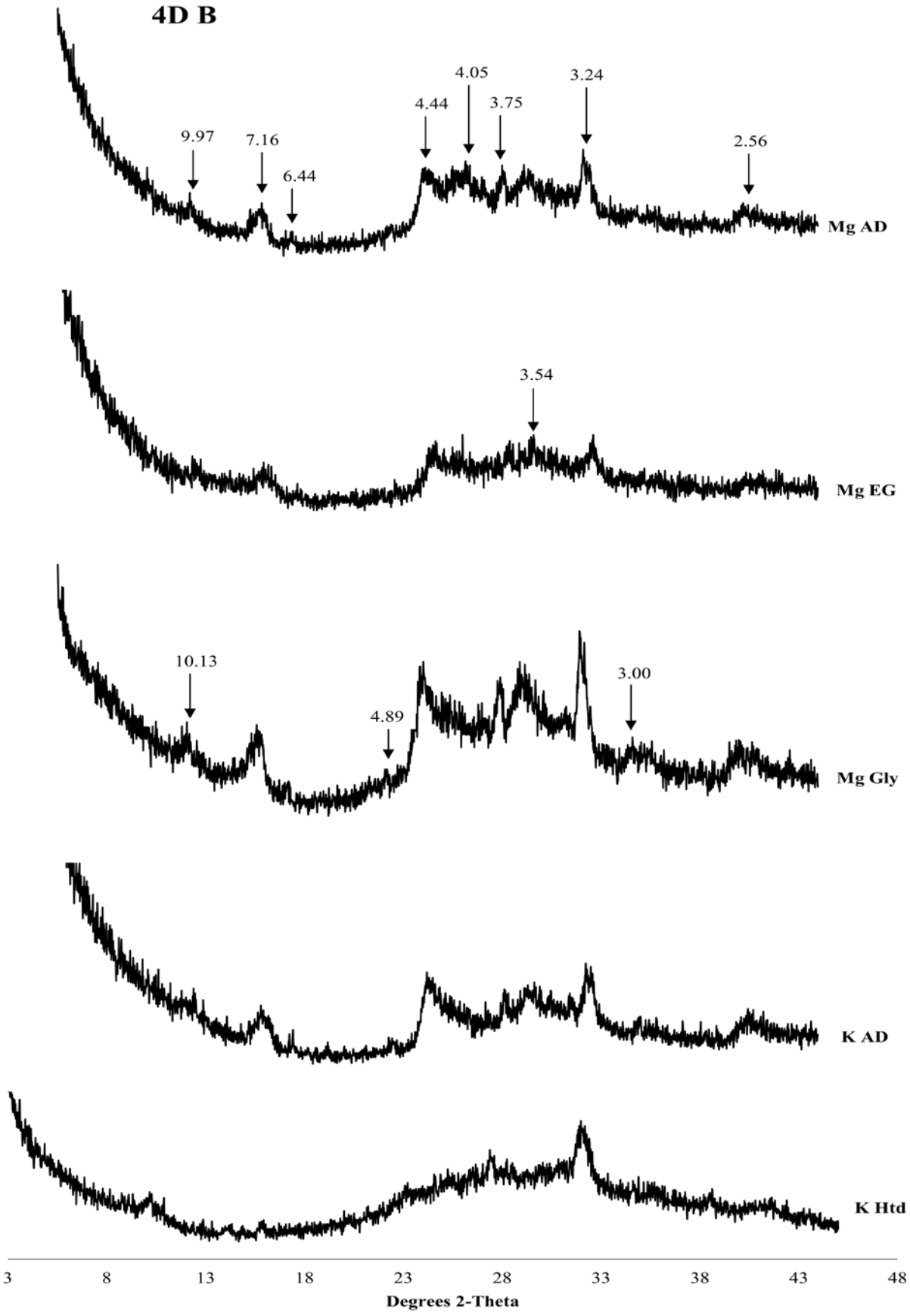
4D B
9.97
7.16
6.44
4.44
4.05
3.75
3.24
2.56
Mg AD
3.54
Mg EG
10.13
4.89
3.00
Mg Gly
K AD
K Htd
3
8
13
18
23
28
33
38
43
48
Degrees 2-Theta

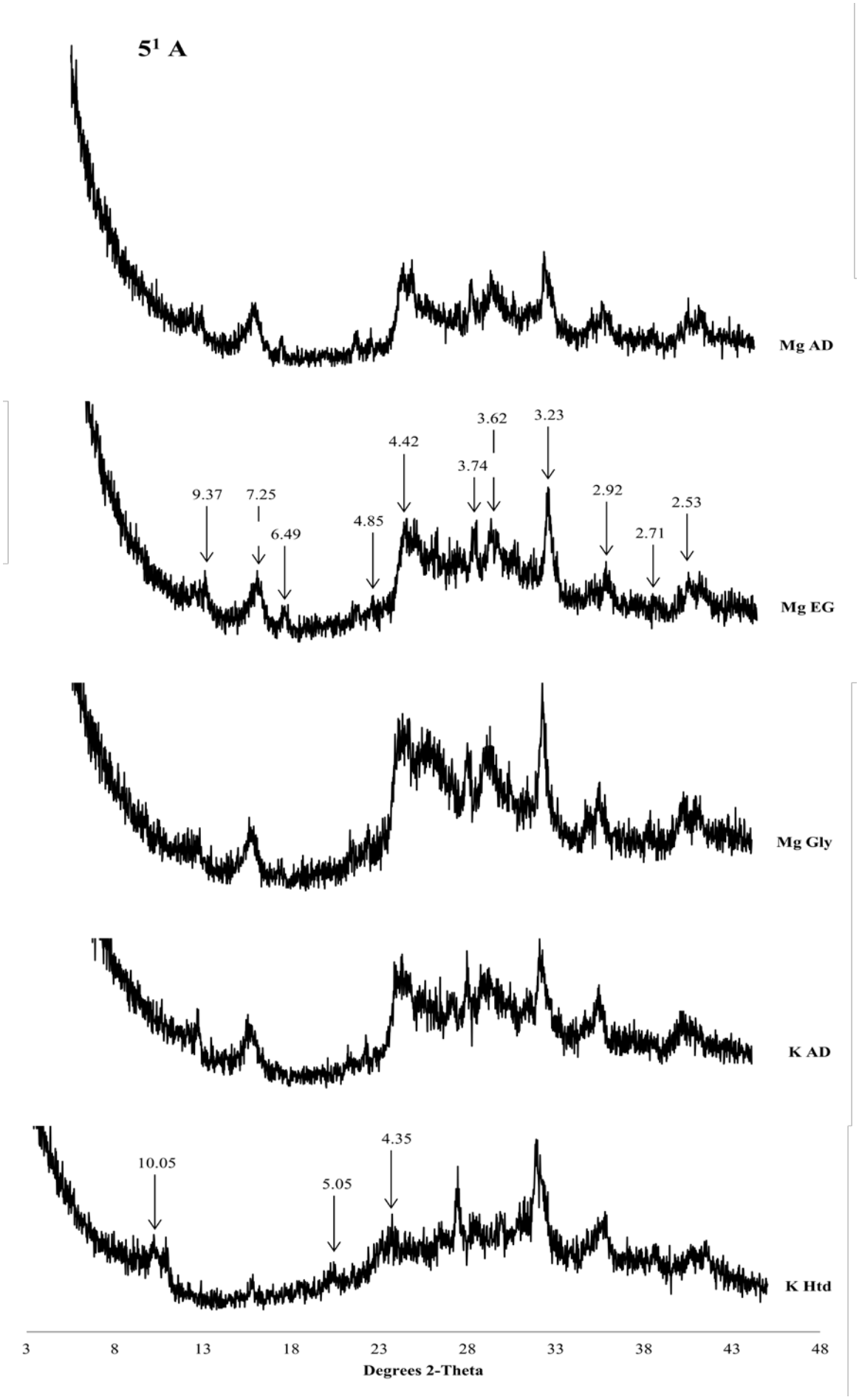
5¹ A
Mg AD
9.37
7.25
6.49
4.85
4.42
3.74
3.62
3.23
2.92
2.71
2.53
Mg EG
Mg Gly
K AD
10.05
5.05
4.35
K Htd
3
8
13
18
23
28
33
38
43
48
Degrees 2-Theta

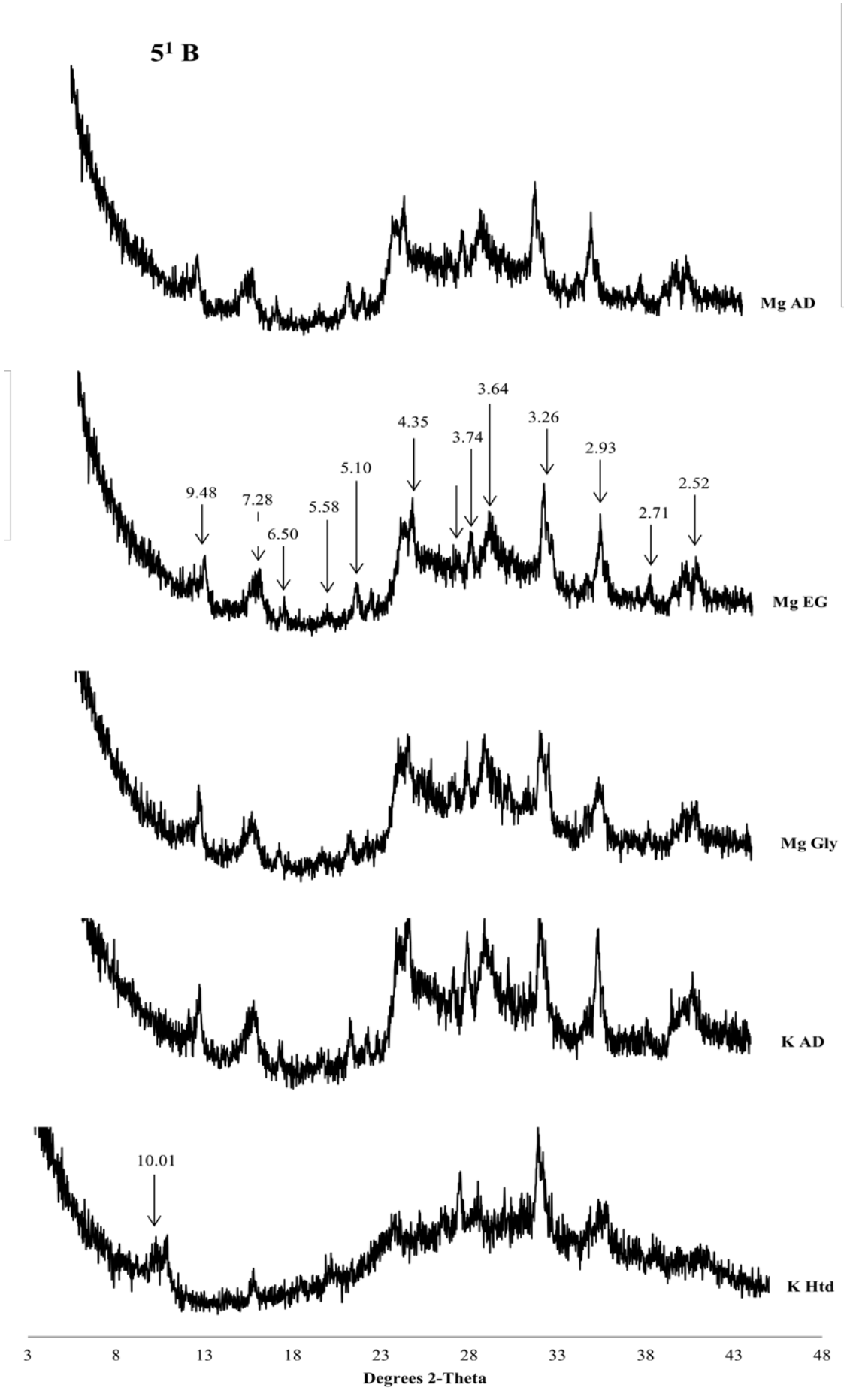
5¹ B
Mg AD
9.48
7.28
6.50
5.58
5.10
4.35
3.74
3.64
3.26
2.93
2.71
2.52
Mg EG
Mg Gly
K AD
10.01
K Htd
3
8
13
18
23
28
33
38
43
48
Degrees 2-Theta

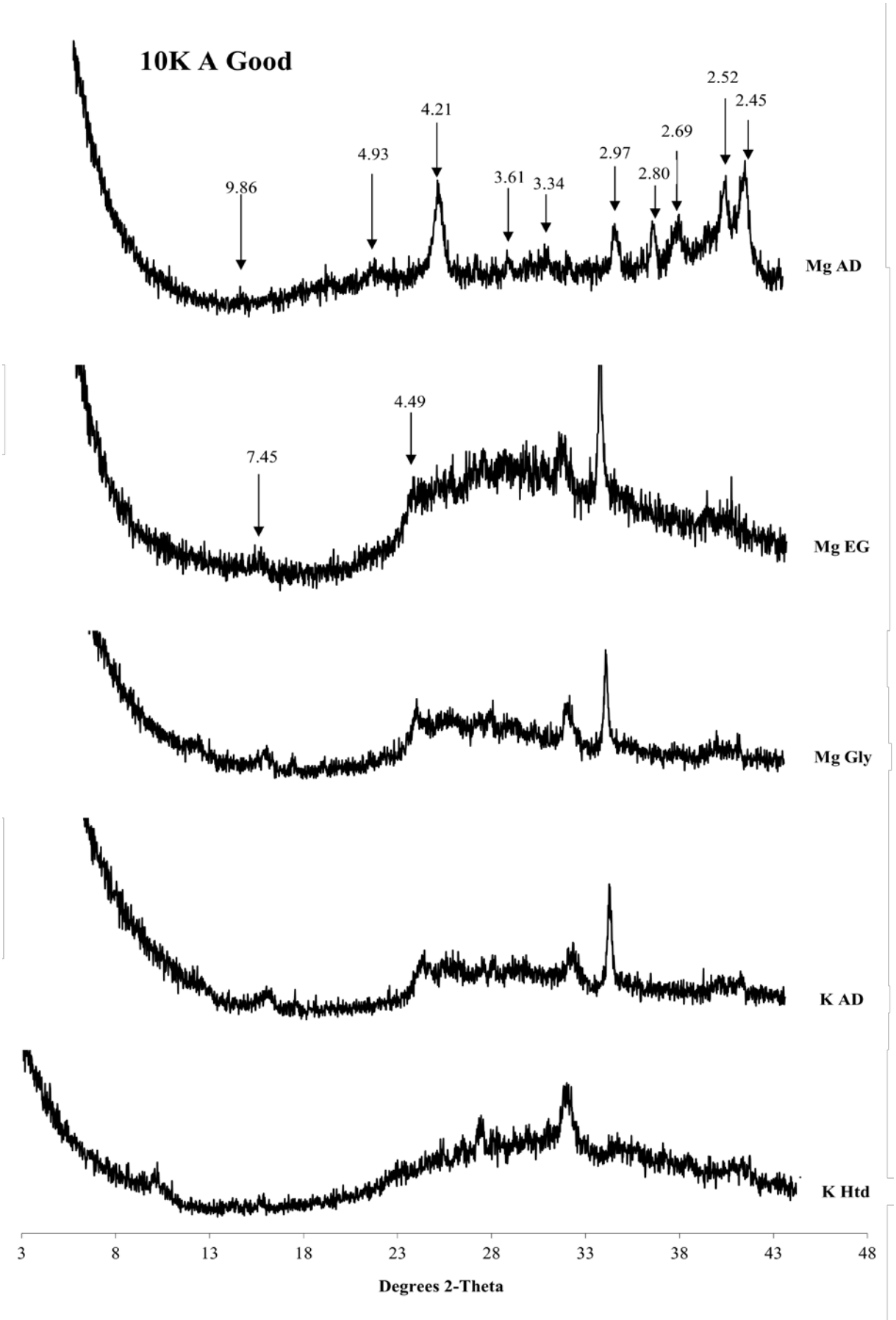
10K A Good
9.86
4.93
4.21
3.61
3.34
2.97
2.80
2.69
2.52
2.45
Mg AD
7.45
4.49
Mg EG
Mg Gly
K AD
K Htd
3
8
13
18
23
28
33
38
43
48
Degrees 2-Theta

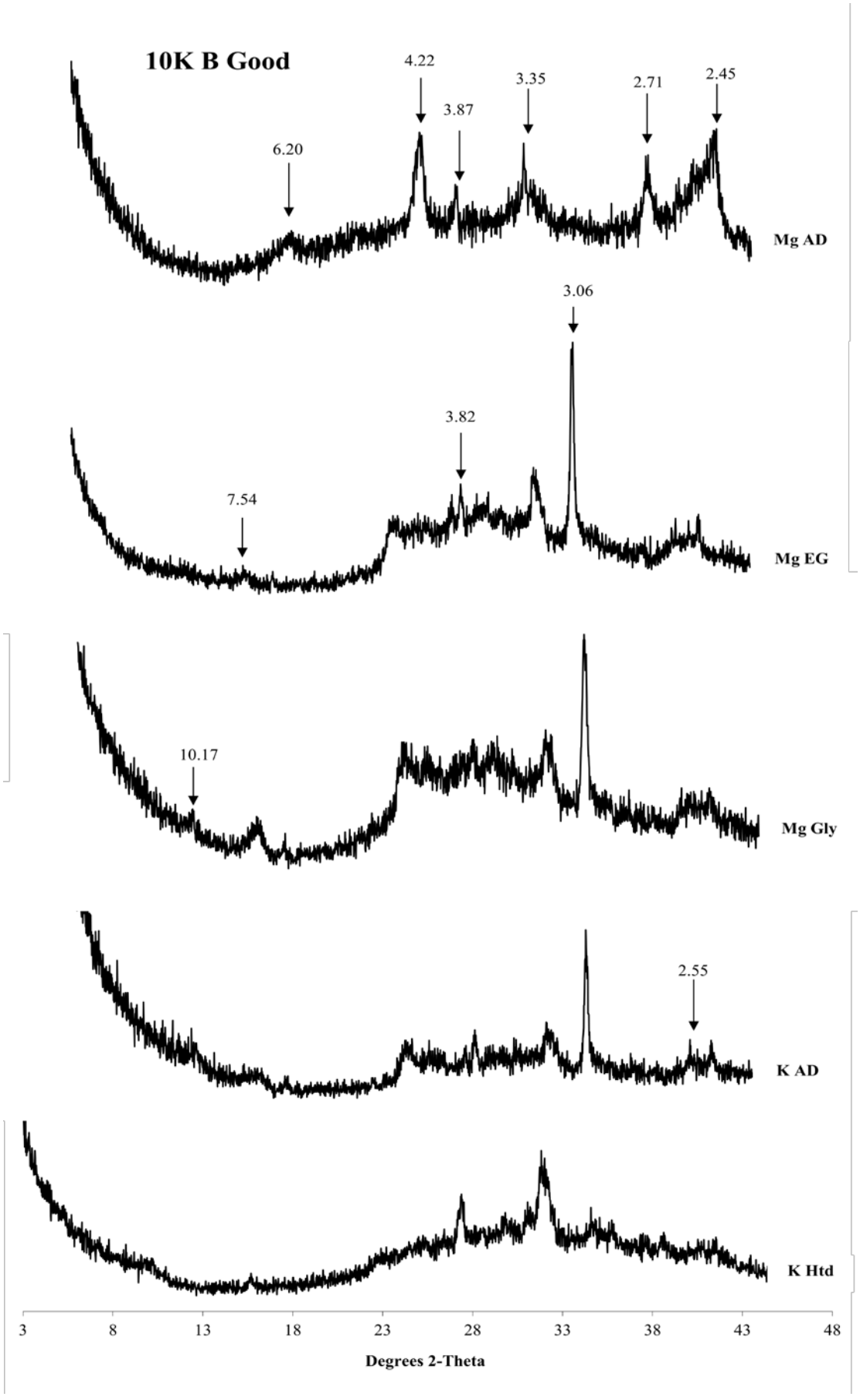
10K B Good
4.22
3.87
3.35
2.71
2.45
6.20
Mg AD
3.06
3.82
7.54
Mg EG
10.17
Mg Gly
2.55
K AD
K Htd
3
8
13
18
23
28
33
38
43
48
Degrees 2-Theta

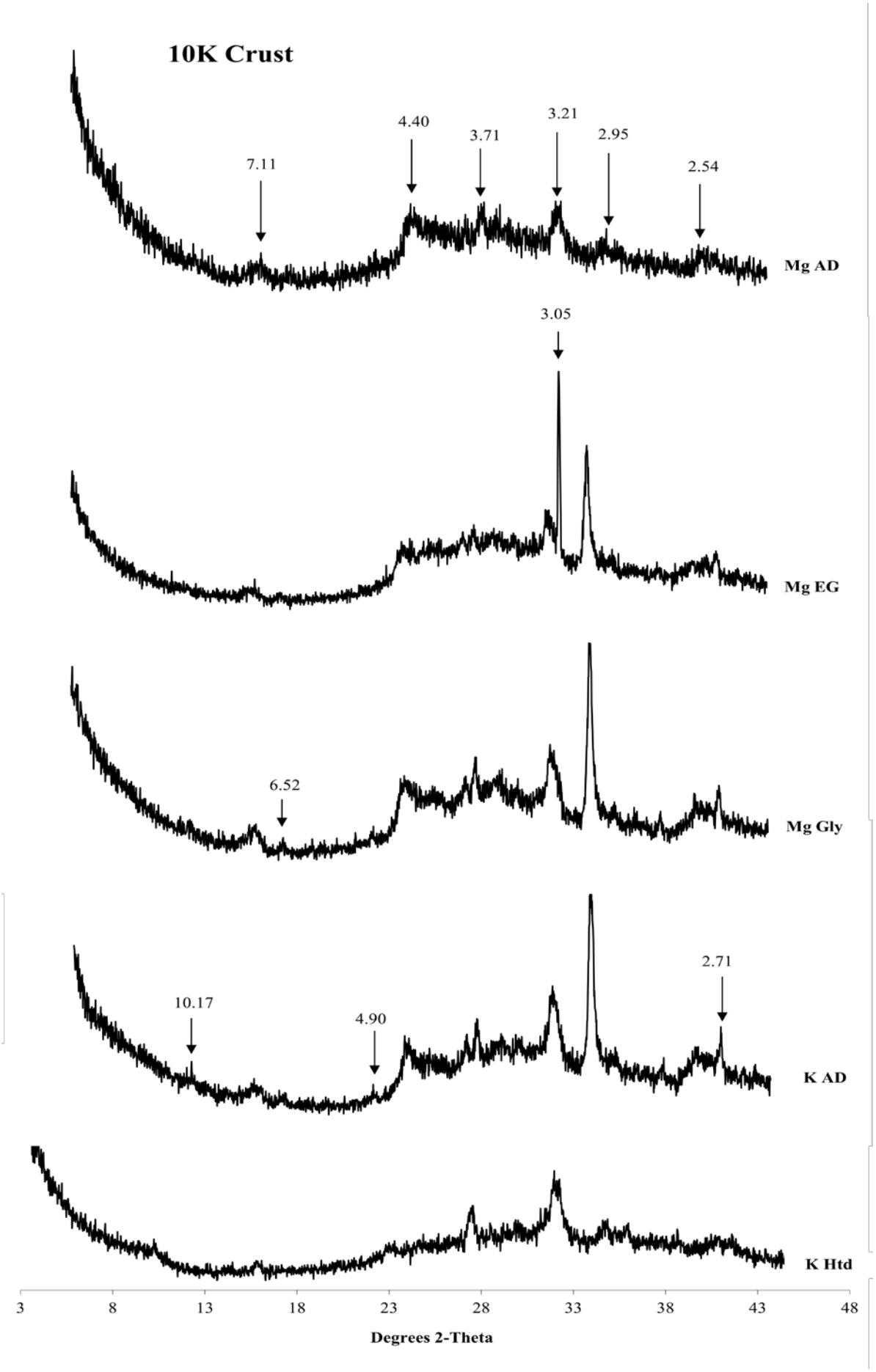
10K Crust
7.11
4.40
3.71
3.21
2.95
2.54
Mg AD
3.05
Mg EG
6.52
Mg Gly
10.17
4.90
2.71
K AD
K Htd
3
8
13
18
23
28
33
38
43
48
Degrees 2-Theta

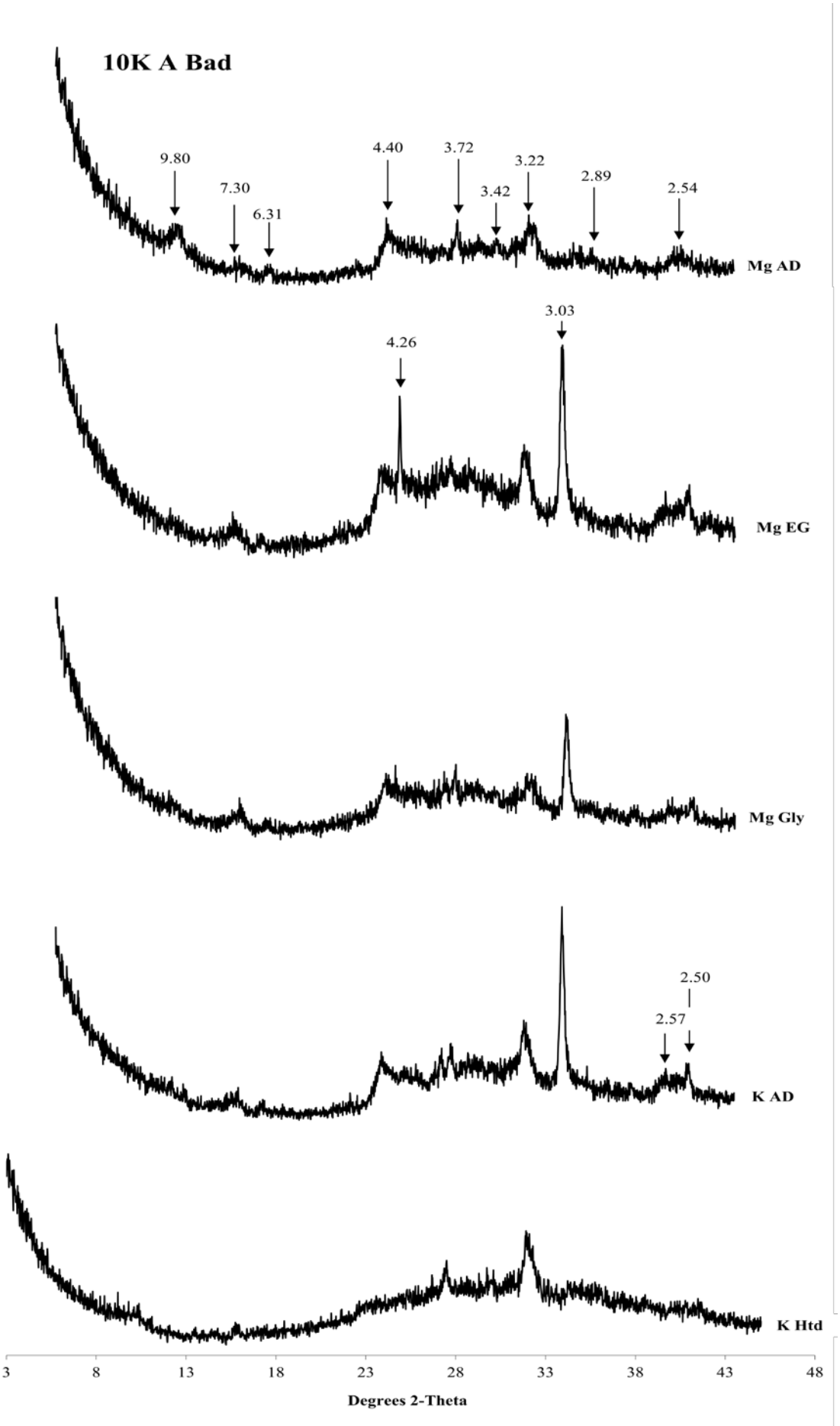
10K A Bad
9.80
7.30
6.31
4.40
3.72
3.42
3.22
2.89
2.54
Mg AD
4.26
3.03
Mg EG
Mg Gly
2.50
2.57
K AD
K Htd
3
8
13
18
23
28
33
38
43
48
Degrees 2-Theta

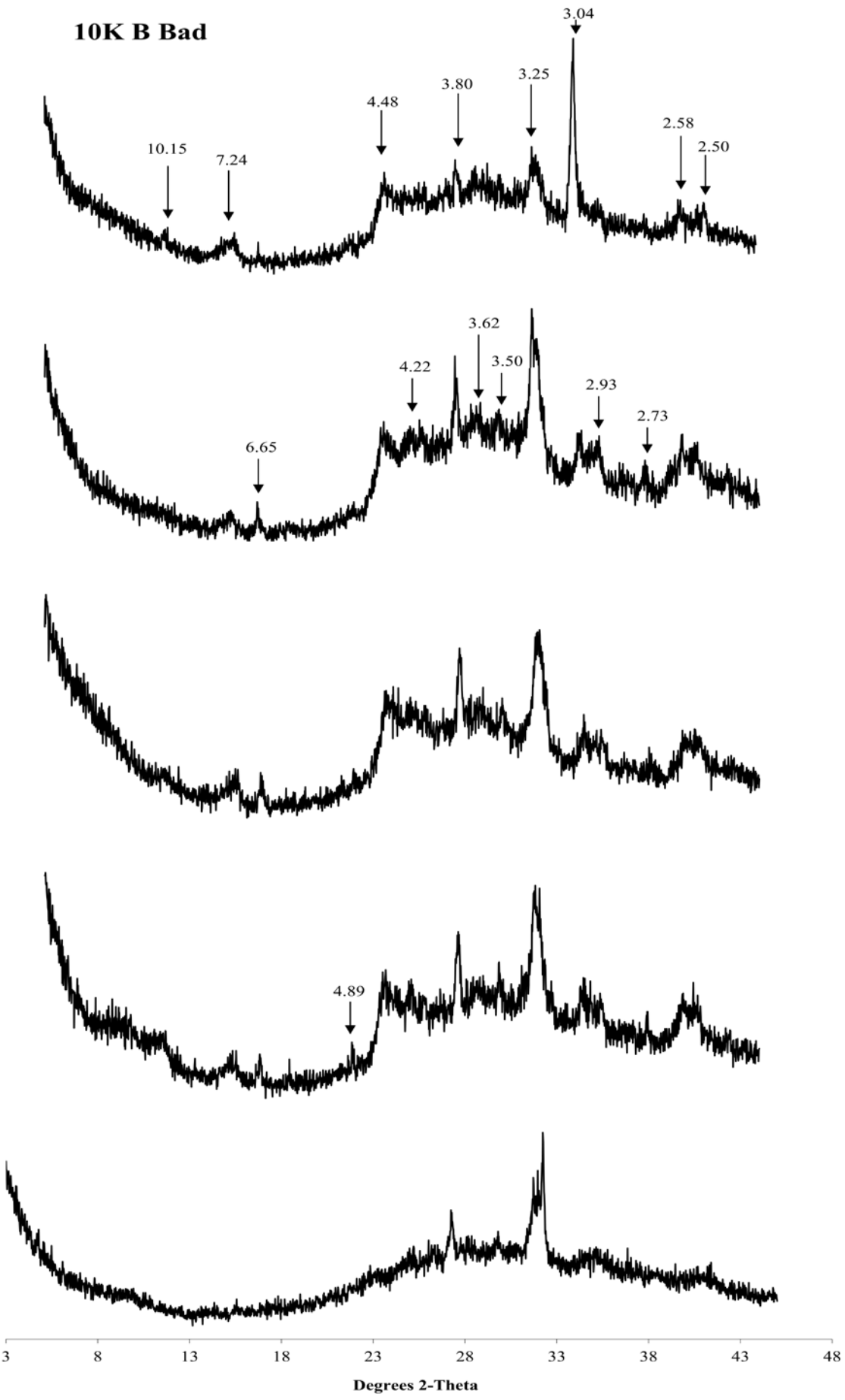
10K B Bad
3.04
3.25
3.80
4.48
2.58
2.50
10.15
7.24
3.62
3.50
4.22
2.93
2.73
6.65
4.89
3
8
13
18
23
28
33
38
43
48
Degrees 2-Theta

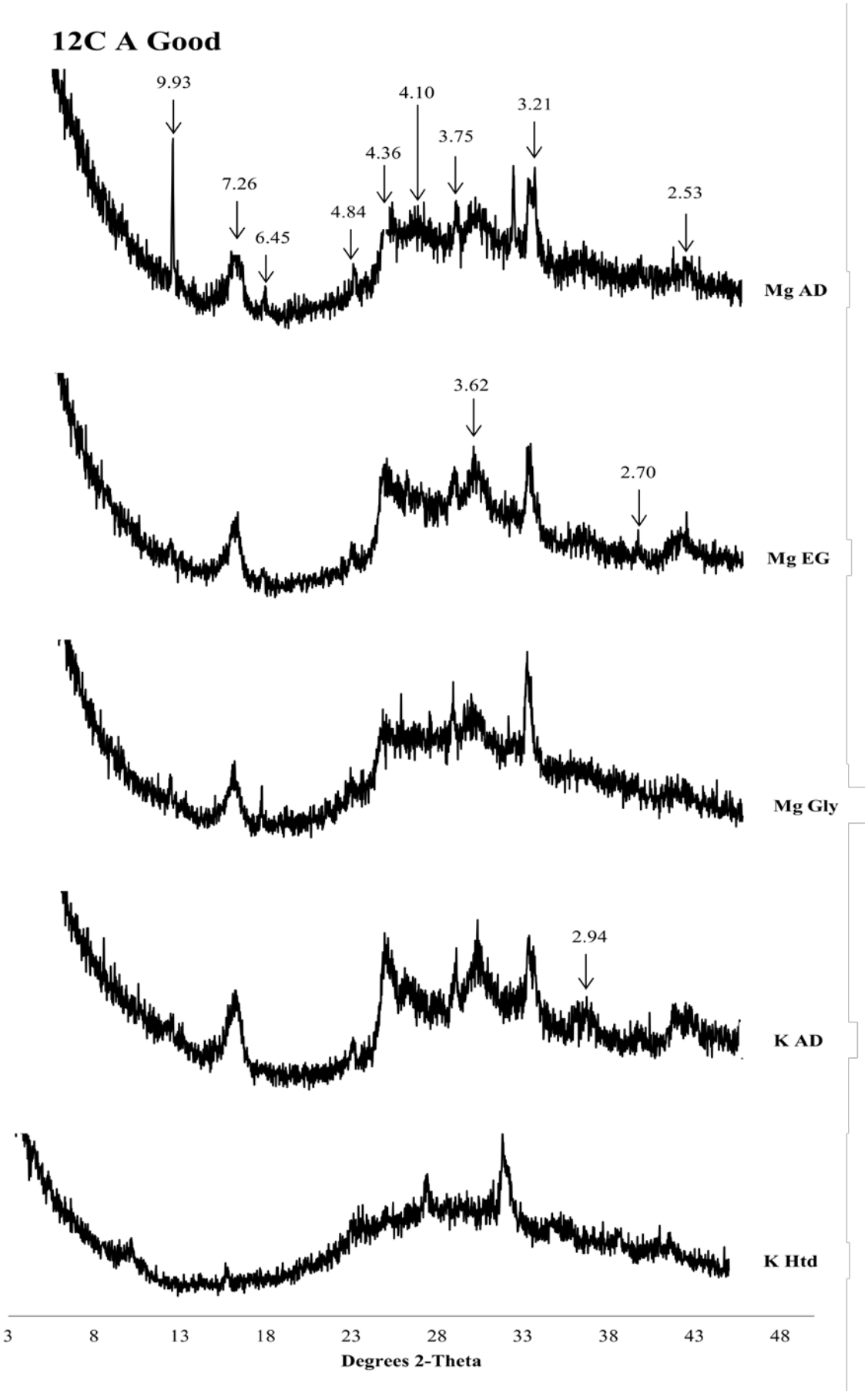
12C A Good
9.93
7.26
6.45
4.84
4.36
4.10
3.75
3.21
2.53
Mg AD
3.62
2.70
Mg EG
Mg Gly
2.94
K AD
K Htd
3
8
13
18
23
28
33
38
43
48
Degrees 2-Theta

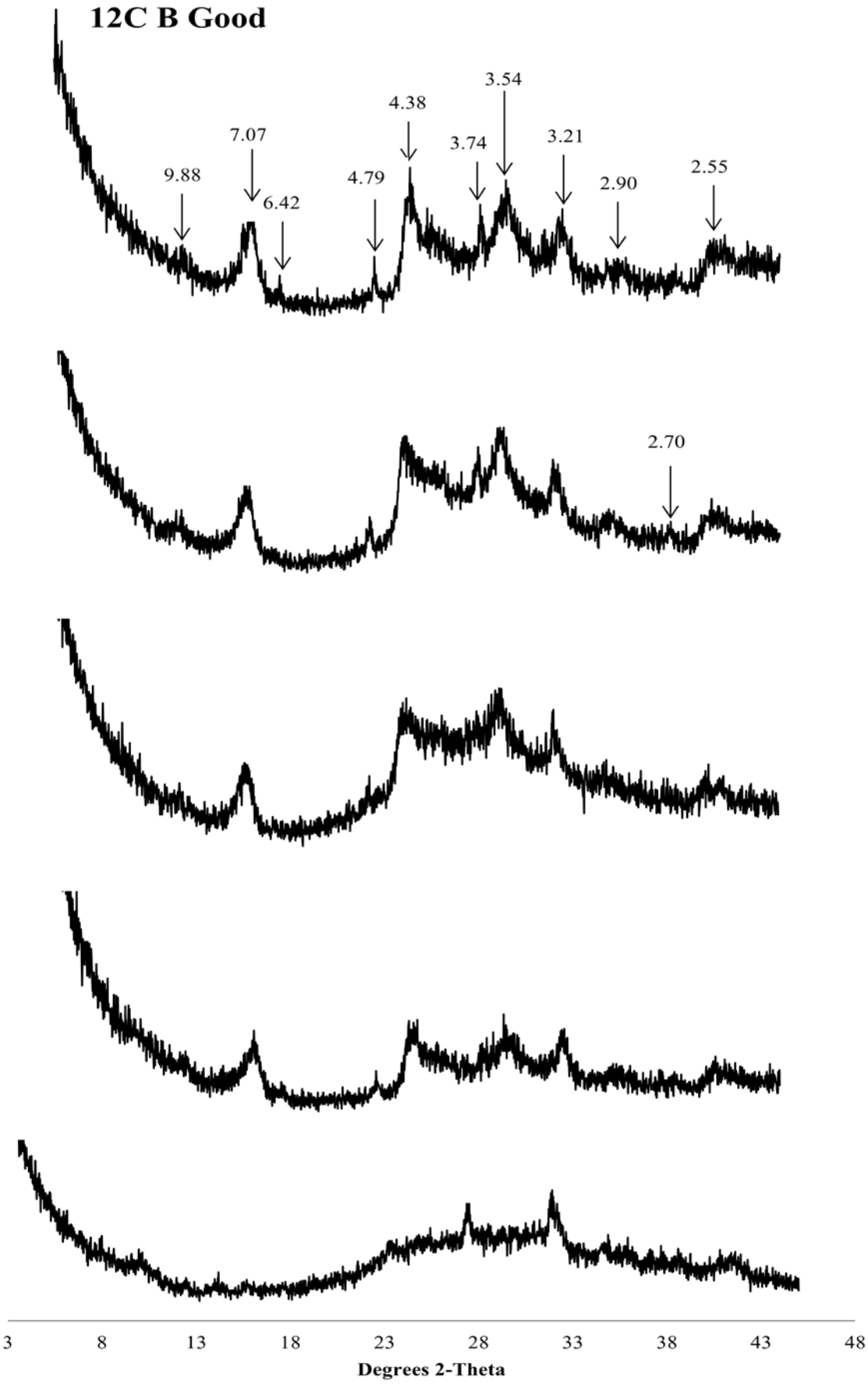
12C B Good
9.88
7.07
6.42
4.79
4.38
3.74
3.54
3.21
2.90
2.55
2.70
3
8
13
18
23
28
33
38
43
48
Degrees 2-Theta

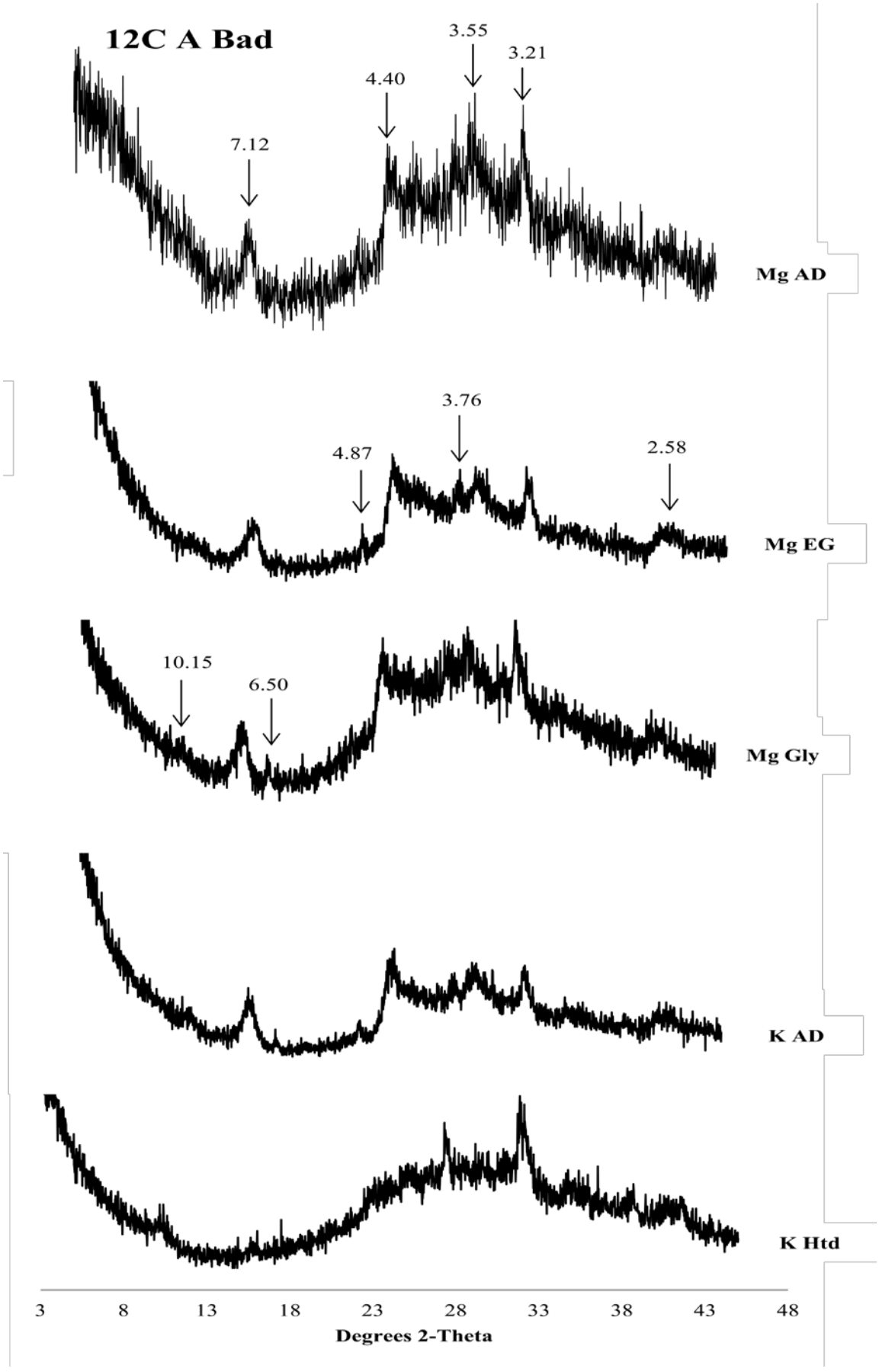
12C A Bad
7.12
4.40
3.55
3.21
Mg AD
4.87
3.76
2.58
Mg EG
10.15
6.50
Mg Gly
K AD
K Htd
3
8
13
18
23
28
33
38
43
48
Degrees 2-Theta

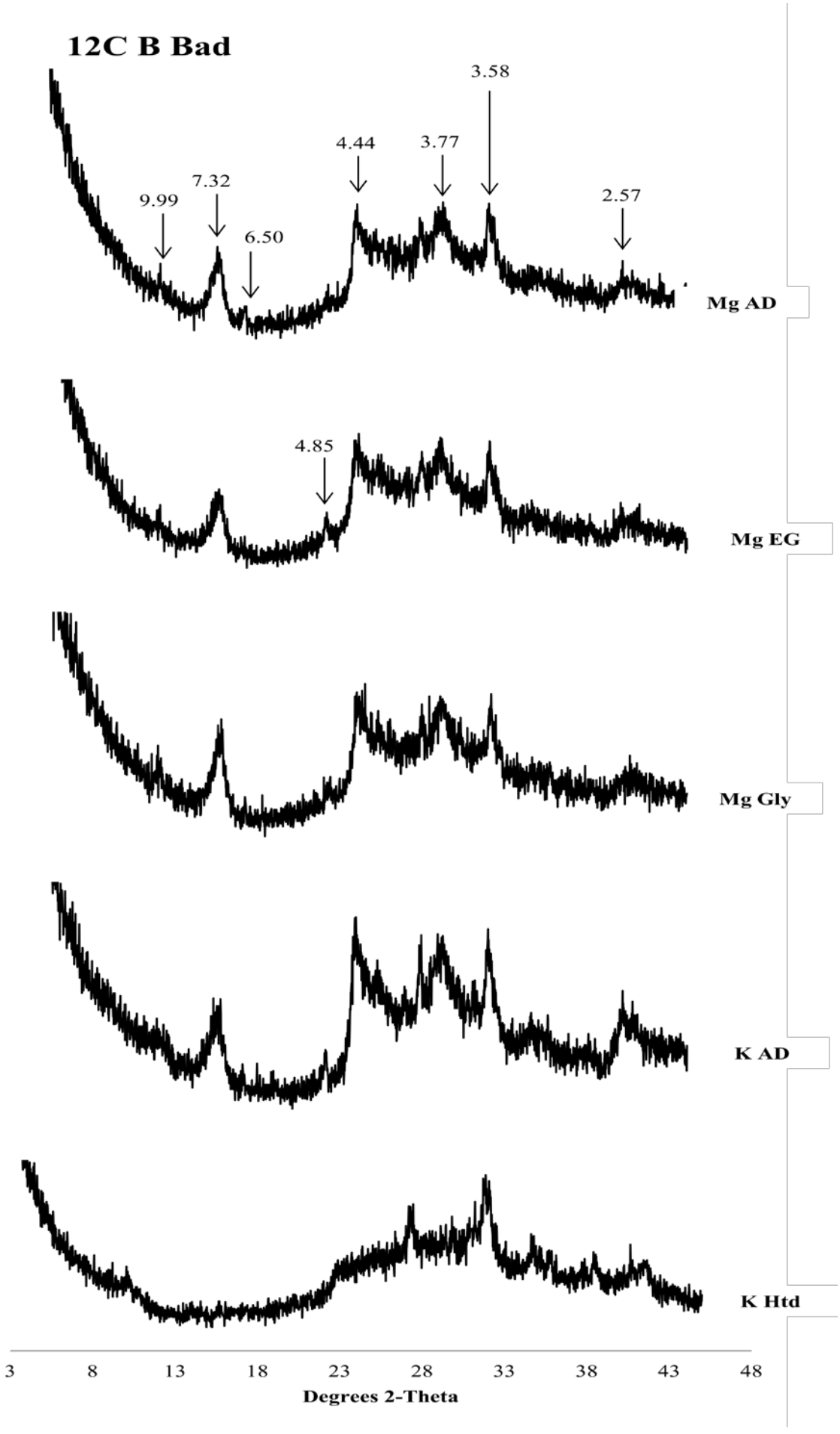
12C B Bad
3.58
4.44
3.77
7.32
9.99
2.57
6.50
Mg AD
4.85
Mg EG
Mg Gly
K AD
K Htd
3
8
13
18
23
28
33
38
43
48
Degrees 2-Theta

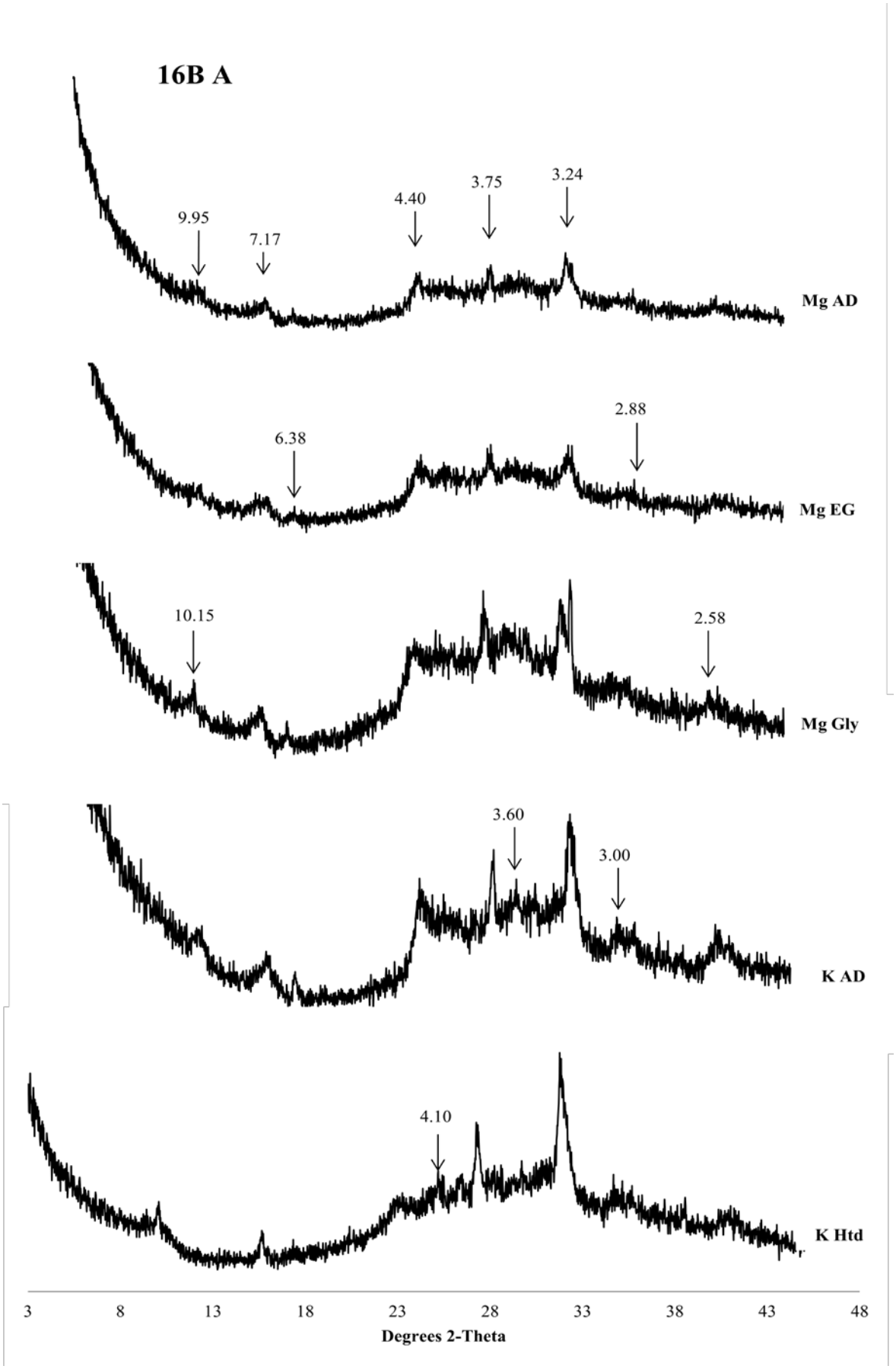
16B A
9.95
7.17
4.40
3.75
3.24
Mg AD
6.38
2.88
Mg EG
10.15
2.58
Mg Gly
3.60
3.00
K AD
4.10
K Htd
3
8
13
18
23
28
33
38
43
48
Degrees 2-Theta

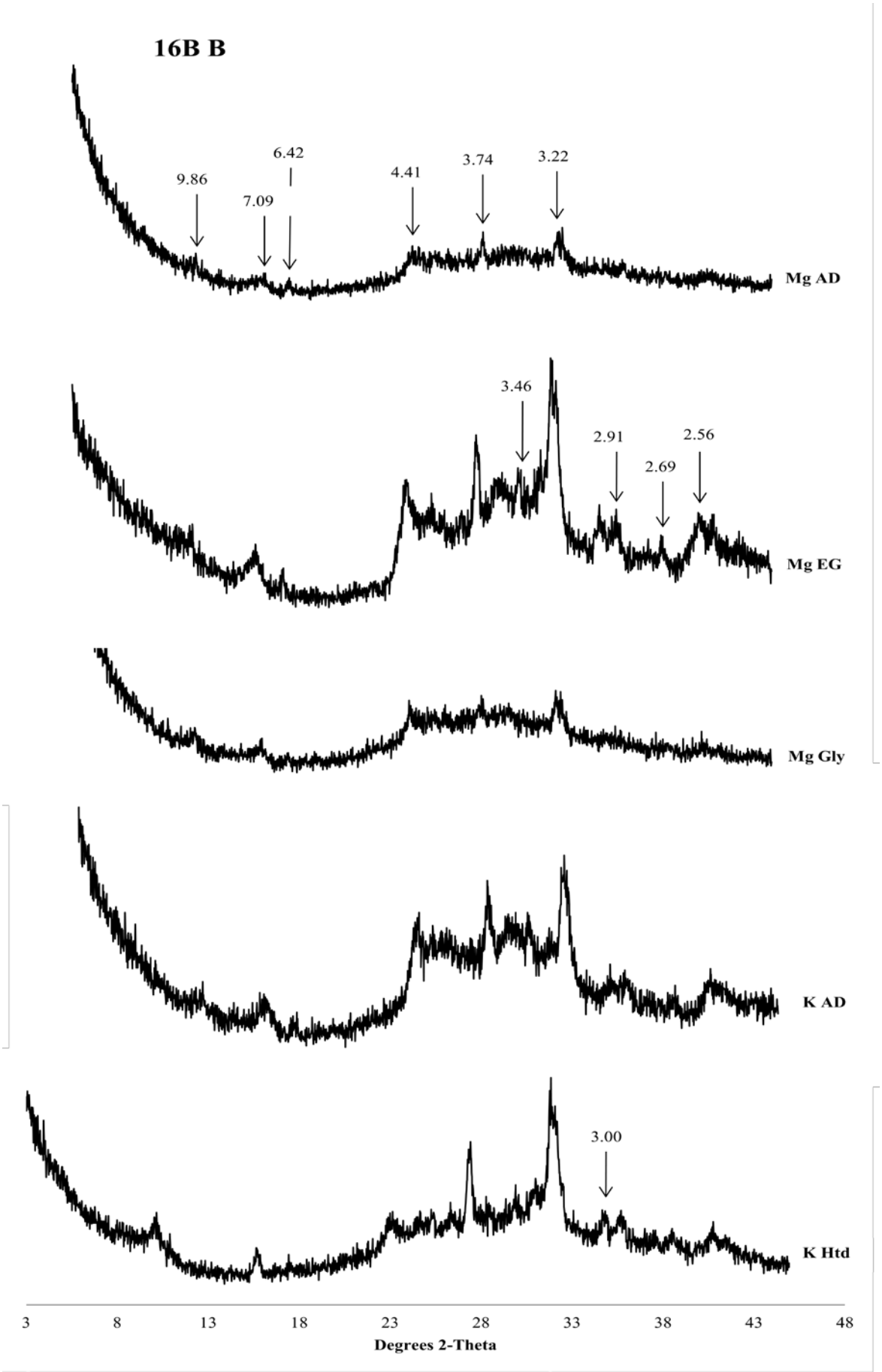
16B B
9.86
7.09
6.42
4.41
3.74
3.22
Mg AD
3.46
2.91
2.69
2.56
Mg EG
Mg Gly
K AD
3.00
K Htd
3
8
13
18
23
28
33
38
43
48
Degrees 2-Theta

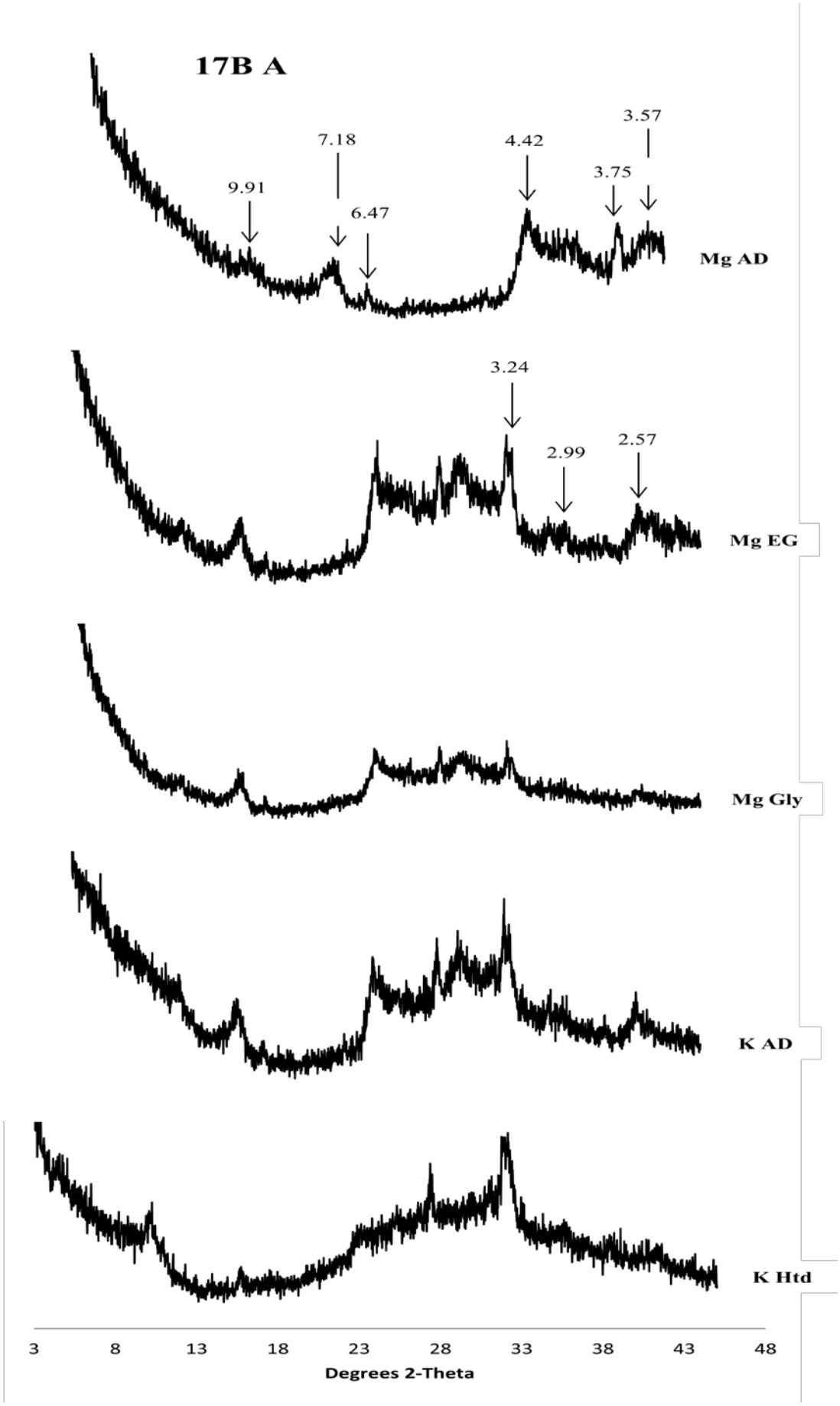
17B A
9.91
7.18
6.47
4.42
3.75
3.57
Mg AD
3.24
2.99
2.57
Mg EG
Mg Gly
K AD
K Htd
3
8
13
18
23
28
33
38
43
48
Degrees 2-Theta

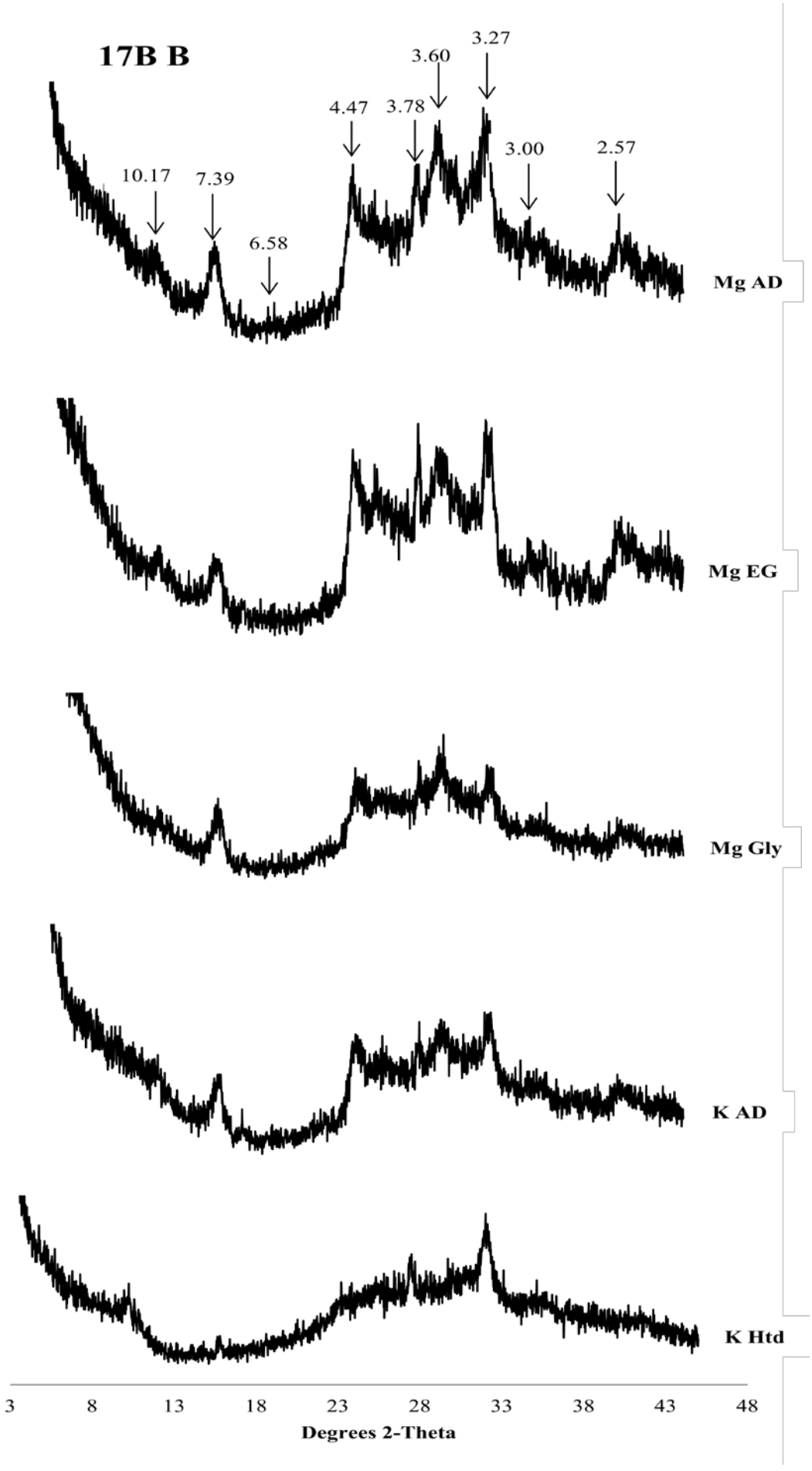
17B B
10.17
7.39
6.58
4.47
3.78
3.60
3.27
3.00
2.57
Mg AD
Mg EG
Mg Gly
K AD
K Htd
3
8
13
18
23
28
33
38
43
48
Degrees 2-Theta

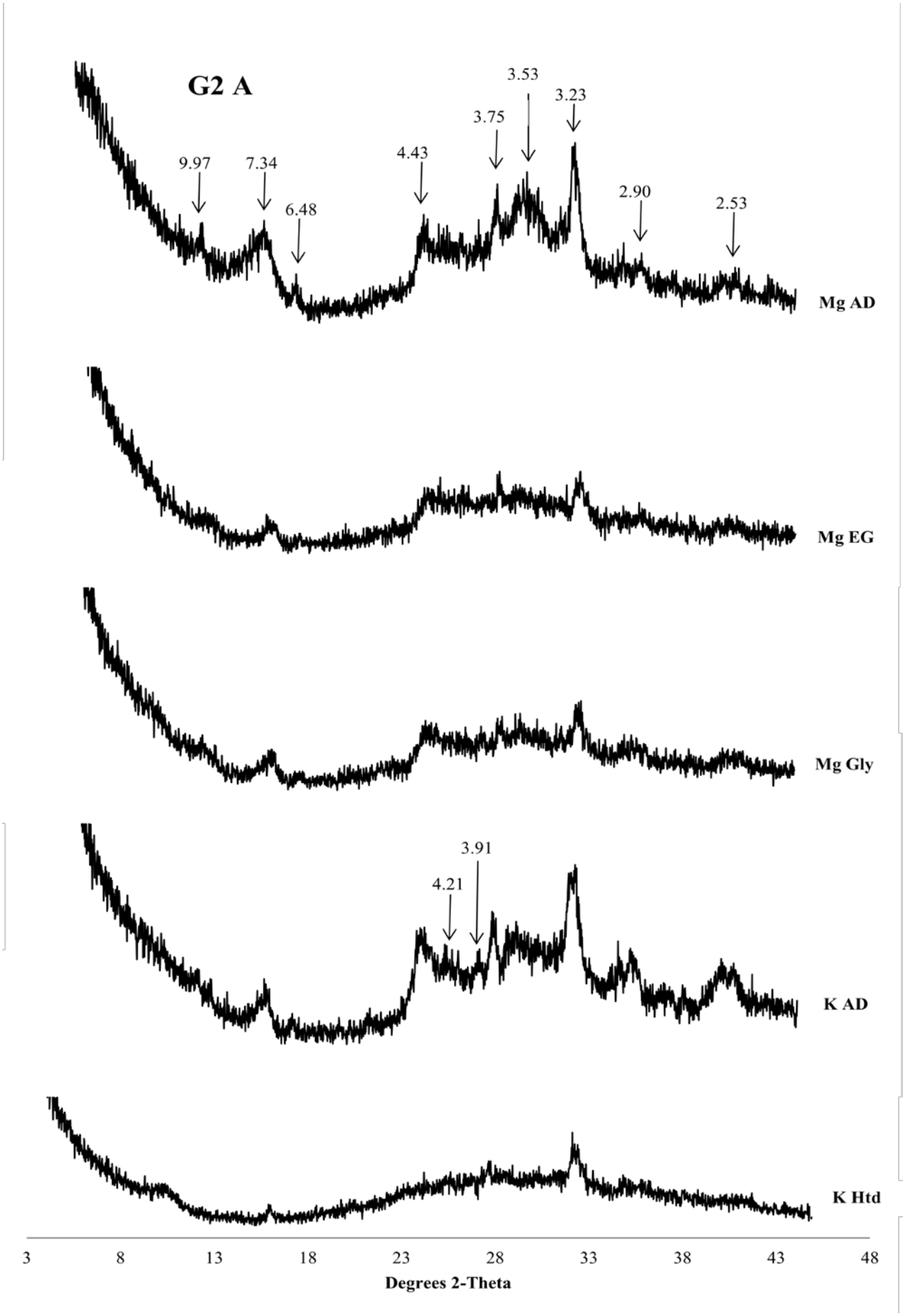
G2 A
9.97
7.34
6.48
4.43
3.75
3.53
3.23
2.90
2.53
Mg AD
Mg EG
Mg Gly
4.21
3.91
K AD
K Htd
3
8
13
18
23
28
33
38
43
48
Degrees 2-Theta

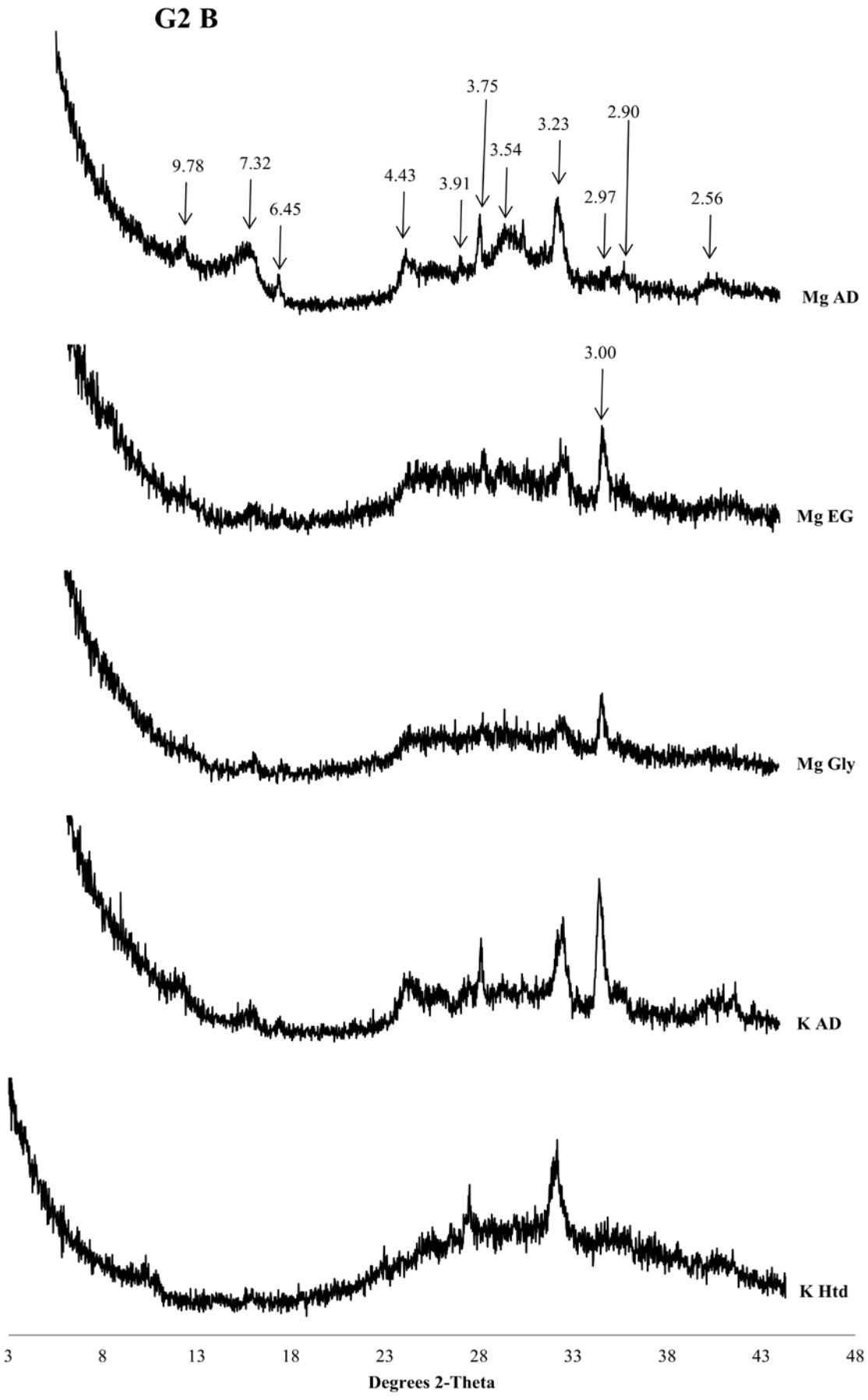
G2 B
9.78
7.32
6.45
4.43
3.91
3.75
3.54
3.23
2.97
2.90
2.56
Mg AD
3.00
Mg EG
Mg Gly
K AD
K Htd
3
8
13
18
23
28
33
38
43
48
Degrees 2-Theta

e)

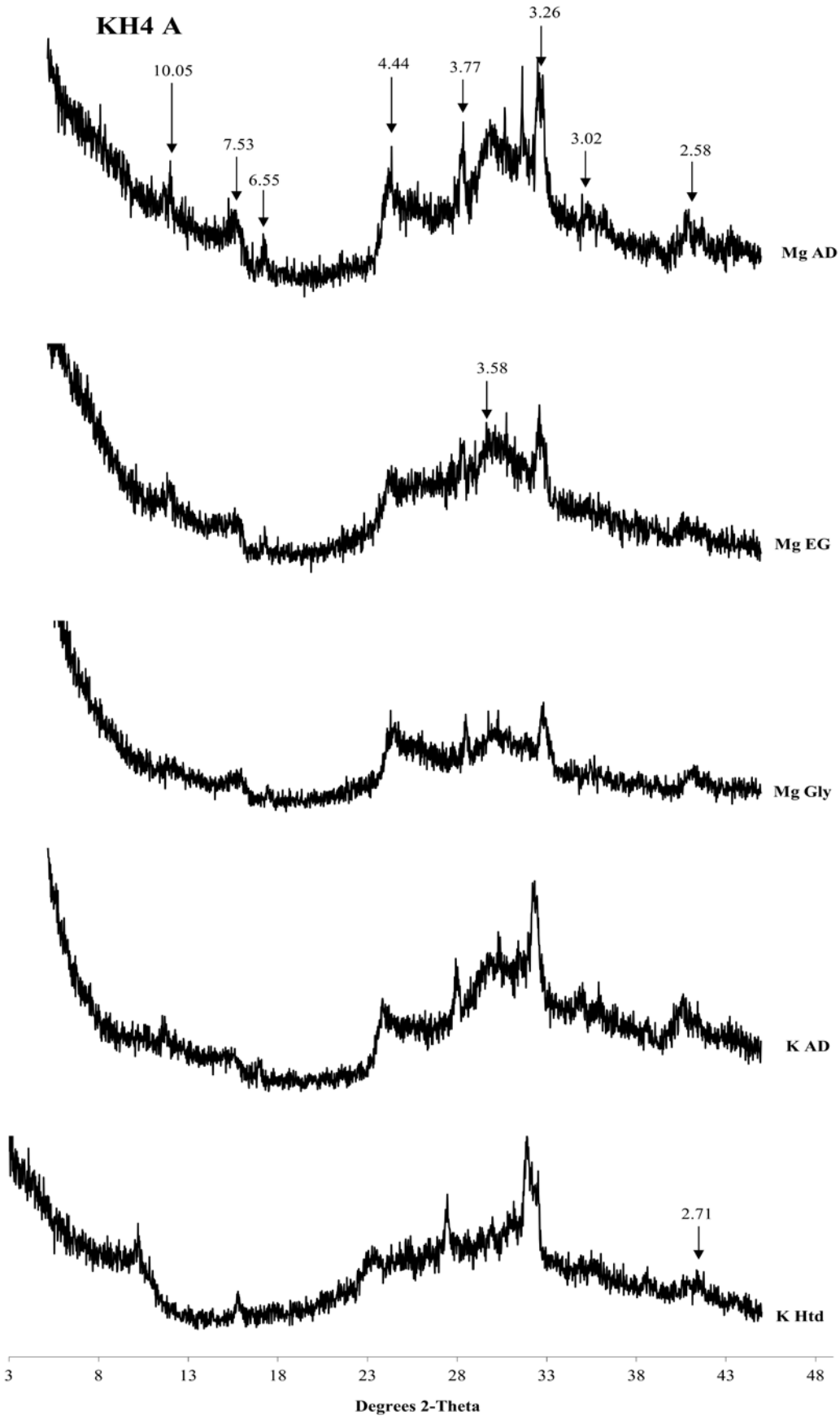
KH4 A
10.05
7.53
6.55
4.44
3.77
3.26
3.02
2.58
Mg AD
3.58
Mg EG
Mg Gly
K AD
2.71
K Htd
3
8
13
18
23
28
33
38
43
48
Degrees 2-Theta

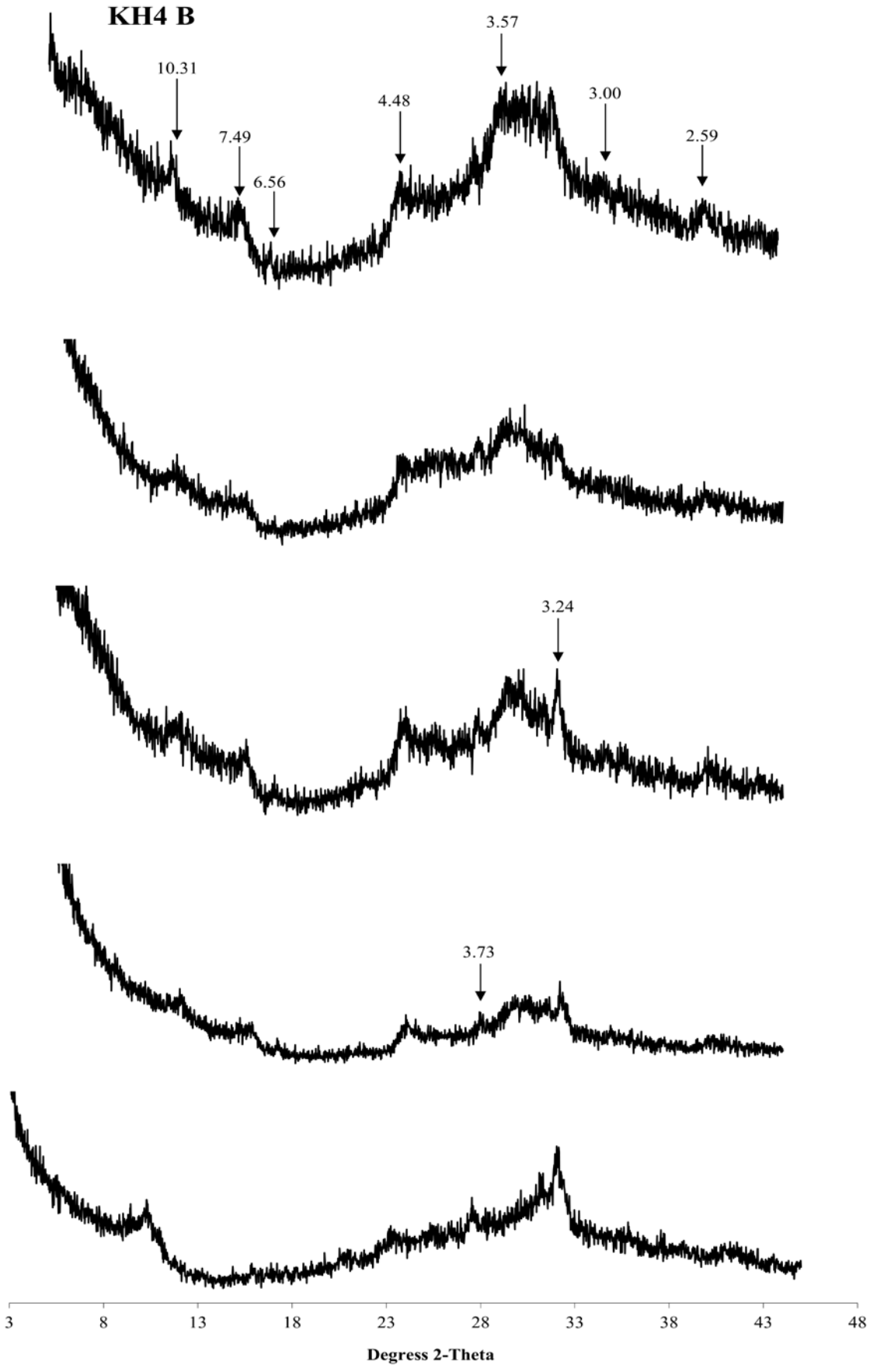
KH4 B
10.31
7.49
6.56
4.48
3.57
3.00
2.59
3.24
3.73
3
8
13
18
23
28
33
38
43
48
Degress 2-Theta

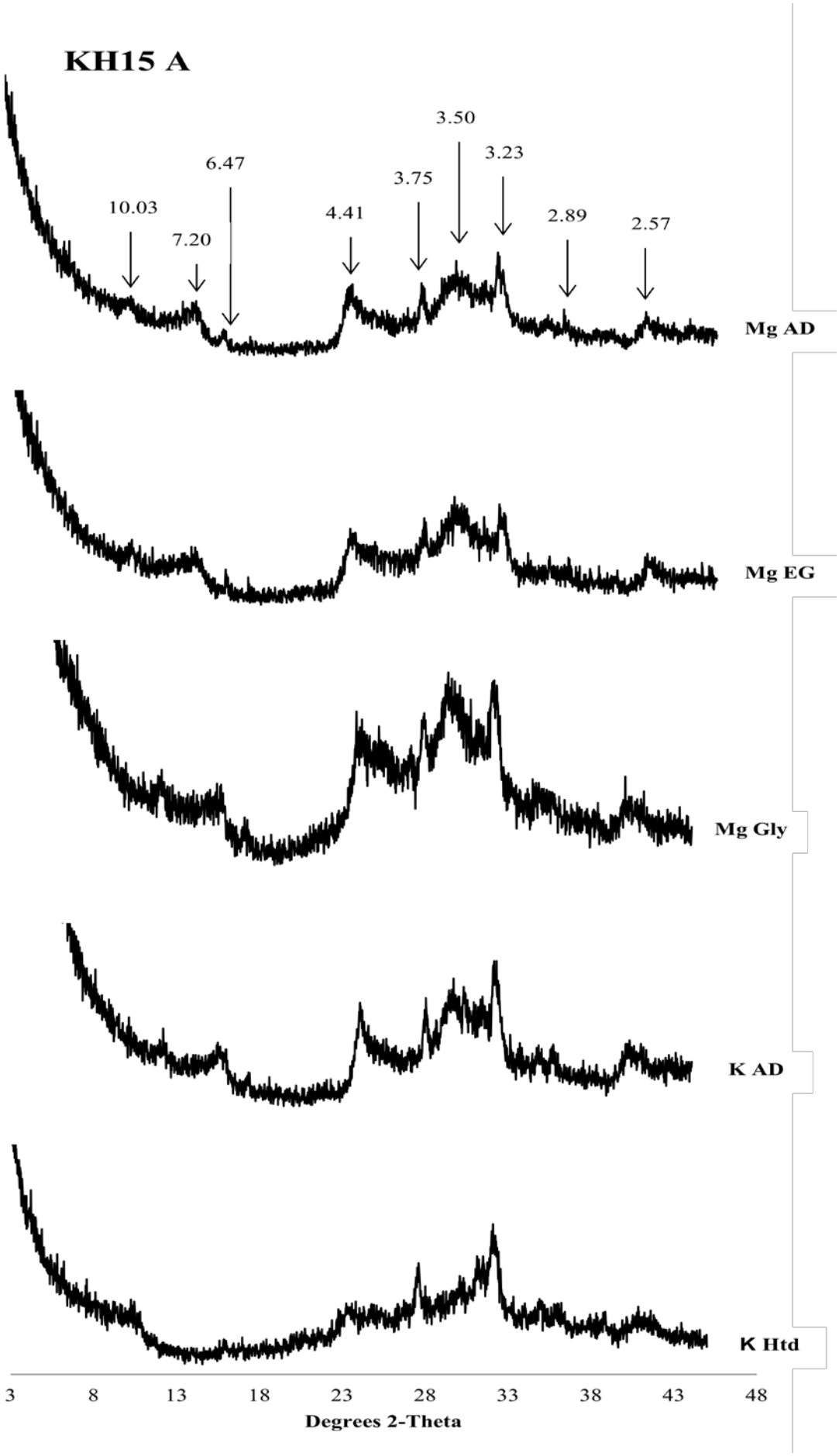
KH15 A
10.03
7.20
6.47
4.41
3.75
3.50
3.23
2.89
2.57
Mg AD
Mg EG
Mg Gly
K AD
K Htd
3
8
13
18
23
28
33
38
43
48
Degrees 2-Theta

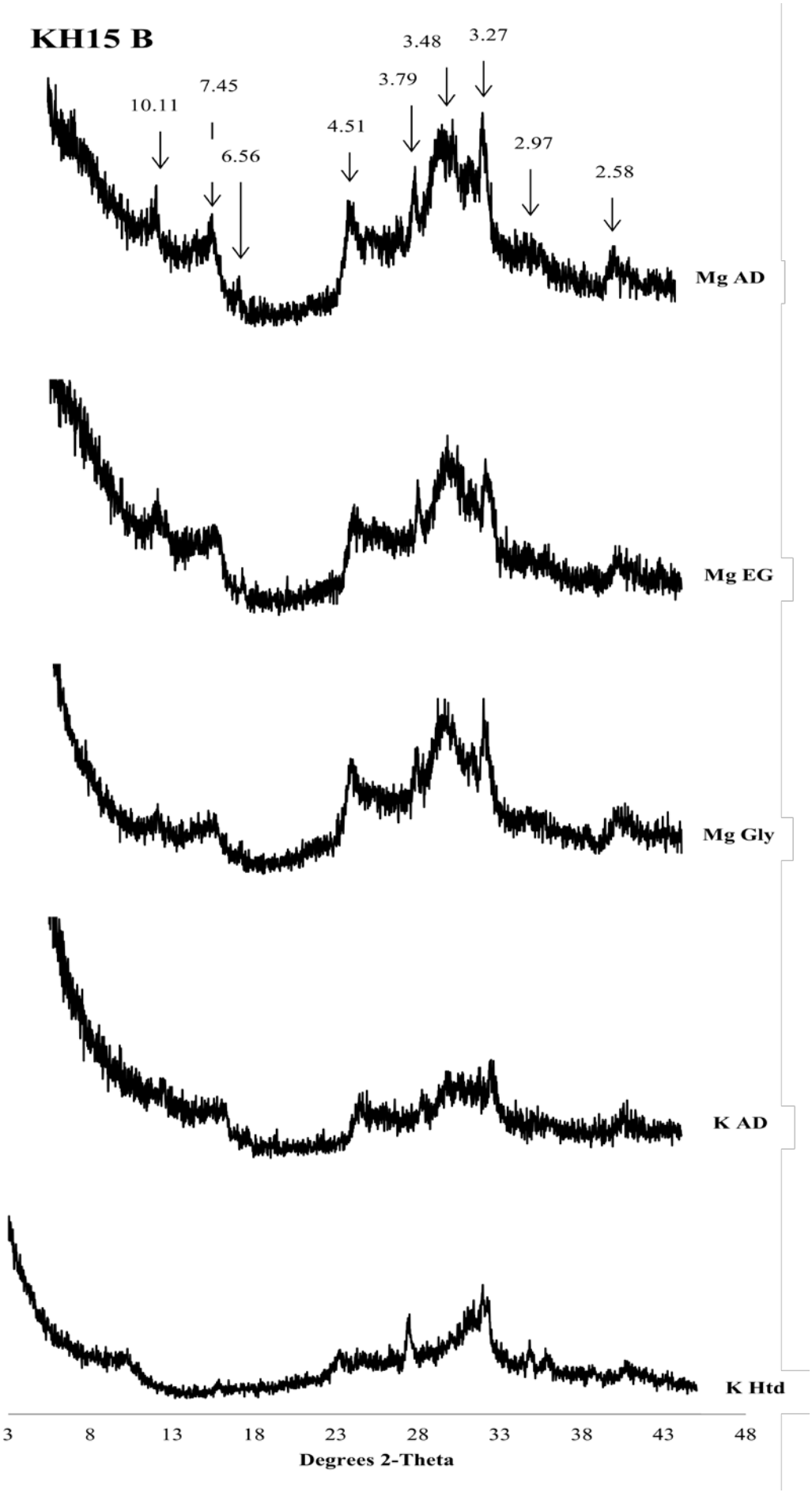
KH15 B
10.11
7.45
6.56
4.51
3.79
3.48
3.27
2.97
2.58
Mg AD
Mg EG
Mg Gly
K AD
K Htd
3
8
13
18
23
28
33
38
43
48
Degrees 2-Theta

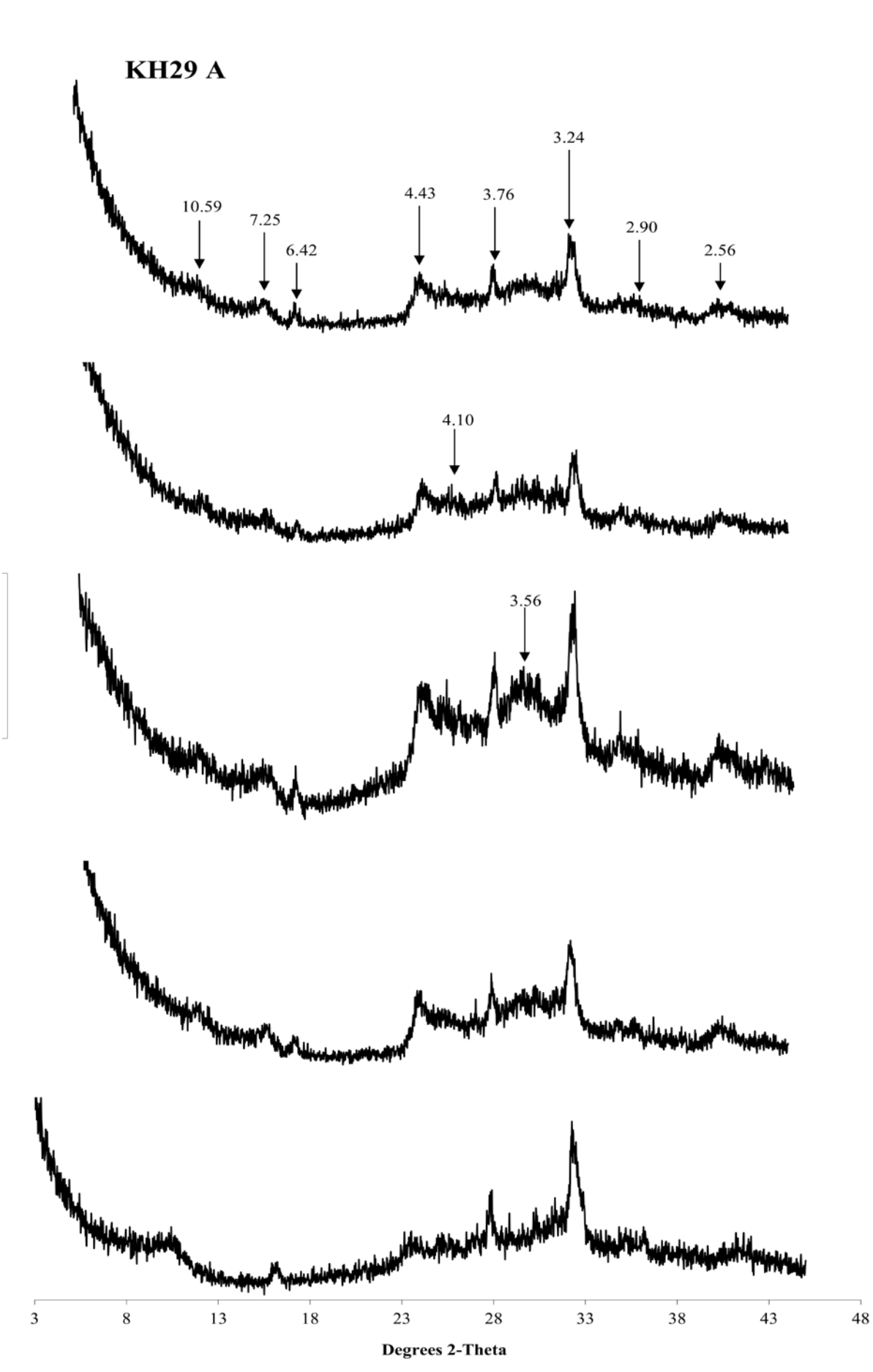
KH29 A
10.59
7.25
6.42
4.43
3.76
3.24
2.90
2.56
4.10
3.56
3
8
13
18
23
28
33
38
43
48
Degrees 2-Theta

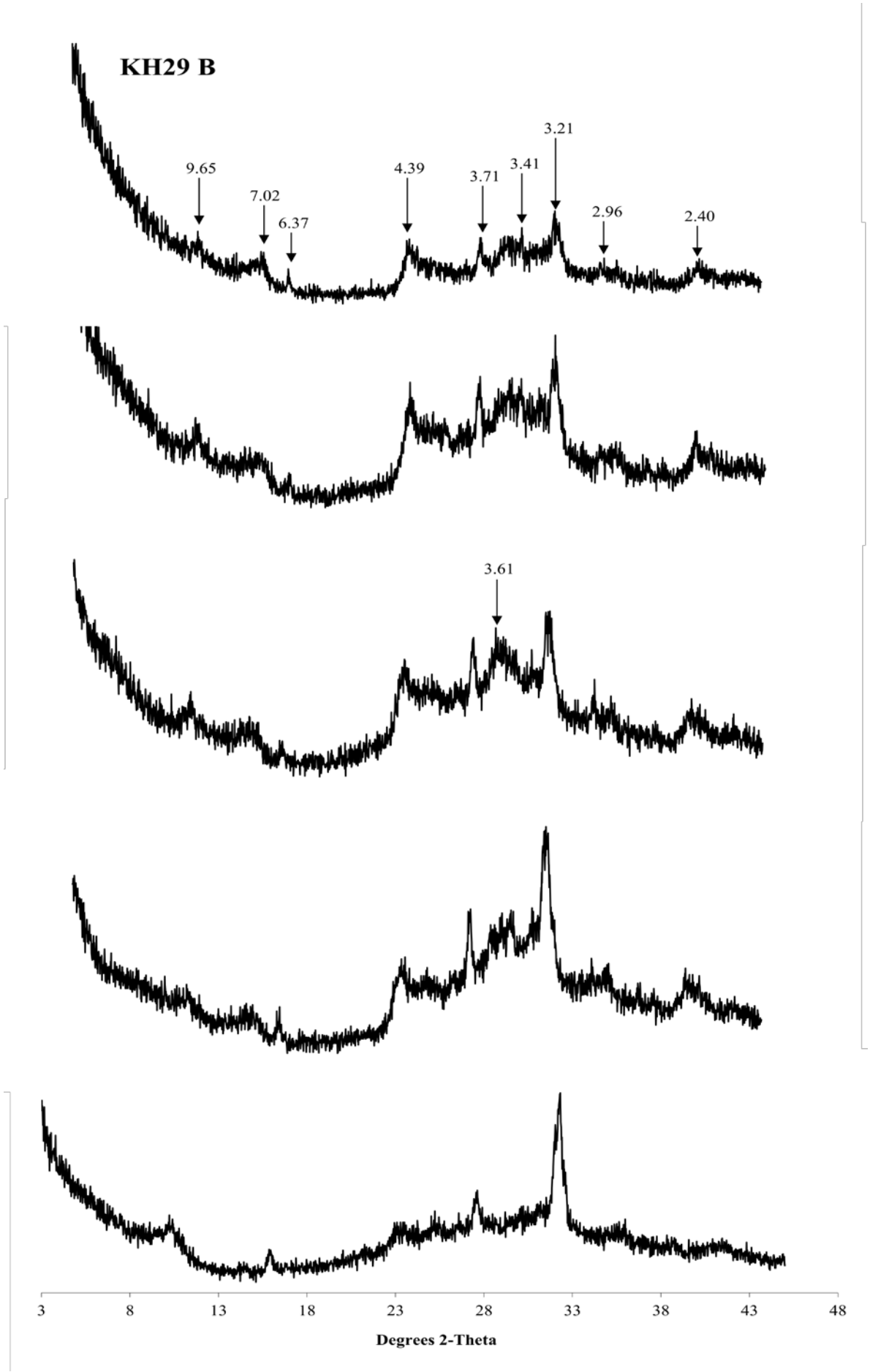
KH29 B
9.65
7.02
6.37
4.39
3.71
3.41
3.21
2.96
2.40
3.61
3
8
13
18
23
28
33
38
43
48
Degrees 2-Theta

f)

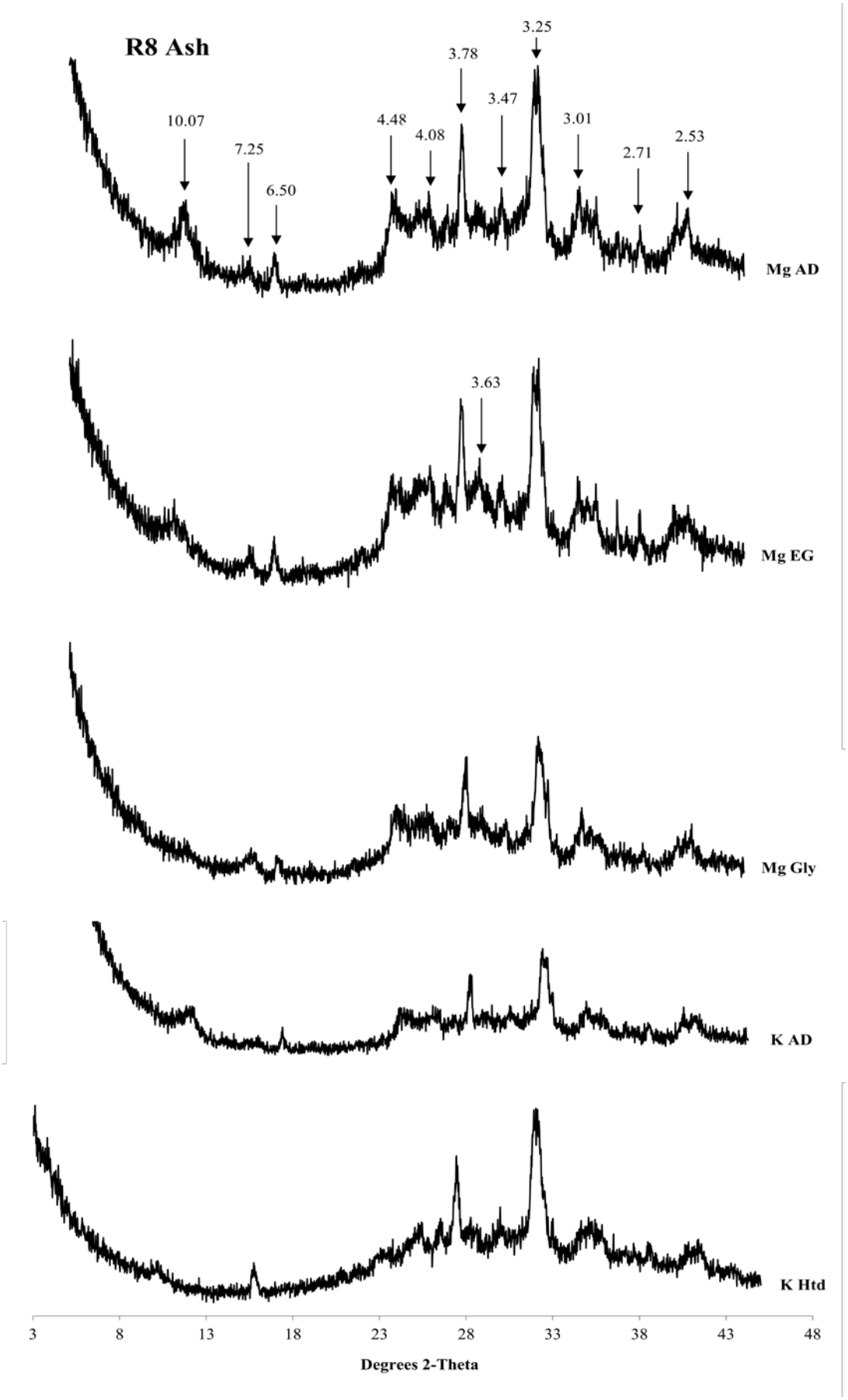
R8 Ash
10.07
7.25
6.50
4.48
4.08
3.78
3.47
3.25
3.01
2.71
2.53
Mg AD
3.63
Mg EG
Mg Gly
K AD
K Htd
3
8
13
18
23
28
33
38
43
48
Degrees 2-Theta

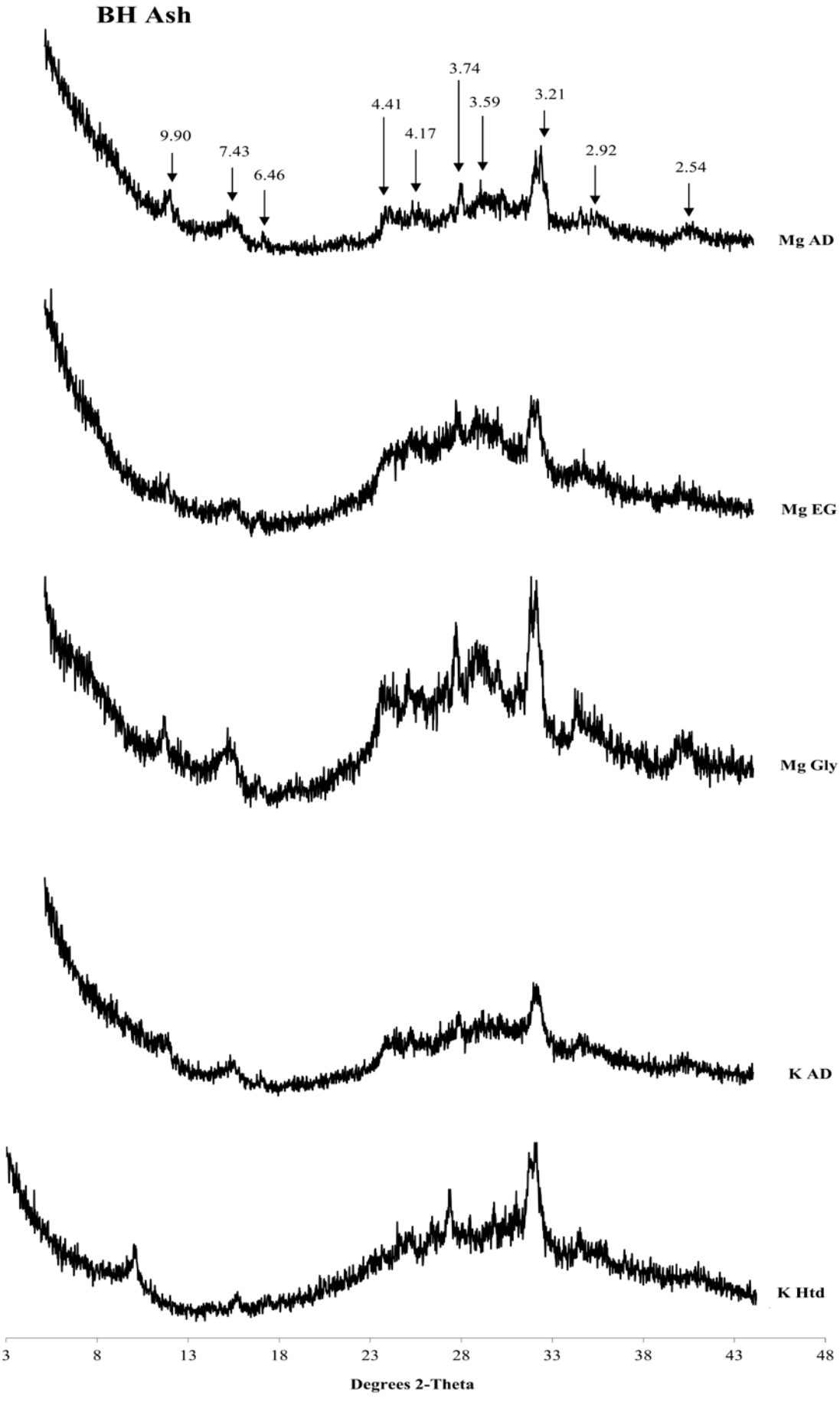
BH Ash
9.90
7.43
6.46
4.41
4.17
3.74
3.59
3.21
2.92
2.54
Mg AD
Mg EG
Mg Gly
K AD
K Htd
3
8
13
18
23
28
33
38
43
48
Degrees 2-Theta